$F_{420}H_2$ dehydrogenation activity and electron transport in the methanoarchaea *Methanospirillum hungatei* GP1, *Methanosarcina barkeri* Fusaro, and *Methanosphaera stadtmanae*

by

Patrick Chong

A thesis submitted in partial fulfillment of
the requirements for the degree of

Doctor of Philosophy

Department of Microbiology
University of Manitoba

2007

THE UNIVERSITY OF MANITOBA

FACULTY OF GRADUATE STUDIES

*****

COPYRIGHT PERMISSION

$F_{420}H_2$ dehydrogenation activity and electron transport in the methanoarchaea *Methanospirillum hungatei* GP1, *Methanosarcina barkeri* Fusaro, and *Methanosphaera stadtmanae*

BY

Patrick Chong

A Thesis/Practicum submitted to the Faculty of Graduate Studies of The University of Manitoba in partial fulfillment of the requirement of the degree

DOCTOR OF PHILOSOPHY

Abstract

The $F_{420}H_2$ dehydrogenase (Fpo complex) of *Methanosarcina mazei* Gö1 catalyzes the $F_{420}H_2$-dependent reduction of methanophenazine, which is used to reduce the heterodisulfide complex (CoM-S-S-CoB) *via* the heterodisulfide reductase (Hdr). This activity is believed to be unique to methylotrophic members of the *Methanosarcinaceae*, but a similar activity, designated $F_{420}H_2$ dehydrogenation, was observed in non-methylotrophic methanoarchaea, independent of growth substrate or phylogeny. A requirement for phenazine-dependent $F_{420}H_2$ dehydrogenation activity is not readily apparent during electron transport in methanoarchaea that possess both the F_{420}-reducing hydrogenase (F_{420} H_2ase) and F_{420}-nonreducing hydrogenase (MV H_2ase); MV H_2ase, along with Hdr, catalyzes the H_2-dependent reduction of CoM-S-S-CoB. In the absence of F_{420} H_2ase or MV H_2ase, could there be a physiological function for the observed $F_{420}H_2$ dehydrogenation activity? Several methanoarchaea were chosen for this study.

Methanospirillum hungatei GP1 has an F_{420} H_2ase, but lacks MV H_2ase; in the absence of the latter enzyme, there is no clear link between H_2 and CoM-S-S-CoB reduction in this methanoarchaeon. Soluble and membrane-bound $F_{420}H_2$ dehydrogenation activities were purified separately to apparent homogeneity and associated with the F_{420} H_2ase; no other sources of $F_{420}H_2$ dehydrogenation activity was detected. Analyses of the genome of *Msp. hungatei* JF1 show that neither a distinct $F_{420}H_2$ dehydrogenase nor an MV H_2ase is encoded by the genome, consistent with biochemical analyses. Genomic analyses did reveal the presence of genes encoding for a non-catalytic MV H_2ase subunit that may provide an electronic link between the F_{420} H_2ase and Hdr, providing a possible means for $F_{420}H_2$-dependent CoM-S-S-CoB reduction in *Msp. hungatei* GP1.

Methanosarcina barkeri Fusaro, a methylotrophic member of the *Methanosarcinaceae*, was expected to be a model for the study of the $F_{420}H_2$ dehydrogenase. Biochemical and/or genomic analyses indicate the presence of F_{420} H_2ase, MV H_2ase, and $F_{420}H_2$ dehydrogenase in this methanoarchaeon. Kinetic analyses of the membrane-bound phenazine-dependent $F_{420}H_2$ dehydrogenase activities of *Ms. barkeri* Fusaro and *Ml. tindarius* produced unexpectedly different activity profiles.

Purification to apparent homogeneity of the soluble and membrane-bound $F_{420}H_2$ dehydrogenation activities resulted in the isolation of the F_{420} H_2ase; no other source of $F_{420}H_2$ dehydrogenation activity was detected in our studies. While the phenazine-dependent $F_{420}H_2$-oxidation activity was not associated with a distinct $F_{420}H_2$ dehydrogenase, the observed activity shares some similarities with the $F_{420}H_2$ dehydrogenase activity of *Ms. mazei* Gö1. In the presence of F_{420} H_2ase and MV H_2ase, it is possible that, under the growth conditions tested, a distinct $F_{420}H_2$ dehydrogenase may not be needed for CoM-S-S-CoB reduction.

Methanosphaera stadtmanae possesses an MV H_2ase, but an F_{420} H_2ase activity has not been reported. O_2-labile, phenazine-dependent $F_{420}H_2$ dehydrogenation activity was observed at much lower levels relative to other methanoarchaea. The $F_{420}H_2$ dehydrogenation activity was enriched, but could not be purified to homogeneity. This activity appears to be associated with two proteins: $F_{420}H_2$ oxidase and F_{420} H_2ase.

Analysis of the cell-free extract of *Msph. stadtmanae* indicated very low levels of F_{420}-reducing activity; this activity was partially characterized, and possesses distinctive qualities relative to other methanoarchaea. The genome of *Msph. stadtmanae* contains gene sequences encoding for subunits of a putative F_{420} H_2ase; BLAST analyses of these sequences indicate similarity with the corresponding enzyme from *Methanothermobacter thermoautotrophicus* ΔH, a H_2/CO_2 metabolizing member of the *Methanobacteriales*. The finding of an F_{420} H_2ase activity provides a better understanding of electron transport in *Msph. stadtmanae*.

$F_{420}H_2$ oxidase activity ($F_{420}H_2$-dependent reduction of O_2) was also detected in cell-free extract. $F_{420}H_2$ oxidase and phenazine-dependent $F_{420}H_2$ dehydrogenation activities declined rapidly when stored under aerobic conditions, indicating possible co-association of the two activities. Further studies are required to resolve the F_{420} H_2ase and $F_{420}H_2$ dehydrogenation/$F_{420}H_2$ oxidase activities of *Msph. stadtmanae*.

While much has been elucidated of the electron transport pathways in the methanoarchaea, our studies show that variations in these pathways do occur in individual methanoarchaea. This is not unexpected as the methanoarchaea are a taxonomically diverse group of microbes, unified by the capacity to couple the production of methane with energy conservation.

Acknowledgements

To Dr. Richard Sparling, thank you for your guidance and patience throughout the course of my studies. You have always been very generous with your time, and extremely helpful at all times. You have been more than just my advisor, you have also been a friend and mentor, and a source of encouragement and inspiration, through good times and bad.

I would especially like to thank Dr. Kathleen Londry, Dr. Barbara Triggs-Raine, and Dr. Isamu Suzuki (retired) for all of their helpful comments, as well as their efforts to keep me on the straight and narrow during the course of my studies.

To Ayush, Kari, Rahul, George, Tamiko, Denny, Reuben, and to all my friends and colleagues in the Department of Microbiology, past and present; you have all made coming to work each day a pleasure, and have given me many fond memories of my time as a graduate student. I wish you all well in your future endeavors. Sharon, I am certainly going to miss all the little chats that we used to have!

To my family- Mom, Dad, Ivy, Peter, Noreena, Phoenix, and Little Dragon - thank you for all the love and encouragement that you have given me as I toiled through the years, and for always believing in me.

Table of Contents

Page

List of Figures

Chapter one

Chapter six

Chapter seven

List of Tables

Chapter four

Chapter five

Chapter six

Chapter seven

List of Abbreviations

ADH.....Alcohol dehydrogenase
CH_3OH.....Methanol
CoB.....Coenzyme B, 7-mercaptoheptanoylthreoninephosphate
CODH/ACS.....Carbon monoxide dehydrogenase/Acetyl-CoA synthase
CoM.....Coenzyme M, 2-mercaptoethanesulfonic acid
CoM-S-S-CoB.....Heterodisulfide complex
DEAE.....Diethylaminoethyl
DNase.....Deoxyribonuclease
DPI.....Diphenyleneiodonium chloride
DSZM.....Deutche Sammlung von Zellkulturen und Mikroooranismen
Ech.....Energy conserving hydrogenase
DTT.....Dithiothreitol
EDTA.....Ethylenediaminetetraacetic acid
F_{420}.....8-hydroxy-5-deazaflavin
$F_{420}H_2$.....reduced 8-hydroxy-5-deazaflavin
FAD.....Flavin adenine dinucleotide
Fd.....Ferredoxin
Fd_{red}.....Reduced ferredoxin
Fno.....$F_{420}H_2$:$NADP^+$ oxidoreductase
Fpo.....$F_{420}H_2$:phenazine oxidoreductase
Frh.....F_{420}-reducing hydrogenase
Fqo.....$F_{420}H_2$:quinone oxidoreductase
H_4MPT.....Tetrahydromethanopterin
H_4SPT.....Tetrahydrosarcinopterin
Hdr.....Heterodisulfide reductase
HEPES.....(N-[2-Hydroxyethyl]piperazine-N'-[2-ethanesulfonic acid]
kDa.....kilodalton
Mb.....*Methanobacterium*
Mc.....*Methanococcus*
MCAC.....Metal chelate affinity chromatography
Ml.....*Methanolobus*
MP.....Methanophenazine
Ms.....*Methanosarcina*
Msp.....*Methanospirillum*
Msph.....*Methanosphaera*
Mst.....*Methanosaeta*
Mtb.....*Methanothermobacter*
MTZ.....Metronidazole
MV.....Methyl viologen
Mvh.....Methyl viologen-reducing hydrogenase
NAD^+.....Nicotinamide adenine dinucleotide
NADH.....Reduced nicotinamide adenine dinucleotide
$NADP^+$.....Nicotinamide adenine dinucleotide phosphate
NADPH.....Reduced nicotinamide adenine dinucleotide phosphate

PAGE.....Polyacrylamide gel electrophoresis
RNase.....Ribonuclease
SDS PAGE.....Sodium dodecyl sulfate polyacrylamide gel electrophoresis
Tris.....Tris(hydroxymethyl)aminomethane
Tris/Cl.....Tris(hydroxymethyl)aminomethane Chloride

1. Methanogenesis and electron transport in the methanoarchaea

1.1. The Production of Methane

Methane (CH_4, MW = 16.0426 g/mol), the chief constituent of natural gas, is the simplest and most abundant of the hydrocarbons (Stafford *et al.* 1978). There are three natural sources of methane: (1) in the various natural gases originating from the physical and chemical breakdown of prehistoric plant material; (2) from biogenic sources such as flooded rice paddies and wetlands, where methane is produced *via* the decomposition of plants by anaerobic microorganisms; (3) from the gastrointestinal tracts of ruminant animals such as cattle or sheep, where methane is produced through the concerted activity of symbiotic anaerobic microorganisms who produce or consume H_2 (Meynell 1978, Bodelier *et al.* 2000). Methane is also produced in various man-made constructs, including sewage digesters, landfills, food plant waste fermenters, and oil wells (Garcia 1998). Anaerobic decomposition of organic matter results in the production of a gas containing 50-75% methane, 25-45% carbon dioxide, and small amounts of hydrogen, nitrogen, and hydrogen sulfide (Price and Cheremisinoff 1981).

The concentration of atmospheric methane has steadily increased over the last 300 years from 0.7 parts per million (p.p.m.) to 1.7 p.p.m., almost in line with the increase in human population growth (Pearce 1989, Thauer 1998). It has been estimated that 10^9 tons of methane are produced per year by methane-producing microorganisms. As global warming increases, methane is also released from the polar ice caps and the frozen tundra, where methane is trapped in the ice (Pearce 1989). The majority of the combustible gas (two-thirds) diffuses into aerobic zones where it is oxidized by

methanotrophic bacteria to CO_2, with the remaining amount buried as methane deposits or released to the atmosphere where it is photochemically converted to carbon dioxide (CO_2) (Anthony 1986, Ermler *et al.* 1997, Thauer 1998).

Global warming is due to the greenhouse effect, the phenomena where infrared energy emitted by the Earth's surface is absorbed by gases in the atmosphere and redirected back to the Earth (Dickinson and Cicerone 1986, Lorius *et al.* 1990). These gases include H_2O vapor, CH_4, CO_2, ozone (O_3), nitrous oxide (N_2O), and various chlorofluorocarbons (Wang *et al.* 1976, Dickinson and Cicerone 1986). One molecule of methane can have a 20- to 25-fold higher effect on climate compared to CO_2, making methane a highly potent greenhouse gas (Kilgore 1993, Bodelier *et al.* 2000). The contribution of methane to global warming has enhanced interest in the microbial processes that contribute to the global methane cycle (Conrad *et al.* 2000).

Oxidation of methane by methanotrophic microorganisms in oxic zones is a process that helps to regulate the levels of methane emanating from freshwater and marine environments. Within anaerobic marine sediments, significant quantities of methane that (> 80%) can be removed by a consortium of microorganisms that use methane as a source of electrons to reduce SO_4 to H_2S (Boetius *et al.* 2000, Orphan *et al.* 2001, Sowers and Ferry 2002). This involves species of anaerobic methanotrophic (ANME) *Archaea* that convert methane to CO_2 and H_2, and H_2-scavenging sulfate-reducing bacteria, likely species of *Desulfobacteraceae* or *Desulfobulbaceae* (Hoehler *et al.* 1994, Orphan *et al.* 2001, Lloyd *et al.* 2006). A novel microbial sink for methane was recently reported by Raghoebarsing *et al.* (2006) in freshwater sediments, where methane oxidation is coupled to nitrate or nitrite reduction to N_2. While the exact mechanism is

largely unknown, it is believed that the reaction involves a microbial consortium, with an archaeon (ANME) oxidizing the methane, and a novel bacterium that catalyzes the denitrification step. This process occurs in anaerobic sediments containing low levels of oxidizable substrates (other than methane) and high levels of nitrate.

A potential source of biofuel, methane can be siphoned from landfills and used for the following: fire kilns, furnaces, and boilers; internal combustion engines or turbines to generate electricity; or it may be cleaned and processed to a higher grade fuel (Richards 1989). Many commercial products are indirectly synthesized using methane. Carbon black, a substance formed *via* the incomplete combustion of methane, is used to make commercial items such as rubber tires, tubes, converyor belts, electronics components, and black pigment for printing cartridges.

1.2. The microbial basis for the production of methane – the methanoarchaea

The first report on the isolation of an organism from river mud that could oxidize H_2 and reduce one carbon compounds (such as CO_2, CO, and formate) to methane was made by Stephenson and Strickland in 1933; this landmark paper marked the beginning of the modern era for the study of methanogenesis (Thauer 1998). While the isolated culture was not pure, it was significant to note that the culture did not yield methane from compounds containing two or more carbon atoms (Wolfe 1993).

The development of the Hungate technique, for cultivation of anaerobic microorganisms, allowed for isolation of these fastidious microorganisms for whole cell physiological studies in the 1950s, followed by cell extract studies in the 1960s (Hungate 1950, Wolfe 1993). In the ensuing years, many of the key enzymes, cofactors, and genes

of methanogenesis would be elucidated. In the 1970s, a pressurized anaerobic atmosphere was used to grow these strictly anaerobic microorganisms (Balch and Wolfe 1976). Another vital discovery was the recognition that the methane-producing "bacteria" were microorganisms belonging to the domain *Archaea* (Woese 1990).

1.2.1. The Archaea

In 1977, Carl Woese and coworkers exploited the partial sequences of the 16S-ribosomal RNA (16S rRNA) to monitor different phylogenetic types of microorganisms (Woese 1981). Prior to 1977 there had been a long held view that all organisms could be divided into two Super-Kingdoms, the prokaryotes and the eukaryotes (Danson 1988). Analysis of the 16S rRNA distinguished a group of microorganisms from both the eukaryotes and the prokaryotes, and in 1979 allowed them their own branch on the tree of life as a Super-Kingdom (Danson 1988, Cowan 1992). These organisms were christened archaebacteria (later renamed *Archaea*) and include diverse groups of microorganisms that thrive in unusual habitats with extremes of temperature, salinity and pH (Woese *et al.* 1990, Gray 1996, Schäfer *et al.* 1999).

The term *Archaea* represents a once held belief that these organisms originated from life forms preceding the division of the Eukaryal and Eubacterial domains; however, based on the sequence of universally present proteins, the *Archaea* have been placed on the branch leading to the Eukarya (Schäfer *et al.* 1999). *Archaea* are also distinguished from the Eukarya and Eubacteria by unique metabolic activities, suggesting uncommon structures of proteins and cofactors (Ferry 1997). Phylogenetically, most current isolates can be placed into two major kingdoms of *Archaea*, the *Crenarchaeota*

and the *Euryarchaeota*; a third kingdom, the *Korarchaeota* and possibly a fourth, the *Nanoarchaeota* have been proposed (Woese *et al.* 1990, Aravalli *et al.* 1998, Huber *et al.* 2002).

The kingdom *Euryarchaeota* includes a diverse group of microbes, known collectively as the methanoarchaea, that couple the generation of energy with the production of methane; thus far, all organisms capable of energy-coupled methane generation are found within this single group (Woese *et al.* 1990).

1.2.2. Enter the methanoarchaea

Over two billion years ago, methane-producing microorganisms thrived in all types of habitat, but once O_2 saturated the oceans, these anaerobic microbes were forced to seek refuge in environments outside the reach of O_2 (Pearce 1989). The microbial degradation of organic material in an anaerobic environment forces the microorganisms to use molecules other than O_2 as electron acceptors (Price and Cheresinoff 1981). The methanoarchaea comprise the largest and most phylogenetically diverse members of the *Archaea*, and are ubiquitous in anaerobic environments, residing in diverse habitats, including aquatic sediments, bogs, marshes, tundra, from the wetwood of infected trees, in the rumen of animals, the mammalian large intestine, human dental plaque, guts of insects such as termites, in marine picoplanktons, and in deep-sea, hyperthermophilic geothermal vents (Zeikus and Henning 1975, Baross and Deming 1983, Belay *et al.* 1988, Cowan 1992, Aravalli *et al.* 1998, Leadbetter and Breznak 1996). Collectively, methanoarchaea are found in environments with wide ranges in salinity, temperature, and pH (Zinder 1993).

Methanoarchaea require an oxidation/reduction potential in the growth medium more negative than -0.3 V, where the O_2 concentration is approximately 10^{-56} M (Zinder 1993). Pure methanogenic cultures have been observed surviving aerobic conditions for no more than 30 hours, with methane production decreasing after 200 minutes exposure to air (Kiener and Leisinger 1983, Fetzer *et al.*1993). Certain methanoarchaea, including *Methanothermobacter* (*Mtb.*) *thermoautotrophicus* and *Methanocaldococcus* (*Mc.*) *jannaschii*, form biofilms which may aid in limiting contact with O_2 (LePaglia and Hartzell 1997). Some methanoarchaea also possess enzymes to detoxify O_2 and reactive O_2 species, such as superoxide dismutase, catalase, or $F_{420}H_2$ oxidase (Takao *et al.* 1991, Brioukhanov *et al.* 2000, Shima *et al.* 2001, Seedorf *et al.* 2004).

In natural ecosystems, the indigenous microflora can also develop a protective effect on the methanoarchaea against O_2 toxicity (Wagner *et al.* 1999). As a result, methanoarchaea can reside in communities under O_2-limited conditions (i.e. microaerophilic), where O_2 is consumed by facultative microbes, and their metabolic byproducts are scavenged by the methanoarchaea for their own metabolic processes (Schink 1997). These communities make methanoarchaea a valuable resource in the biological treatment of wastewater pollution, where they coexist with O_2-consuming bacteria (Kato *et al.* 1993).

The methanoarchaea derive their metabolic energy from the conversion of a restricted number of substrates to methane (Cowan 1992, Ferry 1999). The metabolic capacity to couple energy conservation with methane production, known as methanogenesis, is unique to the methanoarchaea (Zeikus 1977, Balch *et al.* 1979). Traces amounts of methane, which is not linked to energy conservation, are produced by

some sulfate-reducing bacteria well as from the sulfate-reducing archaeon *Archaeoglobus fulgidus*, during growth on lactate and sulfate (Beeder *et al.* 1994, Klenk *et al.* 1997, Shcherbakova and Vaĭnshteĭn 2000).

Methanogenesis represents the essential terminal step in the anaerobic breakdown of organic material under light-, nitrate-, and sulfate-limited conditions (Garcia *et al.* 2000, Sowers and Ferry 2006). Microbial partnerships are required for the complete breakdown of complex carbon substrates, such as cellulose, proteins, fatty acids, alcohols other than methanol (CH_3OH), etc, to CO_2 and methane. The mineralization of organic matter typically follows four steps: hydrolysis; fermentation; acetogenesis/hydrogenesis (syntrophic); and methanogenesis (Pankhania and Robinson 1984). Various species of hydrolytic, fermentative, syntrophic, and acetogenic bacteria break down the complex carbon molecules to H_2, acetate, CO_2, and formate, which are then metabolized by the methanoarchaea as methanogenic substrate (McInerney *et al.* 1979, Mah 1982, Daniels 1984). The methane generated is oxidized to CO_2 by other microbial processes, and made available for photosynthetic fixation, completing the carbon cycle (Sowers and Ferry 2006).

The major energy-yielding step is associated with the reduction of a methyl (CH_3-) moiety to methane ($\Delta G^{\circ\prime} = -40$ kJ/mol), with the electrons for the reductive step obtained from the oxidation of H_2 or formate (80% of species), CH_3OH, methylamines or dimethylsulfide (under marine conditions, high sulfate) (26% of species), acetate (11% of species), and in a few instances ethanol or propanol (Rouvière and Wolfe 1988, Garcia 1998).

Interspecies H_2 transfer between bacteria and methanoarchaea is a physiologically important process in microbial communities, maintaining low partial pressures of H_2 (Mah 1982). H_2 produced by bacterial metabolic processes is removed by the methanoarchaea and used as a source of electrons. Partnerships of H_2-producers with an H_2 consumer allows for the complete breakdown of organic polymers (Zinder 1993, Sowers 1995). In natural habitats, partnerships with methanoarchaea can only take place in the absence of sulfate, as sulfate-metabolizing bacteria, such as the *Desulfovibrio* spp., have a higher affinity (Km = 2 μM) and lower threshold for H_2, allowing these microbes to use H_2 at low partial pressures more readily than their methanogenic competitors (Km = 4-8 μM) (Kristjansson *et al.* 1982, Zinder 1993).

1.2.3. Phylogeny of the methanoarchaea

Presently, the methanoarchaea are divided into five distinct orders: *Methanobacteriales*, *Methanococcales*, *Methanomicrobiales*, *Methanopyrales*, and *Methansarcinales* (Thauer 1998). Recently, it has been suggested, on the basis of studies of the gene sequences encoding the enzymes from the methanogenic pathway (H_2:CO_2) and coenzyme F_{420} synthesis, that the methanoarchaea should be separated into two independently evolving classes: Class I, encompassing the *Methanobacteriales*, *Methanococcales*, and *Methanopyrales*, and Class II which contains the *Methanomicrobiales* and *Methanosarcinales* (Bapteste *et al.* 2005).

The *Methanosarcinales* also have a number of non-methanogenic relatives, such as the *Halobacteriales*, *Thermoplasmatales*, and *Archaeoglobales*, *Archaea* which may be considered to be "degenerated methanoarchaea that have lost most of the proteins

involved in methanogenesis..." (Bapteste *et al.* 2005). Members of the *Archaeoglobales*, which are hyperthermophilic *Archaea* that contain many of the proteins required for reverse-methanogenesis (production of CO_2), are hypothesized to be the missing link between the methanoarchaea and the sulfur-metabolizing *Archaea* (Bapteste *et al.* 2005).

The *Methanosarcinales* have evolved more extensively than the other methanogenic orders and show more variation in environmental niche and phenotypic characteristics; this is exemplified by the recently published genome of *Methanosarcina mazei* Gö1 which contains a significant number of bacterial genes, indicating that numerous lateral gene transfers may have played a significant role in the evolution of *Ms. mazei* Gö1, as well as for other members of the *Methanosarcinales* (Deppenmeier 2002). Members of the order *Methanosarcinales* are the most metabolically versatile of the methanoarchaea, as demonstrated by their collective ability to metabolize CO_2, acetate, CH_3OH, and methylamines (Rouvière *et al.* 1992). This is also evident by the presence of enzymes and structures involved in electron transport in members of the *Methanosarcinales* that are apparently not found in the *Methanomicrobiales* or in the methanoarchaea comprising Class I, which possess a single pathway for methanogenesis and are typically limited to the use only one or two methanogenic substrates (Deppenmeier *et al.* 2002, Galagan *et al.* 2002, Maeder *et al.* 2006).

1.3. An overview of methanogenesis and electron transport in the methanoarchaea

The process of methanogenesis is comprised of a series of oxidation/reduction reactions using H_2, formate, CH_3OH, or acetate as the source of carbon and/or electrons

for the production of CH_4 and ultimately to energy conservation. The metabolic pathways of methanogenesis involve a number of unusual cofactors, many of which are also found in ANME, cousins of the methanoarchaea that reside in methane-rich deep sea marine sediments (Deppenemier *et al.* 1996, Hallam *et al.* 2004).

Barker (1956) speculated that the production of methane from CO_2, CH_3OH, or acetate metabolism occurred *via* single-carbon (C_1) reduction reactions partially carried out on pteridine and tetrapyrrole conenzyme carriers (Zeikus *et al.* 1985). In the ensuing years, these carriers – methanofuran, tetrahydromethanopterin, component B, and coenzyme M - were isolated and characterized. In the following section, the three main methanogenic pathways will be discussed: the reduction of CO_2 with H_2 (hydrogenotrophic); the reduction and/or disproportionation of CH_3OH or methylamines (methylotrophic); and the fermentation of acetate (aceticlastic).

1.3.1. The hydrogenotrophic pathway

The conservation of hydrogenotrophic machinery in the vast majority of methanoarchaea suggests that this pathway may have been the ancestral form of methanogenesis (Bapteste *et al.* 2005). Approximately 80% of known methanoarchaea are hydrogenotrophic (Garcia 1998). H_2 is a major fermentation product of many species of anaerobic bacteria, fungi, and protozoa in many natural habitats, providing a steady source of electrons for methanogenesis (Zinder 1993).

The reduction of CO_2 to CH_4 consumes four molecules of H_2 (Fox *et al.* 1987):

$$CO_2 + 4H_2 \rightarrow CH_4 + 2H_2O,\ \Delta G^{\circ\prime} = -131\ \text{kJ/mol}\ CH_4$$

Formate (HCOOH) is another common microbial fermentation product used by some methanoarchaea as a carbon and electron source for methanogenesis; formate is converted to CO_2 and $2H^+ + 2e^-$ *via* **formate dehydrogenase** (FDH) (Sparling and Daniels 1986, Ferry 1990, Zinder 1993):

$$HCOO^- \rightarrow CO_2 + H^+ + 2e^-$$

FDH has been purified from a number of methanoarchaea; studies with *Methanococcus* (*Mc.*) *thermolithotrophicus* indicate that synthesis of FDH may be regulated by the presence of H_2 (Sparling and Daniels 1990).

An overview of the hydrogenotrophic pathway is depicted in Figure 1.1. The first step in this pathway begins with the reduction of CO_2 to *N*-formyl-methanofuran ($\Delta G°' =$ +16 kJ/mol), catalyzed by the **formyl-methanofuran dehydrogenase** (Thauer *et al.* 1993). Formyl-methanofuran dehydrogenase has been purified from a number of methanoarchaea, including *Methanothermobacter* (*Mtb.*) *marburgensis*, *Methanobacterium* (*Mb.*) *formicicum*, and *Methanosarcina* (*Ms*) *barkeri* strain Fusaro (Ferry 1999). The enzyme from *Ms. barkeri* consists of five subunits (FmdEACDB), with a molybdopterin guanine dinucleotide, using CO_2 as substrate and forming N-carboxymethanofuran as an intermediate (Karrasch *et al.* 1990, Vorholt and Thauer 1997, Bartoschek *et al.* 2000).

Mtb. thermoautotrophicus possesses two isoforms of formyl-methanofuran dehydrogenase, containing either molybdenum or tungsten (Hochheimer *et al.* 1995).

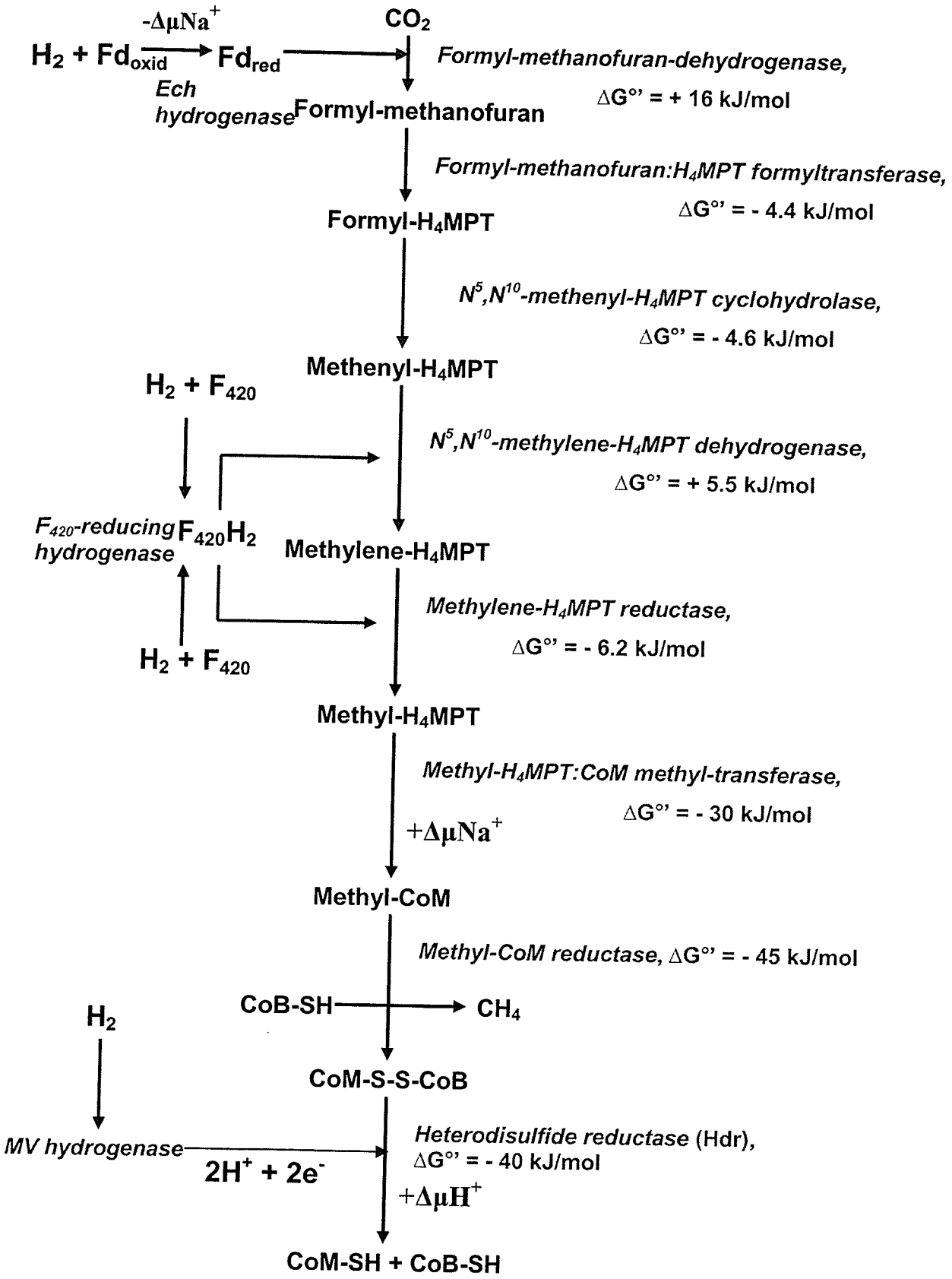

Figure 1.1. Pathway of methanogenesis from H_2 and CO_2 in *Mtb. thermoautotrophicus* ΔH and other hydrogenotrophic methanoarchaea (Deppenmeier *et al.* 1996, Shima *et al.* 2002).

The genes encoding the tungsten-dependent enzyme are transcribed when tungsten or molybdenum is present in the growth medium, whereas the molybdenum-dependent enzyme is only transcribed when molybdate is present (Hochheimer *et al.* 1996). The tungsten-containing isoform is comprised of four subunits (FwdABCD), while the molybdenum variant is a three subunit enzyme (FmdABC) (Hochheimer *et al.* 1995). Interestingly, the FmdA subunit is apparently identical to the FwdA subunit, and it has been proposed that the A-subunit for both variants is encoded by the same gene, in the *fwd* operon encoding the tungsten-dependent enzyme (Hochheimer *et al.* 1996).

Originally dubbed CDR (carbon dioxide reduction factor), methanofuran (Figure 1.2) was renamed for the uncommon presence of a furan ring (Leigh and Wolfe 1983, Leigh *et al.* 1984).

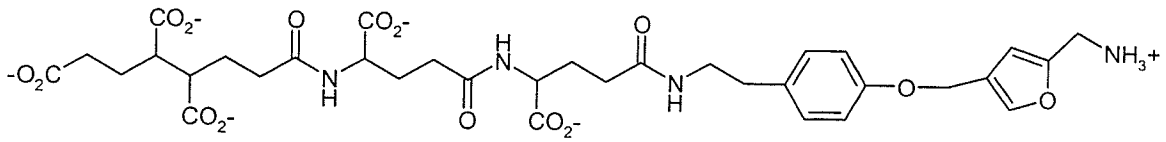

Figure 1.2. Structure of methanofuran

The requirement for methanofuran during methanogenesis on CO_2 was initially reported by Romesser and Wolfe (1982), and established by Leigh *et al.* (1985) as a formyl-carrier. The fixation of CO_2 to methanofuran (Figure 1.3) is an endergonic reaction ($\Delta G^{\circ\prime} = +16$ kj/mol) that requires reducing equivalents produced by the membrane-bound Ech hydrogenase, with an energy conserving sodium gradient (2-4 Na^+) driving the reaction (Kaesler and Schönheit 1989a, 1989b, de Poorter *et al.* 2006). The reducing equivalents are in the form of reduced ferredoxin ($FD\text{-}H_2$) generated *via* an

H_2-oxidizing Ech hydrogenase that is driven by consumption of a Na^+ gradient ($-\Delta\mu Na^+$) (Figure 1.1) (Deppenmeier 2002, Meuer *et al.* 2002, Hedderich 2004).

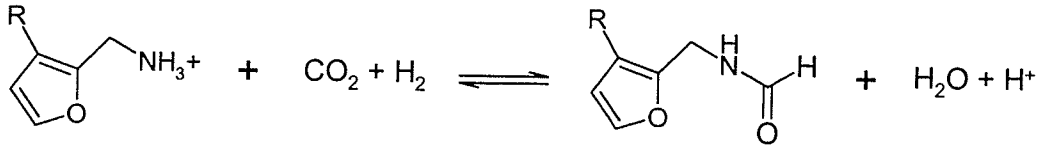

Figure 1.3. Reduction of CO_2 to formyl-methanofuran

The formyl group is then transferred to tetrahydromethanopterin (H_4MPT) to form N^5-formyl- H_4MPT *via* **formylmethanofuran: H_4MPT formyltransferase** (Figure 1.4) ($\Delta G°'$=-4.4 kJ/mol) (Brietung and Thauer 1990, Thauer *et al.* 1993).

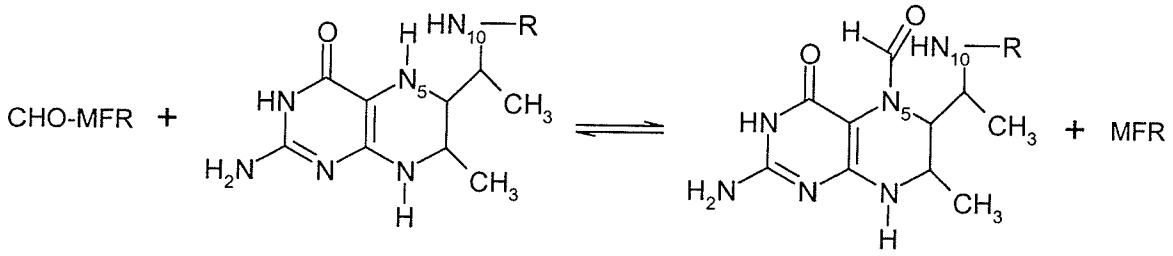

Figure 1.4. Formation of N^5-formyl- H_4MPT from formyl-MFR and H_4MPT

Formylmethanofuran: H_4MPT formyltransferase has been purified from *Mtb. thermoautotrophicus*, *Ms. barkeri*, *Methanopyrus* (*M.*) *kandleri*, as well as the sulfate-reducing archaeon *A. fulgidus*. It is a monomer or tetramer of a polypeptide of apparent molecular mass 32-41 kDa (Thauer *et al.* 1993). H_4MPT (Figure 1.5), which was discovered from deproteinated extracts of *Mtb. thermoautotrophicus*, acts as a C_1 carrier at various oxidation states, existing in a derivatized form with a bound formyl, methenyl, methylene, or methyl group linked at either or both N^5 or N^{10} positions of the pterin group (Keltjens *et al.* 1983, Escalante-Semerena *et al.* 1984a, 1984b).

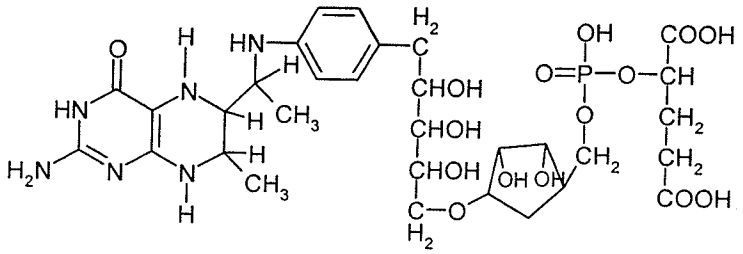

Figure 1.5. Structure of tetrahydromethanopterin (H_4MPT)

H_4MPT resembles tetrahydrofolate (H_4F), a C_1 carrier in humans and bacteria although the two compounds are not functionally equivalent (Edward and Maden 2000). H_4MPT and H_4F both consist of a pterin ring linked to an arylamine with the C_1 moiety binding at N^5 and N^{10}. H_4F contains glutamate residue(s) linked to the benzene ring, while H_4MPT consists of a ribitol residue linked to ribose-5-phosphate, followed by hydroxyglutarate (Edward and Maden 2000). H_4MPT is also a carbon carrier in the biosynthesis of cell carbon, providing units for amino acids and purines (DiMarco 1990). Methanoarchaea of the order *Methanosarcinales* contain tetrahydrosarcinopterin (H_4SPT), which possesses an additional glutamate residue attached to the hydroxyglutarate *via* an amide linkage to the α-carboxylic acid group (van Beelen *et al.* 1984).

The next three reactions cover the reduction of N^5-formyl- H_4MPT to N^5-methyl-H_4MPT. **N^5,N^{10}-methenyl-H_4MPT cyclohydrolase** catalyzes the conversion of N^5-formyl- H_4MPT to N^5,N^{10}-methenyl-H_4MPT ($\Delta G°'$=-4.6 kJ/mol) (Figure 1.6) (Thauer *et al.*1993). The respective enzymes from *Mtb. thermoautotrophicus*, *M. kandleri*, and *Ms. barkeri* contain two identical subunits of 37-41 kDa with no identifiable prosthetic groups (Ferry 1999).

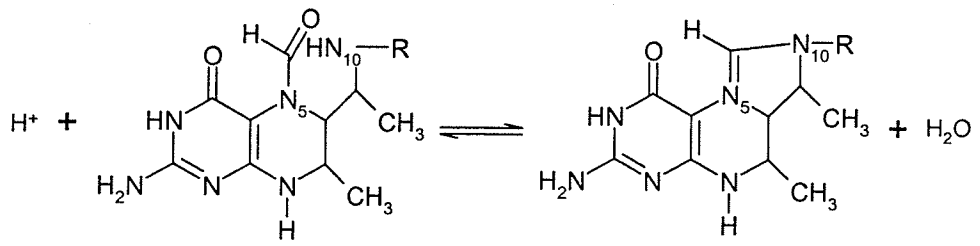

Figure 1.6. Conversion of N^5-formyl- H_4MPT to N^5,N^{10}-methenyl-H_4MPT

N^5,N^{10}-methylene- H_4MPT dehydrogenase catalyzes the reversible reduction of N^5,N^{10}-methenyl-H_4MPT to N^5,N^{10}-methylene- H_4MPT, using reducing equivalents provided by reduced coenzyme F_{420} ($F_{420}H_2$) ($\Delta G°'$=-5.5 kJ/mol) (Figure 1.7) or H_2 (von Bünau *et al.* 1991, Thauer *et al.* 1993). Coenzyme F_{420} (8-hydroxy-5-deazaflavin) is the major electron carrier found in all methanoarchaea, although the amount varies in each methanoarchaeon. It is an obligate hydride donor/acceptor that is essential during methanogenesis in the hydrogenotrophic as well as methylotrophic pathways, and also for biosynthetic reactions. During growth on H_2:CO_2, $F_{420}H_2$ is regenerated by the F_{420}-reducing hydrogenase (Thauer *et al.* 1993).

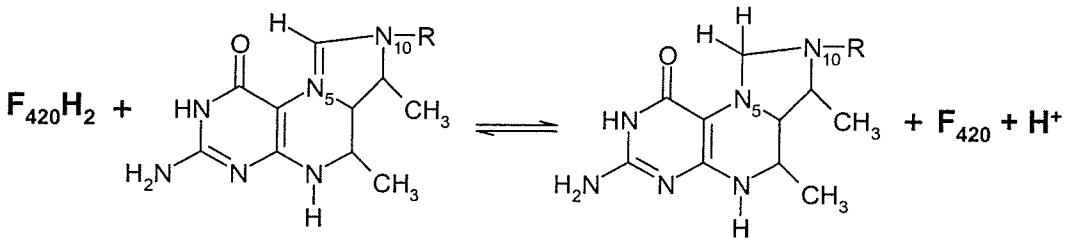

Figure 1.7. Reduction of N^5,N^{10}-methenyl-H_4MPT, with electrons from reduced coenzyme F_{420}, to N^5,N^{10}-methylene- H_4MPT

The F_{420}-dependent enzyme has been purified from *Ms. barkeri*, *Mtb. thermoautrophicus*, and *M. kandleri* (Mukhopadhyay and Daniels 1988, te Brommelstroet *et al.* 1991a, te Brommelstroet *et al.* 1991b, Klein *et al.* 1993). The enzyme is found as either a hexamer or an octamer, consisting of identical subunits (30-36 kDa) (Ferry 1999).

The H_2-dependent variant has been described for *Mtb. marburgensis*, *M. kandleri*, and *Mc. thermolithotrophicus* (Zirngibl *et al.* 1990, Ma *et al.* 1991, Hartmann *et al.* 1996). The native enzyme consists of only one type of subunit, and is the only known hydrogenase that does not contain iron sulfur (FeS) clusters (Zirngibl *et al.* 1992, Albracht 1994). The presence of a tightly bound cofactor containing Fe was recently reported for this enzyme (Buurman *et al.* 2000, Lyon *et al.* 2004).

Studies with *Mtb. marburgensis* indicate that under conditions with non-limited H_2, the H_2-dependent enzyme is transcribed, whereas the F_{420}-dependent version is produced when H_2 is limited (Nölling *et al.* 1995). Under Ni-limited conditions, the H_2- and F_{420}-dependent N^5,N^{10}-methylene- H_4MPT dehydrogenases together catalyze the reduction of F_{420} with H_2, as the Ni-dependent F_{420}-reducing hydrogenase activity is essentially zero (Afting *et al.* 1998).

$F_{420}H_2$-dependent **methylene-H_4MPT reductase** catalyzes the reversible reduction of N^5,N^{10}-methylene-H_4MPT to N^5-methyl-H_4MPT ($\Delta G^{\circ\prime}$=-17.2 kJ/mol)

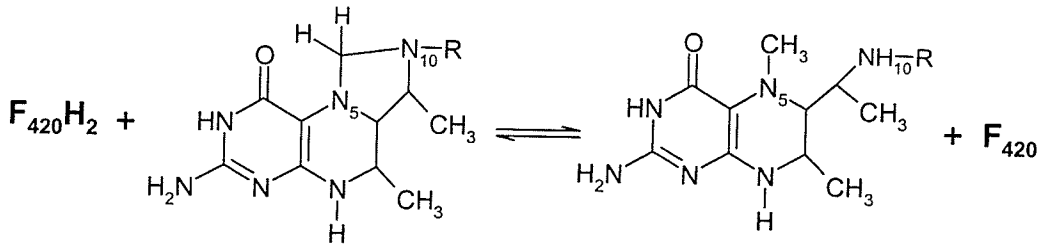

Figure 1.8. Reduction of N^5,N^{10}-methylene-H_4MPT to N^5-methyl-H_4MPT.

(Figure 1.8) (Thauer *et al.* 1993).

The reductase has been purified from *Mtb. thermoautotrophicus*, *Mtb. marburgensis* and *Ms. barkeri* (Ma and Thauer 1990, Ma and Thauer 1990b, te Brommelstroet *et al.* 1990). The enzymes contain one subunit (35-38 kDa) without a prosthetic group, and directly transfer a hydride ion from $F_{420}H_2$ to N^5,N^{10}-methylene-H_4MPT (Vaupel and Thauer 1995, Ferry 1999).

The next major step involves transfer of the methyl group from N^5-methyl-H_4MPT to coenzyme M (2-mercaptoethanesulfonic acid, CoM-SH), *via* **methyl-H_4MPT:CoM methyltransferase** ($\Delta G°'$=-29.7 kJ/mol) (Figure 1.9) (Thauer *et al.* 1993).

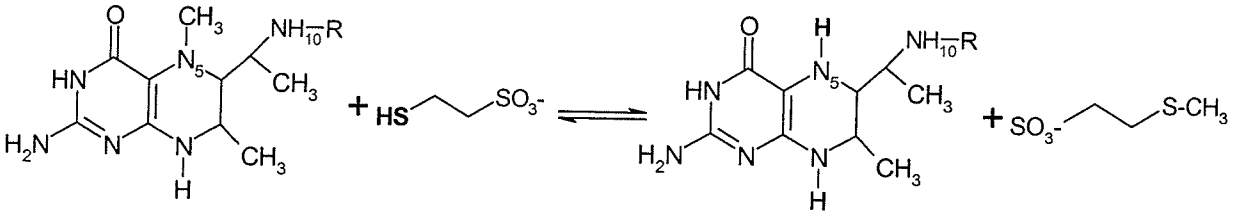

Figure 1.9. Transfer of the methyl group from H_4MPT to CoM-SH.

CoM-SH, the simplest coenzyme known (to date), functions as a methyl carrier during methanogenesis (Taylor and Wolfe 1974, DiMarco 1990). Cell extracts from *Methanobacterium* M.o.H. (*Methanobacterium bryantii*) were separated *via* dialysis by McBride and Wolfe (1971), who discovered a factor that was required for methanogenesis from CH_3-Cbl; as this factor was necessary for methyl transfer, it was named coenzyme M. Studies by Taylor and Wolfe (1974) distinguished CoM-SH as a novel coenzyme. CH_4 is produced from CH_3-S-CoM, the terminal intermediate of

methanogenesis from all substrates (McBride and Wolfe 1971). In addition, CoM-SH also acts as an electron donor for the fumarate reductase reaction in *Mtb. thermoautotrophicus* (Bobik and Wolfe 1989). Previously believed to be restricted exclusively to the methanogenic *Archaea*, CoM-SH also plays an important role in the carboxylation of epoxypropane in the Gram-negative bacterium *Xanthobacter* strain Py2, where it acts as a C_3 carrier (Balch *et al.* 1979, Allen *et al.* 1999). Several analogs of CoM have been synthesized, including 2-bromoethanesulfonic acid which acts as a methyl-CoM reductase inhibitor (Gunsalus *et al.* 1978).

Methyl-H_4MPT:CoM methyltransferase, characterized in *Mtb. marburgensis* and *Ms. mazei* Gö1, is an integral membrane-bound complex that contains a corrinoid cofactor (5'-hydroxybenzimidazolyl cobamide) (Gärtner *et al.* 1993, Becher *et al.* 1992b). Transfer of CH_3 to CoM-SH involves two steps. In the first step, the reduced corrinoid cofactor (Co(I)) accepts the methyl group from methyl-H_4MPT; in the second reaction the methyl group is transferred to CoM-SH, a step that is dependent on the presence of Na^+ (Gärtner *et al.* 1994, Weiss *et al.* 1994). The latter step results in the generation of a transmembrane electrochemical Na^+ gradient ($\Delta\mu Na^+$); studies with the purified methyl-transferase reconstituted into liposomes catalyzed an electrogenic Na^+ transport with a stoichiometric ratio of 1.7 mol Na^+ per mol methyl-H_4MPT demethylated (Schäfer *et al.* 1999). Inhibition of methyl-H_4MPT:CoM methyltransferase activity results in the inhibition of Na^+ transport, indicating that methyl-H_4MPT:CoM methyltransferase is a primary Na^+ pump (Becher *et al.* 1992a). The $\Delta\mu Na^+$ generated is used to drive the reduction of CO_2 to formyl-MF (Shima *et al.* 2002).

ATP synthases uses protonmotive force across the membrane to drive the synthesis of ATP from ADP and Pi, but some organisms also synthesize ATP using sodium-motive force (Junge *et al.* 1997). There has been some experimental evidence suggesting that the Na^+ gradient generated may be used to produce ATP in *Mc. voltae*, *Mtb. thermoautotrophicus* ΔH and *Ms. mazei* Gö1 (Dybas and Konisky 1992, Becher and Müller 1994, Šmigán *et al.* 1994), such that ATP production in methanoarchaea may be mediated by transmembrane chemiosmotic gradients of proton and/or sodium ions (Chen and Konisky 1993)

Extensive studies have been conducted on the methyl-H_4MPT:CoM methyltransferase from *Mtb. marburgensis*, which contains eight non-identical subunits (34 (MtrH), 28 (MtrE), 24 (MtrC), 23 (MtrA), 21 (MtrD), 13 (MtrG), 12.5 (MtrB), and 12 (MtrF) kDa) encoded by *mtrEDCBAFGH* (Harms *et al.*1995). The *Mtr* operon is located between the methyl-CoM reductase operon (*mcr*) and a downstream open reading frame that is predicted to encode a Na^+/K^+ exchanger (Ferry 1999). The 23 kDa subunit MtrA contains a corrinoid and is believed to be partially associated with the cytoplasmic face of the cell membrane, with the corrinoid-binding site protruding into the cytoplasm. Na^+ translocation is believed to be coupled to conformational changes in MtrA upon methylation, leading to the methyl group being released and transferred to CoM-SH, forming CH_3-S-COM (Harms *et al.* 1995). The genes encoding the eight subunits from the methyl-H_4MPT:CoM methyltransferase from *Ms. mazei* Gö1 have also been cloned and sequenced (Lienard and Gottschalk 1998).

CH_3-S-CoM is reduced to produce methane, requiring the activity of **methyl-CoM reductase** to catalyze the reduction of the methyl group with electrons from 7-

mercaptoheptanoyl-*O*-phospho-L-threonine (HTP-SH, **CoB-SH**) (Ellermann *et al.* 1987, 1988, Thauer *et al.* 1993). In the process, free methane is released and the heterodisulfide complex CoM-S-S-CoB is formed ($\Delta G^{\circ\prime}$ = -45 Kj/mol) (Figure 1.10).

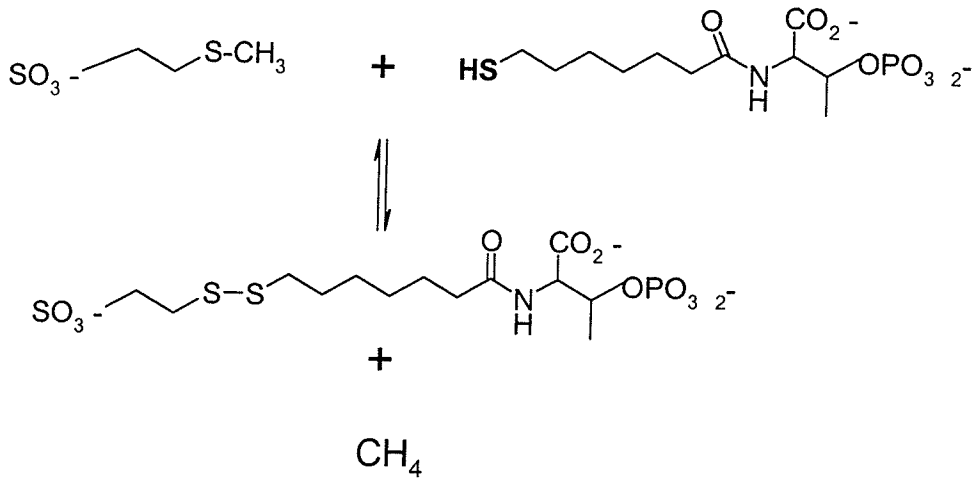

Figure 1.10. Reduction of CH_3-S-CoM with CoB-SH and formation of CH_4 and CoM-S-S-CoB

The methyl-CoM reductase has been purified from a number of methanoarchaea, but has been studied in greatest detail from *Mtb. thermoautotrophicus* and *Mtb. marburgensis* (Ferry 1999). This enzyme consists of 3 subunits, α, (65 ± 3 kDa), β (46 ±2 kDa), and γ (35 ± 5 kDa), in a $\alpha_2\beta_2\gamma_2$ arrangement (300 kDa) (Rospert *et al.* 1990). Methyl-CoM reductase contains two molecules of coenzyme F_{430}, a yellow nickel porphinoid that is tightly bound to the enzyme (Ellefson *et al.* 1982).

Two isoforms of the reductase (MCR I and MCR II) were purified from *Mtb. thermoautotrophicus* and *Mtb. marburgensis*, which differ only by a 5 kDa difference in the γ-subunit: there are also differences in the N-terminus amino acid sequences of the subunits in the respective isoforms (Rospert *et al.* 1990). MCR II is predominantly found when cells are grown in an excess of H_2 and CO_2, while MCR I is

found in greater amounts when the gas supply becomes limited (Rospert *et al.* 1990, Bonacker *et al.* 1993).

The major energy conserving step in methanogenesis has long been associated with the reductive cleavage of CoM-S-S-CoB formed during the release of methane from methyl-CoM. CoM-S-S-CoB is an important intermediate since it is a substrate for the ultimate energy conservation reaction step catalyzed by the **heterodisulfide reductase** (Hdr) (Shima *et al.* 2002). It had been speculated that the reduction of methyl-CoM with CoB-SH was the site of energy conservation ($\Delta G^{\circ\prime}$=-45 kJ/mol), but this has since been abandoned (Blaut *et al.* 1987, Thauer *et al.* 1993).

Hdr catalyzes the reductive cleavage of CoM-S-S-CoB back to the free cofactors CoM-SH and CoB-SH ($\Delta G^{\circ\prime}$=-40 kJ/mol) (Thauer *et al.* 1993). During growth on H_2/CO_2, the source of reducing equivalents is provided by H_2, *via* the F_{420}-nonreducing hydrogenase (*aka* methyl viologen (MV)-reducing hydrogenase) (Hedderich and Thauer 1988). Studies with *Mtb. thermoautotrophicus* have demonstrated that the free energy change ranges from -55 to -80 kJ/mol, depending on the dissolved hydrogen partial pressure (de Poorter *et al.* 2003). Hdr is part of a membrane-associated H_2:hetero-disulfide oxidoreductase complex that is found in most hydrogenotrophic methanoarchaea, as well as methanoarchaea capable of growth on CH_3OH or acetate (Heiden *et al.* 1993, Deppenmeier *et al.* 1991, Simianu *et al.* 1998). Electrons extracted by the F_{420}-nonreducing hydrogenase are transported to Hdr and then to CoM-S-S-CoB, restoring pools of CoM-SH and CoB-SH (Hedderich *et al.* 1990). The reduction of CoM-S-S-CoB by the H_2:hetero-disulfide oxidoreductase complex generates an energy conserving transmembrane electrochemical proton gradient ($\Delta\tilde{u}H^+$); studies with

Ms. barkeri demonstrate that the transmembrane proton gradient leads to ATP synthesis from ADP + Pi, *via* the A_1A_0 ATP synthase (Müller *et al.* 1999, Deppenmeier 2002).

Hdr from *Mtb. marburgensis* was isolated as part of a complex consisting of six subunits: 80, 51, 41, 36, 21, and 17 kDa: the 80, 36, and 21 kDa subunits comprise Hdr, while the 51, 41, and 17 kDa subunits form an F_{420}-nonreducing hydrogenase (Mvh) (Hedderich *et al.* 1990, Setzke *et al.* 1994). The H_2:heterodisulfide oxidoreductase complex was found to be loosely bound to the cell membrane, and the bulk of the activity was isolated from the soluble fraction (Hedderich *et al.* 1994, Setzke *et al.* 1994, Deppenmeier 2004). Hedderich *et al.* (1994) described the *Hdr* operon, which contains 3 genes; *HdrA*, *HdrB*, and *HdrC* encode the 72.2, 33.5, and 21.8 kDa subunits, respectively. HdrA contains a flavin binding site, while the HdrC subunit contains FeS clusters (Hedderich *et al.* 1994, Stojanowic *et al.* 2003). HdrB, which contains the active site for CoM-S-S-CoB reduction, is believed to be the membrane anchor for the complex, although transmembrane helices typically observed in integral membrane proteins are not part of the secondary structure of HdrB (Fricke *et al.* 2006).

The H_2:heterodisulfide oxidoreductase complex of *Ms. barkeri* also consists of an F_{420}-nonreducing hydrogenase and Hdr; unlike the complex isolated from *Mtb. thermoautotrophicus*, the H_2:heterodisulfide oxidoreductase complex of *Ms. barkeri* was found to be tightly associated to the cell membrane (Heiden *et al.* 1993). This multienzyme complex includes the electron carrier cytochrome *b*, which wasn't found in the *Mtb. thermoautotrophicus* complex (Heiden *et al.* 1993). Hdr from *Ms.barkeri* is a heterodimer consisting of 46 and 23 kDa subunits; the 23 kDa subunit contains cytochrome *B*, and the 46 kDa subunit was predicted to be the active site for CoM-S-S-

CoB reduction (Heiden *et al.* 1994). Künkel *et al.* (1997) reported the discovery of the *MbHdrDE* operon encoding the Hdr in *Ms. barkeri*, where *MbHdrD* encodes the 46 kDa subunit, and *MbHdrE* encodes the 23 kDa cytochrome subunit. MbHdrD was found to be equivalent to the MtHdrBC subunits, indicating that the flavin component isolated from *Mtb. thermautotrophicus* is not essential for CoM-S-S-CoB reduction (Künkel *et al.* 1997).

Studies with *Ms. mazei* Gö1 indicate that methanophenazine may be an intermediate between the F_{420}-nonreducing hydrogenase and Hdr; this scenario is not observed in methanoarchaea outside of the *Methanosarcinaceae* (Abken *et al.* 1998, Ide *et al.* 1999).

1.3.2. The methylotrophic pathway

Approximately 26% of methanoarchaea are capable of using the methylotrophic pathway (Garcia 1998). In marine, hypersaline, and other high sulfate environments, methylotrophic metabolism predominates over H_2 and acetate utilization, since sulfate-reducers are able to utilize H_2 more readily (Ollivier *et al.* 1994). Methyl amines are formed through the degradation of osmoregulatory amines, such as choline, creatine, and betaine, or the bacterial reduction of trimethyl oxide, a common metabolite and excretory product of marine animals (Neil *et al.* 1978, Hippe *et al.* 1979, Strøm *et al.* 1979, Oremland *et al.*1982). CH_3OH is a substrate used by methylotrophic methanoarchaea, though it is not a major precursor for CH_4 in anaerobic environments; CH_3OH is produced *via* bacterial degradation of lignin and pectin (Donnelly *et al.* 1980, Oremland *et al.*1982).

Methanogenesis with CH_3OH occurs *via* the following pathways:

$$4CH_3OH \rightarrow 3CH_4 + CO_2 + 2\ H_2O,\ \Delta G°'=-105\ kJ/mol\ CH_4$$

(CH_3OH disproportionation)

or

$$CH_3OH + H_2 \rightarrow CH_4 + H_2O,\ \Delta G°'=-113\ kJ/mol$$

(reduction of CH_3OH with H_2)

Methylamines are also metabolized in a similar manner to CH_3OH disproportionation (Hippe *et al.* 1979, Keltjens and Vogels 1993):

$$4CH_3NH_3Cl + 2H_2O \rightarrow 3CH_4 + CO_2 + 4NH_4Cl,\ \Delta G°'=-76.7\ kJ/mol$$

$$2(CH_3)_2NH_2Cl + 2H_2O \rightarrow 3CH_4 + CO_2 + 2NH_4Cl,\ \Delta G°'=-74.8\ kJ/mol$$

$$4(CH_3)_3NHCl + 6H_2O \rightarrow 9CH_4 + 3CO_2 + 4NH_4Cl,\ \Delta G°'=-75.8\ kJ/mol$$

CH_3OH is transformed into methane in a series of oxidation/reduction reactions by which the initial steps differ from the metabolism of CO_2 and H_2 (Zeikus *et al.* 1985). The process of CH_3OH disproportionation can be subdivided into two separate parts, one oxidizing and one reducing. In the oxidizing part of the pathway, one mole of CH_3OH is oxidized to CO_2 in order to provide reducing equivalents that are used in the reducing part of the methylotrophic pathway to reduce the remaining 3 moles of CH_3OH to methane. An overview of CH_3OH disproportionation is given in Figure 1.11.

Throughout the CH_3OH oxidation process, the enzymes of the hydrogenotrophic pathway are used, but in the reverse direction. The metabolism of CH_3OH is initiated

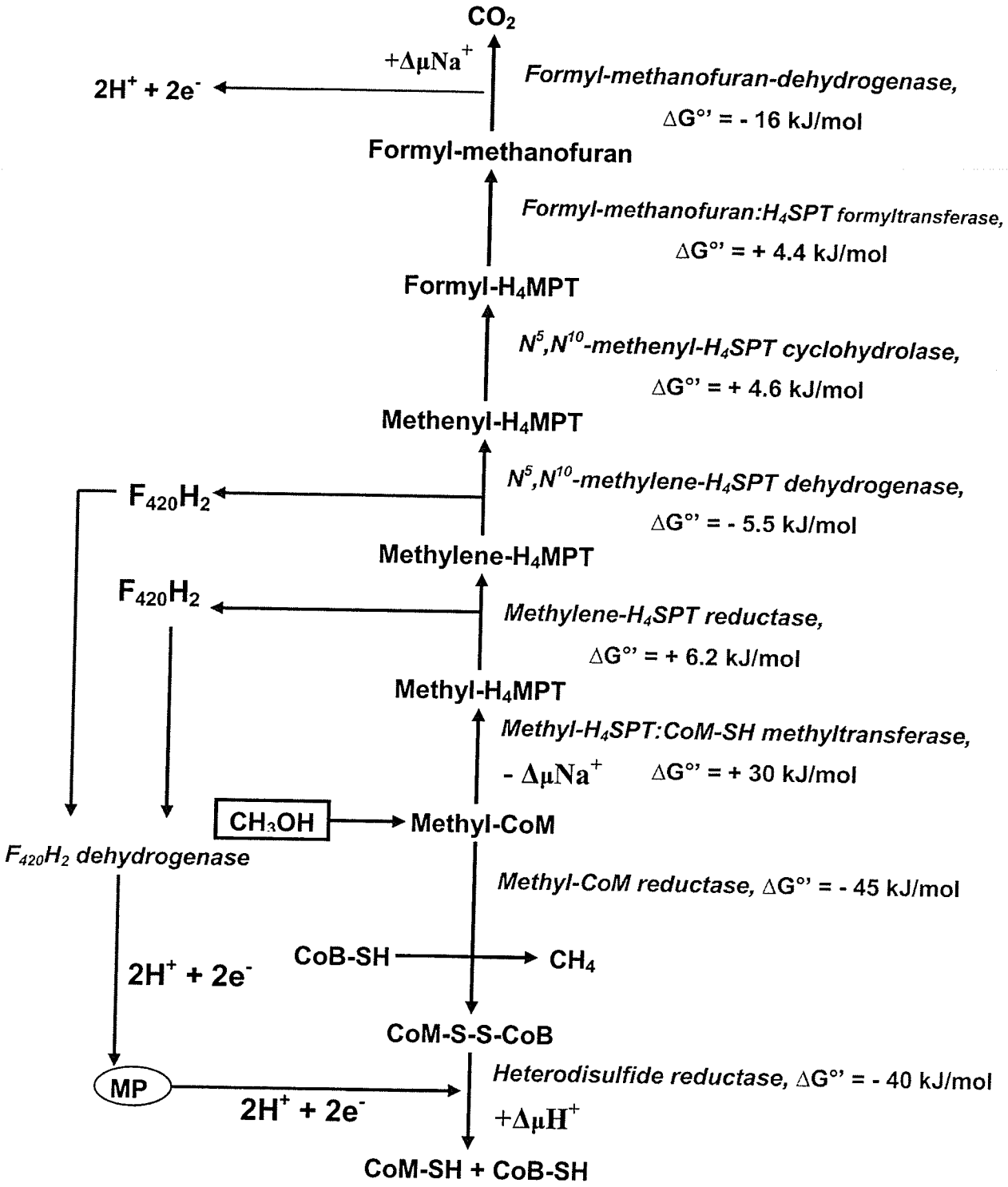

Figure 1.11. Expected pathway of methanogenesis in *Methanosarcina* spp. growing on methanol (Keltjens and Vogels 1993, Deppemeier *et al.*1996, Deppenmeier 2004).

by two methyl transferases, as described below (van der Meijden *et al.* 1983, Zeikus *et al.* 1985).

The **methanol :coenzyme M methyltransferase** system (MtaABC), comprise a two enzyme system, MT1 (MtaBC) and MT2 (MtaA). The first enzyme in this system is the **methanol:corrinoid methyltransferase** (MT1), which autocatalyzes the transfer of the CH_3OH methyl group to its corrinoid cofactor (Keltjens and Vogels 1993, Sauer *et al.* 1997). MT1 consists of two subunits, MtaB (49 kDa) and the corrinoid-containing MtaC (24 kDa) (Sauer *et al.* 1997). MtaB and MtaC form a tight complex, while MtaA is purified separately (Sauer and Thauer 1998).

The second enzyme, **methyl-corrinoid:CoM methyl transferase** (MT2), catalyzes the transfer of the methyl group from MT1 to coenzyme M, forming methyl-S-CoM (Keltjens and Vogels 1993, Ferry 1999). MT2 consists of only one 36 kDa subunit (MtaA) which does not contain any prosthetic groups. The methyl group of methyl-S-CoM is transferred to tetrahydrosarcinopterin (H_4SPT), a step leading either to the oxidation of the C_1-bound intermediate to CO_2 and generation of 2 molecules of $F_{420}H_2$, or reduction to methane with electrons donated by CoB-SH (Ferry 1999). Two isoforms of MT2 have been reported, MtaA and MtbA (Grahame 1989, Yeliseev *et al.* 1993). MtaA predominates when *Ms. barkeri* is grown on CH_3OH, while MtaB is produced when *Ms. barkeri* is grown on H_2/CO_2 or trimethylamine (Harms and Thauer 1996).

As in the hydrogenotrophic pathway, CH_3-CoM is reduced by the CH_3-CoM reductase using CoB-SH as electron donor. Free CH_4 is released and CoM-S-S-CoB is formed. In methylotrophic methanoarchaea such as *Ms. mazei* Gö1, a membrane-bound $F_{420}H_2$:heterodisulfide oxidoreductase complex, consisting of the enzymes $F_{420}H_2$

dehydrogenase (Fpo complex) and Hdr, catalyzes the $F_{420}H_2$-dependent reduction of CoM-S-S-CoB to regenerate CoM-SH and CoB-SH (Deppenmeier 2002, 2004). $F_{420}H_2$ is generated *via* methyl-group oxidation (Deppenmeier *et al.* 1996). Methanophenazine (MP) is believed to be the intermediate linking electron transfer between the enzymes $F_{420}H_2$ dehydrogenase and Hdr (Abken *et al.* 1998, Bäumer *et al.* 1998, Deppenmeier *et al.* 1999). Reduction of methanophenazine and CoM-S-S-CoB generates $\Delta\tilde{u}H^+$ that is used to drive the synthesis of ATP (Deppenmeier 2002, 2004).

Msph. stadtmanae, *Msph. cuniculi*, and *Methanomicrococcus blatticola* can also produce methane *via* the reduction of CH_3OH with H_2 (*M. blatticola* can also reduce methyl-amines), requiring only the terminal reductive steps of the hydrogenotrophic pathway following methyl transfer to CoM-SH (Miller and Wolin 1985, Biavati *et al.* 1988, Sprenger *et al.* 2000). Unlike the CH_3OH -metabolizing methanoarchaea from the *Methanosarcinaceae*, cytochromes are not found in *Msph. stadtmanae*, *Msph. cuniculi*, or *M. blatticola* (Fricke *et al.* 2006). *M. blatticola* cannot reduce CO_2 to methyl-CoM, nor can it or produce CO_2 from CH_3OH (Sprenger *et al.* 2005); it has not been reported whether the undetected components of the pathway are present only in quantities sufficient for cellular biosynthesis.

The recently elucidated genome of *Msph. stadtmanae* indicates that all of the coding sequences for the enzymes required for CO_2 reduction to CH_3-CoM and CH_3OH oxidation to CO_2 are present, with the exception of the genes for the biosynthesis of molybdopterin, an essential component of the formyl-methanofuran dehydrogenase (Fricke *et al.* 2006); indeed, Lin and Sparling (1995, 1998) showed the *Msph. stadtmanae* were able to produce limited amounts of methane using H_2 and serine, which indicates a

requirement for H_4MPT and methylene-H_4MPT reductase. Low activities of the CO_2 reduction/ CH_3OH oxidation enzymes have been detected in cell extracts, consistent with a requirement of this pathway for biosynthesis (Schwörer and Thauer 1991, van de Wijngaard *et al.* 1991, Fricke *et al.* 2006).

1.3.3. The aceticlastic pathway

Under natural physiological conditions, acetate is the most important methanogenic substrate as it is the ultimate endproduct of many fermentative pathways (Gottschalk 1979, Zinder 1993). Only about 11% of the methanoarchaea are capable of metabolizing acetate, but this substrate, produced by homoacetogenic microorganisms, accounts for the majority (~ two/thirds) of the methane produced under natural and man-made conditions (Jetten *et al.* 1992, Ferry 1993, Garcia 1998). During aceticlastic growth, acetate is both a carbon and electron source for methanogenesis. The methyl group is reduced to methane, while the electrons generated from the oxidation of the CO moiety are used for the reduction of CoM-S-S-CoB.

The breakdown of acetate by aceticlastic methanoarchaea is essential in the maintenance of pH homeostasis in anaerobic environments, preventing the acidification of the environment (Jetten *et al.*1992, Zinder 1993). The fermentation of acetate to methane by *Methanosarcina* spp. proceeds *via* the following pathway (Figure 1.12), and is coupled to the smallest change of free energy of all methanogenic substrates (Schäfer *et al.* 1999):

$$CH_3COO^- + H^+ \rightarrow CH_4 + CO_2,\ \Delta G^{\circ\prime} = -36\ kJ/mol\ CH_4$$

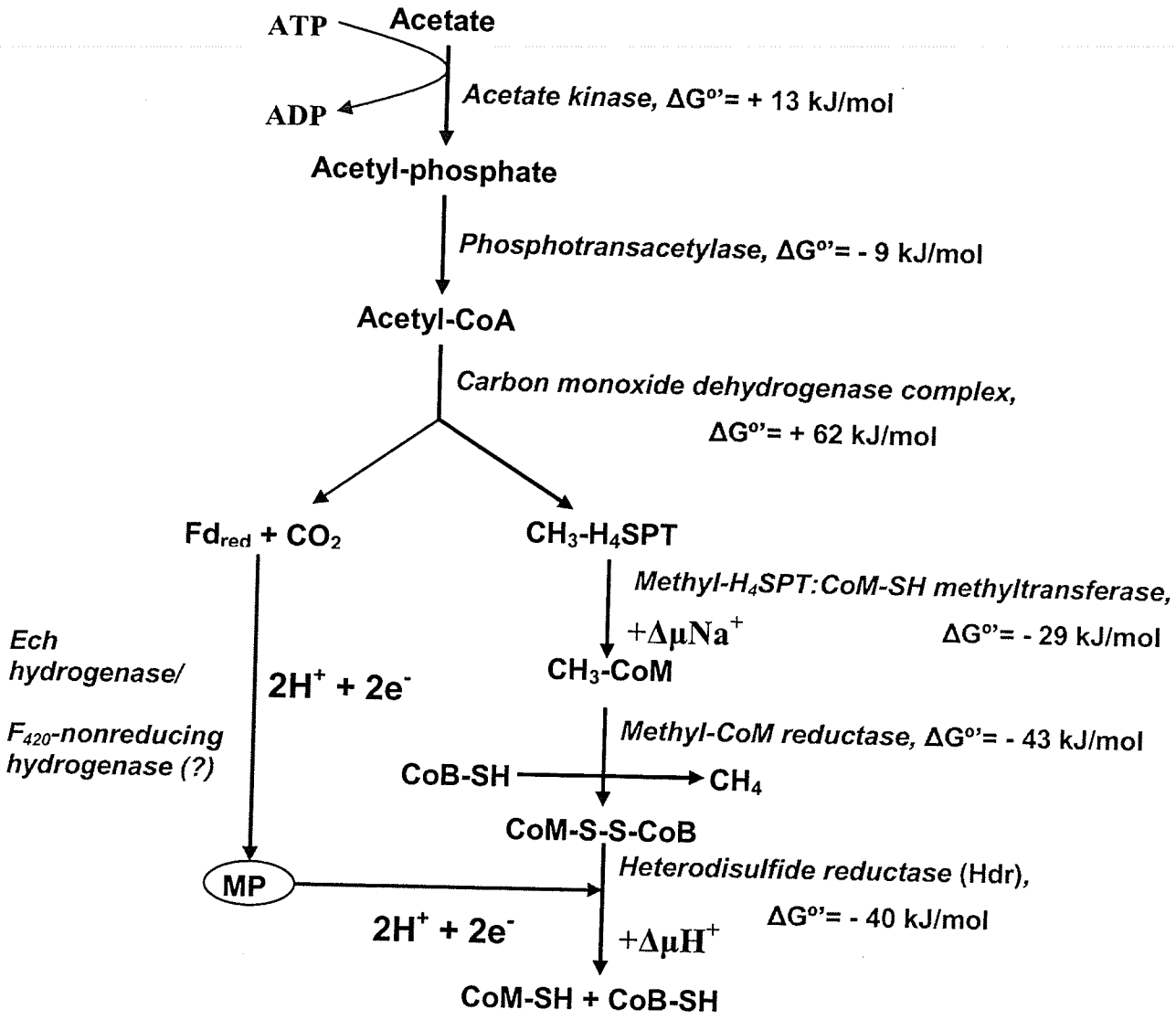

Figure 1.12. Pathway of methanogenesis from acetate for members of the *Methanosarcinaceae* (Ferry 1993, Deppenmeier *et al.* 1996, Deppenmeier 2004).

Approximately 60-70% of the methane produced in nature results from the aceticlastic pathway by *Methanosarcina* and *Methanosaeta* spp. (formerly known as *Methanothrix*) (Patel 1984). *Methanosarcina* spp. have a higher growth rate relative to *Methanosaeta*, but *Methanosaeta* spp. have a higher affinity for acetate and can be found in environments with lower concentrations of acetate (Jetten *et al.* 1992).

Methanogenesis from acetate by *Ms. barkeri* begins with its activation to acetyl-CoA *via* **acetate kinase** and **phosphotransacetylase** prior to cleavage by the CO dehydrogenase/acetyl-CoA synthase complex (Ferry 1993, Ferry 1999):

$$CH_3COO^- + ATP + CoA \rightarrow CH_3CO\text{-}S\text{-}CoA + ADP + Pi\ ,\ \Delta G^{\circ\prime} = +4.0\ kJ/mol$$

In *Methanosaeta* species, **acetate thiokinase** (*aka* acetyl-CoA synthetase) performs a similar step (Teh and Zinder 1992, Kemner and Zeikus 1994):

$$CH_3COO^- + CoA + ATP \rightarrow CH_3CO\text{-}S\text{-}CoA + AMP + PPi\ ,\ \Delta G^{\circ\prime} = -6.0\ kJ/mol$$

The central enzyme in the pathway of methanogenesis from acetate is **carbon monoxide dehydrogenase** (CODH) (Ferry 1993, Ferry 1999). CODH is actually part of a dual function system that also includes the **acetyl-CoA synthase** (ACS), forming the CODH/ACS complex. The primary function of this complex is the formation or cleavage of the C-C and C-S bonds of acetyl-CoA, but is commonly referred to as CODH because the enzyme complex also oxidizes CO to CO_2 (Ferry 1993). Acetyl-CoA is cleaved into methyl- and carbonyl- groups *via* CODH.

There have been extensive studies of the CODH/ACS complex from *Ms. thermophila* (Simianu *et al.* 1998). The subunits of the CODH/ACS complex are encoded by the *cdh* operon, transcription of which is regulated in response to the growth substrate (Simianu *et al.* 1998). The complex consists of five subunits (α (CdhA), β

(CdhC), γ (CdhE), δ (CdhD), ε (CdhB)) resolved into two enzyme components (Ferry 1999). This includes a 200 kDa CO-oxidizing Ni/Fe-S component containing the α- and ε-subunits, and a 100 kDa corrinoid/iron-sulfur component containing the δ-and γ-subunits (Ferry 1999). The β-subunit is unstable and has not yet been characterized (Ferry 1999). There are three metal clusters, A, B, and C, found within the nickel/iron-sulfur (Ni/Fe-S) component: Cluster A is believed to be responsible for cleavage of acetyl-CoA, while cluster C is the proposed site for the oxidation of CO, with electrons transferred to and from cluster C *via* cluster B (Ferry 1999). Likewise, the CODH/ACS complex of *Ms. barkeri* also consists of a five subunit complex with biochemical properties that are identical to that of *Ms. thermophila*. The CODH/ACS complex from *Methanosaeta soehngenii* and *Methanosarcina frisia* have similar properties as *Ms. thermophila*, but lack cluster A (Ferry 1999).

A mechanism for acetyl-CoA cleavage has been proposed by Ferry (1999). In this scheme, acetyl-CoA binds to the CdhC subunit, where the C-S bond is cleaved, followed by transfer of the acetyl-group to the nickel atom of cluster A in CdhA. C-C bond cleavage then occurs at cluster A and the methyl group is then transferred to the CdhE subunit. Finally, the CO-group is released to cluster C of CdhA where it is oxidized to CO_2.

Following cleavage of acetyl-CoA by the CODH/ACS complex, the carbonyl group is oxidized by CODH to produce CO_2 and reducing equivalents, which are transferred to CoM-S-S-CoB *via* the electron carrier ferredoxin (Fd). Coenzyme F_{420} is not an electron carrier for CODH, but may be involved during the oxidation of the methyl group of acetate to CO_2 to provide electrons for reductive biosynthesis (Ferry 1999).

Meanwhile, the methyl group is transferred to H_4SPT, and then to CoM-SH, generating energy conserving $\Delta\mu Na^+$ (Ferry 1993, 1999). The final steps are similar to those described for the hydrogenotrophic and methylotrophic pathways, specifically the production of methane, formation of CoM-S-S-CoB and regeneration of CoM-SH and CoB-SH. As with the other pathways, reduction of CoM-S-S-CoB leads to the generation of an energy conserving $\Delta\mu H^+$.

The CO:heterodisulfide oxidoreductase system, studied in *Methanosarcina* spp., executes the reduction of CoM-S-S-CoB *via* reduced ferredoxin (Fd_{red}), and a membrane-bound Fd_{red} oxidizing complex, including methanophenazine, that transfers the electrons to Hdr (Deppenmeier *et al.* 1996, Schäfer *et al.* 1999, Deppenmeier 2004). The Ech hydrogenase produces H_2 from Fd_{red}, while the F_{420}-nonreducing hydrogenase and Hdr catalyze CoM-S-S-CoB reduction; it has also been suggested that the Ech alone might catalyze the oxidation of Fd_{red} and transfer of electrons to Hdr without the F_{420}-nonreducing hydrogenase (Kemner and Zeikus 1994b, Deppenmeier 2002). Methanophenazine (MP) is expected to be the electronic link between the hydrogenase(s) and the Hdr (Deppenmeier 2002, 2004). This scenario is unlikely in *Methanosaeta concilii*, which contains low levels of hydrogenase activities (Sowers *et al.* 1984, Patel 1984, Deppenmeier *et al.* 1996).

Methanosarcina acetivorans lacks the Ech hydrogenase, but instead contains a multisubunit membrane bound protein complex, the ***Ms. acetivorans* Rhodobacter nitrogen fixation** complex (Ma-Rnf) (Li *et al.* 2006). Ma-Rnf is believed to be an electron transferring complex, interacting with reduced ferredoxin and transferring the electrons to methanophenazine. As is the case for other RNF proteins, this complex is

also hypothesized as being an ion pump, translocating either protons or sodium ions through the membrane (Li *et al.* 2006).

Under physiological conditions, where the environmental concentrations of acetate are low (0.5-5 mM), the catabolic reactions yield very small amounts of energy, often not enough to form 1 ATP from ADP; the process itself also requires an investment of 1 ATP to activate acetate prior to degradation (Jetten *et al.* 1992). Additional means to generate energy must be present in aceticlastic methanoarchaea.

One prospect is the energy conserved *via* cleavage of the pyrophosphate (PPi) bond. PPi is formed by *Methanosaeta* spp. when ATP is hydrolysed to AMP and PPi, during activation of acetate to acetyl-CoA (Kohler and Zehnder 1984), and also during various biosynthetic processes, including DNA/RNA synthesis, amino acid activation, polysaccharide synthesis, and fatty acyl-CoA formation (Maeshima 2000). Jetten *et al.* (1992) reported the presence of membrane-bound pyrophosphatase in *Methanosaeta* similar to proton translocating pyrophosphatases found in plant vacuoles and phototrophic bacteria, possibly linking the hydrolysis of PPi to energy conservation.

Bäumer *et al.* (2002) reported the presence of genes encoding two separate proton-translocating pyrophosphatases in *Ms. mazei* Gö1. Using inverted membrane vesicles from CH_3OH -grown cells, it was shown that hydrolysis of 1 mol of PPi was coupled to translocation of 1 mol of protons across the membrane.

1.4. Elements of electron transport in the methanoarchaea – Electron carriers

A number of electron carriers are present in methanoarchaea, ranging from cytochromes and methanophenazine, which are found exclusively in members of the

Methanosarcinaceae (Garcia *et al.* 2000), to electron carriers such as coenzyme F_{420} or $NADP^+$ which are found in all methanoarchaea (Schäefer *et a*l. 1999). In the following sections, the electron carriers Coenzyme F_{420}, cytochrome, ferredoxin, and methanophenazine will be discussed.

1.4.1. Coenzyme F_{420}

8-hydroxy-5-deazaflavin (coenzyme F_{420}, Figure 1.13) was originally isolated from methanoarchaea, but similar compounds have also been found in sulfate-reducing *Archaea*, halophilic *Archaea*, various *Streptomyces* species, *Mycobacterium tuberculosis*, *Nocardia aurantia*, and some eukaryotes (Daniels *et al.* 1984, Lin and White 1986, Shima *et al.* 2002).

F_{420} was first isolated from *Methanobacterium* strain MoH by Cheeseman *et al.* (1972), and later identified as the N-(N-L-lactyl-γ-L-glutamyl)-L-glutamic acid phosphodiester of 7,6-didemethyl-8-hydroxy-5-deazariboflavin 5'phosphate by Eirich *et al.* (1978), who characterized coenzyme F_{420} as an intensely yellow-blue-green fluorescent compound present in all of the methanoarchaea tested (Lin and White 1986, White and Zhou 1993). While not exclusive to the methanoarchaea, F_{420} acts as an important indicator as a molecular marker for the preliminary screening and identification of the presence of methanoarchaea because of its (generally) high cellular abundance (up to 100 mg F_{420}/kg of cells) and its intense fluorescence (Eirich *et al.* 1979, Fox *et al.* 1987, Peck and Archer 1989, Zhou and White 1993). The reduced form does not exhibit fluorescence (DiMarco 1990). Heine-Dobbernack *et al.* (1988) demonstrated that F_{420}

could be used as a parameter to estimate the biomass of methanoarchaea, using *Mb. bryantii* and *Ms. barkeri* as test subjects.

F_{420} is the major redox carrier in methanoarchaea (DiMarco 1990). F_{420} is functionally equivalent to NAD; it is an obligate hydride (H^-) acceptor/donor and its redox potential is ~ -350 mV (-320 mV for NAD) (Jacobson and Walsh 1984).

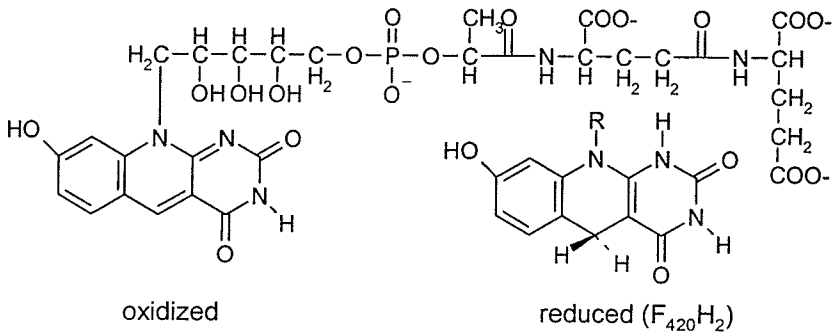

Figure 1.13. Oxidized and reduced forms of coenzyme F_{420}

Coenzyme F_{420} also acts as a sensor for the presence of O_2. Spectral analysis by Schönheit *et al.* (1981) observed that the majority of F_{420} (>70%) was lost after a culture of *Mtb. thermoautotrophicus* was exposed to air for 50 minutes. F_{420} is converted to factor 390 (F_{390}) upon exposure to oxygen: AMP or GMP couples to the 8-OH group of the deazaflavin to form derivatives which show an absorbance maximum at 390 nm (Kiener *et al.* 1988, van de Wijngaard and van der Drift 1991). Studies by Gloss and Hausinger (1988) indicated that O_2 was the only trigger for F_{390} formation, and that the addition of heavy metals or methanogenesis inhibitors did not lead to F_{390} synthesis. Accumulation of F_{390} leads to a stoppage of cell metabolic activities, since the active substrate F_{420} would not be accessible as substrate for the various methanogenic enzymes (Hausinger *et al.* 1985). Once anaerobic conditions are restored, F_{390} is then converted

back to F_{420} by the F_{390} hydrolase (Vermeij *et al.* 1985, Gloss and Hausinger 1988, Kengen *et al.* 1991).

In methylotrophic methanoarchaea, reduced F_{420} ($F_{420}H_2$) plays a significant role in the $F_{420}H_2$:heterodisulfide oxidoreductase system, using the reversed CO_2 reduction pathway to oxidize one mol of CH_3OH (or methylamine) to provide $F_{420}H_2$ for the reduction of CH_3OH /methylamine to methane (Keltjens and Vogels 1993, Deppemeier *et al.* 1996). In hydrogenotrophic methanoarchaea, methanogenesis from CO_2 and H_2 involves two $F_{420}H_2$-dependent reduction reactions: N^5,N^{10}-methenyl-H_4MPT to N^5,N^{10}methylene-H_4MPT, and N^5,N10-methylene-H_4MPT to N^5-methyl-H_4MPT (Shima *et al.* 2002). Hydrogenotrophic methanoarchaea reduce coenzyme F_{420} *via* the H_2-dependent F_{420}-reducing hydrogenase (Thauer *et al.* 1993). Under Ni^+-limiting conditions some methanoarchaea may use the tandem activities of the $F_{420}H_2$- and H_2-dependent N^5,N^{10}-methylene- H_4MPT dehydrogenases to produce $F_{420}H_2$, when the F_{420}-reducing hydrogenase is inoperative (Ferry 1999).

Coenzyme F_{420} is also used to generate NADPH for reductive biosynthetic metabolism *via* the $F_{420}H_2$:NADPH oxidoreductase (Tzeng *et al.* 1975, Kell *et al.* 1980, Yamazaki *et al.* 1980, Elias *et al.* 2000). F_{420} appears to be essential for photorepair (reduction of thymine dimers) of UV-damaged DNA in *Mtb. thermoautotrophicus* (Kiener *et al.* 1985). $F_{420}H_2$ is also used to detoxify O_2 by way of the recently reported $F_{420}H_2$ oxidase from *Methanobrevibacter arboriphilus*, which catalyzes the oxidation of two $F_{420}H_2$ with one O_2, to two F_{420} and two H_2O (Seedorf *et al.* 2004).

Methanoarchaea that use ethanol or isopropanol to reduce CO_2 to methane *via* $NADP^+$-dependent alcohol dehydrogenase also possess an F_{420}-dependent $NADP^+$

reductase that is able to oxidize NADPH + H^+ to provide electrons for the reduction of F_{420} (Berk and Thauer 1997):

$$2\ NADPH + H^+ + F_{420} \rightarrow 2\ NADP^+ + 2\ F_{420}H_2$$

NADPH-dependent F_{420}-reduction has been observed in *Methanogenium organophilum* and *Methanobacterium palustre*, both of whom possess the NADP-dependent alchohol dehydrogenase (Bleicher and Winter 1991, Berk and Thauer 1997).

F_{420} can be reduced from a number of sources (H_2, NADPH, etc), and can be used as a source of reductant to for many compounds (CoM-S-S-CoB, O_2, $NADP^+$, etc), making it a versatile, but not universal electron carrier.

1.4.2. Cytochrome

Cytochromes are proteins with iron-containing porphyrin ring (heme) prosthetic groups attached to them. A variety of cytochromes of the *b*- and *c*-type have been identified in methylotrophic members of the family *Methanosarcinaceae*: the presence of this particular electron carrier is restricted solely to members of this family (Kuhn *et al.* 1983, Kamlage and Blaut 1992, Müller *et al.* 1993, Deppenmeier *et al.* 1996). Heiden *et al.* (1993, 1994) reported that cytochrome *b* was purified as part of the H_2:heterodisulfide oxidoreductase complex of *Ms. barkeri* (cytochrome *b2*, HdrE). Cytochrome *b* was reduced by H_2 (*via* F_{420}-nonreducing hydrogenase) and oxidized by CoM-S-S-CoB *via* Hdr, although the reaction rate was too quick to be resolved (Heiden *et al.* 1993). Experiments with *Ms. mazei* Gö1, which contains two *b*-type (midpoint potentials: -135 and -240 mV) and two *c*-type (midpoint potentials: –140 and -230 mV) cytochromes,

have illustrated that cytochromes are reduced by $F_{420}H_2$ and also oxidized by CoM-S-S-CoB rapidly (Kamlage and Blaut 1992, Schäfer *et al.* 1999).

The two operons encoding F_{420}-nonreducing hydrogenase (*vhoGAC/vhtGAC*) also contain genes encoding b-type cytochromes (*vhoC/vhtC*); expression studies have concluded that the F_{420}-nonreducing hydrogenase and cytochrome *b1* participate as part of the H_2:heterodisulfide oxidoreductase system; in contrast, the F_{420}-nonreducing hydrogenases from methanoarchaea outside of the *Methanosarcinaceae* do not encode genes encoding for cytochrome(Deppenmeier *et al.* 1996), suggesting other means for electron transport.

1.4.3. Ferredoxin

Electron-transporting iron-sulfur proteins called ferredoxins, as well as polyferredoxin (12[Fe-4S]), have been isolated from members representing all the methanogenic orders. Ferredoxins generally mediate electron transfer between enzymatic systems (Moura *et al.* 1982). Ferredoxin is required for methanogenesis when acetate is used as substrate, where reduced ferredoxin acts an electron acceptor for the Ech hydrogenase, and is used for the reduction of CoM-S-S-CoB (Deppenmeier 2002). In *Ms. barkeri* Fusaro, reduced ferredoxin (formed by the Ech hydrogenase from H_2 by sodium-motive force) is also a source of electrons for CO_2 fixation to formyl-methanofuran in the initial CO_2 reduction stage, during growth on H_2 and CO_2 (Meuer *et al.* 2002, Deppenmeier 2002).

Reeve *et al.* (1989) reported that polyferredoxin was encoded as part of the *mvh* (*mvhB*) operon of *Mtb. thermoautotrophicus* ΔH; this gene has also been conserved

Methanothermus fervidus (Steigerwald *et al.* 1990). Polyferredoxin contains low electron accepting activity, so its function as the physiological electron acceptor of the methylviologen-reducing hydrogenase is questionable (Schäfer *et al.* 1999). *mvhB* is not encoded by *Msph. stadtmanae*, suggesting that the polyferredoxin may not be essential for activity of the F_{420}-nonreducing hydrogenase (Fricke *et al.* 2006).

1.4.4. Methanophenazine

Phenazines, discovered in the late nineteenth century, are naturally occurring pigments formed by bacteria, such as the *Pseudomonas* and *Streptomyces* species, which are excreted into the medium (Ingram and Blackwood year, Turner and Messenger 1986). Many of the phenazine compounds are secondary metabolites which have antibiotic activity, and participate in redox reactions under *in vitro* conditions (Turner and Messenger 1986). Non-natural phenazines are synthesized as analogues of the natural bacterial product and tested as bactericides, fungicides, herbicides, and anti-tumour agents (Turner and Messenger 1986). There are approximately 100 different naturally occurring phenazines, of which all but one are of bacterial origin (Beifuss and Tietze 2005).

A low molecular weight redox active (-165 ± 6 mV) compound identified as methanophenazine was purified from the membranes of CH_3OH -grown *Ms. mazei* Gö1 (Figure 1.14) (Abken *et al.* 1998, Beifuss and Tietze 2005). This was the first phenazine compound to be reported from an archaeon, and the first phenazine derivative involved in electron transport of biological systems (Beifus *et al.* 2000, Deppenmeier 2002). Methanophenazine is similar in function to menaquinone, redox active pigments found in

the cell membranes of bacteria, such as *Clostridium thermoaceticum* and *Clostridium thermoautotrophicum*, as well as the sulfate-reducing archaeon *Archaeoglobus fulgidus* (Das et al. 1989, Brüggemann et al. 2000).

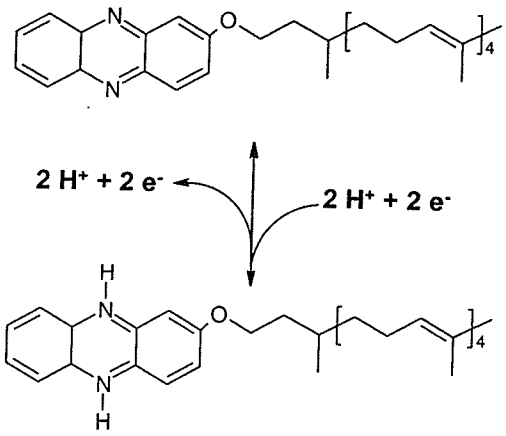

Figure 1.14. Structure and reactivity of methanophenazine (Beifuss *et al.* 2000).

This highly hydrophobic compound is expected to be the link between the $F_{420}H_2$ dehydrogenase complex and the Hdr, playing an important role in membrane-bound electron transport (Abken *et al.* 1998, Beifuss *et al.* 2000). To date, methanophenzine has not been purified from any other methanoarchaeon outside of the *Methanosarcinaceae* (Beifuss and Tietze 2005). The genes for the synthesis of this cofactor have not been identified.

Because of the extremely hydrophobic character of methanophenazine, and also because of the low yields and time consuming extraction process, the water soluble phenazine derivative 2- hydroxy-phenazine (2-OH-phenazine, -191 ± 8 mV) was chemically synthesized and used in subsequent redox experiments (Beifuss *et al.* 2000, Beifuss and Tietze 2005). 2-OH-phenazine is reduced by the $F_{420}H_2$ dehydrogenase and by the F_{420}-nonreducing hydrogenase of *Ms. mazei* Gö1 (Abken *et al.* 1998) :

$$F_{420}H_2 + \text{2-OH-Phen} \rightarrow F_{420} + \text{2-OH-Phen}H_2$$

$$H_2 + \text{2-OH-Phen} \rightarrow \text{2-OH-Phen}H_2$$

It is clear that phenazine compounds can receive and transfer electrons with some of the key enzymes in the methanogenesis pathways in various members of the *Methanosarcinaceae*. Furthermore, the reduced form, dihydro-2-OH-phenazine, acts as a source of electrons for the reductive cleavage of CoM-S-S-CoB (-177 ± 5 mV), *via* Hdr (Abken *et al.* 1998, Ide 1999, Murakami *et al.* 2001):

$$\text{2-OH-Phen}H_2 + \text{CoM-S-S-CoB} \rightarrow \text{2-OH-Phen} + \text{CoM-SH} + \text{CoB-SH}$$

Reduced phenazine has recently been used as an *in vitro* electron donor for the reduction of CoM-S-S-CoB in *M. blatticola*; phenazine was reduced by membrane-bound hydrogenase activity (Sprenger *et al.* 2005). It is not clear whether methanophenazine is present in this methanoarchaeon.

1.5. Elements of electron transport - Redox enzymes

1.5.1. Hydrogenases

Hydrogen is a key substrate for methanogenic *Archaea*, providing reducing equivalents for biosynthetic reactions as well as catabolic methane formation, with various hydrogenases being central for this metabolism (Kemner and Zeikus 1994). The existence of this enzyme was discovered by Stephenson and Strickland (1931) who observed the biological activation of H_2 in *E. coli*. Hydrogenases are found in a wide variety of microorganisms and catalyze the simplest chemical reaction in nature:

$H_2 \leftrightarrow 2H^+ + 2e^-$ (Hedderich 2004). Based on the metal groups found in the various hydrogenases, there are three classes of hydrogenases: [NiFe]-hydrogenases; [Fe]-hydrogenases; and the FeS-free hydrogenases (Vignais *et al.* 2001).

Two roles have been described for hydrogenases in the metabolism of anaerobic bacteria. Fermentative bacteria use hydrogenases to produce H_2 *via* oxidation of reduced electron carriers during fermentation, allowing the carriers to be recycled for the continuous production of ATP *via* substrate-level phosphorylation (Adams *et al.* 1981). Secondly, H_2 is also a source of electrons for the reduction of various terminal electron acceptors, such as sulfate, nitrate, CO_2, or fumarate, generating ATP *via* membrane-bound electron transport chains (Adams *et al.* 1981).

Methanoarchaea possess various hydrogenase activities that function in the reduction of C_1-moieties to methane, reduction of CoM-S-S-CoB to CoM-SH and CoB-SH, and CO_2 fixation to methanofuran. Most methanogenic hydrogenases are [NiFe] hydrogenases containing the two metals in a bimetallic reaction center involved in the H_2 cleavage reaction, with the exception being the H_2-dependent methylene-H_4MPT dehydrogenase (discussed in section 1.3.1.) (Albracht 1994, Sorgenfrei *et al.* 1997, Vignais *et al.* 2001). Hydrogenases that will be discussed in detail include: the coenzyme F_{420}-reducing hydrogenase; the coenzyme F_{420}-nonreducing (*aka* methyl viologen-reducing) hydrogenase; and the Ech hydrogenase (energy conserving hydrogenase). Each hydrogenase is specialized in its capacity to transfer electrons from H_2 to different electron carriers/acceptors in the methanogenic pathways, with some also being able to transfer from sources other than H_2.

1.5.1.1. F_{420}-reducing hydrogenase

The coenzyme F_{420}-reducing hydrogenase has been purified and characterized from a number of methanoarchaea, including *Ms. barkeri* strains MS and Fusaro, *Methanospirillum* (*Msp.*) *hungatei* GP1, *Mtb. thermoautotrophicus*, *Mtb. marburgensis*, *Mc. voltae*, *Mc. jannaschi*, *Methanococcus* (*Mc.*) *vannielii*, and *Mb. formicicum* (Yamazaki 1982, Jacobson *et al.* 1982, Fauque *et al.* 1984, Fox *et al.* 1987, Muth *et al.* 1987, Sprott *et al.* 1987, Baron et al. 1989, Fiebig and Friedrich 1989, Shah and Clark 1990, Choquet and Sprott 1991, Michel *et al.* 1995). F_{420}-reducing hydrogenase appears to be universal in all hydrogenotrophic methanoarchaea, with the apparent exceptions of *Methanosphaera cuniculi* and *Methanobacterium* strain G2R (McKellar and Sprott 1979, Biavati *et al.* 1988). This enzyme, which is reversibly inactivated by O_2, catalyzes the H_2-dependent reduction of both coenzyme F_{420} and synthetic electron acceptors such as methyl viologen. Immunogold labeling studies indicate that this enzyme is located on the inner face of the cytoplasmic membrane (Baron *et al.* 1989b, Lünsdorf *et al.* 1991, Braks *et al.* 1994). While the enzyme has hydrophobic character, the F_{420}-reducing hydrogenase is not an integral membrane protein, as the sequences encoding for the subunits do not encode the twin arginine signal sequence required for traffic of proteins into the cell membrane (Vignais *et al.* 2001).

The enzyme is composed of three different subunits, α, β, and γ, with the largest subunit (α) containing the active [NiFe]-site (Künkel *et al.* 1998, Vaupel and Thauer 1998, Vignais *et al.* 2001). The β-subunit binds FAD, which acts as a 1 e-/2 e- switch during electron transfer from $F_{420}H_2$, which donates a hydride ion, to the single-electron carrying Fe-S clusters (Thauer *et al.* 1993). The γ-subunit contains FeS clusters which

mediate the transfer of electrons between the α- and β-subunits (Thauer *et al.* 1993, Vignais *et al.* 2001).

Electrophoresis of the purified F_{420}-reducing hydrogenase from the respective methanoarchaea on non-denaturing native PAGE gels results in the separation of 2-3 distinct bands, 1-2 large molecular weight bands at 500 kDa -1300 kDa, and a lower molecular weight band of 89 kDa – 115 kDa (Sprott *et al.* 1987, Michel *et al.* 1995). Activity staining using F_{420} or methyl viologen reveals that both bands possess hydrogenase activity. The smaller band represents the minimal functional subunit (containing α, β, and γ subunits) capable of F_{420}-reduction. The large band is an aggregate containing a number of the functional subunits.

The F_{420}-reducing hydrogenase of the hydrogenotrophic methanoarchaeon *Mtb. thermoautotrophicus*, has been well studied (Jacobson *et al.* 1982, Jacobson *et al.* 1987, Livingston *et al.* 1987). This enzyme, encoded by the *frhADGB* cluster, can be assayed *via* the reduction of viologen dyes or coenzyme F_{420} with H_2 (Alex *et al.* 1990, Braks *et al.* 1994). Activity stained native PAGE gels indicate that there are two distinct protein bands with F_{420}-reducing activity, consistent with observations of the homologous protein in other methanoarchaea; a high molecular weight band of approximately 800 kDa, and a lower molecular weight band of 115 kDa (Fox *et al.*1987). Like most typical F_{420}-reducing hydrogenases, the enzyme consists of three distinct subunits; α (FrhA, 47 kDa), β (FrhB, 31 kDa), γ (FrhG, 26 kDa); (Fox *et al.*1987). A fourth subunit is also encoded by the *frh* operon, δ (FrhD, 18 kDa); this subunit, found in the homologous gene clusters in other methanoarchaea, does not copurify with the holoenzyme and is expected to encode a protease involved with hydrogenase maturation (Ficke *et al.* 2006).

Immunogold labeling studies of a related methanoarchaeon, *Mtb. marburgensis*, indicated that the majority of the F_{420}-reducing hydrogenase (90%) was associated with the membrane, bound to the cytoplasmic side with 10-20 kDa linker particles (Braks *et al.* 1994).

The properties of the F_{420}-reducing hydrogenases are fairly consistent amongst the methanoarchaea, but there are some variations between different genera, and even between strains of the same species.

Mc. voltae possesses two different isoenzymes (Fru and Frc) that differ in that an active-site cysteine is replaced with a selenocysteine (Fru)(Halboth and Klein 1992, Sorgenfrei *et al.* 1997). The genes encoding the selenium-free hydrogenase (Frc) are expressed in the absence of selenium (Sorgenfrei *et al.* 1997). Based on information derived from its genome, *Mc. jannaschii* also possesses two F_{420}-reducing isoenzymes (Künkel *et al.* 1998).

Similarly, the genome of *Ms. barkeri* Fusaro also encodes two F_{420}-reducing hydrogenases (*frhADGB* and *freAEGB*), although neither isoenzyme contains selenium (Vaupel and Thauer 1998)). Both operons are transcribed during growth on H_2 and CO_2 or CH_3OH, but not during growth on acetate. While expression of the F_{420}-reducing hydrogenase is not necessary for F_{420}-reduction during methylotrophic growth, *Ms. barkeri* Fusaro produces significant levels of the F_{420}-reducing hydrogenase, comparable to levels during growth on H_2 and CO_2 (Mukhopadhyay *et al.* 1993). The physiological significance of the F_{420}-reducing hydrogenase of *Ms. barkeri* Fusaro during methylotrophic growth is unclear.

While most of the known F_{420}-reducing hydrogenase holoenzymes consist of three separate subunits, the F_{420}-reducing hydrogenase from *Ms. barkeri* strain MS consists of one 60 kDa subunit (overall molecular mass 800 kDa): the corresponding enzyme from *Ms. barkeri* strain Fusaro consists of three subunits (kDa) (Fauque *et al.* 1984, Michel *et al.* 1995). Thus, significant variations can exist even within a species.

Immunological studies using antibodies against the purified F_{420}-reducing hydrogenase from *Msp. hungatei* GP1 only reacted against the cell extract from *Msp. hungatei* JF1 and *Ms. barkeri* strain MS: no reaction was observed against the extracts of *Methanobacterium* strain G2R, *Mc. voltae*, *Mb. formicicum*, *Ms. mazei* Gö1, two strains each of *Mtb. thermoautotrophicus* and *Mb. bryantii*, *Methanobrevibacter arboriphilus*, or *Methanosaeta concilii* (Sprott *et al.* 1987). These differences may reflect the evolutionary divergence among the methanoarchaea (Sprott *et al.* 1987).

1.5.1.2. F_{420}-nonreducing hydrogenase

The F_{420}-nonreducing hydrogenase does not interact with coenzyme F_{420}, but has been assayed using artificial electron acceptors such as methyl viologen (MV) or benzyl viologen (BV). The F_{420}-nonreducing hydrogenase is a [NiFe] hydrogenase that is also reversibly inactivated by O_2 (Thauer *et al.* 1993). This enzyme has been purified from a number of hydrogenotrophic methanoarchaea, including *Mtb. thermoautotrophicus*, *Mb. formicicum*, *Mb. fervidus*, *Mc. jannaschii*, and *Mc. voltae*, as well as from the methylotrophic methanoarchaea, *Ms. barkeri* MS and *Ms. mazei* Gö1 (Jin *et al.* 1983, Adams *et al.* 1986, Shah and Clark 1990, Hedderich *et al.* 1990, Deppenmeier *et al.* 1992, Kemner and Zeikus 1994, Deppenmeier *et al.* 1995). Interestingly, the F_{420}-

nonreducing hydrogenase apparently is not found in the hydrogenotrophic methanoarchaeon *Msp. hungatei* GP1 (Sprott *et al.* 1987). As such, the mechanism by which this methanoarchaeon reduces CoM-S-S-CoB is unresolved.

In the hydrogenotrophic methanoarchaea outside of the *Methanosarcinales*, the F_{420}-nonreducing hydrogenase has primarily been detected in the cytoplasm after cell breakage, whereas the enzyme isolated from methylotrophic methanoarchaea of the *Methanosarcinales* has been located as an integral membrane protein (Deppenmeier *et al.* 1992, Vignais *et al.* 2001).

The F_{420}-nonreducing hydrogenase of *Mtb. thermoautotrophicus* is encoded by *mvhDGAB* (Reeve *et al.* 1989). The MvhA (α) (53 kDa) and MvhG (γ) (33 kDa) subunits form the basic hydrogenase unit typical of all [NiFe] hydrogenases; MvhD (δ) (15.8 kDa) may be the contact site of the hydrogenase for the Hdr (Thauer *et al.* 1993, Vignais *et al.* 2001, Stojanowic *et al.* 2003). MvhB, a 44 kDa subunit, is predicted to be a polyferredoxin (Reeve *et al.* 1989, Steigerwald *et al.* 1990). Interestingly, MvhB is not encoded by the *mvh* operon of *Msph. stadtmanae*, indicating that the MvhB subunit isn't essential for hydrogenase activity (Fricke *et al.* 2006).

The F_{420}-nonreducing hydrogenase has been purified from the cell membranes of *Ms. barkeri* strain MS and *Ms. mazei* Gö1 (Deppenmeier *et al.* 1992, Kemner and Zeikus 1994). The enzyme from *Ms. barkeri* is composed of two subunits, 57 and 35 kDa, with an overall molecular weight estimated as 98 kDa (Kemner and Zeikus 1994). Cytochrome *b* was reduced in the presence of H_2, but ferredoxin, F_{420}, FAD/FMN, and $NAD(P)^+$ were not. The F_{420}-nonreducing hydrogenase of *Ms. mazei* Gö1 has a similar structure, with subunits of 60 and 40 kDa, and a molecular weight between 77 and 79

kDa (Deppenmeier *et al.* 1992). Two separate operons, *vhoGAC* and *vht GAC* encode two nearly identical isoforms of F_{420}-nonreducing hydrogenase (92-97% amino acid identity) (Deppenmeier *et al.* 1995). *vhoG/vhtG* and *vhoA/vhtA* encode the 40 and 60 kDa subunits, respectively, while *vhoC/vhtC* encode *b*-type cytochromes; additionally, a twin arginine signal motif (RRxFxK) is encoded at the 5'ends of the *vhoG* and *vhtG* genes from *Ms. mazei* Gö1, which explains the localization of the F_{420}-nonreducing hydrogenase to the periplasmic face of the cell membrane (Deppenmeier *et al.* 1996, Vignais *et al.* 2001). F_{420}-nonreducing hydrogenase I, encoded by *vhoGAC*, has been purified from cells grown in CH_3OH, H_2:CO_2, or acetate, whereas hydrogenase II, encoded by *vht GAC*, has only been isolated in cells grown in CH_3OH or H_2:CO_2 (Deppenmeier *et al.* 1996). As such, it was concluded that hydrogenase I is likely part of the H_2:heterodisulfide oxidoreductase system as described by Deppenmeier *et al.* (1991), while hydrogenase II is probably involved in electron flow to CO_2 in the course of the formyl-MF dehydrogenase reaction (Schäfer *et al.* 1999).

Abken *et al.* (1998) have proposed a model in which the Vho hydrogenase extracts electrons from H_2, which then progress to the Hdr, *via* methanophenazine; this comprises the proposed H_2:heterodisulfide oxidoreductase complex in *Ms. mazei* Gö1 and for other members of the *Methanosarcina* spp. (Figure 1.15A) (Ide *et al.* 1999, Deppenmeier *et al.* 1999, Deppenmier 2002, 2004). The oxidation of H_2/reduction of methanophenazine (MP) by Vho, and the oxidation of reduced methanophenazine (MPH_2)/reduction of CoM-S-S-CoB, generates $\Delta\mu H^+$ used to synthesize ATP (Deppenmeier *et al.* 2002, 2004).

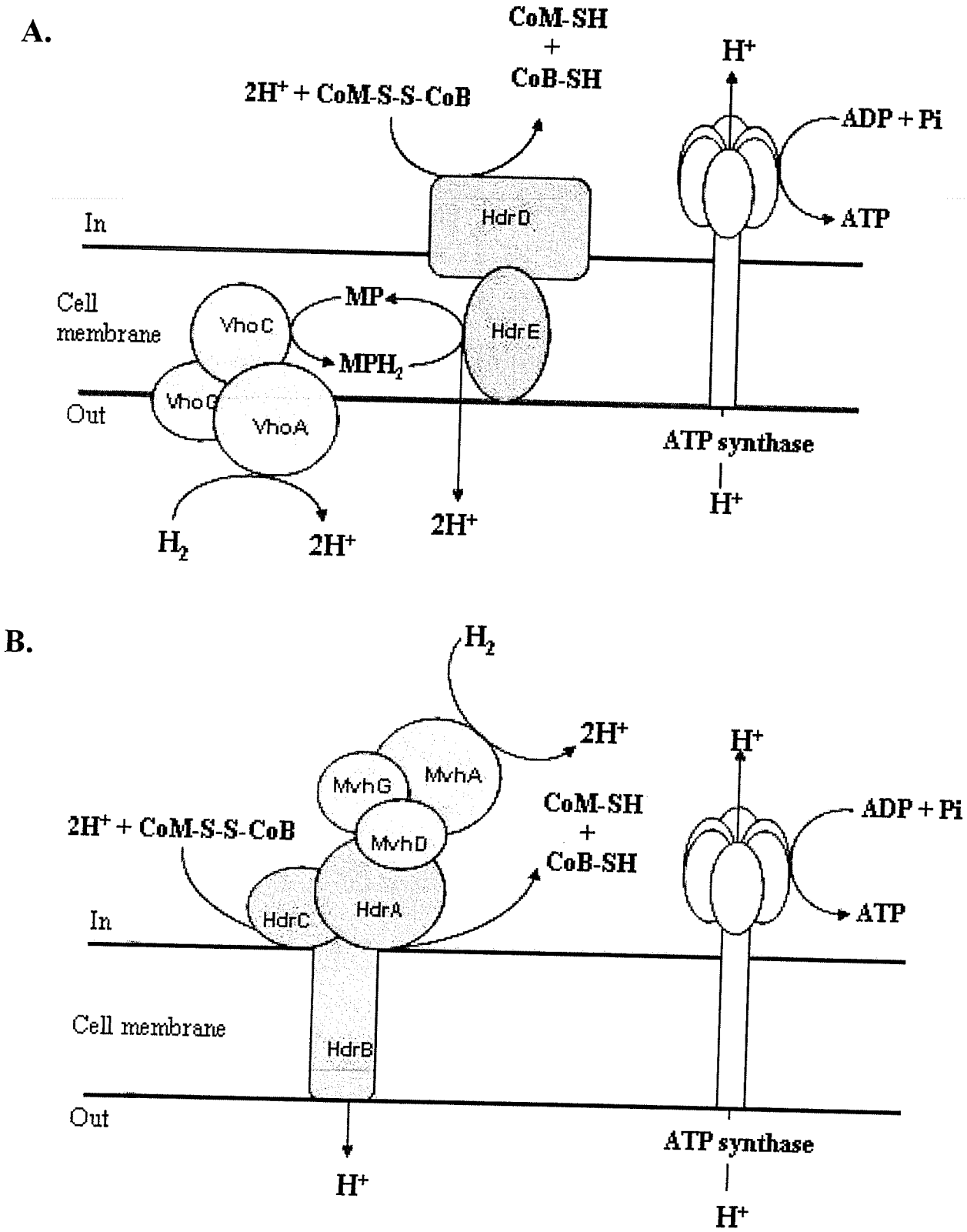

Figure 1.15. Model of electron transport and energy conservation *via* the H_2:CoM-S-S-CoB oxidoreductase complex in (A) the *Methanosarcinales*, and (B) the *Methanobacteriales* (Ide *et al.* 1999, Deppenmeier *et al.* 2002, 2004, Setzke *et al.* 1994, Stojanowic *et al.* 2003, Fricke *et al.* 2006). MP, methanophenazine. MPH_2, reduced methanophenazine.

Until recently, the physiological electron acceptor for the F_{420}-nonreducing hydrogenase of methanoarchaea outside of the *Methanosarcinales* was not entirely clear. The best studied system amongst the hydrogenotrophic methanoarchaea has been described using *Mtb. thermoautotrophicus* as a model, which contains several proteins that may participate as electron acceptors for the F_{420}-nonreducing hydrogenase. These include: polyferredoxin; a flavoprotein (flavoprotein A) that copurifies with the H_2:heterodisulfide oxidoreductase complex; and possibly rubredoxin (Nölling *et al.* 1995b). Neither polyferredoxin nor flavoprotein A were effectively reduced by the purified hydrogenase (Nölling *et al.* 1995b).

Recent models indicate that there are likely no intermediates between the F_{420}-nonreducing hydrogenase and Hdr, with the F_{420}-nonreducing hydrogenase docking directly onto the Hdr. The F_{420}-nonreducing hydrogenase (Mvh) and Hdr are isolated together as a large, tightly bound complex from the soluble cytoplasmic fraction of *Mtb. thermoautotrophicus* (Figure 1.15B) (Setzke *et al.* 1994, Stojanowic *et al.* 2003). Electron transfer from Mvh to Hdr is likely facilitated at the contact site of the MvhD subunit to HdrA; in the respective genomes of *Methanosarcina* spp. and *Msph. stadtmanae,* an *mvhD* homologue is fused to the 5' end of an *hdrA* homologue, indicating a potential link between the F_{420}-nonreducing hydrogenase and Hdr without the need for intermediates, although this has not been shown experimentally (Fricke *et al.* 2006).

1.5.1.3. Ech hydrogenase

H_2-evolving respiratory hydrogenases are membrane-bound, multimeric hydrogenases couple the oxidation of a carbonyl group (from formate, acetate, or carbon

monoxide), with the reduction of $2H^+$ to produce H_2 (Vignais *et al.* 2001). For example, the *E. coli* hydrogenase 3 is a [NiFe] hydrogenase produced under strictly anaerobic conditions and part of the formate hydrogen lyase (FHL) complex (Künkel *et al.* 1998, Vignais *et al.* 2001). This enzyme, coupled with the formate dehydrogenase, couples the oxidation of formate to CO_2 with the concomitant production of H_2. The FHL complex is encoded by eight genes in the hyc operon (hycBCDEFG and fdhF), where hycGE encode the hydrogenase portion of the complex: HycE contains the Ni-binding motif found in all [NiFe] hydrogenases (Sauter *et al.* 1992, Hedderich 2004). The remaining hyc-encoded subunits function as membrane anchors and electron carriers between formate dehydrogenase and hydrogenase 3 (Vignais *et al.* 2001). A similar hydrogenase system has been described for *Rhodospirillum rubrum*, where the hydrogenase activity is carbon monoxide-induced: the hydrogenase operates in tandem with the CODH to oxidize CO and to produce H_2 (Fox *et al.* 1996a, b).

Similar hydrogenases have been described from *Ms. barkeri* strain Fusaro, *Mtb. thermoautotrophicus* and *Mtb. marburgensis* (Meuer *et al.* 1999, Tersteegen and Hedderich 1999, Hedderich 2004). The enzyme was purified from the membranes of acetate-grown *Ms. barkeri* and given the designation Ech hydrogenase (energy-conserving hydrogenase) (Künkel *et al.* 1998, Meuer *et al.* 1999). The Ech hydrogenase from *Ms. barkeri* is encoded by a six gene operon, *echABCDEF*. The hydrogenase large subunit, EchE, shares very little sequence similarity with the respective subunits from the F_{420}-reducing and F_{420}-non reducing hydrogenases, with the exception of the [NiFe]-binding motifs. The hydrogenase small subunit EchC is also poorly conserved, with similarities restricted to an N-terminus cysteine cluster involved in the formation of a

[4Fe-4S] cluster (Künkel *et al.* 1998, Hedderich 2004). The integral membrane subunits of the Ech hydrogenase have closely related counterparts to the NADH:quinone oxidoreductase (Complex I), and functions as an ion pump with a role in energy-conservation during H_2 evolution, or reverse electron transport during H_2 uptake/ reduction of ferredoxin (Fd) (Meuer *et al.* 2002, Hedderich 2004). Ech provides the cell with reduced Fd that is required as electron donors for the various oxidoreductase activities in the catabolic and anabolic pathways (Meuer *et al.* 2002).

There have been several hypotheses put forth regarding the physiological importance of Ech in methanoarchaea during growth on the various methanogenic substrates. Anti-Ech serum was used to detect the presence of Ech in the cell extract of *Ms. thermophila*, indicating a potentially essential function of Ech in the acetate metabolism of *Methanosarcina* species (Meuer *et al.* 1999). Cell suspensions of *Ms. barkeri* mutants (Δech) could not grow on acetate; this was attributed to the mutants' inability to catalyze the oxidation of CO to CO_2 and H_2 (Meuer *et al.* 2002). During acetoclastic methanogenesis, it is believed that Ech catalyzes Fd-dependent H_2-evolution (Meuer *et al.* 2002, Hedderich 2004). The CO-group of acetyl-CoA is oxidized to CO_2, with the electrons transferred to Fd; Fd-H_2 is then used to provide electrons, in the form of H_2, for the reduction of CoM-S-S-CoB (Deppenmeier 2004).

During growth on H_2 and CO_2, it is suggested that Ech couples the consumption of an ion gradient with ferredoxin reduction, thus allowing for a thermodynamically unfavorable reaction to proceed (Meuer *et al.* 1999, 2002, Deppenmeier 2004). Meuer *et al.* (2002) reported that cell suspensions of Δech *Ms. barkeri* mutants could not grow on H_2 and CO_2, and that cell extracts from the mutants could not catalyze the reduction of

FD, the electron donor for the reduction of CO_2 to formyl-methanofuran. The genome of *Ms. acetivorans* indicates that this methanoarchaeon does not encode an Ech; this was one explanation as to why this *Ms. acetivorans* could not grow using H_2 and CO_2 (Galagan *et al.* 2002).

Mtb. thermoautotrophicus encodes two Ech-type hydrogenases, Eha and Ehb; based on the abundance of transcripts produced, Ehb is likely involved with catabolic reactons, while Eha is involved with anabolic reactions (Tersteegen and Hedderich 1999). Tersteegen and Hedderich (1999) hypothesized that the function of these hydrogenase complexes may be to act as multisubunit integral membrane proteins that form large electron transfer complexes, driving the reduction of CO_2 to formyl-methanofuran, or aiding in the synthesis of cellular components such as pyruvate, and 2-oxoglutarate.

Analysis of the respective genomes for *Mc. jannaschii*, *M. kandleri*, *Methanococcus maripaludis*, and *Msp. hungatei* JF1 indicates that these methanoarchaea also contain open reading frames that encode for the Ech hydrogenase (Bult *et al.* 1996, Slesarev *et al.* 2002, Porat *et al.* 2006). The genome of *Msph. stadtmanae* also encodes an Ehb hydrogenase, but lacks the gene encoding EhA hydrogenase; Ehb is likely involved with pyruvate synthesis in this methanoarchaeon (Fricke *et al.* 2006).

1.5.2. The $F_{420}H_2$ dehydrogenase

The $F_{420}H_2$ dehydrogenase is part of the methylotrophic methanogenesis pathway (Figure 1.11, section 1.3.2.). The $F_{420}H_2$ dehydrogenase is an essential component of the membrane-bound $F_{420}H_2$:heterodisulfide oxidoreductase system in some members of the *Methanosarcinales*, functioning as the entry point for electrons derived from the

oxidation $F_{420}H_2$. These electrons are then ferried through a membrane-bound electron transport chain that leads to Hdr and ultimately reduction of CoM-S-S-CoB and generation of an energy conserving, transmembrane proton gradient (Müller *et al.* 1993, Bäumer *et al.* 1998). While the $F_{420}H_2$ dehydrogenase plays an important role in the metabolism of methylotrophic methanoarchaea, its existence and function in non-methylotrophic methanoarchaea has yet to be determined. Electron transport and energy conservation has been well studied in the *Methanosarcinales*, particularly with *Ml. tindarius* and *Ms. mazei* Gö1 (Scheel and Schäfer 1990, Deppenmeier *et al.* 1990a, 1990b, Deppenmeier *et al.* 1996, Deppenmeier 2002, 2004).

Deppenmeier *et al.* (1990a) analyzed the role of $F_{420}H_2$ in the reduction of CoM-S-S-CoB by the $F_{420}H_2$ dehydrogenase, using inverted vesicle preparations of *Ms. mazei* Gö1 and *Ml. tindarius*. These vesicles coupled $F_{420}H_2$ oxidation with the reduction of CoM-S-S-CoB in a concomitant and stoichiometeric reaction (Deppenmeier *et al.* 1990a):

$$\text{CoM-S-S-CoB} + F_{420}H_2 \rightarrow \text{CoM-SH} + \text{CoB-SH} + F_{420}$$

The $F_{420}H_2$-dependent reduction of CoM-S-S-CoB was coupled to the generation of a transmembrane proton gradient $\Delta\mu H^+$, which led to the formation of ATP from ADP + Pi *via* A_1A_0 ATP synthase: 1 mole of ATP was formed per 2-3 moles of $F_{420}H_2$ oxidized (Deppenmeier *et al.* 1990b).

Thus far, the $F_{420}H_2$ dehydrogenase has only been purified from *Ml. tindarius* (Haase *et al.* 1992), *Ms. mazei* Gö1 (Abken and Deppenmeier 1997), and the closely related sulfate-reducing archaeon *A. fulgidus* , which may be a methanoarchaeon that has lost the ability to generate methane (Kunow *et al.* 1994, Bapteste *et al.* 2005).

1.5.2.1. Purification of the $F_{420}H_2$ dehydrogenase from Methanolobus tindarius

$F_{420}H_2$ dehydrogenase was first purified by Haase *et al.* (1992) from *Ml. tindarius*. As described by Haase *et al.* (1992), the oxygen-stable enzyme was extracted from the cell membrane, and contains five subunits with apparent molecular masses of 45, 40, 22, 18, and 17 kDa (total molecular mass: 120 kDa). The enzyme contained 16 ± 2 mol iron and 16 ± 3 mol acid-labile sulfur per mole of enzyme. Enzyme activity was assayed using the methyl viologen/metronidazole system. Methyl viologen is reduced *via* electrons donated from $F_{420}H_2$ and transferred by $F_{420}H_2$ dehydrogenase; metronidazole reoxidizes the reduced methyl viologen in order to prevent spectroscopic interference with $F_{420}H_2$. Curiously, flavins were not detected, although the electron transfer from the hydride donor $F_{420}H_2$ to the one-electron acceptor requires a 2-electron/1e-electron switch; as well, the iron-sulfur (FeS) clusters themselves are single electron acceptors, thus necessitating the 2-electron/1-electron switch (Abken and Deppenmeier 1997).

Westenberg *et al.* (1999), using the N-terminal amino acid sequence of the 40 kDa subunit of the $F_{420}H_2$ dehydrogenase, discovered the gene *ffdB* in the *Ml.tindarius* chromosome. It was apparent that the *ffdB* gene was part of an operon containing three additional reading frames: *ffdA*, *ffdC*, and *ffdD*. The genes were cloned into *E. coli* and the protein products were examined. While *ffdB* encoded the 40 kDa subunit, the products from the other genes were not found to be identical to any of the other known subunits, although it has been surmised that *ffdC* and *ffdD* may encode two of the smaller subunits (22, 18, or 17 kDa). However, the purified $F_{420}H_2$ dehydrogenase from *Ml.*

tindarius consists of five subunits, indicating that there must be one gene that was not discovered.

1.5.2.2. Purification of the $F_{420}H_2$ dehydrogenase from Methanosarcina mazei *Gö1*

The discovery of $F_{420}H_2$ dehydrogenase in *Ml. tindarius* was followed by the purification of the homologous enzyme in *Ms. mazei* Gö1 by Abken and Deppenmeier (1997). The oxygen-stable holoenzyme (115 kDa) consisted of five different polypeptide subunits with molecular masses of 40, 37, 22, 20, and 16 kDa (Abken and Deppenmeier 1997). The enzyme from *Ms. mazei* Gö1 contains FeS clusters as well as FAD (0.2 mol/mol enzyme). Abken and Deppenmeier (1997) suggested that the low amounts of FAD may be due to the flavin not being covalently bound and that most may have been lost during the process of purification. It was also suggested that much of flavin from the *Ml. tindarius* $F_{420}H_2$ dehydrogenase may have been lost entirely during purification, since FAD was not detected in the enzyme, with the remaining traces of FAD masked by the buffer components. FAD is essential for the dehydrogenase activity as it acts as a two electron/one electron switch during the transfer of electrons from $F_{420}H_2$ to electron acceptor. The physiological electron carrier for the $F_{420}H_2$ dehydrogenase is believed to be methanophenazine (section 1.4.4.)

1.5.2.3. DPI-mediated inhibition of the phenazine-dependent $F_{420}H_2$ dehydrogenase

The heterodisulfide reductase (Hdr), the key enzyme for energy conservation, can receive electrons from FD_{red}, H_2, or $F_{420}H_2$ for the reduction of CoM-S-S-CoB (Deppenmeier *et al.* 1996). In methylotrophic methanoarchaea of the

Methanosarcinacaea, methanophenazine is proposed to be the electronic link to Hdr (Bäumer *et al.* 1998, Ide *et al.* 1999, Deppenmeier et al. 2002, Deppenmeier 2004). Brodersen *et al.* (1999) discovered that the compound diphenyleneiodonium (DPI) was specifically able to inhibit both the H_2- (F_{420}-nonreducing hydrogenase) and $F_{420}H_2$-dependent ($F_{420}H_2$ dehydrogenase) heterodisulfide oxidoreductase systems. From this study, it was concluded that DPI competitively inhibits the 2-OH-phenazine-dependent $F_{420}H_2$ dehydrogenase activity, increasing the Km from 35 to 100 μM 2-OH-phenazine (Brodersen *et al.*1999).

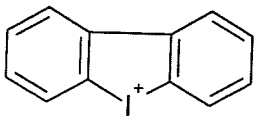

Diphenyleneiodonium Chloride

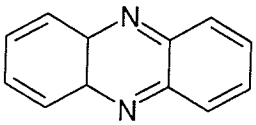

Phenazine

Figure 1.16. Structures of Diphenyleneiodonium (DPI) chloride and phenazine.

A model was proposed that suggests that the inhibition occurs at the site of 2-OH-phenazine reduction (at the two N atoms). The observed inhibition is not surprising since DPI has a chemical structure that is very similar to phenazine; this provided additional support for the role of methanophenazine as an e- carrier in the oxidation of $F_{420}H_2$, and ultimately to the reduction of CoM-S-S-CoB *via* Hdr (Figure 1.16).

1.5.2.4. $F_{420}H_2$ dehydrogenase as a redox-driven proton pump

Bäumer *et al.* (2000) reported the discovery of the gene locus in a DNA fragment that contained a cluster of genes encoding the $F_{420}H_2$ dehydrogenase from *Ms. mazei* Gö1; the name given to this locus was *fpo* ($F_{420}H_2$:phenazine oxidoreductase). Analysis of the *fpo* genes and their products revealed similarities between the $F_{420}H_2$ dehydrogenase and the genes (*nuoA-N*) encoding the proton-translocating NADH:ubiquinone oxidoreductase (NDH-1, complex I) from *E. coli*, and to analogous structures found in the mitochondria of eukaryotic organisms (Yagi *et al.* 1998, Bäumer *et al.* 2000). The purified $F_{420}H_2$ dehydrogenase reported by Abken and Deppenmeier (1997) was actually not the holoenzyme as predicted, but the cytoplasmic portion of a much more sophisticated integral membrane structure.

In accordance with the organization of the gene sequences of the *nuo* operon in *E. coli*, the genes of the *fpo* operon were designated *fpoA, B, C, D, H, I, J, K, L, M, N*, and *O*; *fpoF*, which encodes the 37 kDa subunit, is found at a different location in the chromosome away from the *fpo* cluster (Bäumer *et al.* 2000). This gene is believed to encode the electron input device of $F_{420}H_2$ dehydrogenase. Overexpression of *fpoF* from *Ms. mazei* Gö1 in *E. coli* produced a flavoprotein containing non-heme iron and acid-labile sulfur; the FpoF subnit was capable of oxidizing $F_{420}H_2$ in the presence of methyl viologen (Bäumer *et al.* 2000).

A model of electron transport in the membranes of *Ms. mazei* Gö1 was proposed by Bäumer *et al.* (2000) (Figure 1.17). The protein originally isolated by Abken and Deppemeier (1997) from *Ms. mazei* Gö1, consisting of FpoB (22 kDa), C (20 kDa), D (40 kDa), I (16 kDa), and F (37 kDa), are clustered together on the cytoplasmic side of

the cell membrane. FpoF is predicted to be the point of entry for electrons from $F_{420}H_2$, which are shuttled through FeS clusters to FpoBCDI. FpoBCDI forms the membrane-associated FeS-containing module that transfers electrons to the membrane-integral FpoAHJKLMN component, and finally to methanophenazine. The role of FpoO is not entirely clear, but does not appear to be essential for activity.

This model is supported by the finding of significant identity and similarity between the primary sequences of 11 proteins encoded by *fpoA* to *fpoN*, excluding *fpoF*, with analogous subunits found in bacterial and mitochondrial NADH dehydrogenase (Bäumer *et al.* 2000). The homologues of complex I, found in the respiratory chains of bacteria, the mitochondria of eukaryotes, and chloroplasts of plants, generate a proton motive force for the synthesis of ATP, and also regenerate NAD^+ by removing excesses of reducing equivalents (Yagi *et al.* 1998, Friedrich 1998, Friedrich and Scheide 2000). The electrons are passed to membrane-bound hydrophobic electron carriers called quinones (Friedrich and Weiss 1997).

The Fpo complex is expected to operate in a similar manner, interacting with $F_{420}H_2$ instead of NADH, and methanophenazine in place of ubiquinone; ubiquinone is not found in methanoarchaea (Bäumer *et al.* 2000, Deppenmeier 2002). It is speculated that the $F_{420}H_2$ dehydrogenase and the NADH dehydrogenase both evolved from a common ancestral ion-pumping hydrogenase (Friedrich and Scheide 2000, Hedderich 2004). Indeed, there is sequence similarity of the subunits from the [NiFe] hydrogenases (including the F_{420}-reducing/nonreducing hydrogenases, and the Ech hydrogenase) with the subunits of the *E. coli* complex I and the Fpo complex (Friedrich and Scheide 2000). FpoF does not show homology to any of the subunits of complex I, but does show

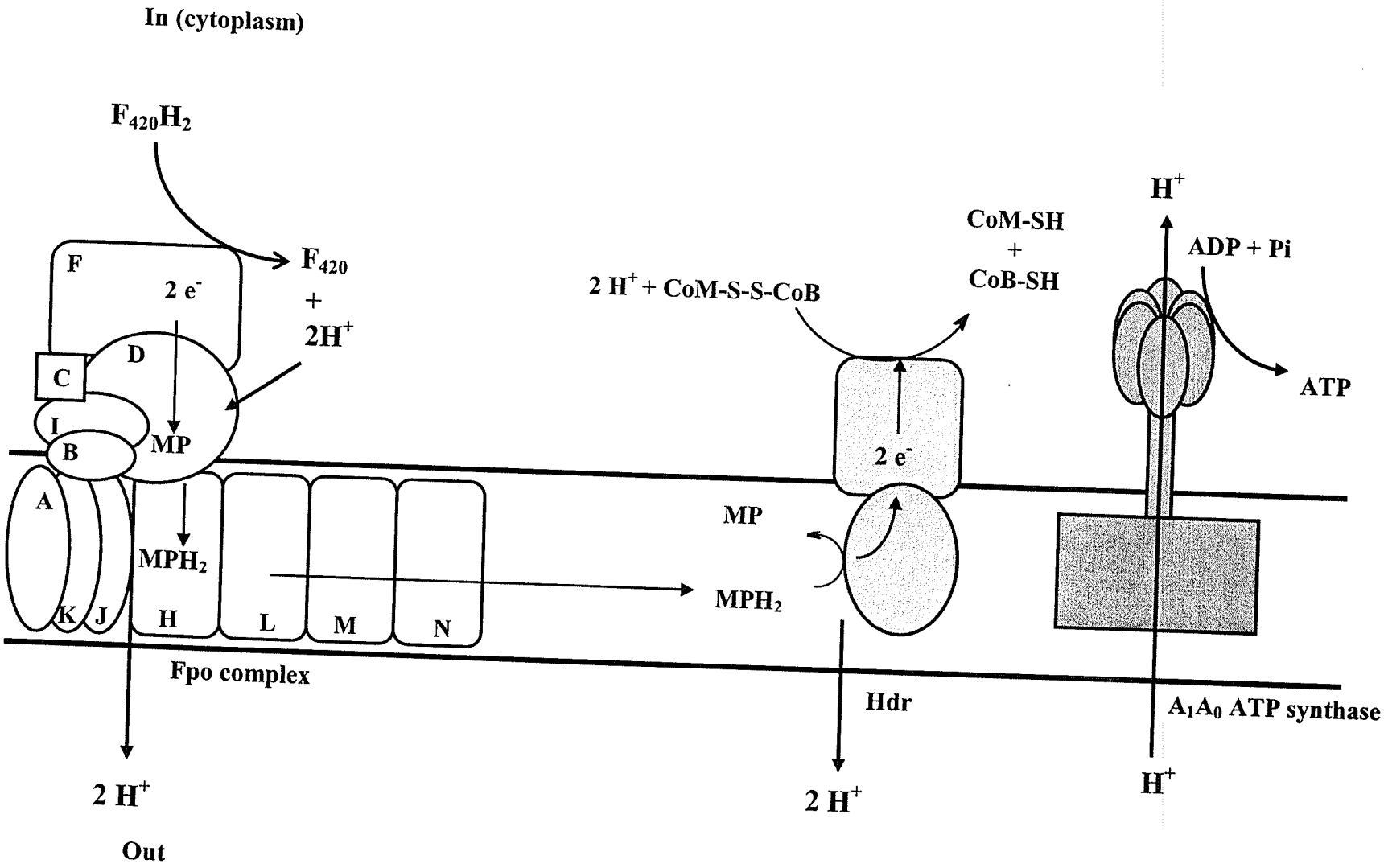

Figure 1.17. Hypothetical model of membrane-bound electron transport and energy conservation in CH_3OH-grown *Methanosarcina mazei* Gö1 as described in text (Bäumer *et al.* 2000, Deppenmeier *et al.* 2002). Fpo, $F_{420}H_2$ phenazine oxidoreductase. Hdr, heterodisulfide reductase. MP, methanophenazine. MPH_2, reduced methanophenazine.

homology to the subunits of several methanogenic F_{420}-dependent enzymes such as the F_{420}-reducing hydrogenases (β-subunit) and the F_{420}-dependent formate dehydrogenases, all of which are FAD-containing proteins (Bäumer *et al.* 2000).

Bäumer *et al.* (2000) have also provided experimental evidence that indicates that the activity of the $F_{420}H_2$ dehydrogenase resembles a proton pump in *Ms. mazei* Gö1. Using inverted membrane vesicles, protons flow into the lumen of the vesicles concurrent with $F_{420}H_2$-dependent reduction of 2-OH-phenazine. Two protons are pumped into the lumen during reduction of 2-OH-phenazine *via* Fpo, with another pair of protons translocated during the course of CoM-S-S-CoB reduction. In contrast, 4 protons are pumped out by complex I of *E. coli* (Deppenmeier 2004). A model depicting the activity of the $F_{420}H_2$ dehydrogenase complex and CoM-S-S-CoB reduction is shown in Figure 1.17.

Several lines of evidence support the homology between the $F_{420}H_2$ dehydrogenase and the NADH dehydrogenase: both are membrane-bound proteins containing flavins and Fe-S clusters; both $F_{420}H_2$ (-350 mV) and NADH (-320 mV) are reversible hydride donors with similar midpoint potentials; both proteins use small membrane-bound hydrophobic non-protein electron acceptors (methanophenazine and ubiquinone, respectively); and DPI inhibits $F_{420}H_2$ dehydrogenase as well as NADH dehydrogenase (Bäumer *et al.* 2000).

1.5.2.5. The Fqo complex of Archaeoglobus fulgidus

A similar complex was isolated from the membranes of the hyperthermophilic marine archaeon *A. fulgidus* by Kunow *et al.* (1994), while Brüggermann *et al.* (2000)

reported the genes coding for the subunits of the complex. As with the methanogenic homologue, the *fqo* ($F_{420}H_2$:quinone oxidoreductase) gene cluster, encompassing 11 genes (A, BC, D, H, I, J, K, L, M, N, and F), shows significant homology to subunits of the prokaryotic and eukaryotic NADH-quinone oxidoreductases (Brüggermann *et al.* 2000). Unlike the *fpo* operon of *Ms. mazei* Gö1, the *fqo* operon contains all of the genes that encode for the Fqo complex, including *fqoF*. Genes *fqoB* and *fqoC* are fused into one gene, whereas the homologous genes in *Ms. mazei* Gö1 are two separate genes. The structure of the Fqo complex is expected to be similar to the Fpo complex of *Ms. mazei* Gö1, with FqoBCDIF extruding from the cell membrane into the cytoplasm, and FqoAHJKLMN forming the membrane-integral module (Brüggermann *et al.* 2000). There does not appear to be an analogue for *fpoO* in the *fqo* operon.

The Fqo complex oxidizes $F_{420}H_2$ and likely transfers the electrons to menaquinone, present in the cytoplasmic membrane of *A. fulgidus* (Brüggermann *et al.* 2000). Like the analogous component in *Ms. mazei* Gö1, FqoF is predicted to be the electron input device for the Fqo complex: overexpression of the *fqoF* gene in *E. coli* resulted in the production of a 39 kDa protein (containing non-heme iron, acid-labile sulfur, and FAD) that was able to oxidize F_{420} with the concurrent reduction of methyl viologen (plus metronidazole) (Brüggermann *et al.* 2000).

1.6. $F_{420}H_2$ dehydrogenase activity in other methanoarchaea?

While the methanophenazine-dependent $F_{420}H_2$ dehydrogenase activity is essential for methylotrophic growth in members of the *Methanosarcinaceae* (Figure 1.18), a similar activity, using methyl viologen as electron acceptor, appears to be

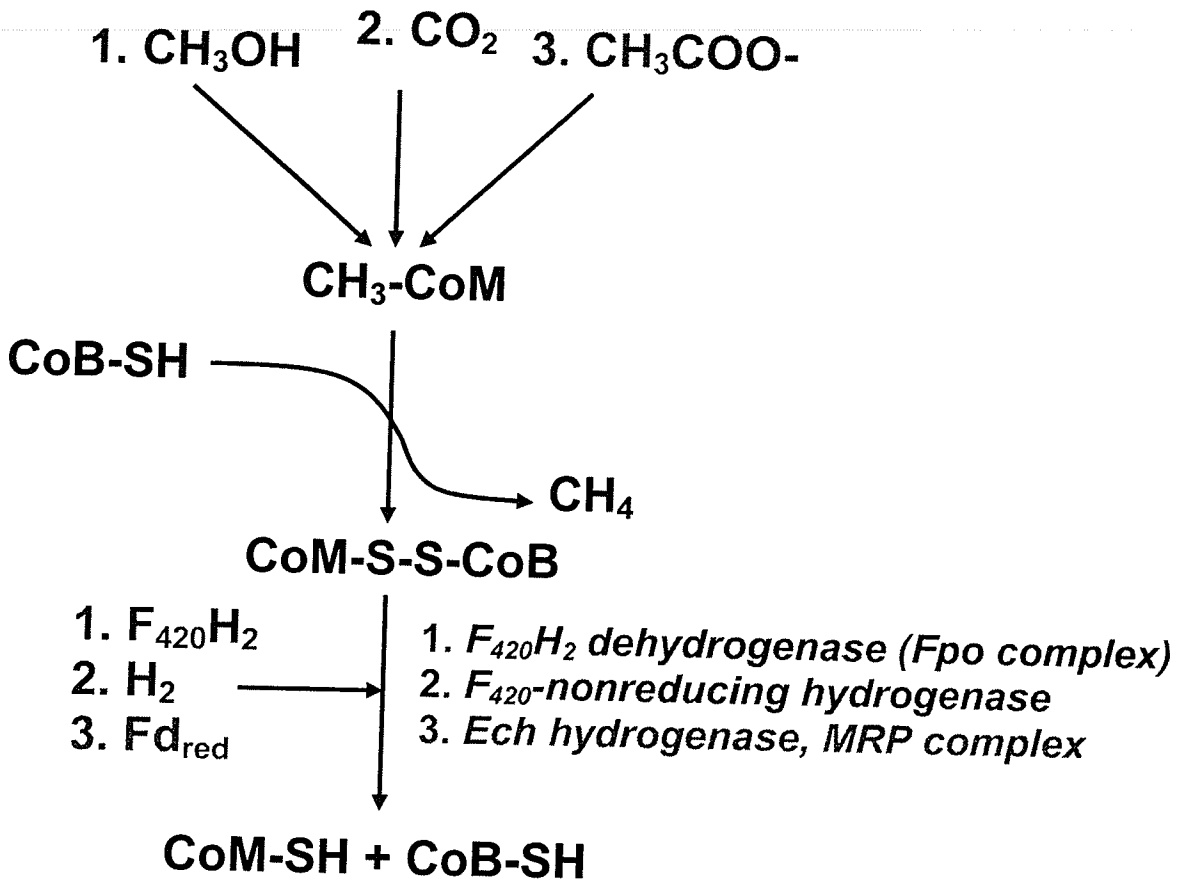

Figure 1.18. Methanogenesis, electron transport, and CoM-S-S-CoB reduction in the methanoarchaea. 1. Growth on CH_3OH. 2. Growth on H_2:CO_2. 3. Growth on acetate. (Thauer *et al.* 1993, Shima *et al.* 2002, Deppenmeier 2004, Li *et al.* 2006).

ubiquitous amongst the methanoarchaea, regardless of methanogenic substrate or phylogeny (Wong *et al.* 1994, Wong PhD thesis 1999). This activity is referred to as $F_{420}H_2$ dehydrogenation, to avoid confusion with the protein purified from the *Ms. mazei* Gö1 and *Ml. tindarius*. The physiological significance of this activity in non-methylotrophic methanoarchaea is unclear. Based on the studies with *Ml. tindarius* and *Ms. mazei* Gö1, $F_{420}H_2$ dehydrogenase activity does not appear to be essential for methanogenesis on substrates other than CH_3OH; along with Hdr, the F_{420}-nonreducing hydrogenase (H_2) and the Ech hydrogenase or MRP complex (Fd_{red}) should provide the pmf for hydrogenotrophic or acetoclastic methanogenesis, respectively (Figure 1.18). It is currently not known how non-methylotrophic methanoarchaea may couple $F_{420}H_2$ oxidation to CoM-S-S-CoB reduction, or if this activity might be required for some other pathway outside of methanogenesis.

However, the hydrogenotrophic methanoarchaeon *Msp. hungatei* GP1 apparently lacks an F_{420}-nonreducing hydrogenase (Sprott *et al.* 1987), which is an important component of the H_2:heterodisulfide oxidoreductase complex found in hydrogenotrophic methanoarchaea that catalyzes the energy conserving reduction of CoM-S-S-CoB (Thauer *et al.* 1993, Shima *et al.* 2002). In the absence of the F_{420}-nonreducing hydrogenase, another mechanism must exist for the reduction of CoM-S-S-CoB. An $F_{420}H_2$ dehydrogenase-like activity has been detected in the cell-free extract of *Msp. hungatei* GP1 (Wong, PhD thesis 1999). Given the close phylogenetic relationship between the *Methanomicrobiales* and *Methanosarcinales* (Bapteste *et al.* 2005), it would not be surprising if an Fpo complex was present in *Msp. hungatei* GP1.

Some methanoarchaea can grow on formate ($HCOO^-$) as an energy source (Livingston *et al.* 1987).

$$HCOO^- + F_{420} \rightarrow CO_2 + F_{420}H_2$$

This reaction is catalyzed by F_{420}-dependent formate dehydrogenase, purified from the hydrogenotrophic methanoarchaea *Methanococcus vannielii* (Jones and Stadtman 1980) and *Methanobacterium formicicum* (Schauer and Ferry 1983), and is also found in *Methanococcus voltae* (Brodersen *et al.* 1999b). As $F_{420}H_2$ is the primary carrier of electrons, could it not be used as an alternative to H_2 for CoM-S-S-CoB reduction? Indeed, membrane-bound CoM-S-S-CoB reduction in *Mc. voltae* is coupled to $F_{420}H_2$ oxidation; the source of $F_{420}H_2$ oxidation associated with the F_{420}-reducing hydrogenase of this methanoarchaeon (Brodersen *et al.* 1999b).

Ms. barkeri Fusaro is a methylotrophic member of the *Methanosarcinaceae*, and would be expected to possess a Fpo complex as in *Ml. tindarius* and *Ms. mazei* Gö1. Studies by Wong (PhD thesis 1999) indicated that this protein is apparently not produced by *Ms. barkeri* Fusaro during growth on CH_3OH, although a similar activity appeared to be associated with an F_{420}-reducing hydrogenase activity; in contrast the purified $F_{420}H_2$ dehydrogenases of *Ml. tindarius* and *Ms. mazei* Gö1 do not possess F_{420}-reducing hydrogenase activity (Haase *et al.* 1992, Abken and Deppenmeier 1997). Furthermore, significant amounts of F_{420}-reducing hydrogenase are produced during growth on CH_3OH, at levels higher than during growth on H_2:CO_2 (Mukhopadhyay *et al.* 1993). High levels of F_{420}-reducing hydrogenase would not be necessary during growth on CH_3OH, as F_{420} is produced *via* CH_3OH oxidation. Is there a link between the high levels

of F_{420}-reducing hydrogenase and $F_{420}H_2$ dehydrogenase activity in this methanoarchaeon?

Msph. stadtmanae, a methanoarchaeon that grows solely on H_2 and CH_3OH, also possesses an $F_{420}H_2$ dehydrogenation activity, although the source and physiological significance of this activity is unknown (Miller and Wolin 1983, 1985, Wong *et al.* 1994). $F_{420}H_2$ is not necessary during growth on H_2 and CH_3OH, but would be required during methanogenesis from H_2 and L-serine, or 2-propanol and CH_3OH, as well as for anabolic reactions (Wong, Ph.D thesis 1999). An F_{420}-reducing hydrogenase was not detected in the cell free extract of *Msph. stadtmanae*, such that the means for F_{420}-reduction in this methanoarchaeon are unclear (Deppenmeier *et al.* 1989, Wong *et al.* 1994). It has been suggested that the $F_{420}H_2$ dehydrogenation activity of *Msph. stadtmanae* may be essential for the reduction of F_{420}; F_{420}-reduction has been observed using cell-free extract of *Msph. stadtmanae*, phenazine, and H_2; (Wong PhD thesis 1999). Methanophenazine may be the link between H_2, the primary source of electrons for *Msph. stadtmanae*, and the observed $F_{420}H_2$ dehydrogenation activity.

2. Research objectives

The various electron transport pathways of the methanoarchaea have been well studied, but biochemical and genomic data as presented and discussed in the previous section suggest that there are variations in the electron transport pathways for some methanoarchaea. Thus our laboratory is interested in studying and elucidating these differences and variations in different methanoarchaea, focusing on the role of $F_{420}H_2$ dehydrogenation activity. In some methylotrophic members of the *Methanosarcinaceae*, the $F_{420}H_2$ dehydrogenase plays an important role in electron transport and energy conservation, catalyzing the classic $F_{420}H_2$-dependent reduction of CoM-S-S-CoB during the final stage of methanogenesis (Deppenmeier 2002, 2004). In *Ms. mazei* Gö1, this activity uses various phenazine-containing compounds as electron carriers/acceptors.

Objective 1: Determine the extent of phenazine-dependent $F_{420}H_2$ dehydrogenation activity in the methanoarchaea

A similar activity, referred to as $F_{420}H_2$ dehydrogenation, appears to be ubiquitous in the cell-free extracts of all methanoarchaea. A role for the $F_{420}H_2$ dehydrogenase activity in non-methylotrophic methanoarchaea containing high levels of F_{420}-reducing hydrogenase and F_{420}-nonreducing hydrogenase activities is not readily apparent. However, in the absence of F_{420}-reducing hydrogenase or F_{420}-nonreducing hydrogenase, could there be a physiological role for the observed $F_{420}H_2$ dehydrogenation activity? Could this activity be required for hydrogenotrophic methanoarchaea using electron sources other than H_2, such as formate or 2-propanol? Could there be an $F_{420}H_2$–dependent mechanism for CoM-S-S-CoB reduction? These questions were examined *via*

study of the phenazine-dependent $F_{420}H_2$ dehydrogenation activities of *Methanospirillum hungatei* GP1, *Methanosarcina barkeri* Fusaro, and *Methanosphaera stadtmanae*.

Objective 2: Purify and characterize the $F_{420}H_2$ dehydrogenation activity of *Methanospirillum hungatei* GP1

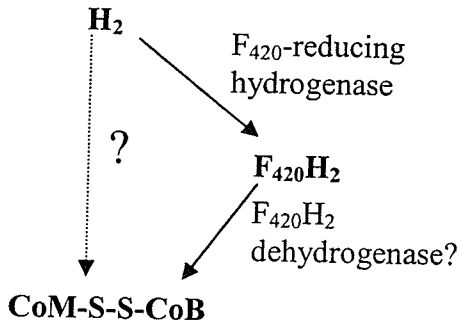

Figure 2.1. Electron transport and CoM-S-S-CoB reduction in *Methanospirillum hungatei* GP1.

Msp. hungatei GP1, a hydrogenotrophic methanoarchaeon of the order *Methanomicrobiales*, possesses an F_{420}-reducing hydrogenase, but lacks an F_{420}-nonreducing hydrogenase (Figure 2.1, Sprott *et al.* 1987). In the absence of F_{420}-nonreducing hydrogenase, it is unclear how H_2 is coupled to CoM-S-S-CoB reduction in this methanoarchaeon. Methyl viologen-dependent $F_{420}H_2$ dehydrogenation activity had been detected in the membranes, suggesting a possible $F_{420}H_2$- and methanophenazine-dependent mechanism for CoM-S-S-CoB reduction. Given the close phylogenetic relationship between the orders *Methanosarcinales* and *Methanomicrobiales* (Bapteste *et al.* 2005), the presence of an $F_{420}H_2$ dehydrogenase in *Msp. hungatei* GP1 would not be surprising. Therefore, one objective of this thesis was to isolate and study the source of

$F_{420}H_2$ dehydrogenation activity in *Msp. hungatei* GP1, and to determine if this activity could substitute for the Mvh with respect to CoM-S-S-CoB reduction in this methanoarchaeon.

Objective 3: Purify and characterize the $F_{420}H_2$ dehydrogenase activity of methanol-grown *Methanosarcina barkeri* Fusaro

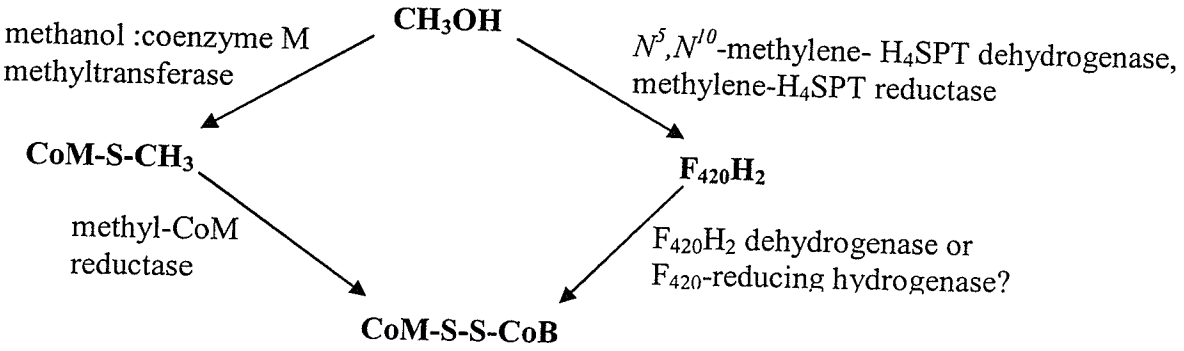

Figure 2.2. Electron transport and CoM-S-S-CoB reduction in *Methanosarcina barkeri* Fusaro.

Ms. barkeri Fusaro, grown on methanol as a source of carbon and electrons, would be expected to produce the $F_{420}H_2$ dehydrogenase, but it had previously been reported that benzyl viologen-dependent $F_{420}H_2$-oxidation was associated with the F_{420}-reducing hydrogenase, rather than a distinct $F_{420}H_2$ dehydrogenase (Keltjens and Vogels 1993). Furthermore, a distinct $F_{420}H_2$ dehydrogenase, assayed with methyl viologen, was not detected in this methanoarchaeon by our laboratory (Wong, Ph.D thesis 1999). However, gene sequences coding for a putative $F_{420}H_2$ dehydrogenase were identified in the incomplete genome of *Ms. barkeri* Fusaro, using sequences coding for subunits of the Fpo complex from *Ms. mazei* Gö1 (circa. 2003-2004, NCBI website). With the discovery

of methanophenazine as a putative electron acceptor for the $F_{420}H_2$ dehydrogenase activity of *Ms. mazei* Gö1 (Abken *et al.* 1998), it was of great interest to see if a phenazine-dependent $F_{420}H_2$ dehydrogenase, similar to that found in *Ms. mazei* Gö1, could be isolated from methanol-grown *Ms. barkeri* Fusaro.

Objective 4: Purify and characterize the $F_{420}H_2$ dehydrogenation activity in *Methanosphaera stadtmanae*

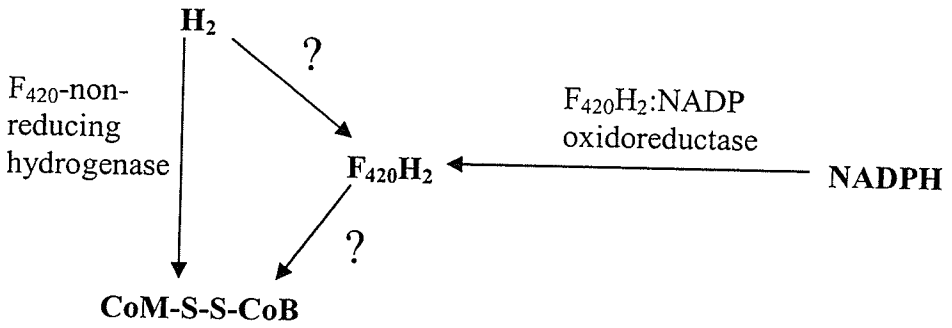

Figure 2.3. Electron transport and CoM-S-S-CoB reduction in *Methanosphaera stadtmanae.*

Various elements of the electron transport pathway have been elucidated in *Msph. stadtmanae*, including the $F_{420}H_2$:NADP oxidoreductase (Fno) and F_{420}-nonreducing hydrogenase (Mvh) (Figure 2.3, Wong PhD thesis 1999, Elias *et al.* 2000), but many steps are still unclear, particularly the relevance of a methyl viologen-dependent $F_{420}H_2$ dehydrogenation activity that was detected in the cell-free extract of *Msph. stadtmanae* (Wong *et al.* 1994). *Msph. stadtmanae*, which grows on H_2 and methanol, possesses an F_{420}-nonreducing hydrogenase (i.e. Mvh), but an F_{420}-reducing hydrogenase activity was not detected in this methanoarchaeon (Deppenmeier *et al.* 1989, van de Wijngaard *et al.*

1991, Wong *et al.* 1994). F_{420} is found at low concentrations in *Msph. stadtmanae* (0.16 nmol·mg protein^{-1}), but $F_{420}H_2$ is required for cellular biosynthesis, and is expected to be necessary during methanogenesis on H_2 and L-serine, or 2-propanol and methanol (Lin and Sparling 1995, Wong *et al.* 1994). Yet there is no obvious connection between H_2 and F_{420}, or $F_{420}H_2$ and Hdr, in the absence of detectable levels of F_{420}-reducing hydrogenase (Deppenmeier *et al.* 1989, Wong *et al.* 1994). Low levels of H_2-dependent F_{420}-reduction activity were observed in the presence of concentrated cell-free extract, F_{420}, and phenazine, suggesting a potential role for the observed $F_{420}H_2$ dehydrogenation activity in methanophenazine-dependent reduction of F_{420} in *Msph. stadtmanae*. The objective was to purify and characterize the activity of the $F_{420}H_2$ dehydrogenation activity, and to complete the electron transport pathway for *Msph. stadtmanae*.

3. Materials and Methods

All chemicals used for this thesis were purchased from Sigma Aldrich or Fisher Scientific.

3.1. Methanoarchaea used for thesis

The methanoarchaea used for this thesis were obtained from the Deutche Sammlung von Zellkulturen und Mikroooranismen (DSZM), Braunschweig, Germany. The primary methanoarchaea studied during the course of this thesis include *Methanosphaera stadtmanae* (DSZM 3091), *Methanosarcina barkeri* Fusaro (DSZM 804), and *Methanospirillum hungatei* GP1 (DSZM 1101). *Methanococcus thermolithotrophicus* (DSZM 2095) was also grown frequently to provide coenzyme F_{420} for various enzymatic assays. *Methanolobus tindarius* (DSZM 2278), *Methanosaeta concilii* GP6 (DSZM 3671), and *Methanothermobacter marburgensis* (formerly *Methanobacterium thermoautotrophicum* Marburg) (DSZM 2133), *Methanobacterium bryantii* (DSZM 863), and *Methanococcus voltae* (DSZM 1533) were also used in this thesis.

3.2. Growth media

Cells were grown in either 1 L Corning bottles, 100 mL serum bottles, or 25 mL Balch tubes; the volume of media depended on the growth substrate used for each methanoarchaeon. Stoppers were wired down to seal the 1 L bottles, while aluminum crimps (Wheaton aluminum seals) were used to seal the Balch tubes and serum bottles.

Media for the respective methanoarchaea were made anaerobic and pressurized to 0.2 atm according to Balch and Wolf (1976), using a water jet vacuum/gas manifold system. Sodium sulfide ($Na_2S \cdot 9\ H_2O$, 200 mM stock) was added to the anaerobic media (final concentration 2 mM) prior to autoclaving. Additions to the sterile media were made through the rubber stoppers using sterile, anaerobic syringes (treated with anaerobic, sterile 2 mM $Na_2S \cdot 9\ H_2O$). The volume of inoculum added was 10% of the volume of the medium (i.e. 50 ml of inoculum added to 500 mL of media).

The media formulations of the primary methanoarchaea most frequently studied (*Msph. stadtmanae*, *Ms. barkeri* Fusaro, and *Msp. hungatei* GP1) and *Mc. thermolithotrophicus* are given here. The media formulations for the other methanoarchaea are given in Appendix A.

Msph. stadtmanae was grown at 37°C according to Miller and Wolin (1985), but in the absence of formate. The media contained (per liter): tryptone (2 g); yeast extract (2 g); K_2HPO_4 (0.3 g); KH_2PO_4 (2.8 g); $(NH_4)_2SO_4$ (0.3 g); NaCl (0.61 g); $MgSO_4 \cdot 7H_2O$ (0.13 g); $CaCl_2 \cdot 2\ H_2O$ (0.08 g); Na acetate (0.5 g); $NaSeO_4$ (0.04 mg); Na_2CO_3 (1.7 g); NH_4Cl (1.0 g); resazurin (0.25 μg); nitrilotriacetic acid (20.2 mg); $FeCl_3 \cdot 6\ H_2O$ (2.1 mg); $CoCl_2 \cdot 6\ H_2O$ (2.0 mg); $MnCl_2 \cdot 4\ H_2O$ (1.0 mg); $ZnCl_2$ (1.0 mg); $NiCl_2 \cdot 6\ H_2O$ (1.0 mg); $CuSO_4 \cdot 2\ H_2O$ (0.5 mg); $Na_2MoO_4 \cdot 2\ H_2O$ (0.5 mg); pyridoxine-HCl (0.1 mg); riboflavin (0.5 mg); thiamine (0.05 mg); nicotinic acid (0.05 mg); *p*-aminobenzoic acid (0.05 mg); lipoic acid (0.05 mg); biotin (0.02 mg); folic acid (0.02 mg); cyanocobalamin (0.01 mg); and $Na_2S \cdot 9\ H_2O$ (0.45 g). The pH of the media prior to gassing/degassing (H_2:CO_2) was approximately 7.4 (final pH 7.0). Methanol (CH_3OH) was added to the media after autoclaving to give a final concentration of 0.4% (100 mM).

Ms. barkeri Fusaro was grown at 37°C according to Kandler and Hippe (1977). The media contained (per liter): yeast extract (2 g); K_2HPO_4 (0.35 g); KH_2PO_4 (0.23 g); NH_4Cl (0.5 g); NaCl (2.25 g); $MgSO_4 \cdot 7\ H_2O$ (0.50 g); $CaCl_2 \cdot 2\ H_2O$ (0.25 g); $NaSeO_4$ (0.04 mg); $NaHCO_3$ (0.85 g); Na_2CO_3 (1.7 g); resazurin (0.25 μg); nitrilotriacetic acid (20.2 mg); $FeCl_3 \cdot 6\ H_2O$ (2.1 mg); $CoCl_2 \cdot 6\ H_2O$ (2.0 mg); $MnCl_2 \cdot 4\ H_2O$ (1.0 mg); $ZnCl_2$ (1.0 mg); $NiCl_2 \cdot 6\ H_2O$ (1.0 mg); $CuSO_4 \cdot 2\ H_2O$ (0.5 mg); $Na_2MoO_4 \cdot 2\ H_2O$ (0.5 mg); pyridoxine-HCl (0.1 mg); riboflavin (0.5 mg); thiamine (0.05 mg); nicotinic acid (0.05 mg); *p*-aminobenzoic acid (0.05 mg); lipoic acid (0.05 mg); biotin (0.02 mg); folic acid (0.02 mg); cyanocobalamin (0.01 mg); and $Na_2S \cdot 9\ H_2O$ (0.45 g). The pH of the media prior to gassing/degassing was approximately 7.5 (final pH 6.5-6.7). For growth on CH_3OH, CH_3OH was added to the media after autoclaving to give a final concentration of 0.4% (100 mM). When acetate was used as methanogenic substrate, $NaCH_3COO$ was added (prior to gassing/degassing) to a final concentration of 200 mM. For growth on CH_3OH or acetate the gas phase was N_2:CO_2; for growth on CO_2, the gas phase was H_2:CO_2.

The hydrogenotrophic methanoarchaeon *Msp. hungatei* GP1, grown on H_2 and CO_2, was grown at 37°C according to Patel *et al.* (1976). The media contained (per liter); NaCl (0.3 g); $MgCl_2 \cdot 6\ H_2O$ (0.064 g); NH_4Cl (0.4 g); Na acetate (0.42 g); K_2HPO_4 (0.82 g); $CaCl_2 \cdot H_2O$ (0.064 g); resazurin (0.25 μg); Na_2CO_3 (1.0 g); nitrilotriacetic acid (20.2 mg); $FeCl_3 \cdot 6\ H_2O$ (2.1 mg); $CoCl_2 \cdot 6\ H_2O$ (2.0 mg); $MnCl_2 \cdot 4\ H_2O$ (1.0 mg); $ZnCl_2$ (1.0 mg); $NiCl_2 \cdot 6\ H_2O$ (1.0 mg); $CuSO_4 \cdot 2\ H_2O$ (0.5 mg); $Na_2MoO_4 \cdot 2\ H_2O$ (0.5 mg); pyridoxine-HCl (0.1 mg); riboflavin (0.05 mg); thiamine (0.05 mg); nicotinic acid (0.05 mg); *p*-aminobenzoic acid (0.05 mg); lipoic acid (0.05 mg); biotin (0.02 mg); folic acid

(0.02 mg); cyanocobalamin (0.01 mg); and $Na_2S \cdot 9\ H_2O$ (0.45 g). The pH of the media prior to gassing/degassing (H_2:CO_2) was approximately 8.5 (final pH 7.0).

Methanococcus thermolithotrophicus was grown at 63 °C according to R.Sparling (PhD thesis). The media contained (per liter); KCl (0.34 g); NH_4Cl (1.0); $MgCl_2 \cdot 6\ H_2O$ (5.1 g); $CaCl_2 \cdot 2\ H_2O$ (0.10 g); K_2HPO_4 (0.25 g); 2-(N-morpholino)-ethanesulfonic acid (MES, 9.75 g); Piperazine-N,N'-bis-2-ethanesulfonic acid (PIPES, 15.12 g); N-2-Hydroxyethylpiperazine-N'-2-ethanesulfonic acid (HEPES, 11.90 g); resazurin (0.25 μg); $NaWO_4 \cdot 2\ H_2O$ (0.07 mg); $NaSeO_3$ (0.04 mg); NaCl (11.68 g); Na Formate (20.40 g); nitrilotriacetic acid (20.2 mg); $FeCl_3 \cdot 6\ H_2O$ (2.1 mg); $CoCl_2 \cdot 6\ H_2O$ (2.0 mg); $MnCl_2 \cdot 4\ H_2O$ (1.0 mg); $ZnCl_2$ (1.0 mg); $NiCl_2 \cdot 6\ H_2O$ (1.0 mg); $CuSO_4 \cdot 2\ H_2O$ (0.5 mg); $Na_2MoO_4 \cdot 2\ H_2O$ (0.5 mg); and $Na_2S \cdot 9\ H_2O$ (0.45 g). The pH of the media prior to gassing/degassing (N_2:CO_2) was approximately 6.5 (final pH 5.8-6.2).

Depending on the methanoarchaeon or enzyme being studied, cultures could be harvested either aerobically or anaerobically in the anaerobic chamber (Coy Laboratory Products) containing an atmosphere of 10% H_2, balance N_2. In the anaerobic chamber, palladium catalysts were used to remove traces of O_2. When $F_{420}H_2$ dehydrogenation or F_{420}-reducing hydrogenase activities were being studied, cultures were harvested aerobically, with the exception of *Msph. stadtmanae*, which was processed under strictly anaerobic conditions. Harvesting of *Mc. thermolithotrophicus* for F_{420} was also conducted under anaerobic conditions. For anaerobic harvesting, all materials were placed in the anaerobic chamber for at least 8 hours prior to usage, usually overnight. Centrifuge bottles capped with rubber o-rings were used to prevent O_2 entry during centrifugation. Cells were centrifuged (15000xg) primarily with a Sorvall RC-5

centrifuge, at 4°C. Cultures were harvested and stored at -60°C in 50 mM HEPES, pH 7.0, containing 15% glycerol, ± 10 mM dithiothreitol, under an atmosphere of N_2. Typically, cells were grown, harvested, and frozen until an appropriate amount of cells have accumulated for experimental purposes.

3.3. Cell lysis

With the exception of *Mc. thermolithotrophicus*, all cultures were lysed *via* 3 passages through the French Press (SLM/Aminco, Rochestor) at either 20,000 psi or 40,000 psi (*Msph. stadtmanae*). When anaerobic conditions were required, cold 2 mM Na_2S was first passed through the press (3 times) to scavenge the O_2 from the pressure cell and from the inlet and outlet tubing. To maintain anaerobic conditions during the lysis process, the inlet and outlet tubing were capped with needles which pierced the rubber stoppers and allowed the extract to pass into the inlet valve and then through the outlet valve into another anaerobic container, minimizing exposure of cell extract to O_2. *Mc. thermolithotrophicus* did not require passage through the French Press, and could be lysed *via* suspension in low salt buffer.

Post lysis, the extract was centrifuged at low speed (22000xg) in a Sorvall RC-5 centrifuge, at 4°C to remove unlysed cells. This step was followed by high speed centrifugation (120000xg) for 45 minutes at 4°C in L8-80 ultracentrifuge to separate the membranous material from the clarified cell-free extract.

3.4. Production of F_{420}

F_{420} was used for a number of assays, including the $F_{420}H_2$ dehydrogenation activity, F_{420}-reducing activity, $F_{420}H_2$ oxidase activity, and for the synthesis of an F_{420}-affinity column. *Mc. thermolithotrophicus* was grown in either 1 L bottles (500 mL/bottle) or in an 11 litre fermentor (10 litre of media, New Brunswick Scientific). The cells were grown to late log phase, harvested anaerobically and then lysed in Tris/Cl, pH 8.0 (60% v/v) with CH_3OH (40% v/v) at 80°C for at least one hour. The lysed cell debris and membranes were removed *via* centrifugation at 22000xg in a Sorvall RC-5 centrifuge, at 4°C. The supernatant was then loaded onto a column of A-25 DEAE Sephadex and washed with 50 mM Tris/Cl, pH 8.0. The bound F_{420}/protein was then washed with stepwise increments of ammonium bicarbonate buffer, from 0.3 to 0.5 M; the F_{420} was separated from the other bound soluble components found in the supernatant, followed by elution from the column using the 1.0 M buffer. The F_{420}:ammonium bicarbonate solution was then heated at 80°C, and the ammonium bicarbonate was evaporated using a rotoevaporator. The F_{420} residue was resuspended in either 50 mM Tris/Cl, pH 8.0, or distilled H_2O.

3.5. Purification of the $F_{420}H_2$ dehydrogenation activity from methanol-grown Methanosarcina barkeri Fusaro and Methanospirillum hungatei GP1

All purification steps were performed aerobically at 4°C; three independent purifications were performed for each methanoarchaeon. Frozen cells were thawed and resuspended in 50 mM HEPES, pH 7.0, containing 5% glycerol, 50 μM phenylmethylsulfonyl fluoride (PMSF), and several crystals of RNase and DNase. The cell suspension was lysed *via* three passages through a French Pressure Cell

(SLM/Aminco, Rochestor), at 20000 psi and the resultant cell-free extract was centrifuged at 22000g. The supernatant was then further centrifuged at 180000g for 6 hours, 4°C. The high speed pellet (HSP) formed, which contains both the soluble cytoplasmic and membrane-bound $F_{420}H_2$ dehydrogenation activities, was homogenized in 10 mM HEPES, pH 7.0, containing 0.5 M NaCl (buffer A).

The homogenate was loaded onto a column of Ni^{2+}-charged iminodiacetic acid (45 mL) on Sepharose fast flow resin equilibrated in buffer A. The membranes, containing up to 20% of the overall $F_{420}H_2$ dehydrogenation activity, flowed through the column without binding, while the soluble activity bound to the Ni^{2+}-affinity column. The protein-loaded column was washed with 2-3 column volumes of buffer A, followed by washing with 2 column volumes of 10 mM HEPES, 0.5 M NaCl, and 0.05% Triton-X-100 (buffer B). The remaining protein, bound on the column as a dark golden-brown band, was eluted with buffer B supplemented with 25 mM imidazole.

Fractions (3.0 mL) containing $F_{420}H_2$ dehydrogenation activity were pooled and desalted using an Amicon ultrafiltrator, with an YM30 membrane. The concentrated protein, suspended in 10 mM HEPES, pH 7.0, 0.05% Triton-X-100, and 10% glycerol, was then loaded onto two 3-20% non-denaturing gradient PAGE gels (Hoeffer systems) and separated by electrophoresis overnight (no more than 15 hours) at a constant 150 V. Protein visualized as high molecular weight yellow-brown bands on the unstained PAGE were excised from the gel and cut into 1-2 mm^3 pieces, placed into the tubes of a Bio-Rad electro-elutor, and eluted from the gel after 8 hours, with fresh buffer exchanged every 2 hours. After electro-elution, the soluble protein was homogenized in 10 mM HEPES, pH 7.0, 0.05% Triton-X-100, and 10% glycerol, and stored at 4°C under N_2. Low molecular

weight bands of similar color were processed in the same manner. For the study of proteins that could not be visualized on the native PAGE, molecular markers were placed in the outermost lanes prior to electrophoresis. After electrophoresis, the lanes containing the markers were stained with coomassie blue and then detained until the molecular marker bands could be visualized. The molecular marker gel strips were washed in distilled water and then realigned with the unstained gel. Gel bands at the approximate molecular weight were then excised and processed as described above.

Membrane-bound $F_{420}H_2$ dehydrogenation activity was isolated from the non-binding fractions collected from the Ni^{2+}-affinity column. The membranes were sedimented, washed, and solubilized using the detergent CHAPS. The solubilized $F_{420}H_2$ dehydrogenation activity was enriched using either a discontinuous (40-45-50%) sucrose gradient ultracentrifugation step (*Msp. hungatei* GP1) or using a Ni^{2+}-affinity column (*Ms. barkeri* Fusaro), followed by desalting/concentration using an Amicon Ultrafiltrator. The concentrated protein was then loaded onto a pair of 3-20% non-denaturing gradient PAGE gels (Hoeffer systems) and electrophoresed overnight (no more than 15 hours) at a constant 150 V.

The protein from the membranes of *Ms. barkeri* Fusaro could be visualized as high molecular weight yellow-brown bands, which were then excised from the gel and cut into 1-2 mm^3 pieces, placed into the tubes of a Bio-Rad electro-elutor, and electrophoresed for 8 hours with fresh buffer exchanged every 2 hours. For the study of proteins that could not be visualized on the native PAGE, molecular markers were placed in the outermost lanes prior to electrophoresis and processed as described above.

The bands of electrophoresed membrane protein from *Msp. hungatei* GP1 were faint and more difficult to visualize, so the native gel was prepared as described above, using molecular markers in the outer gel lanes. After electro-elution, the protein was homogenized in 10 mM HEPES, pH 7.0, 0.05% Triton-X-100, and 10% glycerol, and stored at 4°C under N_2.

3.6. Enzyme assays

3.6.1. $F_{420}H_2$ dehydrogenation assays

Enzyme assays were performed using anaerobic stoppered 12 mm x 75 mm glass cuvettes as described by Daniels and Wessels (1984). The rate of oxidation/reduction of F_{420} ($\varepsilon_{420\,nm} = 45.5\ mM^{-1}\cdot cm^{-1}$) or reduction of methyl viologen ($\varepsilon_{560\,nm} = 8\ mM^{-1}\cdot cm^{-1}$) was followed spectrophotometrically using an LKB Novaspec II spectrophotometer.

The assay buffer for $F_{420}H_2$ dehydrogenation activity normally consisted of 40 mM potassium phosphate, pH 7.0, 0.5 M sucrose, and 10 mM dithiothreitol (DTT), under an atmosphere of N_2. $F_{420}H_2$ dehydrogenation assay tubes for *Msph.stadtmanae* consisted of 200 mM KPO_4 rather than the 40 mM KPO_4 used for other methanoarchaea.

F_{420} was reduced according to Haase *et al.* (1992). Sodium borohydride was added in small increments to the F_{420} (flushed with N_2) until the solution turned colorless. Concentrated HCl was then added to destroy excess sodium borohydride; HCl was added until the solution just turned cloudy. KOH (10 N) was added dropwise to neutralize excess HCl, until the cloudiness just cleared. Reduced F_{420} was gassed/degassed under N_2 and then added to the assay mix immediately prior to measurement, followed by addition of purified enzyme or enzyme extract. As a control, a baseline for $F_{420}H_2$

oxidation in the absence of electron acceptors was established, before the reaction was initiated by addition of electron acceptor. No reaction was observed in the absence of $F_{420}H_2$.

3.6.2. Hydrogenase assays

3.6.2.1. F_{420}-reducing hydrogenase activity

The buffer for assay of the F_{420}-reducing hydrogenase was modified from Choquet and Sprott (1991) and consisted of 100 mM HEPES, pH 7.0, with 10 μM F_{420}, 10 μM FAD, 200 mM KCl, 20 mM $MgCl_2 \cdot 6H_2O$, and 20 mM DTT, under an atmosphere of H_2. Protein was reductively reactivated in the F_{420}-reducing hydrogenase assay tube (until the FAD and F_{420} were reduced), followed by addition of F_{420} (20-25 μM) and measurement of activity. Assays were also performed under an atmosphere of N_2 (control). 50 mM Tris/Cl, pH 8.0, and 200 mM KPO_4, pH 7.0, were also used to test for optimum F_{420}-reducing activity of *Msph. stadtmanae*.

3.6.2.2. F_{420}-nonreducing hydrogenase activity

Assay tubes to measure F_{420}-nonreducing hydrogenase activity contained 50 mM Tris/Cl, pH 8.0, 0.05 mM methyl viologen, 20 mM DTT, and 20 mM $MgCl_2 \cdot 6H_2O$, under an atmosphere of H_2. Protein was reductively activated in the assay tube (until the tubes turned light blue), followed by addition of methyl viologen (final concentration: 2 mM) and measurement of activity.

3.6.2.3. H_2-dependent phenazine reduction

H_2-dependent phenazine reduction was observed using $F_{420}H_2$ dehydrogenation buffer, under an atmosphere of H_2. Protein was incubated in anaerobic buffer for 30 minutes to ensure that the protein was reductively reduced before phenazine (100 μM, $\varepsilon_{365\,nm} = 13\ mM^{-1} \cdot cm^{-1}$) was added to the reaction mix.

3.6.3. $F_{420}H_2$ oxidase activity of Methanosphaera stadtmanae

All manipulations of *Msph. stadtmanae* cultures and extracts were performed in the anaerobic chamber, with the exception of cell lysis (French press) and centrifugation steps. O_2-dependent $F_{420}H_2$ oxidation from the cell-free extract of *Msph. stadtmanae* was assayed according to Seedorf *et al.* (2004). The assay buffer consisted of 50 mM Tris/Cl, pH 7.6 dispensed into 12 mm x 75 mm glass cuvettes sealed with rubber stoppers, and made anaerobic by gassing with N_2. $F_{420}H_2$ was added to a final concentration of 15 μM. Additions of O_2 prior to assay were made using air-saturated water (~250 μM O_2). Distilled water was bubbled with breathing grade air (Welders Supplies) for at least two hours and then dispensed and sealed into a Balch tube, followed by pressurization with breathing grade air. The reaction was measured following addition of the air-saturated water to assay tubes containing cell-free extract and $F_{420}H_2$. A background for $F_{420}H_2$ oxidation was established prior to addition of the air-saturated water. $F_{420}H_2$ oxidase assays were performed at ambient room temperature (~25°C).

A problem that arose during the $F_{420}H_2$ oxidase assays is the presence of O_2 in the tubes prior to addition of O_2-saturated H_2O. Unlike the $F_{420}H_2$ dehydrogenation/F_{420}-

reducing hydrogenase assays, reducing agents are not added to the $F_{420}H_2$ oxidase buffer, to prevent the removal of O_2 necessary for assay of the $F_{420}H_2$ oxidase activity. However, traces of O_2 may be trapped in the assay tubes even after evacuating with N_2. As a result, the addition of cell-free extract to assay tubes containing $F_{420}H_2$ leads to significant $F_{420}H_2$ oxidation in the absence of reducing agent or O_2-saturated H_2O. To alleviate this problem, O_2-saturated H_2O was added only after the O_2 present in the tubes was reduced (i.e. a stable baseline for $F_{420}H_2$ oxidation was reached in the absence of injected O_2).

3.7. Gel electrophoresis

3.7.1. SDS-PAGE gel electrophoresis

SDS-PAGE gels were prepared according to Laemmli (1970), with an acrylamide concentration of 12.8%. Protein samples, mixed with SDS loading buffer, were incubated at 100°C for 5 minutes and loaded immediately onto the SDS PAGE gel followed by electrophoresis using a Bio-Rad mini-protean II electrophoresis unit for 1-2 hours at a constant voltage of 150 V. Following electrophoresis, the SDS-PAGE gels were stained with Coomassie Brilliant Blue R, followed by staining with silver nitrate.

3.7.1.1. Amino-terminus sequencing

For amino (N-) terminus sequencing of individual subunits, unstained SDS PAGE gels were electroblotted immediately after electrophoresis onto nitrocellulose papers for approximately one hour at 4°C, using a Bio-Rad electro blotter. The paper was then stained using ponceau reagent and the bands were aseptically cut out and stored at -20°C

until they were transferred for sequencing. N-terminal sequencing of the purified subunits was performed by the Center of Proteomics at the University of Victoria.

3.7.1.2. Mass Spectroscopy analysis

Mass spectroscopy sequencing of fragments of the purified phenazine-dependent $F_{420}H_2$ dehydrogenation activity of *Msp. hungatei* GP1 was performed in the Department of Physics, at the University of Manitoba. A protocol for sample preparation prior to mass spectroscopy analysis is given here. Following electrophoresis the SDS page gel was stained in coomassie blue for 1-2 hours, followed by destaining of the gel to remove background. The stained bands were then cut out of the gel into 1 mm^3 cubes and placed into eppendorf tubes, using a scalpel wiped with 50% CH_3OH between each sample. Prior to digestion, the gel bands were destained *via* the following steps (constituting one cycle). The bands were washed with 100 mM ammonium bicarbonate to neutralize the acetic acid remaining after destaining, followed by washing in 40% acetonitrile (in ammonium bicarbonate) to remove the coomassie blue dye, with rotation of the eppendorf tubes for 10 minutes. The tubes were then centrifuged to remove liquid. Acetonitrile was added to the gel pieces, which further removed salt and detergent; the gel pieces were then allowed to sit in the acetonitrile for 5 minutes and then spun to remove the acetonitrile (end of cycle). The cycle was repeated, starting with the addition of 100 mM ammonium bicarbonate, until the dyes on the gel were completely removed.

In-gel digestion of the destained gel pieces proceeded with incubation of the gel in freshly made 10 mM dithiothreiotol (DTT), in 100 mM ammonium bicarbonate (2-3x gel volume), for 45 minutes at 57.5°C. The tubes were then centrifuged, and the volume

of DTT removed was noted. The difference in the volume of DTT added and removed indicated the amount required to swell the gel; this volume is equal to the amount of trypsin that was added for digestion of the protein in the gel. 55 mM iodoacetamide in 100 mM ammonium bicarbonate is added to the eppendorf tubes, followed by incubation in the dark for 30 minutes. Afterwards, the tubes were centrifuged and the liquid discarded. Trypsin (5 ng/μl) in 100 mM ammonium bicarbonate was added to the tubes, and incubated at 37°C overnight.

Following trypsin digestion, the tubes were briefly centrifuged and the liquid (referred to as supernatant) was set aside. 0.01% TFA was added to stop digestion of the protein (5 minute incubation). The liquid was then added to the supernatant previously reserved. The following steps constitute a cycle. Peptide extraction began with the addition of 2-3 volumes of 0.01% TFA in 50% ACN, followed by sonication for 10 minutes in cold water. The tubes were centrifuged, and the liquid was collected and pooled with the supernatant. To complete the cycle, the gel pieces were then incubated for 5 minutes in 40% ACN, followed by centrifugation and removal of the liquid to be added to the supernatant. The cycle was then repeated two more times, beginning with the addition of 0.01% TFA in 50% ACN to the gel pieces in the eppendorf tubes. It is important to note that all of the liquid was reserved and stored with their respective pools.

After the extraction process was completed, the peptide samples were concentrated using a Speed Vac. When necessary, gel pieces remaining in the sample were removed with a ZipTip.

3.7.2. Native gradient PAGE gel electrophoresis

Native gradient (3-20% acrylamide) PAGE gels were loaded with 140 μg protein per lane, and electrophoresed for at least 15 hours (no more than 20 hours) at a constant 150 V. The gels were then stained with Coomassie Brilliant Blue R, followed by silver staining according to a protocol ProteoSilver Plus Silver Stain Kit (Prot-Sil2) from Sigma Aldrich.

Activity stains of the native gradient PAGE gels were performed as follows. Following electrophoresis, the native PAGE gels were submerged in anaerobic 50 mM Tris/Cl buffer, pH 8.0, containing 2 mM methyl viologen, 20 mM $MgCl_2$, and 5 mM DTT. The gels were then incubated inside an anaerobic chamber under an atmosphere of (approximately) 10% H_2 (balance N_2) until strong blue bands of reduced methyl viologen could be visualized. Prior to removal of the gels from the anaerobic chamber, 2,3,5-triphenyltetrazolium chloride (1.5 % stock) was added to fix the reduced methyl viologen bands to the gel, producing aerobically-stable red activity-stained bands.

3.8. Genome sequence analysis

BLAST (Basic Local Alignment Search Tool) searches of the *Archaea* database were performed at the NCBI website (National Center for Biotechnology Information, http://www.ncbi.nlm.nih.gov/), using the tblastn program (using a protein query to search the translated nucleotide database). Protein queries are as described in the appropriate chapters.

3.9. Protein determination

Protein concentration was determined using the Bradford (1976) method, using bovine serum albumin as standard.

4. $F_{420}H_2$ dehydrogenation activity in the methanoarchaea

4.1 Introduction

Members of the order *Methanosarcinales* are the most metabolically and physiologically versatile methanoarchaea, containing members capable of metabolizing methylotrophic (methyl-group containing) compounds and/or acetate; some of these methanoarchaea can also grow on H_2 plus CO_2 or CO (Galagan *et al.* 2002, Rother and Metcalf 2004, Maeder *et al.* 2006).

The $F_{420}H_2$ dehydrogenase, also known as the Fpo ($F_{420}H_2$ phenazine oxidoreductase) complex, is a membrane-bound, multi-subunit protein involved with electron transfer reactions and energy conservation in methylotrophic methanoarchaea of the *Methanosarcinaceae* that metabolize methanol or CO (Deppenmeier 2004, J.G. Ferry, personal communication). The complex transfers reducing equivalents from the methanogenic electron carrier coenzyme $F_{420}H_2$ to the electron carrier methanophenazine (Abken *et al.* 1998). Electrons are then transferred from reduced methanophenazine to the heterodisulfide reductase (Hdr), and ultimately leading to reduction of the heterodisulfide complex (CoM-S-S-CoB) to free cofactors CoM-SH and CoB-SH (Figure 17, section 1.5.2.4.) (Deppenmeier 2002, 2004). The two redox reactions are coupled to energy conservation, generating a transmembrane proton gradient used to synthesize ATP *via* A_1A_0 ATP synthase (Bäumer *et al.* 1998, Brodersen *et al.* 2000).

The $F_{420}H_2$ dehydrogenase of *Methanolobus tindarius* and *Methanosarcina mazei* Gö1 were both initially described as holoenzymes (115-120 kDa) consisting of 5 distinct subunits (FpoBCDFI), containing FeS clusters and FAD as prosthetic groups (Haase *et al.* 1992, Abken and Deppenmeier 1997). Analysis of the genome from *Ms. mazei* Gö1

revealed a much more sophisticated complex consisting of 13 subunits, with gene sequences and operon structure reminiscent of the NADH:ubiquinone oxidoreductase (NDH-1, Complex I) of *E. coli*, and also sharing similarities with the subunits of analogous structures from various eukaryotic organisms (Bäumer *et al.* 2000). It has been suggested that the predicted 400 kDa complex was not isolated during the purification process described by Abken and Deppenmeier (1997) due to the use of the detergent CHAPS to solubilize the protein from the cell membranes, which may have led to the fragmentation of the large protein complex; the use of a milder detergent, octylglycoside, resulted in the partial purification of the 400 kDa Fpo complex (Deppenmeier 2002).

As the amount of methanophenazine isolated from the cell membranes of *Ms. mazei* Gö1 was extremely low, and too hydrophobic to be assayed using standard aqueous buffers, 2-hydroxy (2-OH)-phenazine was synthesized and used to assay the dehydrogenase activity (Beifuss and Tietze 2005). Phenazine could also be used as an electron acceptor to assay the $F_{420}H_2$ dehydrogenase activity, although it was not as effective as 2-OH-phenazine; the K_m for phenazine was almost 10-fold higher than the K_m for 2-OH-phenazine. As it is commercially available, phenazine is used in our laboratory to assay the $F_{420}H_2$ dehydrogenation activity. Phenazine is also used to assay membrane-bound hydrogenase activity and CoM-S-S-CoB reduction in the methanoarchaeon *Methanomicrococcus blatticola*, a member of the *Methanosarcinales*; the presence of methanophenazine has not been confirmed in this methanoarchaeon (Sprenger *et al.* 2005). It should be noted that methanophenazine has not been isolated from methanoarchaea other than *Ms. mazei* Gö1; much like cytochromes, this compound

may not exist in methanoarchaea outside of the *Methanosarcinaceae*. The genes coding for methanophenazine biosynthesis proteins have not been identified to date.

The 2-OH phenazine-dependent $F_{420}H_2$ dehydrogenase activity of *Ms. mazei* Gö1 was found to be competitively inhibited by the presence of diphenyleneiodonium (DPI) chloride, a compound with a planar structure similar to phenazine (Brodersen *et al.* 1999). DPI is also an inhibitor of flavoproteins such as mitochondrial and bacterial NADH:ubiquninone oxidoreductase, and neutrophil NADPH oxidase; DPI inhibits (uncompetitive) these enzymes by binding to the FAD component of the respective enzymes (O'Donnell *et al.* 1993, Majander *et al.* 1994). Thus, inhibition of phenazine-dependent $F_{420}H_2$ dehydrogenation activity by DPI could indicate the presence of a protein similar to the $F_{420}H_2$ dehydrogenase of *Ms. mazei* Gö1.

Thus far, the $F_{420}H_2$ dehydrogenase has been isolated from only two methylotrophic methanoarchaea *Ml. tindarius* and *Ms. mazei* Gö1 (Haase *et al.* 1992, Abken and Deppenmeier 1997). The genome of *Methanosarcina* (*Ms.*) *barkeri* Fusaro and *Methanosarcina* (*Ms.*) *acetivorans* C2A, both of which are capable of methylotrophic growth, also contain genes encoding for the subunits of the Fpo complex, (J.G. Ferry, personal communicaton, Maeder *et al.* 2006). A similar complex has also been purified from the sulfate-reducing archaeon *Archaeoglobus fulgidus*, which is phylogenically related to the *Methanosarcinales* (Kunow *et al.* 1994, Brüggermann *et al.* 2000). This complex has not been isolated in methanoarchaea outside of the *Methanosarcinaceae*, and analyses of the published genomes of *Methanocaldococcus jannaschii*, *Methanothermobacter thermoautotrophicus* ΔH and *Methanopyrus kandleri* have not indicated the presence of a distinct Fpo complex, although there are gene sequences

related to complex I that are found in all methanoarchaea, encoding the membrane-bound multi-subunit energy conserving hydrogenase (Ech) (Bult *et al.* 1996, Smith *et al.* 1997, Slesarev *et al.* 2002, Hedderich 2004, Fricke *et al.* 2006).

Research in our laboratory has demonstrated that $F_{420}H_2$ dehydrogenation activity is not restricted by methanogenic substrate or to the *Methanosarcinaceae*, and was apparently ubiquitous in all of the methanoarchaea studied in our laboratory. Phenazine-dependent $F_{420}H_2$ dehydrogenation activity has been detected in the cell free extracts from methanoarchaea metabolizing H_2 and CO_2, acetate, H_2 and methanol. The results of a survey examining the $F_{420}H_2$ dehydrogenation activity and DPI-inhibition are detailed in this chapter. There are several possible candidates for this activity, including the F_{420}-reducing hydrogenase, which are discussed in section 4.7.

4.2. Materials and methods

For a comprehensive look at the materials and methods used for this chapter, the reader is referred to the following sections in Chapter 3:

3.2. Growth media

3.3. Cell lysis

3.6. Enzyme assays

3.6.1. $F_{420}H_2$ dehydrogenation assays

4.3. Results and Discussion

The results of a survey examining the phenazine-dependent $F_{420}H_2$ dehydrogenation activities in cell-free extracts from a number of methanoarchaea across the methanogenic orders are summarized in Table 4.1. This activity is observed in all

methanoarchaea regardless of growth substrate, to varying degrees, but the physiological significance of this activity is unclear. In most instances, phenazine ($E^{\circ\prime}$= -0.265 to -0.165 V) appears to be more effective as an electron acceptor, compared to methyl viologen ($E^{\circ\prime}$= -0.446 V), ranging from a 2- to 10-fold increase in activity. However, methyl viologen and phenazine show little difference in electron accepting capability when looking at the $F_{420}H_2$ dehydrogenation activities of *Msp. hungatei* GP1 and *Msph. stadtmanae*, which contained low activities.

$F_{420}H_2$ ($E^{\circ\prime}$= -0.360 V), when mixed with cell-free extract ± cell membranes, is oxidized to F_{420} and H_2 in the absence of added electron acceptor, a function of the 'reverse' F_{420}-reducing hydrogenase activity. To distinguish between the reverse hydrogenase activity from phenazine- (or another electron acceptor) dependent $F_{420}H_2$ oxidation, a stable baseline of $F_{420}H_2$ oxidation in the absence of electron acceptor is established prior to addition of electron acceptor and subtracted from the activity measured upon addition of electron acceptor.

4.4. Phenazine-dependent $F_{420}H_2$ dehydrogenation activity in the Methanosarcinales

The highest levels of phenazine-dependent $F_{420}H_2$ dehydrogenase activities were observed with *Ml. tindarius* and CH_3OH-grown *Ms. barkeri* Fusaro (Table 4.1). By comparison, cultures of *Ms. barkeri* Fusaro grown on H_2:CO_2 or acetate were approximately 2- and 4-fold lower, respectively. The corresponding activity in *Mst. concilli*, an aceticlastic member of the *Methanosarcinales*, was 5-fold lower. For further study, the phenazine-dependent $F_{420}H_2$ dehydrogenation activity of *Ml. tindarius* and CH_3OH-grown *Ms. barkeri* Fusaro were examined.

Table 4.1. Comparison of the $F_{420}H_2$ dehydrogenation activities found in the cell-free extract of various methanoarchaea. Result are the average of three separate experiments.

Methanoarchaeon	Order	Growth substrate	$F_{420}H_2$ $deH_2ase^{\dagger}$ (phenazine)	$F_{420}H_2$ $deH_2ase^{\dagger}$ (MV)	$K_{m\ phenazine}{}^{\ddagger}$	$Vmax^{\ddagger\ddagger}$	Ic_{50} (µM DPI)
Ml. tindarius	*Methanosarcinales*	Methanol	0.379	0.2	266.7 ± 44.0	0.50 ± 0.04	3
***Ms. barkeri* Fusaro**	*Methanosarcinales*	Methanol	0.421	0.048	95.0 ± 19.6	0.40 ± 0.03	>100
		H_2:CO_2	0.225	0.047	ND	ND	ND
		Acetate	0.116	0.019	ND	ND	ND
Mst. concilli	*Methanosarcinales*	Acetate	0.087	0.042	ND	ND	ND
***Msp. hungatei* GP1**	*Methanomicrobiales*	H_2:CO_2	0.129	0.123	243.0 ± 21.1	0.39 ± 0.01	25
Mc. voltae	*Methanococcales*	H_2:CO_2	0.212	0.067	915.5 ± 213.4	0.60 ± 0.1	25
Mtb. marburgensis	*Methanobacteriales*	H_2:CO_2	0.270	0.07	254.2 ± 60.8	0.41 ± 0.05	30
Mb. bryantii	*Methanobacteriales*	H_2:CO_2	0.296	0.091	318.1 ± 48.5	0.92 ± 0.07	10
Msph. stadtmanae	*Methanobacteriales*	H_2:methanol	0.0023	0.005	138.2 ± 17.5	.003 ± 0.0002	2.5

† µmol $F_{420}H_2$ oxidized·min^{-1}·mg^{-1}
‡ µM phenazine
‡‡ µmol $F_{420}H_2$ oxidized·min^{-1}·mg^{-1}
ND, not determined

4.4.1. Methanolobus tindarius

Ml. tindarius is a mesophilic marine, coccoid methanoarchaeon growing solely on methanol and methylamines as carbon and energy source (König and Stetter 1982). *Ml. tindarius* is a member of the *Methanosarcinaceae* family and one of the first methanoarchaea for which the $F_{420}H_2$-dependent CoM-S-S-CoB reduction was studied, and the first for which the $F_{420}H_2$ dehydrogenase activity was purified (Deppenmeier *et al.* 1990a, Haase *et al.* 1992).

Ml. tindarius contains the Fpo complex, but no F_{420}-reducing hydrogenase, making this methanoarchaeon a suitable model of activity for comparison with the $F_{420}H_2$ dehydrogenation activity found in other methanoarchaea (Deppnemeier *et al.* 1989, Haase *et al.* 1992). The $F_{420}H_2$ dehydrogenase activity was initially assayed using methyl viologen and metronidazole (Haase *et al.* 1992), but this activity was assayed in our studies using phenazine as an electron acceptor; the phenazine-dependent activity was approximately two-fold higher compared to the activity assayed using the same concentration of methyl viologen (Table 4.1).

The apparent K_m for phenazine was determined to be 267 μM (cell-free extract); the apparent K_m for phenazine of the purified $F_{420}H_2$ dehydrogenation activity of *Ms. mazei* Gö1 is 250 μM (Abken *et al.*1998). While the presence of methanophenazine has not yet been reported, it is expected that this compound would be found in the membranes of *Ml. tindarius*. The phenazine-dependent activity was strongly inhibited by the presence of DPI (Ic_{50} ~ 3 μM DPI) (Figure 4.1A). Addition of 3 and 9 μM DPI increased the apparent K_m for phenazine, respectively, 266 μM to 1168 and 2313 μM,

A.

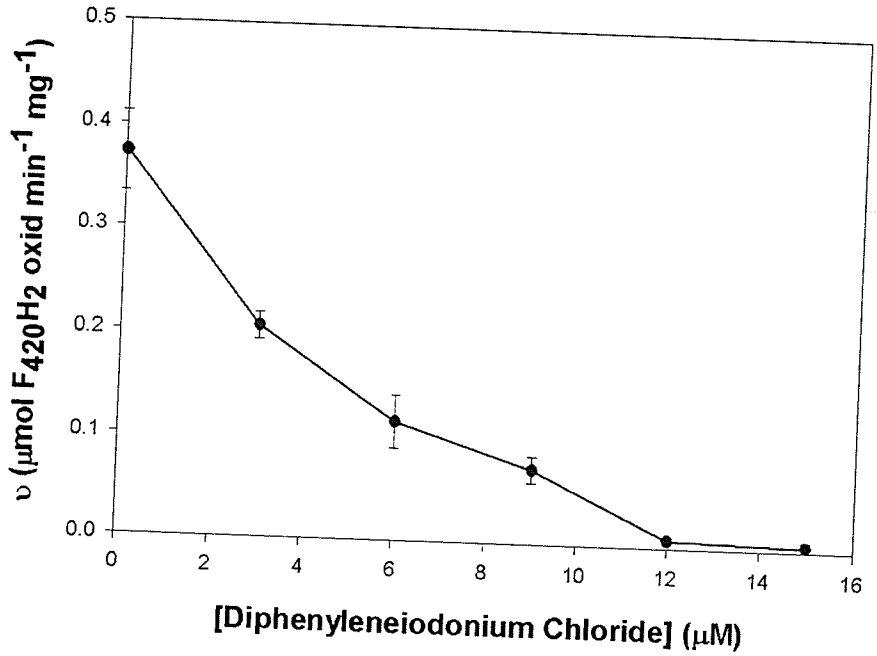

B.

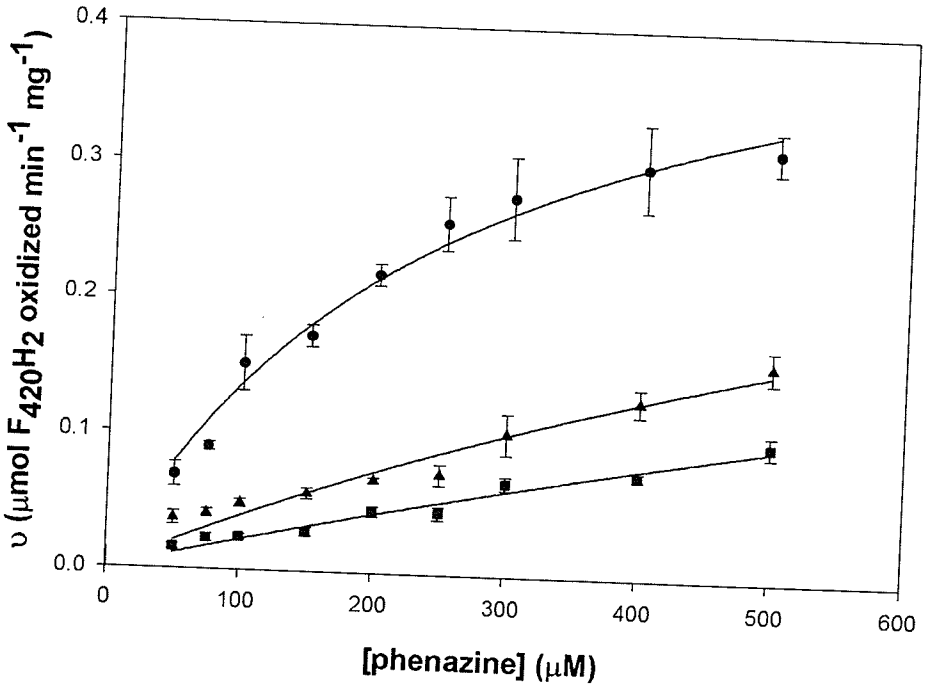

Figure 4.1. (A) Sensitivity of the phenazine-dependent $F_{420}H_2$ dehydrogenase activity of *Methanolobus tindarius* (in cell-free extract) to diphenyleneiodonium (DPI) chloride and (B) Michaelis Menten kinetics plot of the phenazine-dependent $F_{420}H_2$ dehydrogenase activity in the absence/presence of DPI (B). ●, no DPI added. ▲, + 3 μM DPI. ■, + 9 μM DPI.

with Vmax = 0.5 μmol $F_{420}H_2$ oxidized·min^{-1}·mg^{-1} (Figure 4.1B). Similar kinetic parameters were observed were observed when using washed membranes in place of cell-free extract, which contained 15-20% of the overall $F_{420}H_2$ dehydrogenase activity, indicating competitive inhibition of the $F_{420}H_2$ dehydrogenase activity by DPI.

DPI-mediated inhibition of the phenazine-dependent $F_{420}H_2$ dehydrogenase in *Ml. tindarius* was similar to observations made using purified $F_{420}H_2$ dehydrogenase of *Ms. mazei* Gö1(using 2-OH-phenazine), where the addition of 1 μM DPI induced an increase in the apparent K_m for 2-OH-phenazine from 35 to 100 μM (Brodersen *et al.* 1999).

4.4.2. Methanosarcina barkeri *Fusaro*

Ms. barkeri Fusaro is also a member of the *Methanosarcinaceae* and extremely versatile with respect to its selection of methanogenic substrate; like *Ms. mazei* Gö1, *Ms. barkeri* can metabolize methanol ± H_2, H_2:CO_2, or acetate for methanogenesis (Maeder *et al.* 2006). $F_{420}H_2$ dehydrogenation activity was detected in the cell-free extract of *Ms. barkeri* Fusaro when it is grown on the various substrates, to varying levels (Table 4.1).

Phenazine-dependent $F_{420}H_2$ dehydrogenation activity was measured from the cell-free extract and membranes of methanol-grown *Ms. barkeri* Fusaro, but the source of this activity was not immediately clear. Work in our laboratory revealed that the $F_{420}H_2$ dehydrogenation activity of *Ms. barkeri* Fusaro, grown on methanol, elutes with an F_{420}-reducing hydrogenase activity (data not shown, Wong, PhD thesis 1999); on the other hand, the Fpo complex does not possess F_{420}-reducing hydrogenase activity (Abken and Deppenmeier 1997).

A.

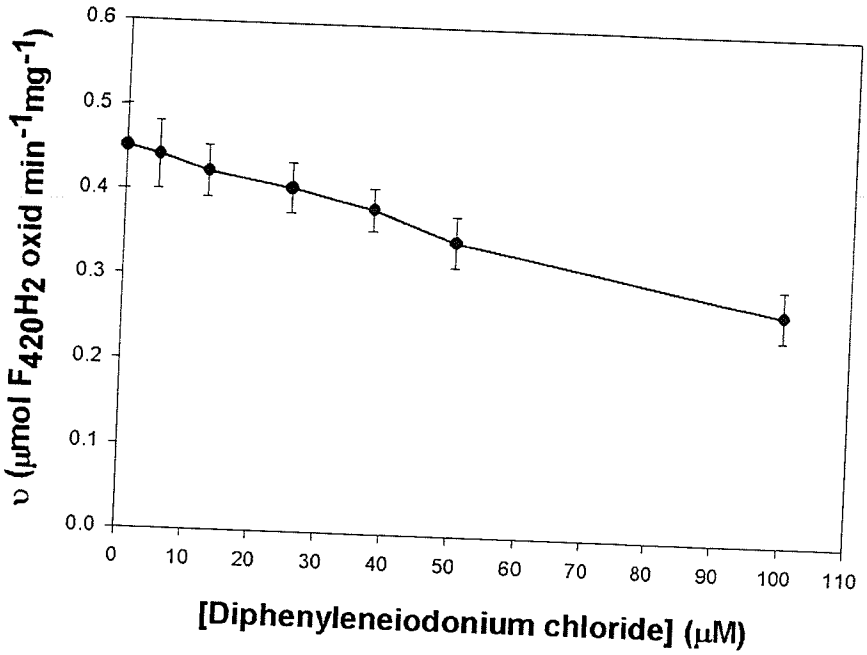

B.

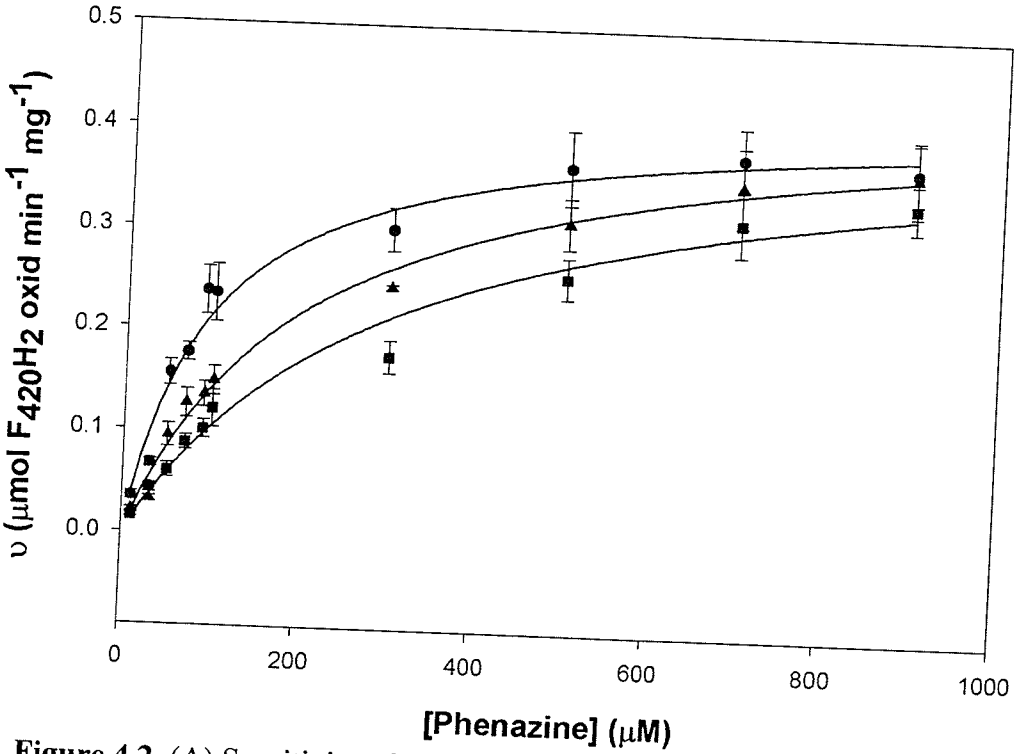

Figure 4.2. (A) Sensitivity of the phenazine-dependent $F_{420}H_2$ dehydrogenase activity of CH_3OH-grown *Methanosarcina barkeri* Fusaro (in cell-free extract) to diphenyleneiodonium (DPI) chloride and (B) Michaelis Menten kinetics plot of the phenazine-$F_{420}H_2$ dehydrogenase activity in the absence/presence of DPI (B). ●, no DPI added. ▲, + 50 μM DPI. ■, + 100 μM DPI.

Phenazine was an effective electron acceptor for the $F_{420}H_2$ dehydrogenation activity, with a 5- to 10-fold increase in $F_{420}H_2$ dehydrogenation activity relative to methyl viologen (Table 4.1). The apparent K_m for phenazine of the $F_{420}H_2$ dehydrogenation activity in cell-free extract from *Ms. barkeri* Fusaro was 95 μM (Vmax = 0.40 μmol $F_{420}H_2$ oxidized·min^{-1}·mg^{-1}), which is approximately 2.5-fold lower than the corresponding K_m for *Ml. tindarius* (266 μM), indicating a higher affinity for the substrate. Similar to the activity of *Ml. tindarius*, the phenazine-dependent $F_{420}H_2$ dehydrogenation activity was competitively inhibited by the presence of DPI, though not to the same extent. There was a substantial difference in the degree of inhibition of the phenazine-dependent $F_{420}H_2$ dehydrogenation activity, as can be seen in Figure 4.2A. Addition of 50 and 100 μM DPI increases the apparent K_m value, from 95 to 213 and 317 μM, respectively (Figure 4.2B).

It is clear that the while both *Ml. tindarius* and *Ms. barkeri* Fusaro possess phenazine-dependent $F_{420}H_2$ dehydrogenation activities, there are several differences that distinguish the respective activities. Addition of DPI has a more significant effect on the activity of *Ml. tindarius*, comparable to the inhibition reported for *Ms. mazei* Gö1 by Brodersen *et al.* (1999). The inhibition curve for *Ml. tindarius* (Ic_{50} = 3 μM DPI) shows a much steeper drop in dehydrogenation activity compared to *Ms. barkeri* Fusaro (Ic_{50} > 100 μM DPI). Low concentrations of DPI (3 μM) were effective in inhibiting the $F_{420}H_2$ dehydrogenation activity in *Ml. tindarius*, the same concentration has a negligible effect on the analogous activity in *Ms. barkeri* Fusaro. The addition of 100 μM DPI only decreased the $F_{420}H_2$ dehydrogenation activity of *Ms. barkeri* Fusaro by 30% (Figure

4.2A); at that same concentration the corresponding activity of *Ml. tindarius* was already completely inhibited (Figure 4.1A).

The differences between the $F_{420}H_2$ dehydrogenation activities of the respective methanoarchaea are also emphasized when examining the Michaels Menten kinetic plots in the presence/absence of DPI of the respective methanoarchaeons (Figure 4.1B and 4.2B). The apparent K_m for phenazine for *Ml. tindarius* drastically increases from 266 μM to 1168 μM (3 μM DPI) and 2313 μM (9 μM DPI) (Vmax = 0.5 μmol $F_{420}H_2$ oxidized·min^{-1}·mg^{-1}); in contrast, the same concentrations of DPI have a minor effect on the $F_{420}H_2$ dehydrogenation activity of *Ms. barkeri* Fusaro, where the K_m increases from 95 μM to 213 μM (50 μM DPI) and 317 μM (100 μM DPI), (Vmax = 0.4 μmol $F_{420}H_2$ oxidized·min^{-1}·mg^{-1}). The phenazine-dependent $F_{420}H_2$ dehydrogenation activity of *Ms. barkeri* Fusaro is further examined in Chapter 6.

4.5. Phenazine-dependent $F_{420}H_2$ dehydrogenation activity in other methanoarchaea

Phenazine-dependent $F_{420}H_2$ dehydrogenation activity was also detected in methanoarchaea outside of the *Methanosarcinaceae*; this activity is not restricted to the use of methanol as methanogenic substrate since this activity could be detected in the cell-free extract of methanoarchaea growing on H_2 and CO_2 or acetate (Table 4.1). The observed activity was also inhibited by the presence of DPI, to varying degrees.

4.5.1. Phenazine-dependent $F_{420}H_2$ dehydrogenation activity in the Methanomicrobiales*: Methanospirillum hungatei GP1*

Methanospirillum hungatei GP1 is a hydrogenotrophic methanoarchaeon from the order *Methanomicrobiales*. An F_{420}-reducing hydrogenase has been purified from this

methanoarchaeon (Sprott *et al.* 1987, Choquet and Sprott 1991), but unlike other hydrogenotrophic methanoarchaea, an F_{420}-nonreducing hydrogenase is apparently not expressed by this methanoarchaeon (Sprott *et al.* 1987). The F_{420}-nonreducing hydrogenase is an important component of the H_2:heterodisulfide oxidoreductase complex which catalyzes the reduction of CoM-S-S-CoB when H_2 and CO_2 are used as methanogenic substrate (Thauer *et al.* 1993, Thauer 1998).

Our studies have detected an $F_{420}H_2$ dehydrogenation activity in the cell-free extract and membranes of this methanoarchaeon. Phenazine acts as an electron acceptor for the $F_{420}H_2$ dehydrogenation activity, but its specificity as an electron acceptor was similar to methyl viologen (Table 4.1). In the absence of an F_{420}-nonreducing hydrogenase, it is of interest that the source of the $F_{420}H_2$ dehydrogenation activity be investigated. The apparent K_m for phenazine of the $F_{420}H_2$ dehydrogenation activity in cell-free extract is 242.6 μM (Vmax = 0.39 μmol $F_{420}H_2$ oxidized $\cdot min^{-1} \cdot mg^{-1}$), which is similar to the value obtained for *Ms. mazei* Gö1 (Abken *et al.* 1998) and *Ml. tindarius* (this thesis). The $F_{420}H_2$ dehydrogenation activity of *Msp. hungatei* GP1 is inhibited by the addition of DPI (Ic_{50} = 25μM, Figure 4.3A), not to the same extent as *Ml. tindarius*, but more similar to the inhibition observed with *Ms. barkeri* Fusaro. Addition of 12.5 and 25 μM DPI increased, respectively, the apparent K_m increased from 242.6 to 308.1 and 403.4 μM (Vmax = 0.38 and 0.37μmol $F_{420}H_2$ oxidized $\cdot min^{-1} \cdot mg^{-1}$, respectively) (Figure 4.3B).

In the absence of the F_{420}-nonreducing hydrogenase, it is possible that *Msp. hungatei* uses an $F_{420}H_2$-dependent mechanism to reduce CoM-S-S-CoB, in a manner

A.

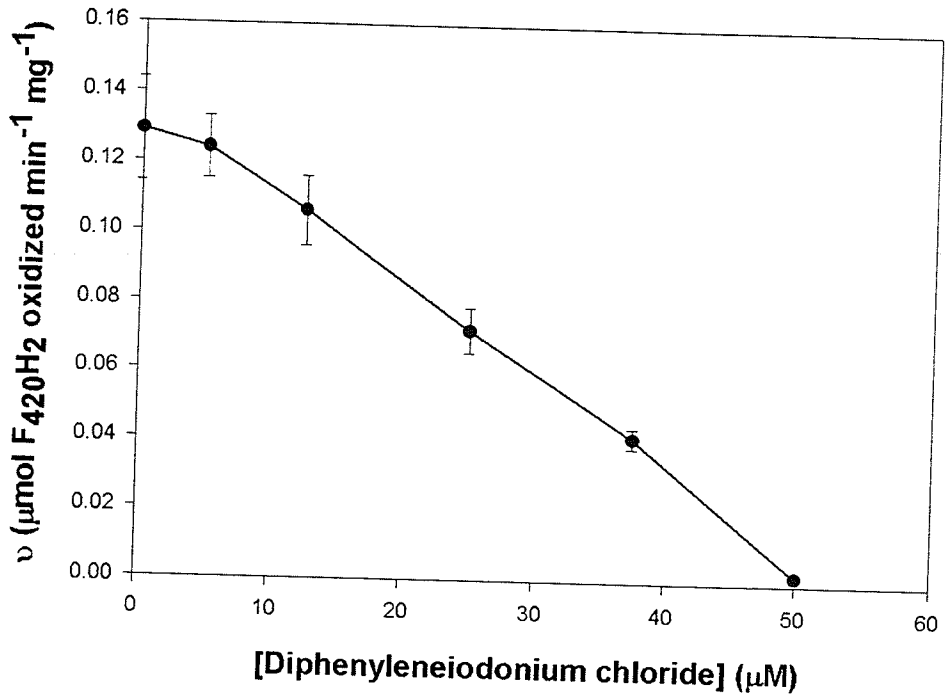

B.

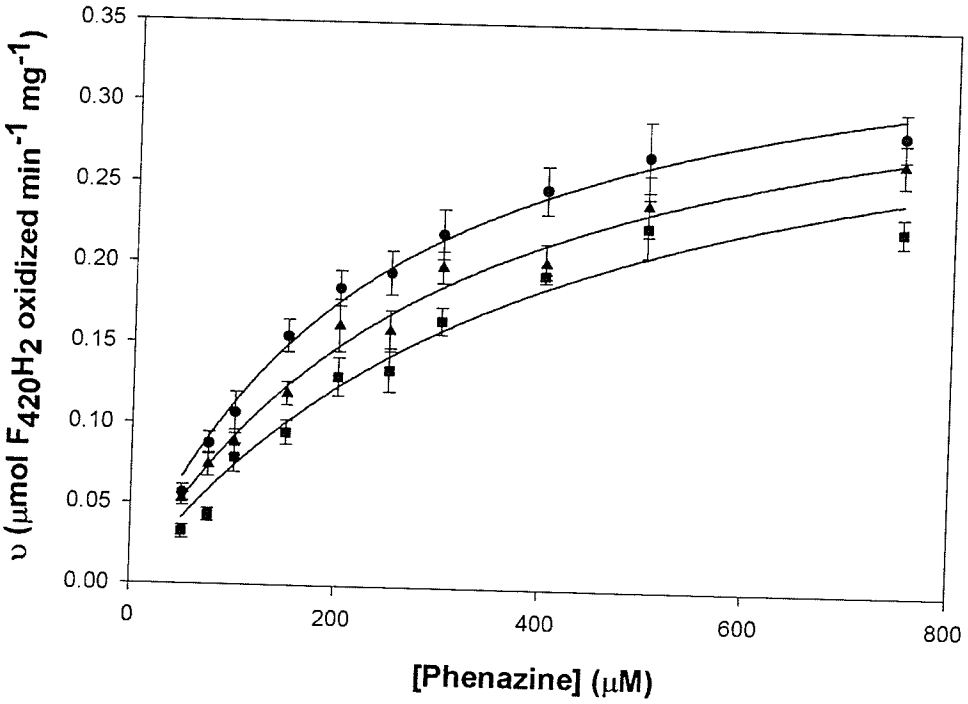

Figure 4.3. (A) Sensitivity of the phenazine-dependent $F_{420}H_2$ dehydrogenase activity of *Methanospirillum hungatei* GP1 (in cell-free extract) to diphenyleneiodonium (DPI) chloride and (B) Michaelis Menten kinetics plot of the phenazine-$F_{420}H_2$ dehydrogenase activity in the absence/presence of DPI. ●, no DPI added. ▲, + 12.5 μM DPI. ■, + 25 μM DPI.

similar to that used by *Methanococcus voltae*, as described by Brodersen *et al.* (1999). This notion is further examined in Chapter 5.

4.5.2. *Phenazine-dependent $F_{420}H_2$ dehydrogenation activity in the* Methanococcales*:* Methanococcus voltae

The order *Methanococcales* consist of coccoid, marine methanoarchaea that grow using H_2 or formate to reduce CO_2 to CH_4, including *Methanocaldococcus jannaschi*, *Methanococcus voltae*, and *Methanococcus thermolithotrophicus* (Boone *et al.* 1993). *Mc. voltae*, named for the Italian physicist Alessandro Volta, possesses two forms each of the F_{420}-reducing hydrogenase and F_{420}-nonreducing hydrogenase (± selenium) (Sorgenfrei *et al.* 1997), but a distinct Fpo complex is not expected to be present in this methanoarchaeon; the genes encoding for the Fpo complex were not found in the genome of *Mc. jannaschi* (Brodersen *et al.* 1999) or *Mc. maripaludis* (NC_005791).

Brodersen *et al.* (1999b) reported membrane-bound $F_{420}H_2$-dependent CoM-S-S-CoB reduction in *Mc. voltae*. The $F_{420}H_2$ oxidation activity was purified from the membranes of *Mc. voltae*; the source of activity was the F_{420}-reducing hydrogenase, whose purification had been previously reported by Muth *et al.* (1987). The activity was assayed using methyl viologen and metronidazole by Brodersen *et al.* (1999b), but our findings indicate that phenazine can also used as an electron acceptor, with 3-fold higher activity (Table 4.1).

The apparent K_m for phenazine for the $F_{420}H_2$ dehydrogenation activity was found to be 915.4 μM phenazine (Vmax = 0.60 μmol $F_{420}H_2$ oxidized·min^{-1}·mg^{-1}), which indicates an extremely low affinity for phenazine as an electron acceptor compared to *Ms. mazei* Gö1 (Abken *et al.* 1998) or *Ml. tindarius* and also relative to the K_m values

A.

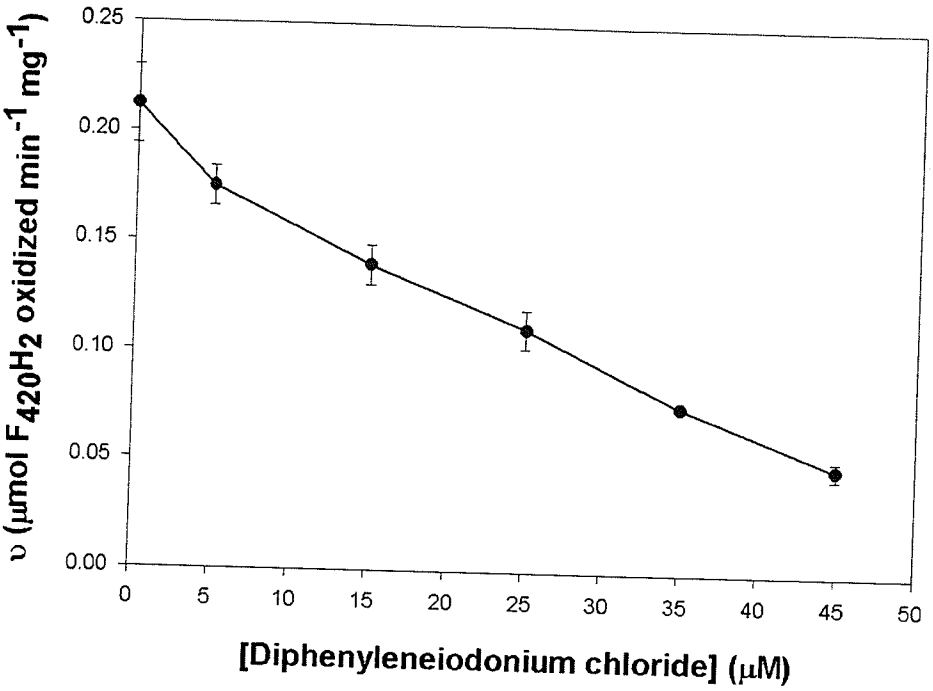

B.

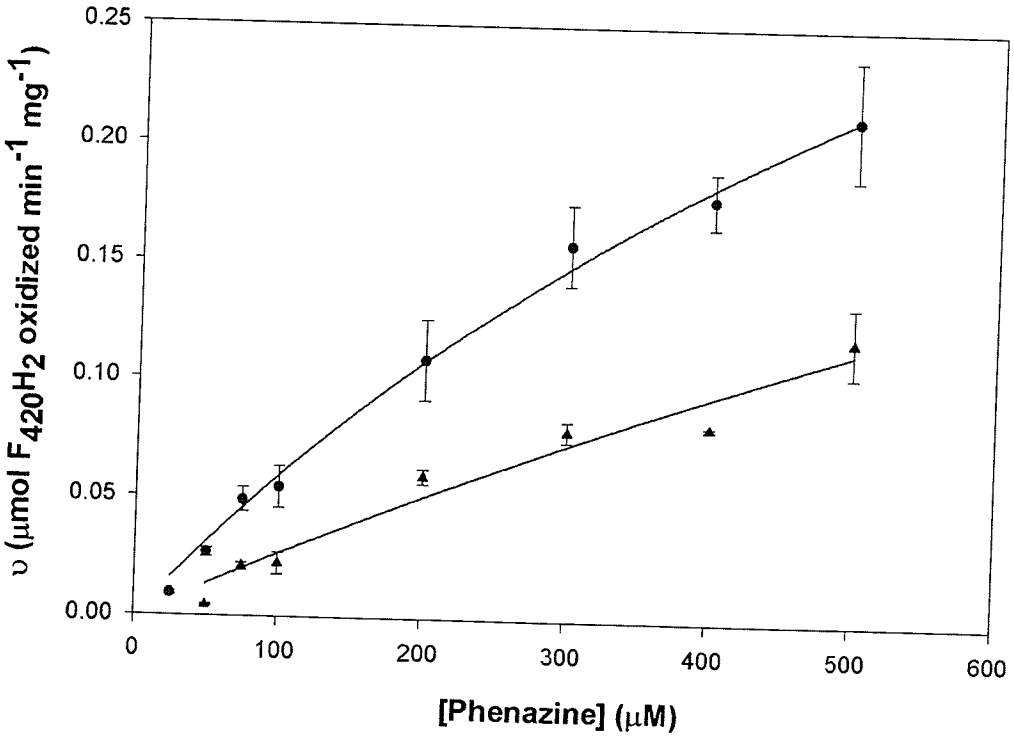

Figure 4.4. (A) Sensitivity of the phenazine-dependent $F_{420}H_2$ dehydrogenase activity of *Methanococcus voltae* (in cell-free extract) to diphenyleneiodonium (DPI) chloride and (B) Michaelis Menten kinetics plot of the phenazine-$F_{420}H_2$ dehydrogenase activity in the absence/presence of DPI.
●, no DPI added. ▲, + 15 μM DPI.

derived for the other methanoarchaea. The $F_{420}H_2$ dehydrogenation activity is also inhibited by the presence of DPI (Ic_{50} = 25 μM DPI, Figure 4A); addition of 15 μM DPI increased the K_m for phenazine from 915.4 to 2295.3 μM phenazine(Vmax = 0.63 μmol $F_{420}H_2$ oxidized $\cdot min^{-1} \cdot mg^{-1}$) (Figure 4.4B).

4.5.3. Phenazine-dependent $F_{420}H_2$ dehydrogenation activity in the Methanobacteriales

Members of the order *Methanobacteriales* form a diverse group that typically grow exclusively on H_2 and CO_2 as substrate for methanogenesis, with the exception of *Msph. stadtmanae* and *Msph. cuniculi*, which cannot use H_2 and CO_2, but reduce methanol to methane only in the presence of H_2 (Miller and Wolin, 1983, 1985, Biavati *et al.* 1988, Boone *et al.* 1993). Several members of this order were tested for phenazine-dependent $F_{420}H_2$ dehydrogenation activity, including *Mtb. marburgensis*, *Mb. bryantii*, and *Msph. stadtmanae*.

4.5.3.1. Methanothermobacter marburgensis

Mtb. marburgensis is a thermophilic methanoarchaeon that uses H_2 and CO_2 as methanogenic substrate. The genome of a related methanoarchaeon, *Mtb. thermoautotrophicus* ΔH, encodes several hydrogenases, including the F_{420}-reducing hydrogenase (Frh), the F_{420}-nonreducing hydrogenase (Mvh), and two isoforms of energy-conserving hydrogenase (Ech), EhA and EhB, but does not encode a distinct Fpo complex (Smith *et al.* 1997, Bäumer *et al.* 2000).

There is no apparent necessity for the $F_{420}H_2$ dehydrogenation activity in *Mtb. marburgensis*, as this methanoarchaeon possesses an F_{420}-nonreducing hydrogenase in

addition to the F_{420}-reducing hydrogenase (Braks *et al.* 1994). Phenazine-dependent $F_{420}H_2$ dehydrogenation activity, which is 4-fold higher relative to the methyl viologen-dependent activity, was detected in the cell-free extract, although this activity was approximately 2-fold lower compared to the activity of *Ml. tindarius* (Table 4.1). The apparent K_m for phenazine of the $F_{420}H_2$ dehydrogenation activity in cell-free extract was determined to be 254.2 μM phenazine (Vmax = 0.41 μmol $F_{420}H_2$ oxidized·min^{-1}·mg^{-1}), which is similar to the K_m value obtained for *Ml. tindarius*. The phenazine-dependent $F_{420}H_2$ dehydrogenation activity was inhibited by the addition of DPI (Ic_{50} = 30 μM DPI, Figure 4.5A), although the degree of inhibition observed with *Mtb. marburgensis* was not as acute as that of *Ml. tindarius*. Addition of 30 μM DPI increased the apparent K_m from 254.2 to 578.0 μM DPI (Vmax = 0.42 μmol $F_{420}H_2$ oxidized ·min^{-1}·mg^{-1}) (Figure 4.5B).

4.5.3.2. Methanobacterium bryantii

Like *Mtb. marburgensis*, *Mb. bryantii* is also a hydrogenotrophic methano-archaeon growing on H_2 and CO_2 that has a phenazine-dependent $F_{420}H_2$ dehydrogenation activity in cell-free extract. In the absence of inhibitor, the apparent K_m for phenzine was determined to be 318.1 μM (Vmax = 0.92 μmol $F_{420}H_2$ oxidized ·min^{-1}·mg^{-1}), indicating lower affinity for phenazine compared to *Ml. tindarius* and *Ms. mazei* Gö1, as well as *Ms. barkeri* Fusaro and *Msp. hungatei* GP1. The $F_{420}H_2$ dehydrogenation activity was more sensitive to DPI than the activity of *Mtb. marburgensis* and *Msp.hungatei* GP1, but less so than *Ml. tindarius* (Ic_{50} = 10 μM DPI, Figure 4.6A). Addition of 7 μM DPI increased the apparent K_m from 318.1 to 415.9 μM phenazine (Vmax = 0.73 μmol $F_{420}H_2$ oxidized ·min^{-1}·mg^{-1}) (Figure 4.6B).

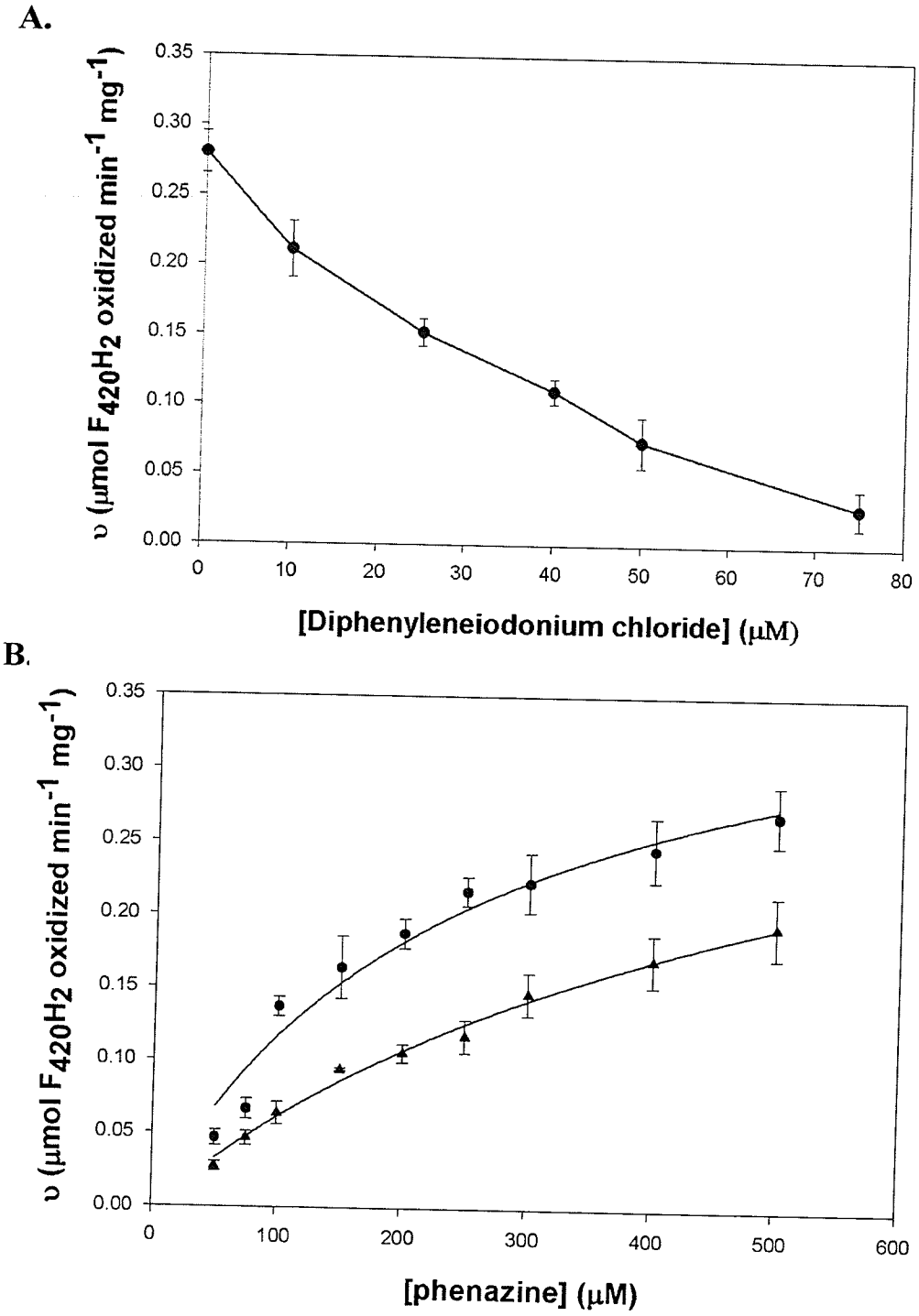

Figure 4.5. Sensitivity of the phenazine-dependent $F_{420}H_2$ dehydrogenase activity of *Methanothermobacter marburgensis* (in cell-free extract) to diphenyleneiodonium (DPI) chloride (A) and Michaelis Menten kinetics plot of the phenazine-dependent $F_{420}H_2$ dehydrogenase activity in the absence/presence of DPI (B). ●, no DPI added. ▲, + 30 μM DPI.

A.

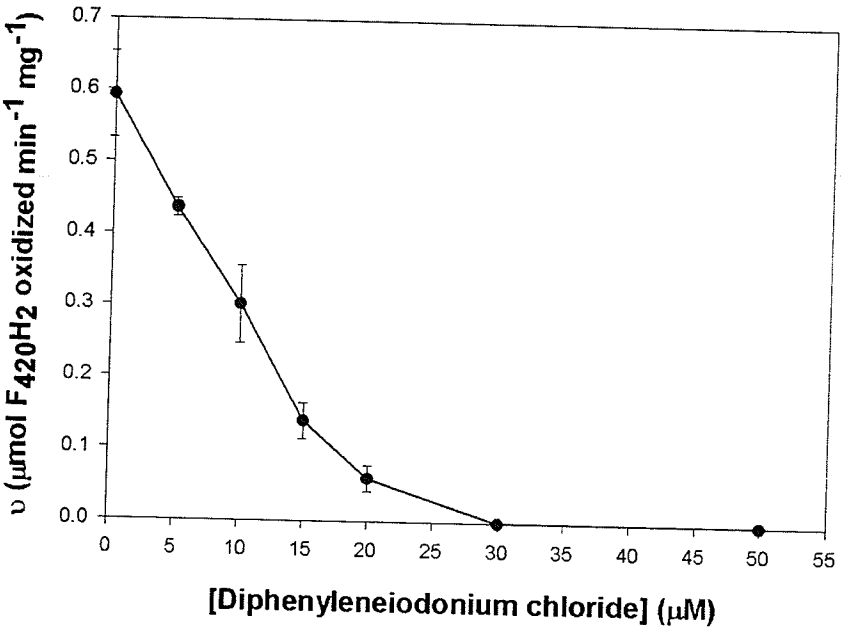

B.

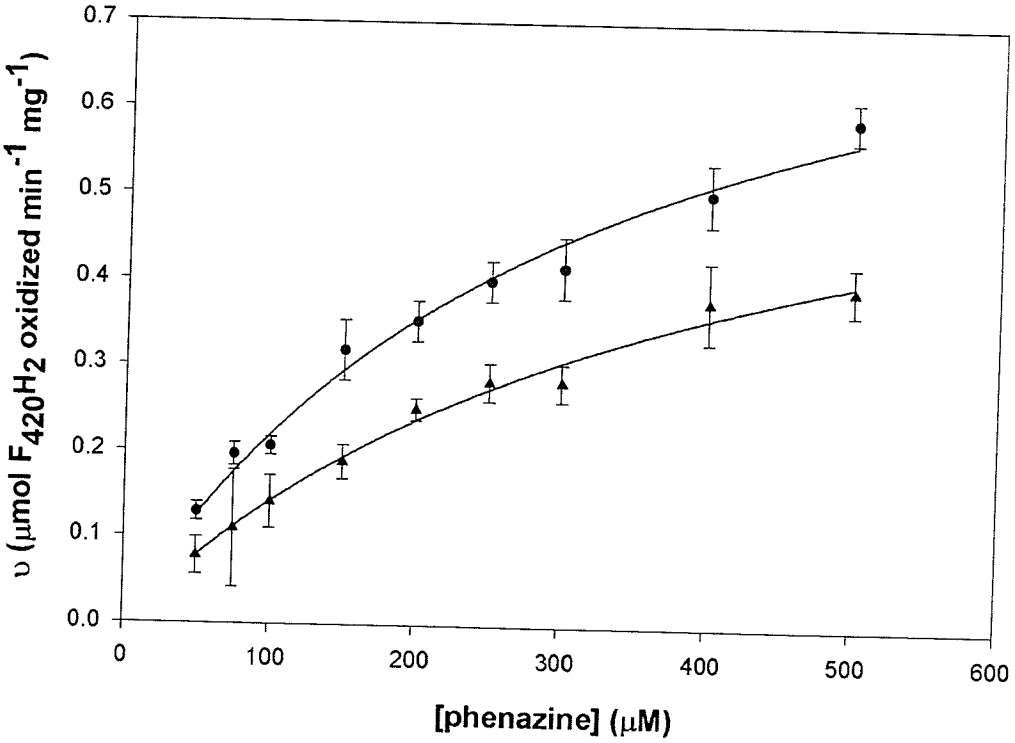

Figure 4.6. (A) Sensitivity of the phenazine-dependent $F_{420}H_2$ dehydrogenation activity of *Methanobacterium bryantii* (in cell-free extract) to diphenyleneiodonium (DPI) chloride and (B) Michaelis Menten kinetics plot of the phenazine-dependent $F_{420}H_2$ dehydrogenation activity in the absence/presence of DPI. ●, no DPI added. ▲, + 7 μM DPI.

4.5.3.3. Methanosphaera stadtmanae

A methyl viologen-dependent $F_{420}H_2$ dehydrogenation activity is present primarily in the cell-free extract of *Msph. stadtmanae* (Wong *et al.* 1994), although the activity measured is significantly lower than the related activities found in the cell-free extracts of most other methanoarchaea tested for this survey, and is also aerobically unstable.

This activity was reinvestigated using phenazine as electron acceptor; the apparent K_m for phenazine was quantified as 138.2 μM phenazine (Vmax = 0.003 μmol $F_{420}H_2$ oxidized·min^{-1}·mg^{-1}), which indicates higher affinity for phenazine relative to *Ms. mazei* Gö1 (Abken *et al.* 1998) and *Ml. tindarius*. The $F_{420}H_2$ dehydrogenation activity is much lower relative to the other methanoarchaea tested, consistent with the low levels of coenzyme F_{420} (0.16 nmol mg^{-1} protein) found in this methanoarchaeon (Wong *et al.* 1994). Moreover, this activity was inhibited by DPI (Ic_{50} = 2.5 μM DPI Figure 7A). Addition of DPI greater than 10 μM did not have a significant effect on the $F_{420}H_2$ dehydrogenation activity, which remains relatively constant as [DPI] increases up to 40 μM (Figure 4.6A).

Addition of 5 μM DPI increased the apparent K_m from 138.2 to 169.9 μM phenazine, but the Vmax decreased from 0.003 to 0.001 (as low as 0.0005) μmol $F_{420}H_2$ oxidized·min^{-1}·mg^{-1} (Figure 7B); this was in contrast to the activity of the other methanoarchaea tested where the Vmax remains constant. These results suggest that there may be a different mechanism of inhibition of the $F_{420}H_2$ dehydrogenation activity of *Msph. stadtmanae* by DPI compared to the inhibition observed in other methano-archaea, or that there may be multiple phenazine-dependent $F_{420}H_2$ oxidizing

A.

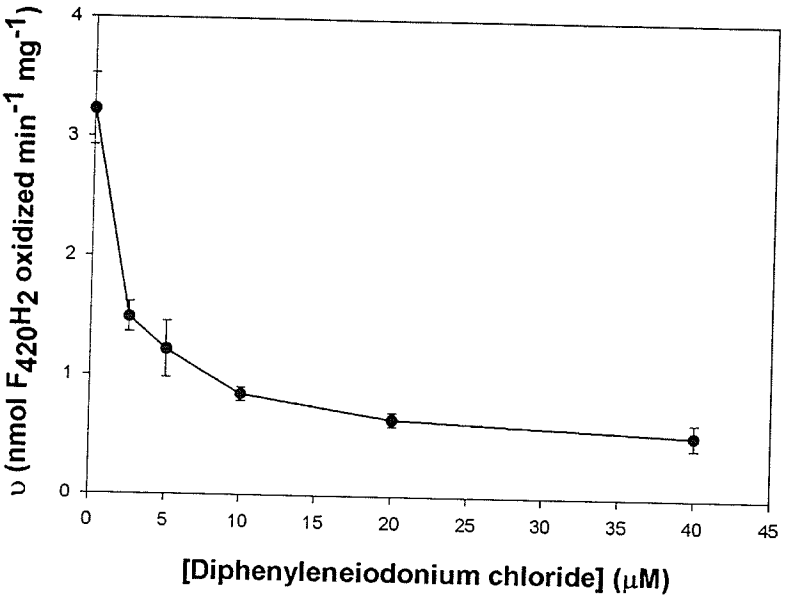

B.

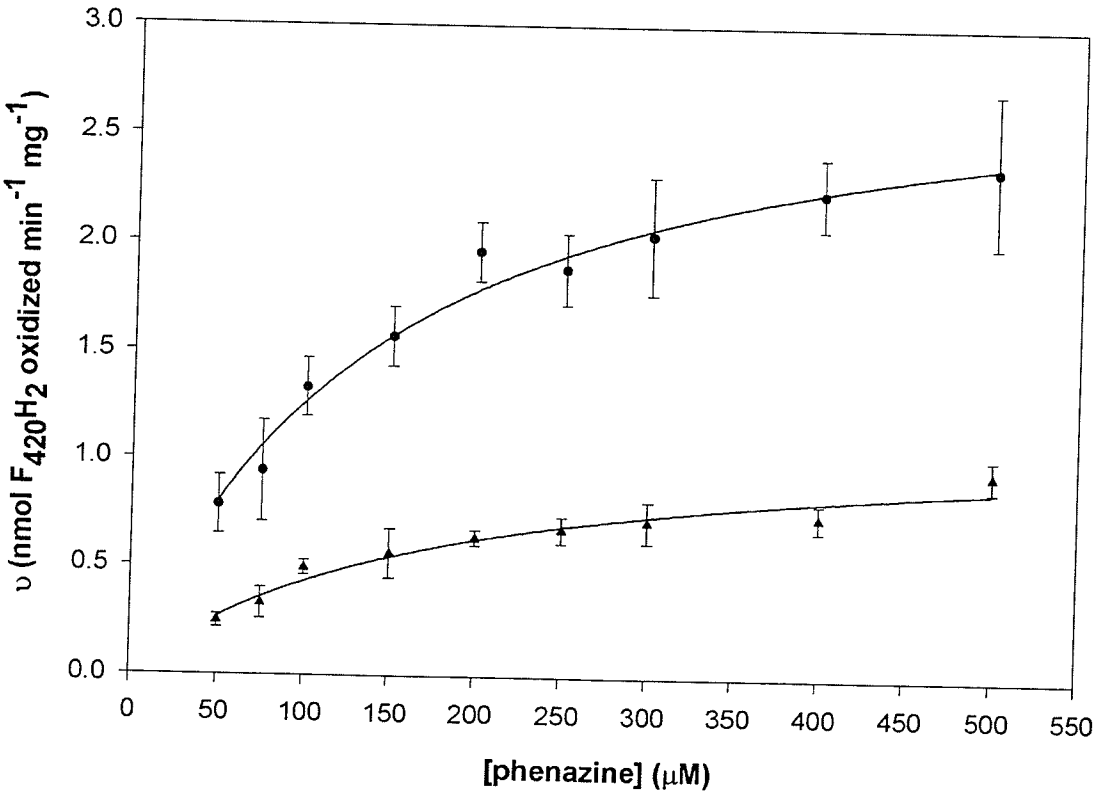

Figure 4.7. (A) Sensitivity of the phenazine-dependent $F_{420}H_2$ dehydrogenation activity of *Methanosphaera stadtmanae* (in cell-free extract) to diphenyleneiodonium (DPI) chloride and (B) Michaelis Menten kinetics plot of the phenazine-dependent $F_{420}H_2$ dehydrogenation activity in the absence/presence of DPI. ●, no DPI added. ▲, + 5 μM DPI.

activities in the cell-free extract of *Msph. stadtmanae*. The $F_{420}H_2$ dehydrogenation activity of *Msph. stadtmanae* is further examined in Chapter 7.

The genome of *Msph. stadtmanae* was recently published, and sequences coding for the subunits of the Fpo complex were not detected in the genome (Fricke *et al.* 2006). However, genes encoding the F_{420}-reducing hydrogenase and an $F_{420}H_2$ oxidase are found in the genome. Could one, or both, of these proteins be the source of the low levels of phenazine-dependent $F_{420}H_2$ dehydrogenation activity?

4.6. Phenazine-dependent $F_{420}H_2$ dehydrogenation – a widespread phenomenon?

The presence of a phenazine-dependent $F_{420}H_2$ dehydrogenation activity appears to be ubiquitous amongst the methanoarchaea regardless of nutritional requirement or phylogeny. In methylotrophic members of the *Methanosarcinaceae*, the $F_{420}H_2$ dehydrogenase activity is an essential component of the $F_{420}H_2$:CoM-S-S-CoB oxidoreductase complex (Deppenmeier *et al.* 2002, 2004). The physiological significance of this activity for methanoarchaea outside of the *Methanosarcinaceae* is unclear; it may be an artifact in the same way as the use of methyl viologen as an electron acceptor for assay of the F_{420}-reducing hydrogenase (Frh) or F_{420}-nonreducing hydrogenase (Mvh, Vho). The genomes of the hydrogenotrophic methanoarchaea *Methanothermobacter thermoautotrophicus* and *Methanocaldococcus jannaschii* indicate that the gene clusters encoding the distinct Fpo complex are not present in these methanoarchaea (Smith *et al.* 1997, Bult *et al.* 1996, Bäumer *et al.* 2000). The methanogenic pathways for these methanoarchaea do not require the presence of this activity, as CoM-S-S-CoB reduction is dependent on the presence of the F_{420}-

nonreducing hydrogenase which is found in all of the aforementioned methanoarchaea as part of the H_2:CoM-S-S-CoB oxidoreductase complex, with the exception of *Msp. hungatei* JF1 which does not possess the F_{420}-nonreducing hydrogenase, based on biochemical and genomic analyses (Sprott *et al.* 1987, this thesis).

The significance of phenazine as an electron acceptor is also not clear, as methanophenazine has not been isolated from methanoarchaea outside of the *Methanosarcinaceae* (Beifuss and Tietze 2005). 2-OH-phenazine can be used as electron acceptor for both the F_{420}-reducing (Frh) and F_{420}-nonreducing (Mvh) hydrogenases of *Mtb. thermoautotrophicus* ΔH, but methanophenazine is not expected to be present in this methanoarchaeon (Meuer *et al.* 1999, Beifuss and Tietze 2005). Although the methanophenazine can be chemically synthesized, the biosynthetic pathway is not known.

4.7. Possible sources of the phenazine-dependent $F_{420}H_2$ dehydrogenation activity outside the Methanosarcinales

The purified $F_{420}H_2$ dehydrogenase of *Ms. mazei* Gö1 is a hydrophobic membrane-bound flavoprotein capable of accepting and converting hydride ions, *via* the FAD component, to single electrons. This is essential as the substrates used to assay the $F_{420}H_2$ dehydrogenase, including methyl viologen, quinones, and various phenazine compounds, are single electron acceptors incapable of reduction *via* hydride transfer (Abken and Deppenmeier 1997, Abken *et al.* 1998). The flavoprotein inhibitor DPI, which is structurally similar to phenazine, competitively inhibits the $F_{420}H_2$ dehydrogenase activity of *Ms. mazei* Gö1 (Brodersen *et al.* 1999). A similar inhibition profile was observed with our studies of the phenazine-dependent $F_{420}H_2$ dehydrogenase

activity of *Ml. tindarius*, a methylotrophic member of the *Methanosarcinaceae* that also contains an Fpo complex (Haase *et al.* 1992).

Methanoarchaea contain several enzymes that can use coenzyme $F_{420}H_2$ as electron donor, including the $F_{420}H_2$:$NADP^+$ oxidoreductase, the methylene-H_4MPT dehydrogenase, the methylene-H_4MPT reductase, the F_{420}-reducing hydrogenase, and the $F_{420}H_2$ oxidase.

$F_{420}H_2$:$NADP^+$ oxidoreductase can be eliminated as a source of the $F_{420}H_2$ dehydrogenase activity as this enzyme reduces $NADP^+$ with $F_{420}H_2$ using a ternary, sequential reaction, *via* direct hydride transfer (Warkentin *et al.* 2001), and can not reduce single electron acceptors such as methyl viologen or phenazine.

The cytoplasmic proteins **methylene-H_4MPT dehydrogenase** and **methylene-H_4MPT reductase** catalyze, respectively, the reversible reduction of N^5,N^{10}-methenyl-H_4MPT to N^5,N^{10}-methylene-H_4MPT and N^5,N^{10}-methylene-H_4MPT to N^5-methyl-H_4MPT (Thauer *et al.* 1993). Both reactions proceed *via* stereospecific hydride transfer, with a ternary complex kinetic mechanism (Ma and Thauer 1990, Vaupel and Thauer 1995). Neither enzyme possesses prosthetic groups such as FAD or FMN, which act as $2e^-/1e^-$ switches. As such, these enzymes cannot be the source of the $F_{420}H_2$ dehydrogenase activity, since reduction of methyl viologen and phenazine both occur *via* single electron transfers.

One plausible source of $F_{420}H_2$ dehydrogenation activity may be the **F_{420}-reducing hydrogenase**. The F_{420}-reducing hydrogenases are flavoproteins that behave on hydrophobic column matrices as very hydrophobic proteins, suggesting a functional association with the cytoplasmic membrane (Sprott *et al.* 1987, Sprott and Beveridge

1993). Immunogold labeling studies of a number of methanoarchaea indicate that the F_{420}-reducing hydrogenase is located on the inner surface of the cytoplasmic membrane (Baron *et al.* 1989b, Lünsdorf *et a*l. 1991, Braks *et al.* 1994). Purified F_{420}-reducing hydrogenase from *Mtb. thermoautotrophicus* also catalyzes the H_2-dependent reduction of 2-OH-phenazine (Meuer *et al.* 1999); it would be plausible to envision an $F_{420}H_2$-dependent mechanism for 2-OH-phenazine-reduction using this enzyme.

Experiments by Brodersen *et al.* (1999b) demonstrated membrane-bound $F_{420}H_2$-dependent reduction of CoM-S-S-CoB in *Mc. voltae*. When the source of the $F_{420}H_2$ dehydrogenation-like activity was purified from the membranes, the end result was the isolation of the F_{420}-reducing hydrogenase; this enzyme catalyzed the $F_{420}H_2$ dependent reduction of methyl viologen. Thus, the F_{420}-reducing hydrogenase may be a physiologically versatile enzyme, being able to transfer e^- to F_{420} from H_2 as a hydrogenase, yet also able to oxidize $F_{420}H_2$ and transferring the e^- to a number of electron carriers, such as methyl viologen and phenazine. A similar scenario may be envisioned for *Msp. hungatei* GP1 and *Ms. barkeri* Fusaro; this is examined further in Chapters 5 and 6, respectively.

Recently, an **$F_{420}H_2$-dependent oxidase** (FlavoproteinA, FprA) was purified from *Methanobrevibacter arboriphilus*, a mesophilic methanoarchaeon isolated from the hindgut of termites (Seedorf *et al.* 2004). FprA catalyzes the following reaction (Seedorf *et al.* 2004, 2005):

$$2F_{420}H_2 + O_2 \rightarrow 2F_{420} + H_2O$$

The presence of an $F_{420}H_2$ oxidase enables the strictly anaerobic methanoarchaeon to thrive in microaerophilic environments (Seedorf *et al.* 2004).

The amino acid sequence of FprA from *M. arboriphilus* was found to be similar to the homologous protein from a number of methanoarchaea, including *Mtb. marburggensis* (71%), *Mc. jannaschii* (69%), and *Ms. acetivorans* (44%) (Seedorf *et al.* 2004). FprA is a cytoplasmic $F_{420}H_2$-dependent flavoenzyme; it is possible that this protein may be a source of the phenazine-dependent $F_{420}H_2$ dehydrogenation activity found in the cell-free extract of methanoarchaea outside of the *Methanosarcinaceae*.

Clearly, the observation of phenazine-dependent $F_{420}H_2$ dehydrogenation activity in cell-free extracts is not an indicator of the importance of this activity in non-methylotrophic methanoarchaea. In order to elucidate a possible physiological role for this activity, the source of the phenazine-dependent $F_{420}H_2$ dehydrogenation activity will have to be purified for further analysis.

5. Purification of the phenazine-dependent $F_{420}H_2$ dehydrogenation activity from *Methanospirillum hungatei* strain GP1

5.1. Introduction

Methanospirillum (*Msp.*) *hungatei* is a hydrogenotrophic spiral-shaped methanoarchaeon discovered by P.H. Smith (1966) in a sample of sewer sludge, and characterized by Ferry *et al.* (1974). *Msp. hungatei* strain GP1, the strain used in our studies, was described by Patel *et al.* (1976), who isolated this methanoarchaeon from a pear waste fermenter. *Msp. hungatei* GP1 is a member of the order *Methanomicrobiales*, which is closely related to the order *Methanosarcinales*, based on phylogenetic analyses of ribosomal proteins, methanogenesis enzymes, and methanogenesis coenzyme biosynthesis enzymes (Bapteste *et al.* 2005). While *Msp. hungatei* GP1 may share some properties with the non-methylotrophic members of the *Methanosarcinales*, like other methanoarchaea outside of this order *Msp. hungatei* GP1 does not possess cytochromes and may share other properties with methanoarchaea from the other methanogenic orders.

In contrast to most other methanoarchaea growing on H_2 and CO_2, an F_{420}-nonreducing hydrogenase is apparently not present in *Msp. hungatei* GP1, but an F_{420} H_2ase has been purified from this methanoarchaeon (Sprott *et al.* 1987, Choquet and Sprott 1991). The F_{420}-nonreducing hydrogenase has been isolated and studied from hydrogenotrophic methanoarchaea such as *Methanothermobacter* (*Mtb.*) *thermoautotrophicus*, *Methanobacterium* (*Mb.*) *formicicum*, *Methanobacterium* (*Mb.*) *fervidus*, *Methanococcus* (*Mc.*) *jannaschii*, and *Methanococcus* (*Mc.*) *voltae*, and also from two methylotrophic methanoarchaea, *Methanosarcina* (*Ms.*) *barkeri* MS and *Methanosarcina* (*Ms.*) *mazei* Gö1 (Jin *et al.* 1983, Adams *et al.* 1986, Shah and Clark

1990, Hedderich *et al.* 1990, Deppenmeier *et al.* 1992, Kemner and Zeikus 1994, Deppenmeier *et al.* 1995). The F_{420}-nonreducing hydrogenase is part of the H_2:heterodisulfide oxidoreductase system, and is essential in most hydrogenotrophic methanoarchaea for the reduction of the heterodisulfide complex (CoM-S-S-CoB), whereas the major physiological role of the F_{420}-reducing hydrogenase (F_{420} H_2ase) is to produce $F_{420}H_2$, which is in turn used to reduce H_4MPT-bound C_1 intermediates to the level of CH_3-H_4MPT (Thauer *et al.* 1993, Shima *et al.* 2002). In the absence of an F_{420}-nonreducing H_2ase, it is not clear how electrons are coupled to the reduction of CoM-S-S-CoB in *Msp. hungatei* GP1.

Work in our laboratory had indicated the possibility of a phenazine-dependent $F_{420}H_2$ dehydrogenation activity in *Msp. hungatei* GP1, similar to the respective activities isolated from *Methanosarcina* (*Ms.*) *mazei* Gö1 (Abken *et al.* 1998) and *Methanolobus* (*Ml.*) *tindarius* (Chapter 4). Given the close phylogenetic relationship between the orders *Methanosarcinales* and the *Methanomicrobiales*, it was not surprising to find such an activity in *Msp. hungatei* GP1. Although significant $F_{420}H_2$ dehydrogenation activities are found in the cytoplasmic fractions (~80%), the $F_{420}H_2$ dehydrogenase (*aka* Fpo ($F_{420}H_2$ phenazine oxidoreductase complex) of *Ml. tindarius* and *Ms. mazei* Gö1 were both purified from the cell membranes of the respective methanoarchaea, the hypothesis being that the $F_{420}H_2$ dehydrogenase is a major component of the membrane-bound electron transport chain (Deppenmeier *et al.* 1990a, Haase *et al.*1992, Abken and Deppenmeier 1997). In these methylotrophic methanoarchaea, methanophenazine is believed to be the physiological electron acceptor for the $F_{420}H_2$ dehydrogenase activity (Abken *et al.* 1998, Bäumer *et al.* 2000). As a substitute for methanophenazine,

2-hydroxy-phenazine (2-OH-phenazine) was synthesized and used to assay the $F_{420}H_2$ dehydrogenase activity of *Ms. mazei* Gö1 in aqueous buffer; this is due to the extremely hydrophobic nature of methanophenazine (Beifuss and Tietze 2005). 2-OH-phenazine is not commercially available and must be synthesized, making phenazine a much more attractive alternative. Our research indicated that phenazine could be used as an electron acceptor when measuring the $F_{420}H_2$ dehydrogenase activity of *Ml. tindarius*: the apparent Km for phenazine was determined to be 267 μM, which is similar to the value derived for the phenazine-dependent $F_{420}H_2$ dehydrogenase activity of *Ms. mazei* Gö1 ($Km_{phenazine}$ = 250 μM, Abken *et al.* 1998). Therefore, phenazine was determined to be a suitable replacement for 2-OH-phenazine in our studies.

Purification of the $F_{420}H_2$ dehydrogenase activity from the cell-free soluble fraction, as well as the membrane fraction, during the course of this thesis did not result in the isolation of a distinct Fpo complex as purified from *Ms. mazei* Gö1. Instead, the purified activity was located on the F_{420} H_2ase of *Msp. hungatei* GP1.

5.2. Materials and methods

For a comprehensive look at the materials and methods used for this chapter, the reader is referred to the following sections in Chapter 3:

3.2. Growth media

3.3. Cell lysis

3.5. Purification of the $F_{420}H_2$ dehydrogenation activity from methanol-grown *Methanosarcina barkeri* Fusaro and *Methanospirillum hungatei* GP1

3.6. Enzyme assays

3.6.1. $F_{420}H_2$ dehydrogenation assays

3.6.2. Hydrogenase assays

5.3. Results

5.3.1. Preliminary results: Soluble vs membrane-bound $F_{420}H_2$ dehydrogenation activity

Following cell lysis, the vast majority (80-90%) of the $F_{420}H_2$ dehydrogenation activity was found in the soluble cytoplasmic fraction of *Msp. hungatei* GP1, with 10-20% of the overall activity located on the washed cell membranes. Various chromatographic techniques were used to resolve the $F_{420}H_2$ dehydrogenation activity of *Msp. hungatei* GP1; from the onset, our results indicated that the $F_{420}H_2$ dehydrogenation activity eluted from the various chromatographic matrices with an F_{420} H_2ase activity. These results were observed on a consistent basis whether the proteins were derived from the soluble cytoplasmic portion, or extracted from solubilized membranes.

DEAE Sephacel (anion exchange chromatography) was a logical first step for the enrichment of the $F_{420}H_2$ dehydrogenation activity since this was the initial step used in the purification of the respective $F_{420}H_2$ dehydrogenase activities from *Ml. tindarius* and *Ms. mazei* Gö1 (Haase *et al.* 1992, Abken *et al.* 1997). The $F_{420}H_2$ dehydrogenation activity was initially studied from the cell membranes of *Msp. hungatei* GP1; the activity was extracted from the CHAPS-solubilized cell membranes. The protein extract was

loaded onto the DEAE Sephacel column, and the $F_{420}H_2$ dehydrogenase activity was eluted using a continuous 0-0.6 M NaCl gradient (Figure 5.1A). Results from previous studies (before this thesis) had demonstrated a small degree of separation of the $F_{420}H_2$ dehydrogenation and F_{420} H_2ase activities, indicating that the two activities might be two separate entities. The use of DEAE Sephacel during the course of this thesis did not result in any separation of the $F_{420}H_2$ dehydrogenation and F_{420} H_2ase activities. Manipulation of the NaCl gradient did not yield any further resolution of the activities. The DEAE Sephacel column was further washed with buffer containing 5 M NaCl to remove tightly bound protein; $F_{420}H_2$ dehydrogenation activity was not detected in the eluate.

The fractions containing $F_{420}H_2$ dehydrogenation activity were pooled and concentrated for a gel filtration step using G-200 (Figure 5.1B); further resolution of the $F_{420}H_2$ dehydrogenation and F_{420} H_2ase activities was not obtained using this chromatographic technique. This seemed to indicate that the $F_{420}H_2$ dehydrogenation activity may be linked to the F_{420} H_2ase of *Msp.hungatei* GP1.

Choquet and Sprott (1991) reported the enrichment of the F_{420} H_2ase of *Msp. hungatei* GP1 using metal chelate affinity chromatography (MCAC), with Ni^{2+} chelated to the affinity matrix, as the initial step in their purification protocol. This appeared to be a viable step in our protocol to separate the F_{420} H_2ase from the $F_{420}H_2$ dehydrogenation activity. However, this step only enriched for the soluble F_{420} H_2ase, as the cell membranes, containing ~10-20% of the overall activity, did not bind to the column. Thus, the membrane-bound activity passed through the column unimpeded, with no affinity for the Ni^{2+} (Choquet and Sprott 1991). However, our results demonstrated that

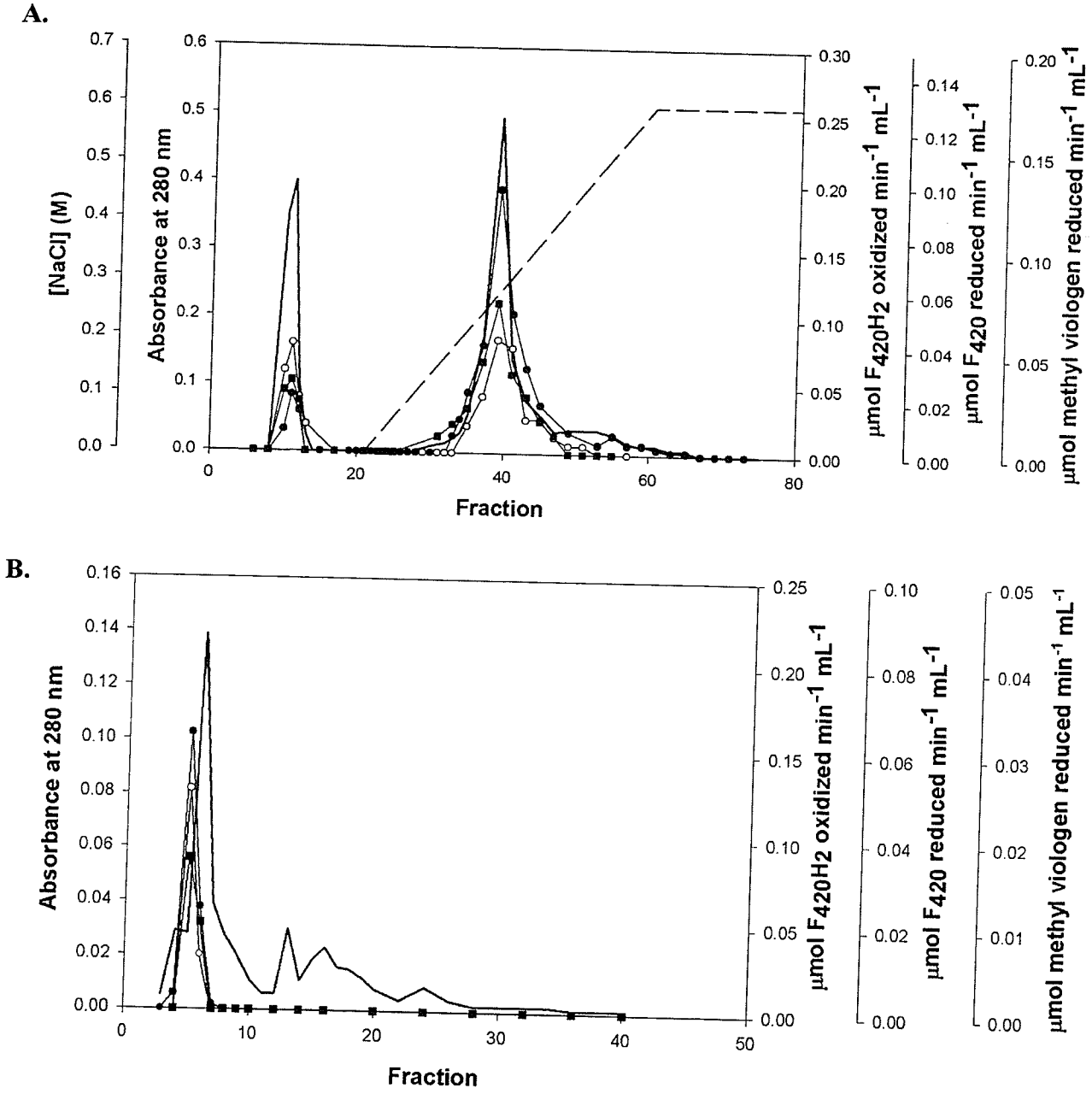

Figure 5.1. (A) Protein and activity profile of fractions collected from a DEAE Sephacel column, eluted using a linear 0-0.6 M NaCl gradient. Protein derived from solubilized cell membranes. Similar profiles observed using lower NaCl gradients (0-0.3 M NaCl). (B) Protein and activity profile of fractions collected from a G-200 column, using pooled and concentrated protein from a DEAE sephacel column. (—), A_{280}. (----), linear 0-0.6 M NaCl gradient. ●, Phenazine-dependent $F_{420}H_2$ dehydrogenation activity. ○, F_{420}-reducing hydrogenase activity. ■, Methyl viologen-reducing hydrogenase.

when the membranes are solubilized with detergent, such as CHAPS, the extracted activity does bind to the Ni^{2+} affinity column.

Since the Fpo complex is expected to be a membrane-bound protein complex, we could not preclude the possibility of an $F_{420}H_2$ dehydrogenase activity located in the membrane fraction that may not be detected in the soluble fraction of the cell-free extract. Simultaneous experiments were set up to identify the source of $F_{420}H_2$ dehydrogenation activity in the soluble and membrane portions.

A typical protein and activity profile of fractions collected from a Ni^{2+} affinity column, using the soluble $F_{420}H_2$ dehydrogenation activity, is shown in Figure 5.2; similar profiles were observed using CHAPS-solubilized membrane-bound protein. The $F_{420}H_2$ dehydrogenation, F_{420}- and methyl viologen-reducing hydrogenase activities all elute in the same peak with no apparent separation. The F_{420}-reducing and methyl viologen-reducing activities reside on the F_{420} H_2ase; a distinct F_{420}-nonreducing H_2ase was not detected in *Msp. hungatei* GP1 (Sprott *et al.* 1987); this was confirmed by our own analyses.

Further steps were introduced in an attempt to separate and enrich the $F_{420}H_2$ dehydrogenation activity; the results of subsequent steps using different chromatographic materials are shown in Figures 5.3 and 5.4 (soluble and membrane-bound proteins, respectively); these results also supported the association of the $F_{420}H_2$ dehydrogenation and F_{420} H_2ase activities on the same protein complex.

Sucrose step gradient profiles are shown in Figures 5.3A and 5.4A, loaded with protein collected and pooled from the Ni^{2+} affinity column. A 45-50% sucrose density

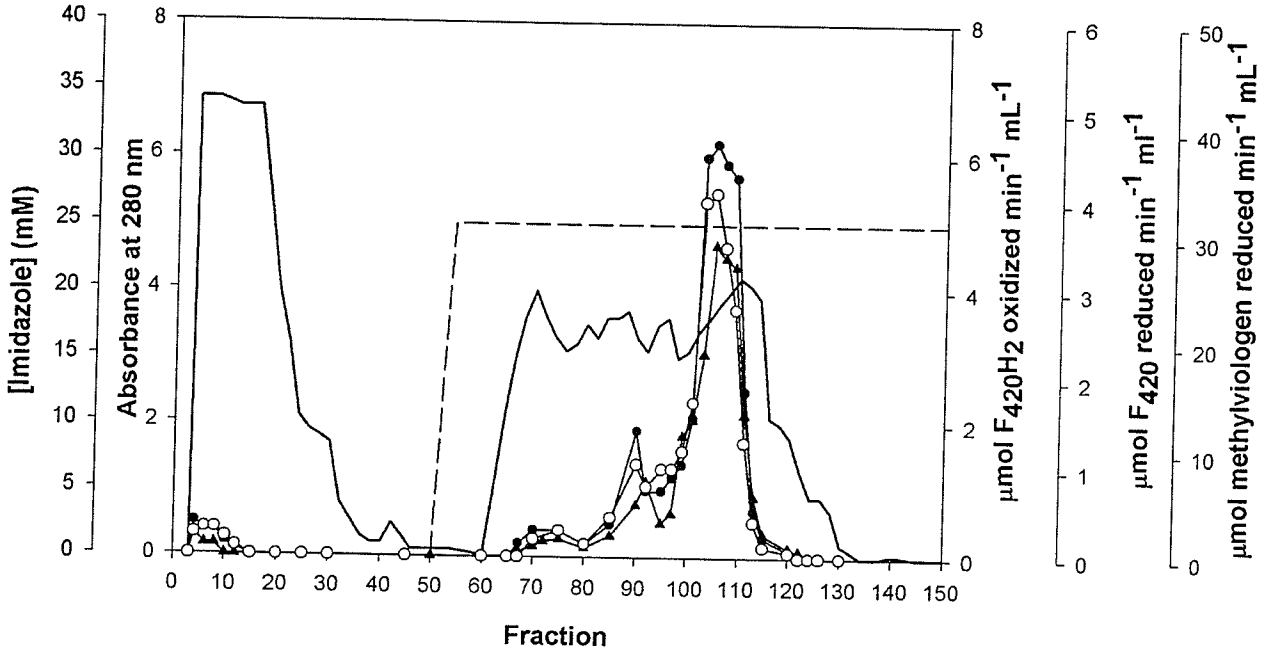

Figure 5.2. Protein and activity profile of fractions collected from a Ni^{2+} affinity column. Protein derived from the clarified cell-free extract (i.e. soluble fraction). Identical profile observed when using protein extracted from the cell membranes. Elution of protein from the column as described under 'Materials and methods'. (—), A_{280}. (----), 25 mM imidazole. ●, Phenazine-dependent $F_{420}H_2$ dehydrogenation activity. ○, F_{420}-reducing hydrogenase activity. ▲, Methyl viologen-reducing hydrogenase.

gradient ultracentrifugation step (10 ml per step) was one of the major enrichment steps in the purification of the F_{420} H_2ase of *Msp. hungatei* GP1 by Choquet and Sprott (1991). The $F_{420}H_2$ dehydrogenation activity could not be separated from the F_{420} H_2ase using the sucrose step gradient; similar results were observed when using a five-step (45-46-47-48-50%) gradient, or from a linear 45-50% sucrose density gradient. Protein pooled and concentrated from the 45-50% sucrose step gradient was then loaded onto a column of Sepharose 6B, an agarose-based gel filtration matrix with broad fractionation range for separating samples with diverse molecular weight ($10 - 4x10^3$ kDa, Pharmacia Biotech). The F_{420} H_2ase is a much larger protein relative to the expected $F_{420}H_2$ dehydrogenase (7- to 8-fold larger), such that one would expect that the two activities should be well separated using this matrix. Figures 5.3B and 5.4B illustrate that both activities have similar molecular weights as they elute together in the same peaks. Furthermore, there are no apparent differences between the activity profiles of the soluble and membrane associated proteins.

However, the activities were not purified to homogeneity, and separation of the proteins from enriched extracts *via* electrophoresis indicated the presence of protein bands with molecular weights similar to the $F_{420}H_2$ dehydrogenase of *Ms. mazei* Gö1.

Since enrichment of the $F_{420}H_2$ dehydrogenation activity appears to occur alongside the hydrogenase activity, a pertinent question was raised at this point: was the $F_{420}H_2$ dehydrogenation activity a distinct entity, or is it located on the F_{420} H_2ase of *Msp. hungatei* GP1? Based on these results, there was indication that the membrane-bound and soluble phenazine-dependent $F_{420}H_2$ dehydrogenation activities of *Msp. hungatei* GP1 were located on the F_{420} H_2ase. On the basis of the above experiments, a protocol

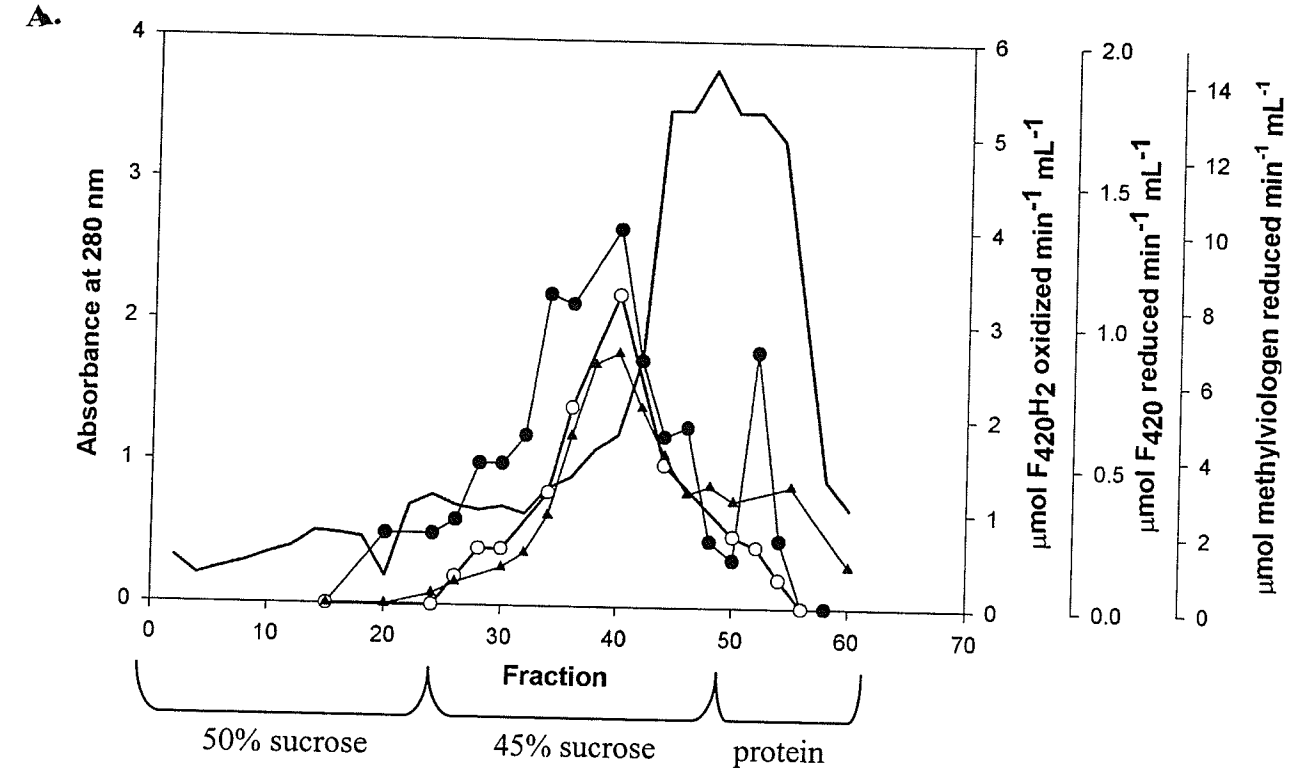

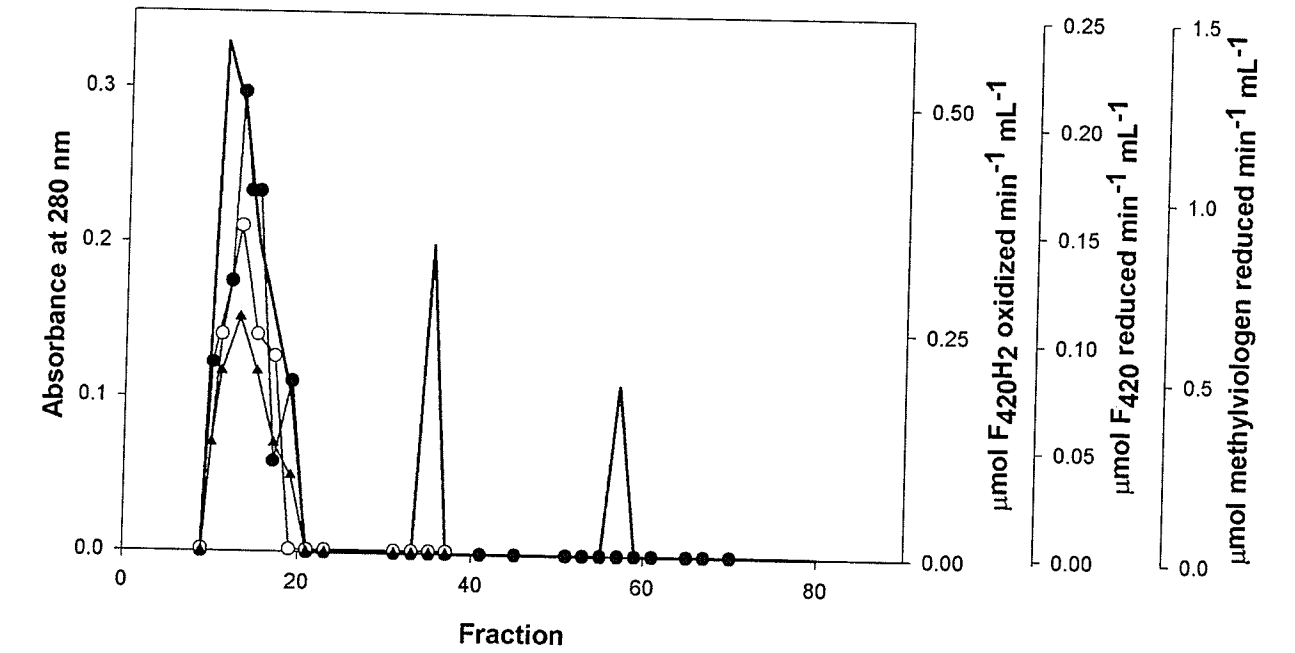

Figure 5.3. Protein and activity profile of fractions collected from: (A) 50-45% sucrose step gradient loaded with protein eluted from a Ni^{2+}-affinity column and (B) Sepharose 6B column loaded with protein collected from the 50-45% sucrose step gradient. Protein derived from the clarified cell-free extract (soluble fraction). (—), A_{280}. ●, Phenazine-dependent $F_{420}H_2$ dehydrogenation activity. ○, F_{420}-reducing hydrogenase activity. ▲, Methyl viologen-reducing hydrogenase activity.

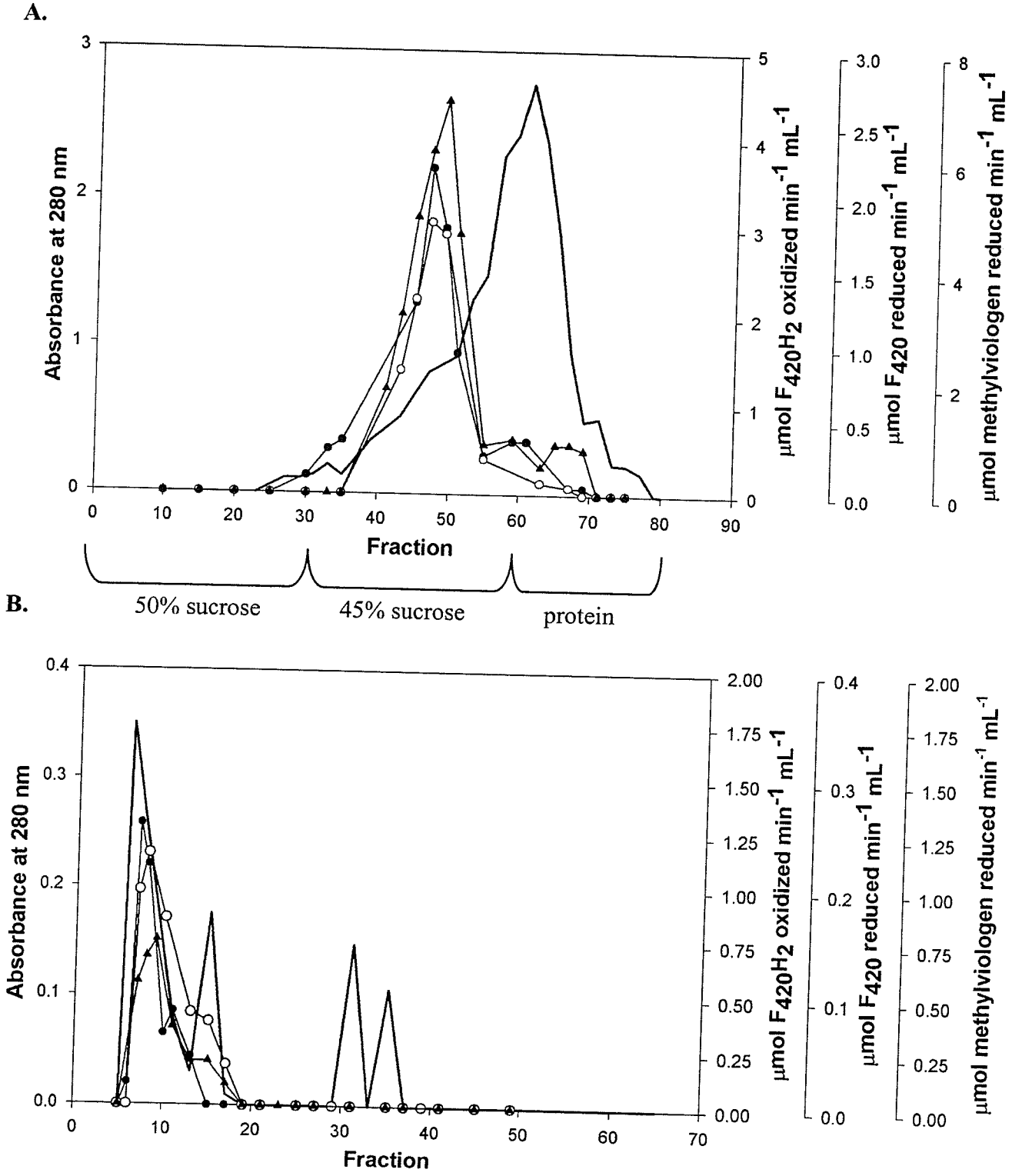

Figure 5.4. Protein and activity profile of fractions collected from: (A) 50-45% sucrose step gradient loaded with protein eluted from a Ni^{2+}-affinity column and (B) Sepharose 6B column loaded with protein collected from the 50-45% sucrose step gradient. Protein solubilized and extracted from washed cell membranes. (—), A_{280}. ●, Phenazine-dependent $F_{420}H_2$ dehydrogenation activity. ○, F_{420}-reducing hydrogenase activity. ▲, Methyl viologen-reducing hydrogenase activity.

was devised for the purification of the $F_{420}H_2$ dehydrogenation activity to homogeneity, in an attempt to separate both activities. The F_{420} H_2ase also catalyzes $F_{420}H_2$ oxidation; by selecting for the purification of this protein, we expected to separate this "artifact" activity from any other source of $F_{420}H_2$ dehydrogenation present in the protein extract.

5.3.2. Purification of the phenazine-dependent $F_{420}H_2$ dehydrogenation activity

The purification of the $F_{420}H_2$ dehydrogenation activity is summarized in Table 5.1; purification of this activity was repeated three times, with representative data presented. Upon cell lysis, and after removal of the unlysed cells and debris, the cell-free extract was further centrifuged at 180000xg for 6 hours. This resulted in the sedimentation of both the soluble and membrane-bound $F_{420}H_2$ dehydrogenation activities into a tight dark brown pellet, referred to as the high speed pellet (HSP). The HSP was homogenized in 10 mM HEPES, pH 7.0, containing 0.5 M NaCl, and loaded onto the Ni^{2+} affinity column where the soluble $F_{420}H_2$ dehydrogenation activity was enriched from the HSP using a single step addition of 25 mM imidazole, along with H_2-dependent F_{420}-reducing and methyl viologen-reducing activites (Figure 5.5). The membranes, containing up to 20% of the $F_{420}H_2$ dehydrogenation activity (and F_{420} H_2ase activity), did not bind to the column and were pooled and stored at 4°C for further analysis.

The pooled fractions containing the soluble $F_{420}H_2$ dehydrogenation activity were desalted and concentrated using an Amicon ultrafiltrator, and then loaded onto linear 3-20% native gradient PAGE gels (in each available lane); electrophoresis of the gels for

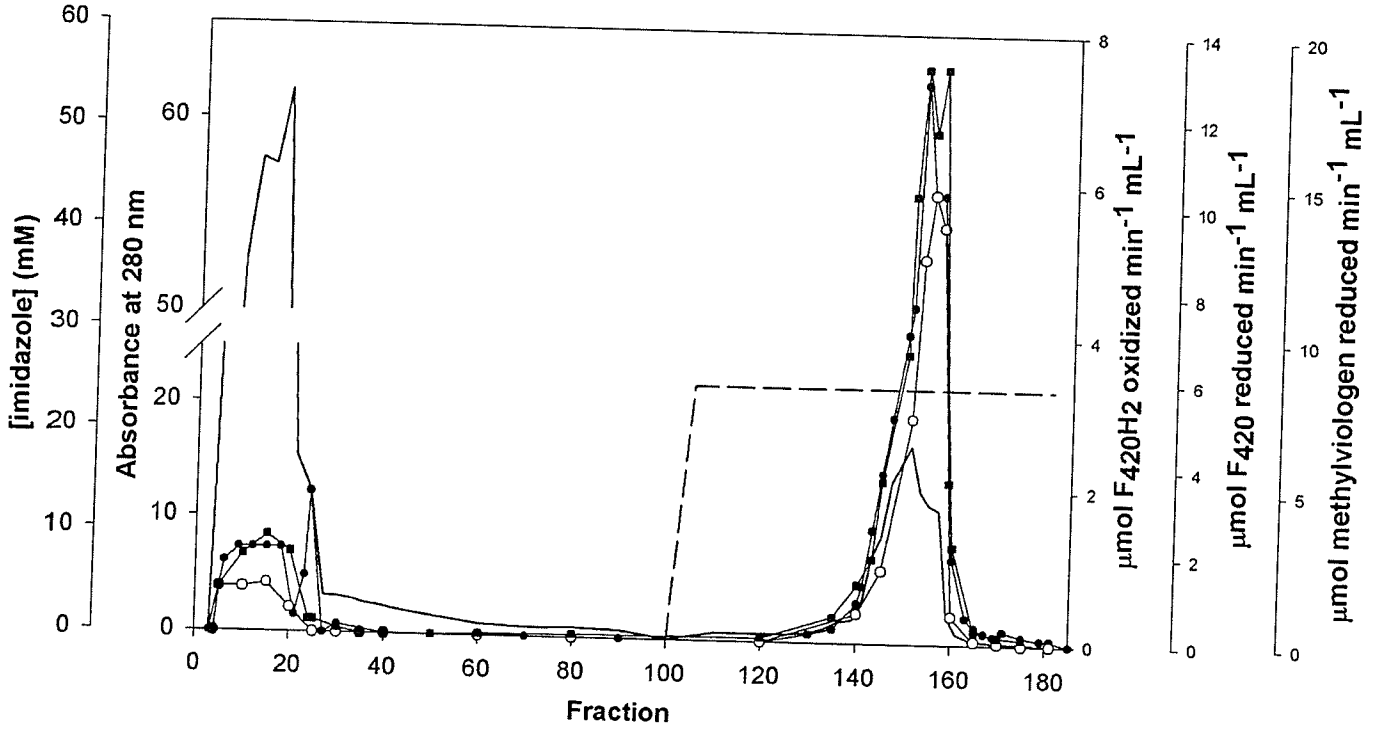

Figure 5.5. Protein and activity profile of fractions collected from a Ni^{2+} affinity column as described in 'Materials and methods'. Cell-free extract from *Methanospirillum hungatei* GP1 was centrifuged at 50 000 rpm, and the soluble and membrane-bound $F_{420}H_2$ dehydrogenation activities were separated from the extract into a tight brown pellet (high speed pellet). The pellet was suspended in buffer and applied to the column. Protein binding to the column was eluted from the column by the addition of 25 mM imidazole, while the membrane-bound activity did not have affinity for the Ni^{2+}. (—), A_{280}. (----), 25 mM imidazole. ●, $F_{420}H_2$ dehydrogenation activity. ○, F_{420}-reducing activity. ■, Methyl viologen-reducing activity.

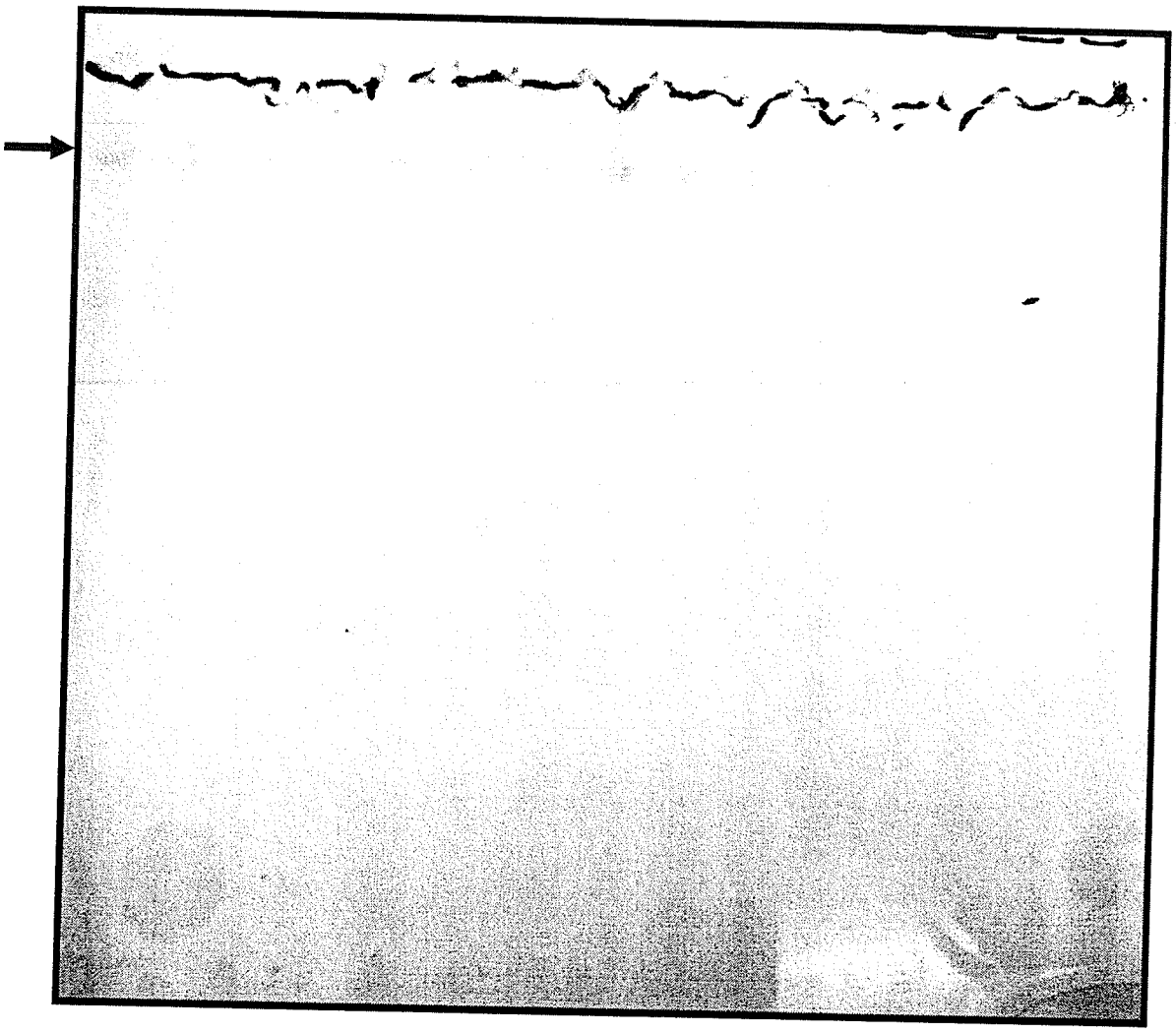

Figure 5.6. Unstained 3-20% native gradient PAGE loaded with protein pooled and concentrated after elution of the soluble $F_{420}H_2$ dehydrogenation activity from Ni^{2+} affinity column. Concentrated extract was loaded into each lane, and the protein was electrophoresed overnight; high molecular weight protein band (marked with arrow) were cut from the gel for elution with Bio-Rad electro elutor. Other colored bands were also processed electro-elution.

Table 5.1. Purification of the soluble phenazine-dependent $F_{420}H_2$ dehydrogenation activity of *Methanospirillum hungatei* GP1. MCAC, metal chelate chromatography.

Purification stage	Protein (mg)	Activity[†]	Yield (%)	Sp. activity[‡]	Purification
Cell-free extract	1808.5	547.8	100	0.3	-
High speed pellet	848.5	391.7	81.7	0.46	1.5-fold
MCAC pool	78.8	124.2	25.9	1.58	5.3-fold
Eluted protein[‡‡]	1.7	23.0	4.8	13.5	45.0-fold

[†]μmol $F_{420}H_2$ oxidized·min^{-1}.
[‡] μmol $F_{420}H_2$ oxidized·min^{-1}·mg^{-1} protein
[‡‡]protein eluted from 3-20% native gradient PAGE

approximately 15 hours (i.e. overnight) resulted in gels with a pattern shown in Figure 6.The presence of FAD and iron-sulfur clusters in the protein allows for the F_{420} H_2ase to be visualized without prior staining.

The distinctive, high molecular weight yellow-brown protein bands (marked in Figure 5.6) were excised from the gel and minced into 1-2 mm^3 pieces, followed by elution of the protein from the gel cubes using a Bio-Rad model 422 Electro Eluter. The eluted protein was resuspended in 50 mM HEPES, pH 7.0, with 5% glycerol and 0.05% Triton-X-100, and stored under N_2 at 4°C for further analysis. Other yellow brown bands are also visualized on the native gradient PAGE (Figure 5.6); neither $F_{420}H_2$ dehydrogenation nor F_{420} H_2ase activities were detected in the protein extracted from the bands.

Table 5.2. Enrichment of the soluble F_{420} reducing hydrogenase activity during the purification of the phenazine-dependent $F_{420}H_2$ dehydrogenation activity of *Methanospirillum hungatei* GP1. MCAC, metal chelate affinity chromatography.

Purification stage	Protein (mg)	Activity[†]	Yield (%)	Sp. activity[‡]	Purification	DeH$_2$ase/ H$_2$ase
Cell-free extract	1808.5	366.1	100	0.22	-	1.37
High speed pellet	848.5	275.8	75.3	0.33	1.5-fold	1.39
MCAC pool	78.8	179.4	49.0	1.70	7.7-fold	0.93
Eluted protein[‡‡]	1.7	23.0	6.3	13.5	61.4-fold	1.00

[†]μmol F_{420} reduced·min^{-1}.
[‡]μmol F_{420} reduced·min^{-1}·mg^{-1} protein
[‡‡]protein eluted from 3-20% native gradient PAGE

The F_{420} H_2ase activity was monitored in tandem with the $F_{420}H_2$ dehydrogenation activity (Table 5.2), confirming the co-migration of the $F_{420}H_2$ dehydrogenation and F_{420} H_2ase activities. No other source of $F_{420}H_2$ dehydrogenation activity was observed.

The purification of the membrane-bound $F_{420}H_2$ dehydrogenation activity is summarized in Table 5.3. The protocol used for isolation of the membrane-bound $F_{420}H_2$ dehydrogenation activity was similar to that of the soluble activity, but with the Ni^{2+} affinity column step replaced with a three step (40-45-50%) sucrose step gradient. The pooled membranes were solubilized with CHAPS, concentrated with an Amicon ultrafiltrator, and loaded onto the three step sucrose gradient, followed by a 48 hour ultracentrifugation step (23,000 rpm). The phenazine-dependent $F_{420}H_2$ dehydrogenation

activity isolated from the solubilized cell membranes eluted from the sucrose step gradient along with methyl viologen- and F_{420} H_2ase activities (Figure 5.7). Similar results are observed when the membrane proteins were separated using various column chromatography techniques with varying chromatographic properties, including DEAE Sephacel (Figure 5.1), Ni^{2+} affinity chromatography (Figure 5.2), gel filtration (Figure 5.4), and Phenyl Sepharose Cl-4B (data not shown).

Fractions containing $F_{420}H_2$ dehydrogenation activity were pooled, diluted of sucrose and concentrated using an Amicon ultrafiltrator, followed by electrophoresis of the concentrated sample on a 3-20% native gradient PAGE. Protein bands could not be directly observed on the unstained gel due to the lower amounts of protein associated with the membrane, but staining of the outermost lanes of the gel revealed the positions of the protein bands in their respective lanes; these bands were cut from the gel, and protein was extracted using the BioRad electro-elutor, followed by homogenization in 50 mM HEPES, pH 7.0, with 5% glycerol and 0.05% Triton-X-100, and storage under N_2 at 4°C. With the exception of the $F_{420}H_2$ dehydrogenation activity located on the F_{420} H_2ase, no other source of $F_{420}H_2$ dehydrogenation activity was detected in the solubilized membrane protein.

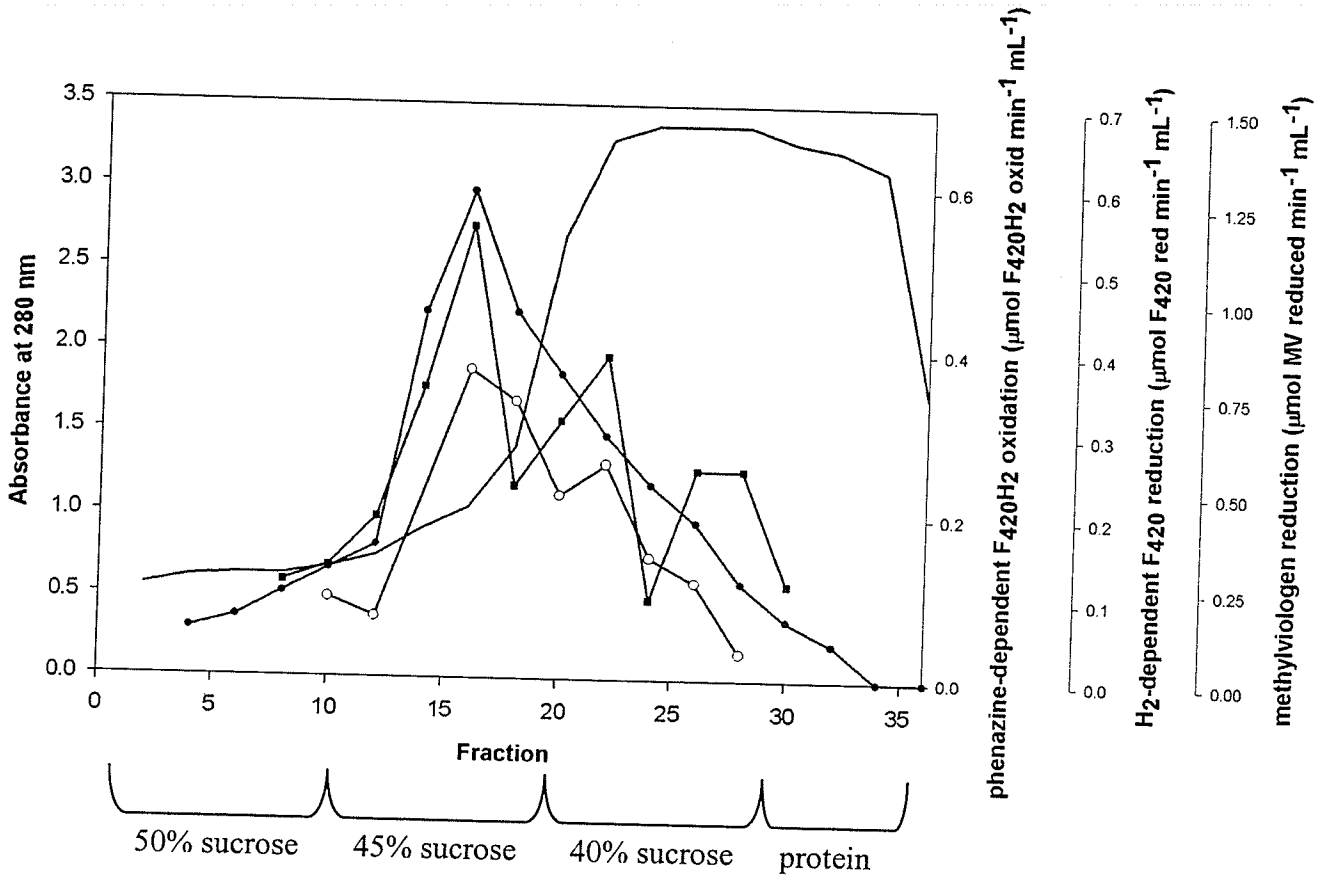

Figure 5.7. Protein and activity profile of fractions collected from a 40-45-50% sucrose gradient ultracentrifugation step. Protein was extracted from CHAPS-solubilized membranes of *Methanospirillum hungatei* GP1. (—), A_{280}. ●, Phenazine-dependent $F_{420}H_2$ dehydrogenation activity. ○, F_{420}-reducing hydrogenase activity. ■, Methyl viologen reducing hydrogenase activity.

Table 5.3. Purification of the membrane-bound phenazine-dependent $F_{420}H_2$ dehydrogenation activity of *Methanospirillum hungatei* GP1.

Purification stage	Protein (mg)	Activity†	Yield (%)	Sp. activity‡	Purification
Washed mem	120.9	27.1	100	0.22	-
Solubilized protein	46	9.0	33.2	0.20	0.9-fold
Sucrose pool	9.6	2.6	7.9	0.27	1.2-fold
Eluted protein‡‡	0.02	0.2	0.7	12.8	58.3-fold

†μmol $F_{420}H_2$ oxidized·min^{-1}.
‡ μmol $F_{420}H_2$ oxidized·min^{-1}·mg^{-1} protein
‡‡protein eluted from 3-20% native gradient PAGE

5.3.3. Properties of the $F_{420}H_2$ dehydrogenation activity of Methanospirillum hungatei *GP1*

5.3.3.1. Molecular properties

Coomassie blue-staining of the purified protein following linear 3-20% native PAGE gel electrophoresis reveal a pair of distinct high molecular weight protein bands (Figure 5.8), both of which exhibit hydrogenase activity when stained with methyl viologen under reducing conditions; this is consistent with the molecular weight of the F_{420} H_2ase (720 ± 84 kDa) of *Msp. hungatei* GP1, determined using gel filtration by Sprott *et al.* (1987).

The polypeptide pattern of the subunits on an SDS PAGE appears to be identical to the profile of the purified F_{420} H_2ase described by Choquet and Sprott (1991) (Figure 5.9 and 5.10). The purified protein from *Msp. hungatei* GP1 consists of 3

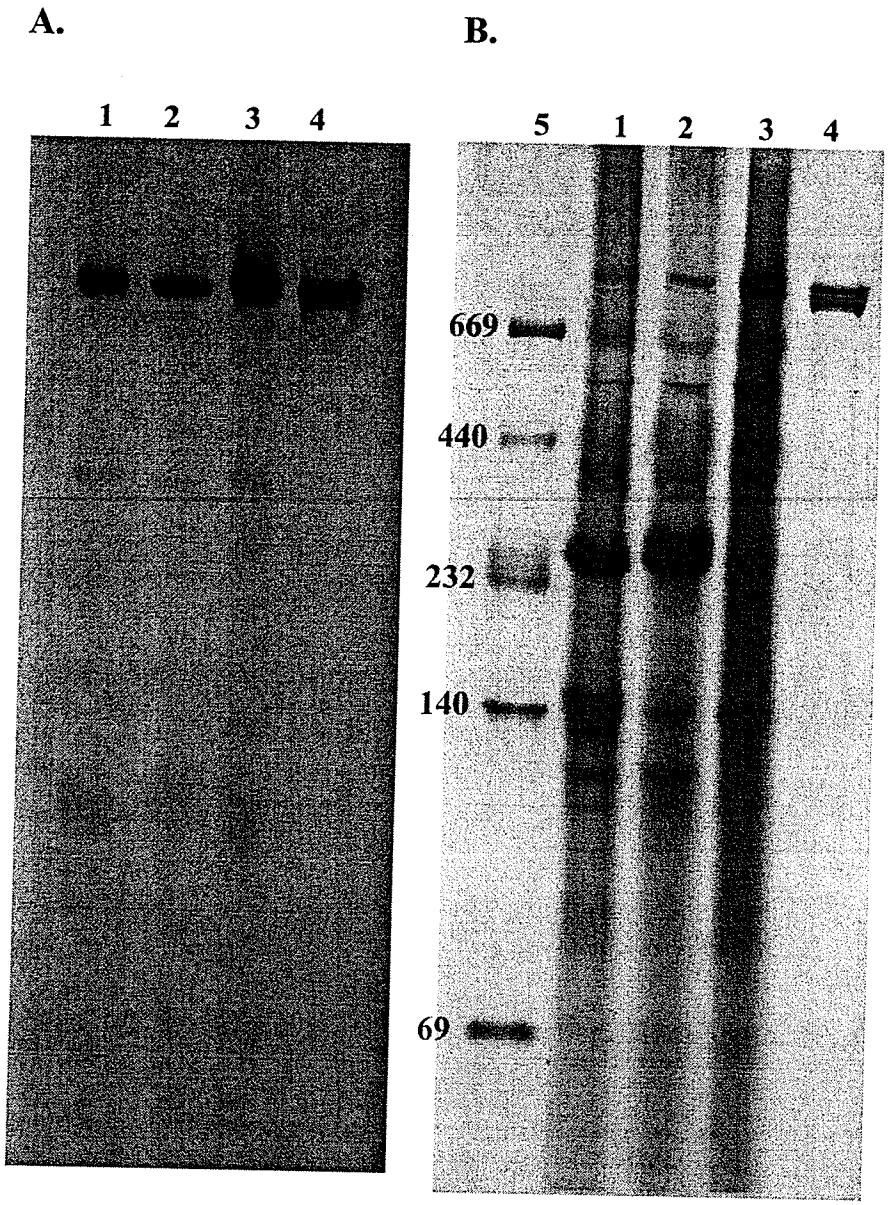

Figure 5.8. (A) Hydrogenase activity- and (B) coomassie blue-stained 3-20% native gradient PAGE showing progression of the purification of the soluble phenazine-dependent $F_{420}H_2$ dehydrogenation activity of *Methanospirillum hungatei* GP1. 1, Cell-free extract. 2, High speed pellet. 3, Ni^{2+} affinity column pool. 4, purified protein. 5, molecular markers (kDa).

subunits of approximately 55 (α), 33 (β), and 30 (γ) kDa, similar to what was previously reported. While the protein has hydrophobic character, it is not an integral membrane protein but is found attached on the inner face of the cytoplasmic membrane (Sprott et *al.* 1987, Sprott and Beveridge 1993).

Figure 5.11 shows an activity-stained and double stained (coomassie blue- and silver-stained) 3-20% native gradient PAGE with loaded with the purified soluble and membrane-bound $F_{420}H_2$ dehydrogenation activities, indicating that the soluble and membrane-bound activities are identical.

From these results, the observed phenazine-dependent $F_{420}H_2$ dehydrogenation activity from *Msp. hungatei* GP1 is a property of the F_{420} H_2ase, and not to a distinct Fpo complex as purified from some methylotrophic members of the *Methanosarcinaceae*.

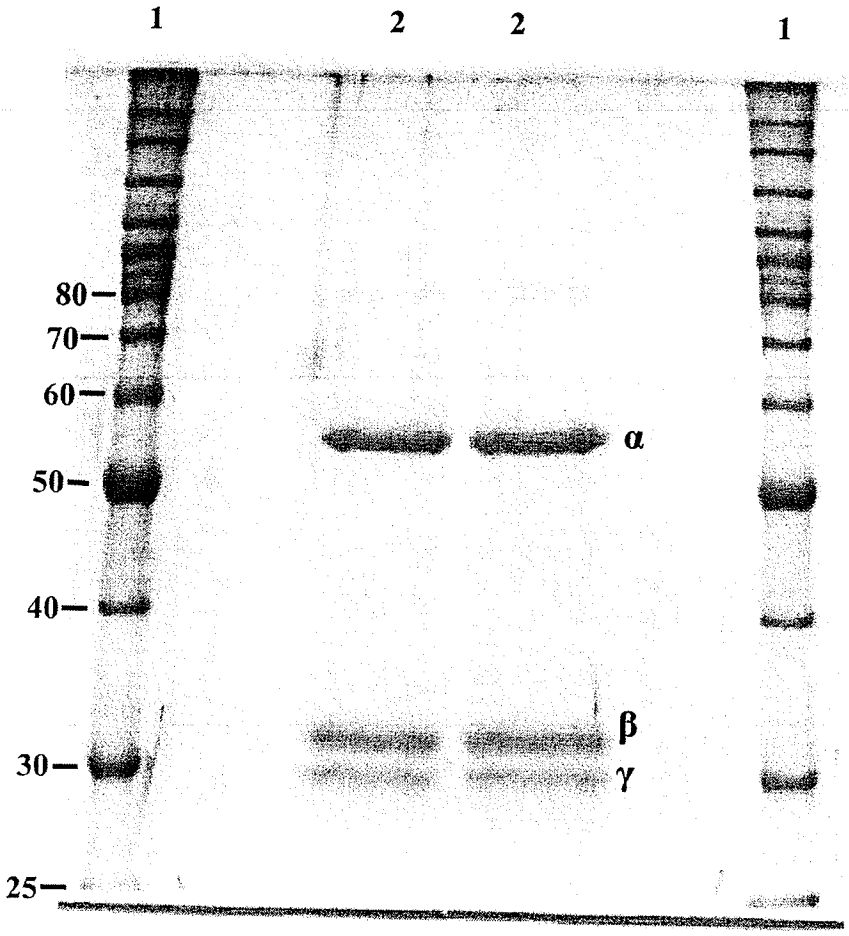

Figure 5.9. Coomassie blue-stained SDS PAGE (12.8% acrylamide) of the purified soluble phenazine-dependent $F_{420}H_2$ dehydrogenation activity from *Methanospirillum hungatei* GP1. 1, molecular markers (kDa). 2, purified protein.

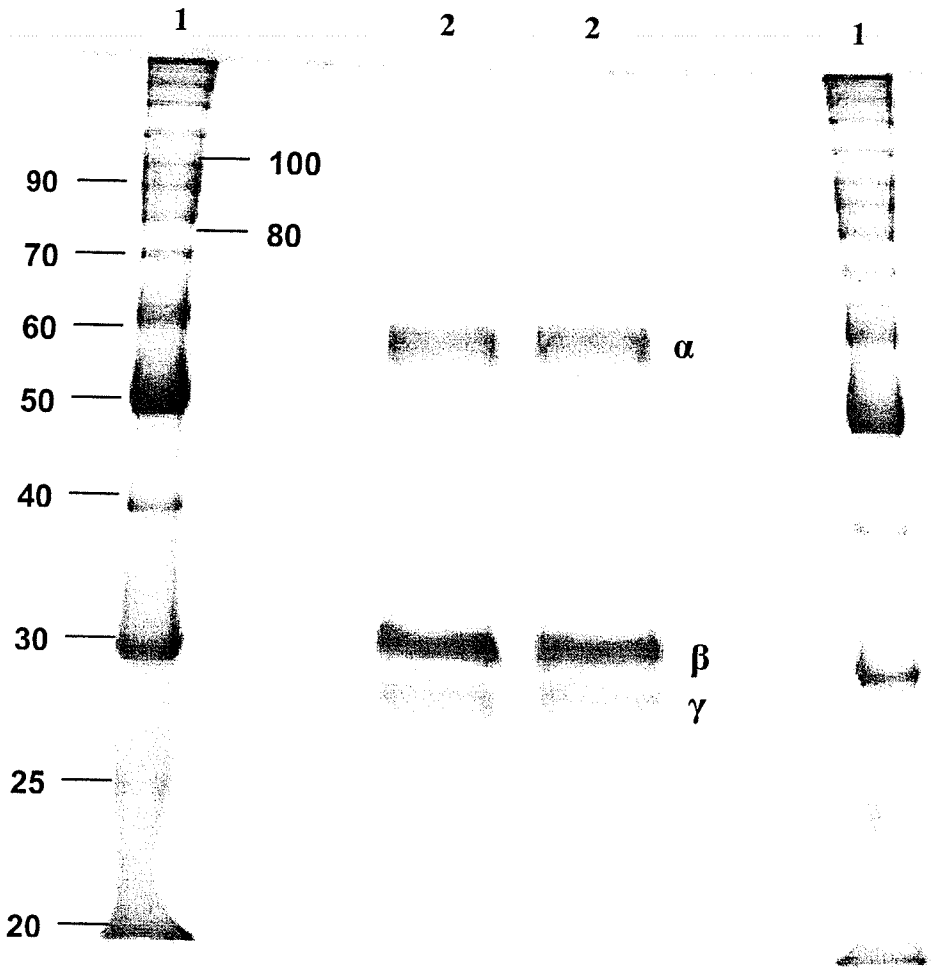

Figure 5.10. Double-stained (Coomassie blue- and silver-stained) SDS PAGE (12.8% acrylamide) of purified soluble phenazine-dependent $F_{420}H_2$ dehydrogenation activity from *Methanospirillum hungatei* GP1. 1, molecular markers (kDa). 2, purified protein.

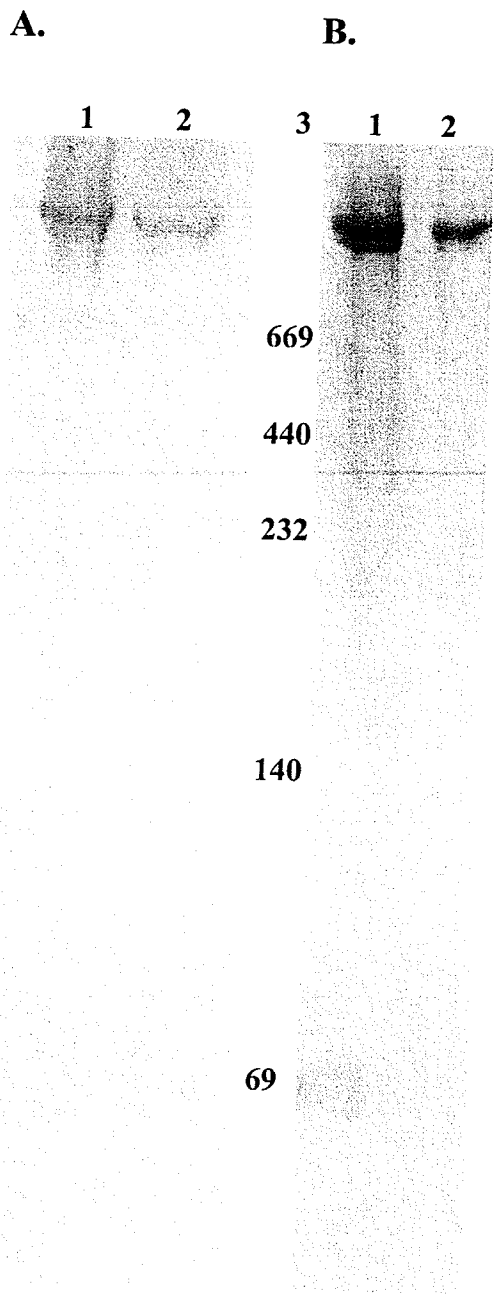

Figure 5.11. (A) Hydrogenase activity-stained and (B) coomassie blue-/silver-stained 3-20% native gradient PAGE comparing the purified soluble and membrane-bound $F_{420}H_2$ dehydrogenation activities.
1, soluble protein. 2, membrane protein. 3, molecular markers (kDa).

5.3.3.2. Mass Spectroscopy sequencing of the purified protein

To confirm that the purified $F_{420}H_2$ dehydrogenation activity was located on the F_{420} H_2ase, mass spectroscopy (MS) analyses of the purified protein was conducted. Two different methods were used to derive sequences from the purified protein. The first method entailed digestion of the holoenzyme with the enzyme trypsin, followed by separation of the fragments by high performance liquid chromatography (HPLC). When the fragment data was compared against the Sonar MS/MS database, the results indicated high similarities with fragments from F_{420} H_2ases from several *Methanosarcina* spp. (Table 5.4).

Table 5.4. Mass spectroscopy analysis results for trypsin-digested fragments of the purified soluble phenazine-dependent $F_{420}H_2$ dehydrogenation activity (holoenzyme) of *Methanospirillum hungatei* GP1. Results compiled using Sonar MS/MS database. Further information regarding the analyses of the holoenzyme is given in Appendix B – Mass Spec data for *Msp. hungatei*.

Expectation	**Significant results (Expectation < 0.1)**	**Methanoarchaeon**	**Accession number**
2.1e-3	F_{420}-reducing hydrogenase isoenzyme II, α subunit	*Methanosarcina barkeri*	CAA74090
2.7e-2	F_{420}-reducing hydrogenase, α subunit	*Methanosarcina acetivorans*	NP_615927
3.5e-2	F_{420}-reducing hydrogenase isoenzyme I, α subunit	*Methanosarcina barkeri*	CAA74094
1.8e-1	F_{420}-reducing hydrogenase isoenzyme I, β subunit	*Methanosarcina barkeri*	CAA74097
7.7e-1	F_{420}-reducing hydrogenase, B subunit	*Methanosarcina mazei* Gö1	NP_635066

The second technique involved in-gel trypsin digestion for each of the purified subunits, as described in 'Materials and methods'. Of the three subunits, only the α-subunit provided data of sufficient quality for analysis. Two independent MS analyses were conducted on the α-subunit. HPLC separation of the digested α-subunit, followed by MS analysis of the fragments, indicated the presence of a fragment with an amino acid sequence that was identical to a fragment derived from the α-subunit of the F_{420} H_2ase from *Ms. mazei* Gö1 (Table 5.5).

MALDI TOF (Matrix-Assisted Laser Desorption Ionization Time of Flight) MS analysis of the trypsin-digested subunit also revealed that the predicted sequence of the polypeptide fragment matched with the sequence of the α-subunit of the F_{420} H_2ase from *Ms. mazei* Gö1 (Table 5.5). Analysis of the amino acid sequence of the α-subunit from the F_{420} H_2ase of *Msp. hungatei* JF1 confirmed the presence of this fragment.

Table 5.5. Mass spectroscopy analysis results for trypsin-digested fragments of the purified soluble phenazine-dependent $F_{420}H_2$ dehydrogenase activity (α-subunit) of *Methanospirillum hungatei* GP1. Fragments predicted to be similar to sequences derived from *Methanosarcina mazei* Gö1. Results compiled using Sonar MS/MS database.

Technique	Expectation	Subunit/Sequence	Accession number
HPLC, MS	8.2e-3	α-subunit, ^{32}GDWLSITPVR^{41}	NP_635069
MALDI TOF	3.1e-3	α-subunit, ^{32}GDWLSITPVR^{41}	NP_635069

BLAST analyses, using amino acid sequences encoding the subunits of the F_{420} H_2ase from various methanoarchaea, confirm that the homologous enzyme from *Msp. hungatei* is most closely related to the enzymes from the *Methanosarcina* spp (Appendix C and D).

5.3.3.3. Catalytic properties

Although our research focused primarily on the $F_{420}H_2$ dehydrogenation activity located in the membranes of *Msp. hungatei* GP1, working with the soluble activity had the benefit of significantly higher yields of purified protein that was indistinguishable from the membrane-bound activity. The soluble phenazine-dependent $F_{420}H_2$ dehydrogenation activity was purified 45-fold to apparent homogeneity with a yield of 5% and a final specific activity of 13.5 μmol $F_{420}H_2$ oxidized·min^{-1}·mg^{-1} protein (Table 5.1); this value ranges from 10-15 μmol $F_{420}H_2$ oxidized ·min^{-1}·mg^{-1} protein.

The $F_{420}H_2$ dehydrogenation activity does not require reductive reactivation prior to assay, as similar activities were measured under aerobic or anaerobic conditions (data not shown). In contrast, the F_{420}-reducing activity must be incubated under reducing conditions in the F_{420} H_2ase reaction buffer before optimal F_{420}-reducing activity is observed. The reactivation process was modified from Choquet and Sprott (1991), with incubation of the protein in 10 μM FAD, 10 μM F_{420} and 20 mM DTT, under an atmosphere of H_2, prior to assay.

NADPH or NADH could not substitute for $F_{420}H_2$ as electron donor, and NAD^+, $NADP^+$, and ferredoxin could not substitute for phenazine, while methyl viologen (with metronidazole) and FAD were both suitable electron acceptors for the $F_{420}H_2$

dehydrogenase activity (Table 5.6). The phenazine-dependent $F_{420}H_2$ dehydrogenation activity was inhibited by the presence of diphenyleneiodonium (DPI) chloride. Dimethyl sulfoxide (DMSO), the solvent used to dissolve DPI did not have any effect on the $F_{420}H_2$ dehydrogenation activity.

DPI is also an inhibitor of flavoproteins, as the purified F_{420} H_2ase was inhibited by the presence of DPI (at 50 μM; the activity was not affected by the addition of 25 μM DPI), but the methyl viologen-reducing activity was not inhibited by DPI

Table 5.6. Electron acceptor specificities of the purified $F_{420}H_2$ dehydrogenase activity of *Methanospirillum hungatei* GP1. $[F_{420}H_2]$ = 10-12 μM.

E^- acceptor and/or inhibitor (μM)	**Activity (μmol $F_{420}H_2$ oxidized·min^{-1}·mg^{-1})**
-	0.3 ± 0.05
Methylviologen (500) + Metronidazole (1000)	12.8 ± 0.7
Phenazine (500)	13.5 ± 1.8
Phenazine (500) + DMSO (50 μl)	12.4 ± 1.5
Phenazine (500) + DPI (25)	9.2 ± 1.2
Phenazine (500) + DPI (50)	5.1 ± 0.4
FAD (40)	5.0 ± 0.4
$NADP^+$ (300)	0.4 ± 0.05
NAD^+ (300)	0.3 ± 0.05
Ferredoxin (1 mg/ml)	0.3 ± 0.03

(Table 5.7). Addition of DMSO did not affect either of the F_{420}- or methyl viologen-reducing H_2ase activities. The presence of phenazine appears to inhibit the F_{420}-reducing activity; this may be due to direct competition for H_2 ($E^{\circ\prime} = -0.420$ V) as phenazine ($E^{\circ\prime} = -0.265$ to -0.165 V) also acts as substrate for the hydrogenase activity. $F_{420}H_2$ may be oxidized by the phenazine-dependent $F_{420}H_2$ dehydrogenation activity concurrent with F_{420}-reduction by the H_2-dependent F_{420}- reducing H_2ase activity.

Table 5.7. Effect of DPI and phenazine on the hydrogenase activities of *Methanospirillum hungatei* GP1. Respective hydrogenase activities were reactivated prior to addition of inhibitor as described under 'Materials and Methods'. [F_{420}] = 20-25 μM. [methyl viologen] = 2 mM.

Electron acceptor	Addition (μM)	Activity
F_{420}	-	$14.3 \pm 2.2^{\dagger}$
F_{420}	50 μl DMSO	$14.7 \pm 1.5^{\dagger}$
F_{420}	DPI (25)	$14.5 \pm 1.2^{\dagger}$
F_{420}	DPI (50)	$4.9 \pm 0.5^{\dagger}$
F_{420}	Phenazine (500)	$3.8 \pm 0.5^{\dagger}$
Methyl viologen	-	$50.1 \pm 2.1^{\ddagger}$
Methyl viologen	50 μl DMSO	$57.0 \pm 3.2^{\ddagger}$
Methyl viologen	DPI (50)	$51.0 \pm 2.1^{\ddagger}$
Methyl viologen	phenazine (500)	$54.2 \pm 4.1^{\ddagger, \dagger\dagger}$

† μmol F_{420} reduced·min^{-1}·mg^{-1}
‡μmol methyl viologen reduced·min^{-1}·mg^{-1}
†† full activity after 5-10 minute lag

In the presence of phenazine, methyl viologen ($E^{\circ\prime} = -0.446$ V) reduction lagged for several minutes (~5-10 minutes), before reaching full activity. This may be due to the preference of the hydrogenase activity for phenazine as substrate, or possibly to transfer of electrons from the reduced methyl viologen to phenazine (either chemical or enzymatic). Addition of 100 μM phenazine to fully reduced methyl viologen (2 mM) resulted in rapid oxidation of the methyl viologen; the reaction was too quick to quantify.

5.3.3.4. Enzyme kinetics and effect of diphenyleneiodonium (DPI) chloride on the $F_{420}H_2$ dehydrogenation activity

The apparent K_m for $F_{420}H_2$ was determined to be 6.3 μM $F_{420}H_2$, with Vmax = 31.1 μmol $F_{420}H_2$ oxidized·min^{-1}·mg^{-1} (Lineweaver Burk: K_m $F_{420}H_2$ = 6.3 μM $F_{420}H_2$, Vmax = 31.2 μmol $F_{420}H_2$ oxidized·min^{-1}·mg^{-1}) (Figure 5.12). The apparent K_m for the phenazine-dependent $F_{420}H_2$ for *Ml. tindarius* and *Ms. mazei* Gö1 are 5.4 and 7 μM $F_{420}H_2$, respectively.

The Michaelis Menten and Lineweaver Burk plots used to determine the apparent K_m for phenazine are shown in Figures 5.13 and 5.14. As determined using the Michaelis Menten kinetics method, the apparent K_m for phenazine was found to be 288.3 μM, while Vmax was 19.5 μmol $F_{420}H_2$ oxidized·min^{-1}·mg^{-1}. Similar values were calculated using the Lineweaver Burk method (K_m = 243.0 μM phenazine, Vmax = 16.9 μmol $F_{420}H_2$ oxidized·min^{-1}·mg^{-1}). The apparent K_m for phenazine as determined for the dehydrogenation activity of *Msp. hungatei* GP1 is similar to the values reported for $F_{420}H_2$ dehydrogenase from *Ms. mazei* Gö1 and *Ml. tindarius* (250 and 288.3 μM, respectively) (Abken *et al.* 1998, this thesis). The turnover number for the $F_{420}H_2$ dehydrogenation activity of *Msp. hungatei* GP1, k_{cat}, was determined to be 164.4 s^{-1}

($k_{cat}/ K_m = 5.6 \times 10^5 M^{-1}s^{-1}$).

Our studies have also demonstrated inhibition of the phenazine-dependent $F_{420}H_2$ dehydrogenation activity of *Msp. hungatei* GP1 (Figures 5.13 and 5.14). Addition of 25 μM DPI increased the K_m for phenazine from 288.3 μM to 370.0 μM (Lineweaver Burk: K_m increased from 243 to 403.5 μM phenazine). In contrast, the apparent K_m increased from 266.7 μM to 1168.1 μM (3 μM DPI) for *Ml. tindarius* (this thesis). These results indicate that the phenazine-dependent $F_{420}H_2$ dehydrogenation activity of *Msp. hungatei* GP1 has a similar affinity for phenazine relative to *Ml. tindarius*, but is much less sensitive to the effects of DPI.

A.

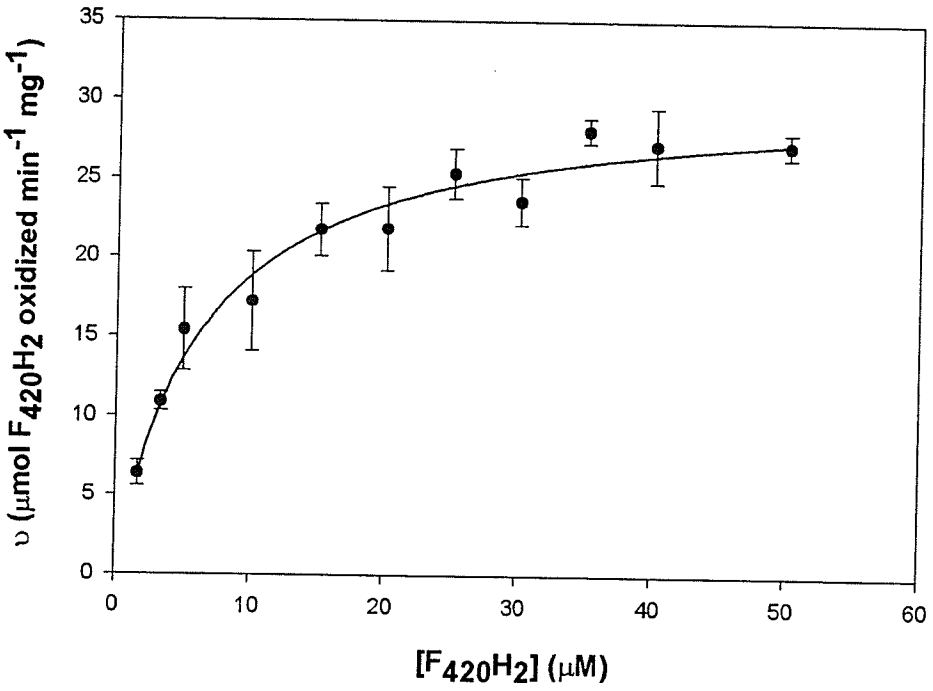

B.

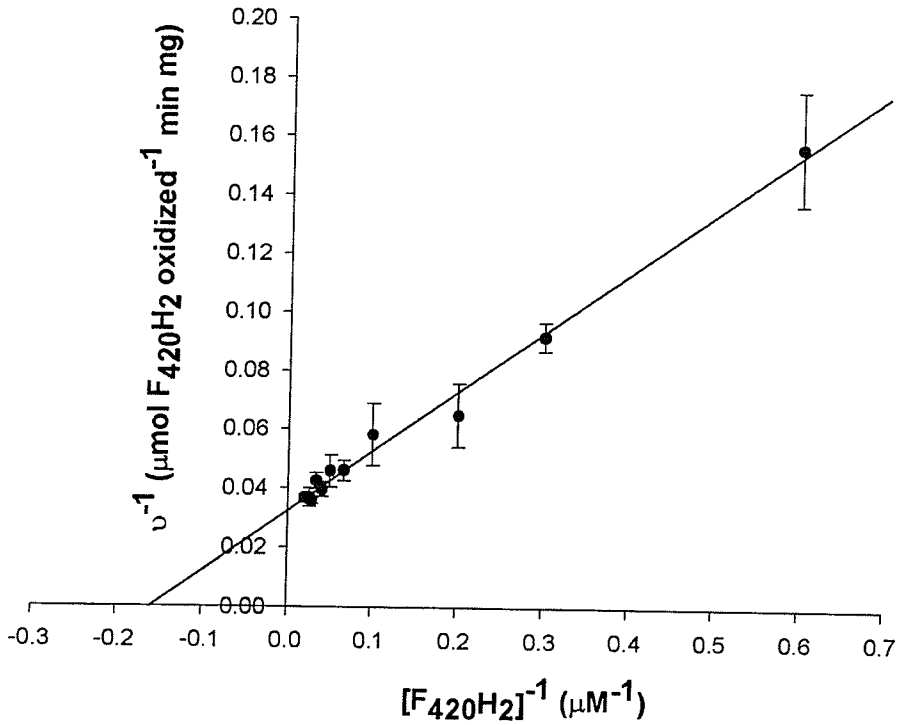

Figure 5.12. Michaelis Menten kinetics (A) and Lineweaver Burk plot for the determination of $KmF_{420}H_2$ for the purified phenazine-dependent $F_{420}H_2$ dehydrogenation activity of *Methanospirillum hungatei* GP1. Each point represents the average of three separate experiments. 500 μM phenazine added per tube.

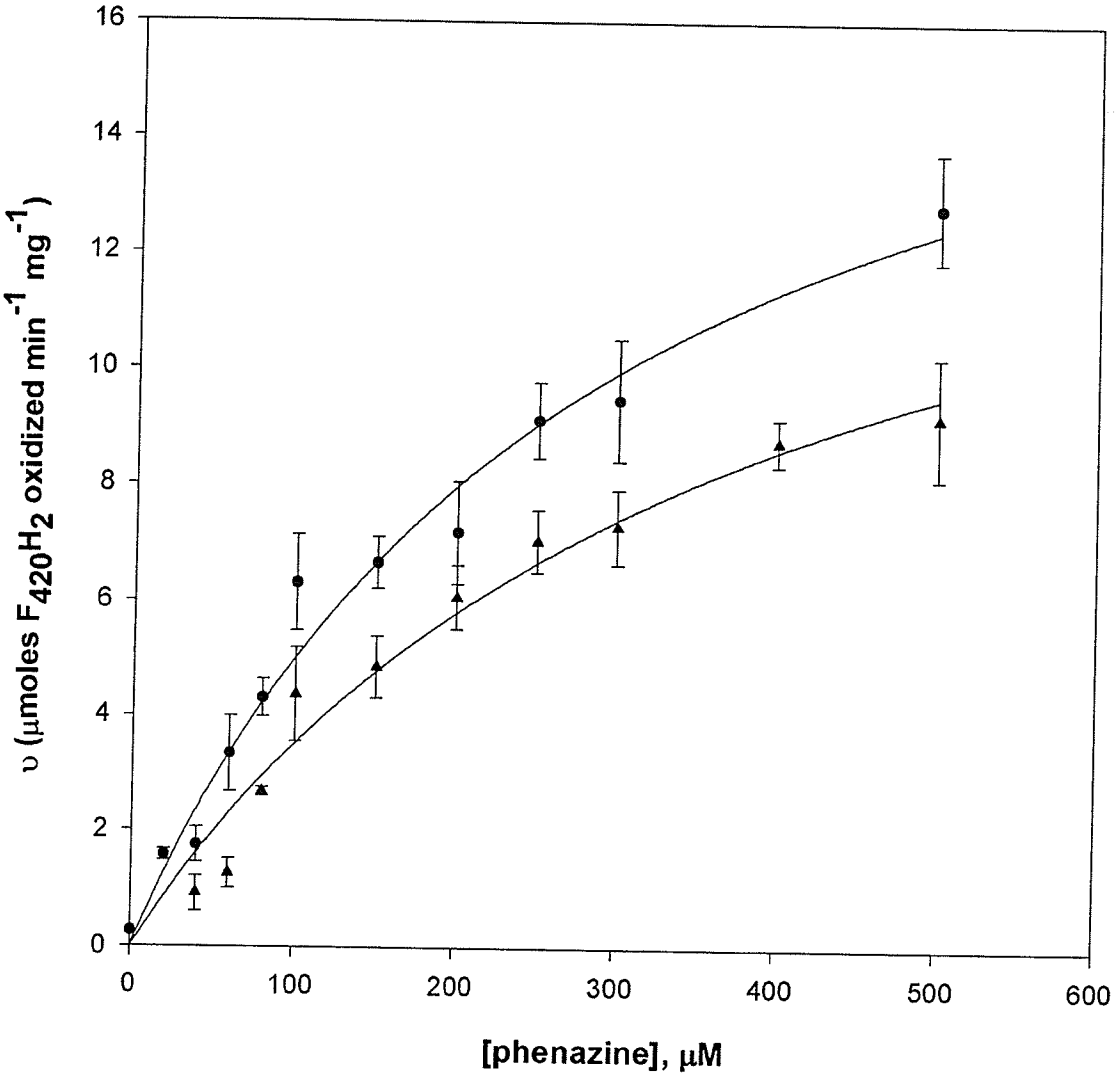

Figure 5.13. Michaelis Menten kinetics plot of the purified phenazine-dependent $F_{420}H_2$ dehydrogenation activity of *Methanospirillum hungatei* GP1 in the presence/absence of DPI. All points represent experiments performed in triplicate. Assay conditions as described under 'Materials and Methods'. ●, No DPI. ▲, 25 μM DPI.

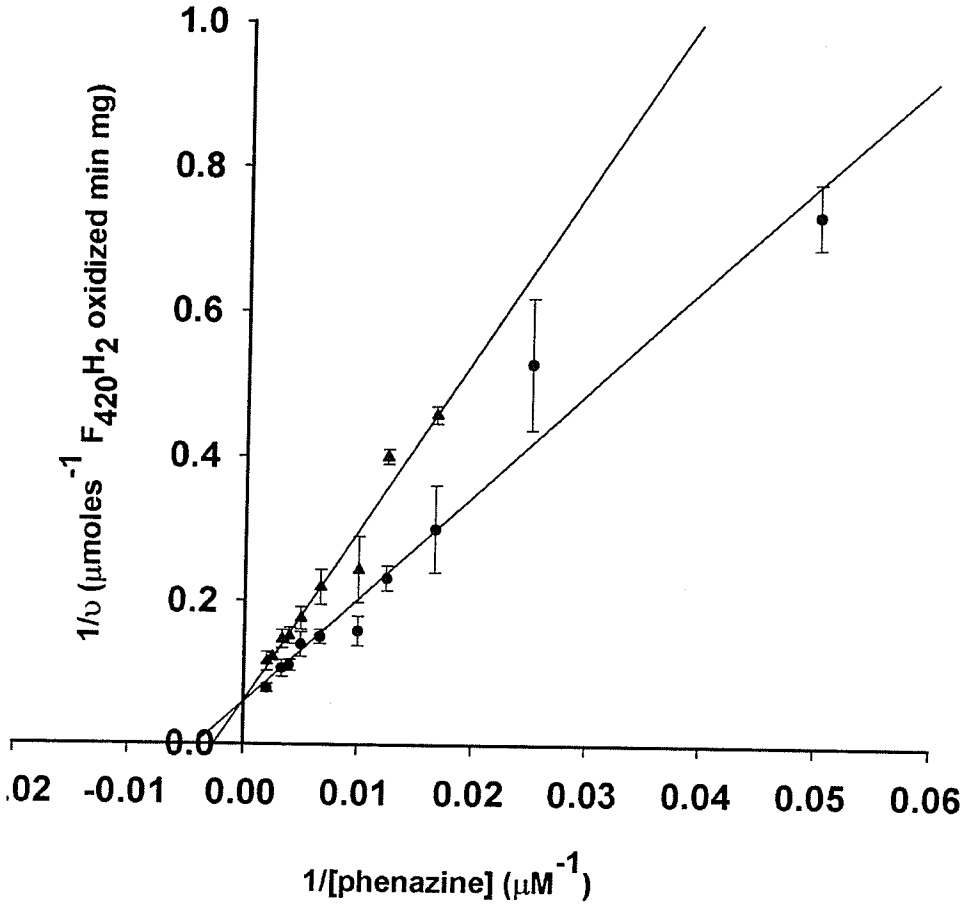

Figure 5.14. Lineweaver Burke kinetics plot of the purified phenazine-dependent $F_{420}H_2$ dehydrogenation activity of *Methanospirillum hungatei* GP1 in the presence/absence of DPI. All points represent experiments performed in triplicate. Assay conditions as described under 'Materials and Methods'. ●, No DPI. ▲, 25 μM DPI.

5.3.3.5. Analyses of the genome of Methanospirillum hungatei *JF1*

The annotated genome of *Msp. hungatei* JF1 (NC_007796) is available for analyses at the National Center for Biotechnology Information (NCBI, http://www.ncbi.nlm.nih.gov) and at the Joint Genome Institute (contig 65, JGI, (http://genome.jgi-psf.org)). Examination of the coding sequences located in contig 65 did not reveal the presence of genes coding for the F_{420}-nonreducing H_2ase, while the operon coding for the F_{420} H_2ase (Frh) was present as expected (Table 5.8).

Table 5.8. Frh operon of *Msp. hungatei* JF1. Sequences of subunits from Contig 65 from the Joint Genome Institute Microbial Sequencing Program.

Gene	Sequence location	Subunit
Mhun2329	2584805-2585671	FrhB (β)
Mhun2330	2585674-2586462	FrhG (γ)
Mhun2331	2586503-2587054	FrhD (δ)
Mhun2332	2587068-2588477	FrhA (α)

BLAST analyses of the Archaea database at NCBI, using the amino acid sequence encoding the FpoF subunit (accession number: AAF65743) of the Fpo complex from *Ms. mazei* Gö1, did not reveal the presence of an FpoF homologue in *Msp. hungatei* JF1 (NC_007796), only sequences coding for the β-subunit (FrhB) of the F_{420} H_2ase were observed (Table 5.9).

Table 5.9. BLAST analyses results using the amino acid sequence coding for the FpoF subunit from *Ms. mazei* Gö1 against the genome of *Msp. hungatei* JF1.

***Ms. mazei* Gö1**	***Msp. hungatei* JF1**			
FpoF subunit/ (accession number)	**Corresponding subunit/ sequence**	**Identity**	**Similarity**	**E value**
FpoF (AAF65743)	FrhB (β) (899494-900231)	84/248 (33%)	139/248 (56%)	4e-32
FpoF (AAF65743)	FrhB (β) (2585602-2584817)	95/264 (35%)	147/264 (55%)	9e-41

BLAST analyses, using the tblastn program, did not indicate the presence of sequences coding for the F_{420}-nonreducing H_2ase, consistent with the findings of Sprott *et al.* (1987) and our own biochemical studies. The amino acid sequences encoding the F_{420}-nonreducing H_2ase s used as query for the BLAST analyses were derived from the following methanoarchaea: *Mtb. thermoautotrophicus* ΔH (Mvh, Table 5.10); *Ms. mazei* Gö1 (Vho, Table 5.11); and *Mc. voltae* (Vhu, Table 5.12). The E values (Expectation) were low, and several of the subunits from the respective F_{420}-nonreducing H_2ases corresponded to subunits of the F_{420} H_2ase of *Msp. hungatei* JF1; this is expected as both enzymes are [NiFe]-hydrogenases (Vignais *et al.* 2001).

Table 5.10. BLAST analyses of the *Msp. hungatei* JF1 genome using the amino acid sequences coding for the F_{420}-nonreducing hydrogenase (Mvh) of *Mtb. thermoautotrophicus* ΔH.

***Mtb. thermoautotrophicus* ΔH**	***Msp. hungatei* JF1**			
MvH subunit/ (accession number)	**Corresponding subunit/ sequence**	**Identity**	**Similarity**	**E value**
MvhA (Q50783)	FrhA (α) (2588417-2587116)	123/465 (26%)	203/465 (44%)	5e-28
MvhG (Q50782)	FrhG (γ) (2586462-2585860)	74/248 (29%)	113/248 (45%)	1e-16
MvhD (Q50781)	MvhD (δ) (2073516-2073926)	75/137 (54%)	97/137 (70%)	8e-39
MvhD (Q50781)	MvhD (δ) (2075475-2075864)	72/130 (55%)	94/130 (72%)	8e-39

Table 5.11. BLAST analyses of the *Msp. hungatei* JF1 genome using the amino acid sequences coding for the F_{420}-nonreducing hydrogenase (Vho) of *Ms. mazei* Gö1.

***Ms. mazei* Gö1**	***Msp. hungatei* JF1**			
Vho subunit/ (accession number)	**Corresponding subunit/ sequence**	**Identity**	**Similarity**	**E value**
VhoA (AAM32009)	FrhA (α) (2588423-2588052)	41/127 (32%)	65/127 (51%)	6e-12
VhoA (AAM32009)	FrhA (α) (2587685-2587116)	66/238 (27%)	94/238 (39%)	3e-7
VhoG (AAM32010)	No match	-	-	-
VhoC (AAM32008)	ABC transporter (312067-312201)	17/50 (34%)	24/50 (48%)	7.3

Table 5.12. BLAST analyses of the *Msp. hungatei* JF1 genome using the amino acid sequences coding for the F_{420}-nonreducing hydrogenase (Vhu) of *Mc. voltae*.

Mc. voltae	***Msp. hungatei* JF1**			
Vhu subunit/ (accession number)	**Corresponding subunit/ sequence**	**Identity**	**Similarity**	**E value**
VhuA (Q00407)	FrhA (α) (2588423-2587155)	115/435 (26%)	194/435 (44%)	6e-27
VhuG (Q00409)	FrhG (γ) (2586462-2586061)	50/158 (31%)	77/158 (48%)	2e-12
VhuD (Q00408)	MvhD (δ) (2073531-2073926)	52/132 (39%)	81/132 (61%)	8e-25
VhuD (Q00408)	MvhD (δ) (2075469-2075804)	52/132 (39%)	81/132 (61%)	6e-25
VhuU (Q00410)	FrhA (α) (2588417-2587116)	72/130 (55%)	94/130 (72%)	8e-39

Although the genes encoding the catalytic subunits of the F_{420}-nonreducing H_2ase were not isolated, sequences coding for the D/δ-subunits from the respective F_{420}-nonreducing H_2ases from *Mtb. thermoautotrophicus* ΔH and *Mc. voltae* are found in the genome of *Msp. hungatei* JF1. These subunits are distinct from the FrhD subunit, and are not found in the *frh* operon of *Msp. hungatei* JF1.

It is interesting to note that on examination of the annotated sequence in Contig 65 (JGI), the genes encoding the D/δ-subunits (Mhun 1839 and Mhun1842, contig 65) are identical repeats found immediately adjacent to the genes of the *hdrABC* operon (Mhun1838-Mhun1836), at the 3' end of *hdrA*. These repeats are related to the δ-subunit of the F_{420}- reducing H_2ase from *M. kandleri*, but also share approximately 50%

Table 5.13. BLAST search results of the gene encoding the putative F_{420}-nonreducing hydrogenase δ-subunit at the 3' end of *hdrA*. The gene encoding the hydrogenase δ-subunit (Mhun1839, 2073516-2073838) is found at the 3' end of *hdrA* gene (Mhun1838, 2071501-2073516).

Methanoarchaeon	subunit	hydrogenase	% Identity	% Similarity	E value
M. kandleri	δ	F_{420}-reducing	55	70	1e-40
Mc. voltae	VhcD	F_{420}-nonreducing	51	72	4e-40
Mc. maripaludis	δ	F_{420}-nonreducing	50	70	2e-38
GZFOS26D6[†]	δ	F_{420}-reducing	55	72	9e-38
Mtb. thermoautotrophicus	MvhD	F_{420}-nonreducing	54	70	1e-37

[†]uncultured methanogenic archaeon

identity (~70% similarity) with various δ-/D-subunits from the F_{420}-nonreducing H_2ases of various Class I methanoarchaea, including MvhD of *Mtb. thermoautotrophicus* ΔH (Table 5.13). MvhD has been suggested to be the electronic link between the F_{420}-nonreducing H_2ase (Mvh) and Hdr in *Mtb. marburgensis* (Figure 1.15B) (Stojanowic *et al.* 2003, Fricke *et al.* 2006). In contrast, FrhD does not copurify with the holoenzyme and is expected to encode a protease involved with maturation (Fricke *et al.* 2006).

5.4. Discussion

5.4.1. Purfication of the phenazine-dependent $F_{420}H_2$ dehydrogenation activity in Methanospirillum hungatei *GP1*

Phenazine-dependent $F_{420}H_2$ dehydrogenation activity has been detected in the cell-free extracts of a number of non-methylotrophic methanoarchaea outside of the *Methanosarcinaceae*, including *Msp. hungatei* GP1 (Chapter 4). Given the close phylogenetic relationship between the orders *Methanosarcinales* and *Methanomicrobiales* (Bapteste *et al.* 2005), the observation of a phenazine-dependent $F_{420}H_2$ dehydrogenase activity in *Msp. hungatei* GP1 was not surprising. In the absence of the F_{420}-nonreducing H_2ase, which is typically found in hydrogenotrophic methanoarchaea associated with the H_2:heterodisulfide oxidoreductase complex, an $F_{420}H_2$-dependent mechanism for CoM-S-S-CoB reduction can be envisioned in *Msp. hungatei* GP1 (Sprott *et al.* 1987, Thauer *et al.* 1993, this thesis).

Following cell lysis, the vast majority (80-90%) of the $F_{420}H_2$ dehydrogenation activity is found in the soluble cytoplasmic portion of *Msp. hungatei* GP1, with 10-20% of the overall activity located on the washed cell membranes. This is consistent with the level of $F_{420}H_2$ dehydrogenase activity found in the membranes of *Ml. tindarius* and *Ms. mazei* Gö1 (Haase *et al.* 1992, Abken and Deppenmeier 1997).

Various chromatographic techniques were used to resolve the $F_{420}H_2$ dehydrogenation activity of *Msp. hungatei* GP1; at the onset, our results indicated that the $F_{420}H_2$ dehydrogenation activity eluted from the various chromatographic matrices with an F_{420} H_2ase activity. These results were observed on a consistent basis whether the proteins were derived from the soluble portion, or extracted from solubilized membranes (Figures 5.1 to 5.4, section 5.3.1).

The profile of the purified $F_{420}H_2$ dehydrogenation activity of *Msp. hungatei* GP1, as observed on native gradient PAGE and SDS PAGE gels indicate the isolation of the F_{420} H_2ase. The native form of the enzyme has a molecular weight greater than 669 kDa (Figure 5.8), consistent with a molecular weight of 720 ± 84 kDa as reported by Sprott *et al.* 1987. The protein is made up of three distinct subunits (Figures 5.9 and 5.10) of approximately 55 (α), 35 (β), and 32 (γ) kDa (Choquet and Sprott 1991). The soluble cytoplasmic- and membrane-bound $F_{420}H_2$ dehydrogenation activities were both isolated on the F_{420} H_2ase (Figure 5.11). No other source of $F_{420}H_2$ dehydrogenation activity was observed in *Msp. hungatei* GP1 during our studies.

Mass spectroscopy analyses indicate that fragments of the purified protein share highest similarity with the F_{420} H_2ase s from the *Methanosarcina* spp. (Tables 5.4 and 5.5). Further analyses of the Archaea database at NCBI indicate that the F_{420} H_2ase of *Msp. hungatei* JF1 is most closely related to the corresponding enzymes from *Methanosarcina* spp. (Appendix C and D).

In contrast, the $F_{420}H_2$ dehydrogenase activity purified from *Ml. tindarius* and *Ms. mazei* Gö1 each consist of 5 distinct subunits with molecular weights ranging from of 45, 40, 22, 18, and 17 kDa (120 kDa overall, *Ml. tindarius*) and 40, 37, 22, 20, and 16 kDa (115 KDa overall, *Ms. mazei* Gö1). The purified activities were not associated with an F_{420} H_2ase activity (Abken and Deppenmeier 1997).

5.4.2. $F_{420}H_2$ dehydrogenase vs. F_{420}-reducing hydrogenase activity

The role of the F_{420} H_2ase is to transfer electrons from H_2 to F_{420}:

$$F_{420} + H_2 \rightarrow F_{420}H_2$$

During growth on H_2 and CO_2, $F_{420}H_2$ is used as a source of electrons for the reduction of C_1-bound H_4MPT intermediates to the level of CH_3-H_4MPT (Figure 1, Chapter 1) (Thauer *et al.* 1993, Deppenmeier *et al.* 1996, Shima *et al.* 2002). This enzyme is typically isolated from the cytoplasm, although immunogold studies have shown that the enzyme is found attached to the inner face of the cytoplasmic membrane (Baron *et al.* 1989, Lünsdorf *et a*l. 1991, Braks *et al.* 1994). A membrane location would be essential if this enzyme is required for energy conservation, as the energy conserving electron transport apparatus is located within the membrane (Schäfer *et al.* 1999).

Similar to the $F_{420}H_2$ dehydrogenase of *Ms. mazei* Gö1, the $F_{420}H_2$ dehydrogenation reaction of *Msp. hungatei* GP1 could be assayed using phenazine as an electron acceptor:

$$F_{420}H_2 + \text{phenazine} \rightarrow F_{420} + \text{phenazine-}H_2$$

Phenazine-dependent $F_{420}H_2$ dehydrogenation was competitively inhibited by the presence of DPI (25 μM). The physiological significance of this activity is unclear, as methanophenazine has not been isolated from methanoarchaea outside of the *Methanosarcinaceae* (Beifuss and Tietze 2005). Also, in contrast to the Fpo complex, the F_{420} H_2ase does not contain membrane integral components resembling a proton pump, so this protein on its own likely is not a site for energy conservation. The purified $F_{420}H_2$ dehydrogenase from *Ml. tindarius* and *Ms. mazei* Gö1 were the soluble cytoplasmic portion of a larger multi-subunit protein complex with integral membrane

components (Deppenmeier 2002, 2004). It is possible that the F_{420} H_2ase may dock onto integral membrane components that would not have been purified using our protocol.

5.4.2.1. Differences in requirement for reductive reactivation

The $F_{420}H_2$ dehydrogenation activity of *Msp. hungatei* GP1 did not require reactivation prior to assay, even after manipulation under aerobic conditions, when the protein would be in an oxidized form. Addition of protein, whether aerobic or anaerobic, to assay buffer containing $F_{420}H_2$ and electron acceptor results in immediate enzyme activity. Addition of FAD to column chromatography or storage buffers did not enhance $F_{420}H_2$ dehydrogenase activity. In contrast, the F_{420} H_2ase activity of *Msp. hungatei* GP1 requires reactivation of the protein under reducing conditions for optimal activity. These conditions, modified from Choquet and Sprott (1991), require incubation of the protein with reducing agent, FAD, and F_{420}, under an atmosphere of H_2. In the absence of reductive reactivation there was a lag in F_{420}-reducing activity lasting several minutes, and approximately 50% decrease in activity compared to the activated enzyme.

Reductive reactivation is a common procedure for aerobically purified hydrogenase. This entails removal of O_2, reduction of the active centers of the hydrogenase in the presence of electron donor(s) and traces of active hydrogenase, under an atmosphere of H_2 (Lissolo *et al.* 1984, Teixeira *et al.* 1985). With respect to the F_{420} H_2ase, reduction of the [NiFe] center, FeS clusters, and flavin moiety is essential, particularly after aerobic manipulation (Kojima *et al.* 1983). Active molecules of hydrogenase catalyze the reduction of F_{420} to $F_{420}H_2$, which would then act as electron donors to the oxidized molecules of hydrogenase (Fox *et al.* 1987). Electrons from

$F_{420}H_2$ enter the protein *via* the FAD component of the β-subunit, which converts the donated hydride ion into 2 single electrons that are transferred through the FeS clusters in the γ-subunit to the [NiFe] center in the α-subunit.

While the mechanism for FAD insertion is not known, a possible model could be suggested based on studies with the heterotetrameric NAD^+ reducing hydrogenase of *Ralstonia* (*R.*) *eutropha* (van der Linden *et al.* 2004). This enzyme consists of two modules, an NADH dehydrogenase (HoxF and HoxU) and a hydrogenase module (HoxH and HoxY). Prolonged exposure of the NAD^+-reducing hydrogenase to NADH leads to a conformational change in the protein, exposing an FMN binding site in HoxY that is normally closed to the environment. NADH is oxidized by HoxF, which contains a fixed molecule of FMN. Electrons are transferred through the FeS clusters from HoxF, through HoxU and HoxY, and finally to HoxH, restoring the protein to a reduced form. At the same time, HoxFU opens up and pivots away from HoxHY, exposing a FMN (bound to HoxY) that slowly dissociates from the protein. This process is reversible, and addition of excess FMN restores the flavin moiety to its site.

Studies with the NAD^+-reducing hydrogenase of *R. eutropha* (van der Linden *et al.* 2004) indicated that FMN could not be restored to the enzyme under oxidized conditions, highlighting the importance of reduced conditions for optimal activation of this protein. Incubation of the oxidized F_{420} H_2ase under reducing conditions (H_2 atmosphere, 20 mM DTT, 10 μM $F_{420}H_2$) may induce a conformational change to the F_{420} H_2ase, perhaps a change in the structure of the β-subunit that exposes the FAD-binding site. The addition of excess FAD may prevent the disassociation of the FAD from its binding site, or more importantly, restore FAD that may have been lost during the course

of purification. This is consistent with the findings of Nelson *et al.* (1984), who observed that FAD dissociated from the F_{420} H_2ase of *Methanobacterium formicicum* during column chromatography, rendering an inactive enzyme; activity was restored after addition of FAD. Spectrophotometric analysis or FAD quantification could be used to confirm the loss of FAD during purification of the $F_{420}H_2$ dehydrogenation activity of Msp. hungatei GP1.

5.4.3. Mechanism of $F_{420}H_2$-dependent phenazine reduction via F_{420}-reducing hydrogenase

The α- and γ- subunits of the methanogenic F_{420} H_2ase form a heterodimeric hydrogenase, capable of reducing synthetic electron acceptors such as methyl or benzyl viologen (Thauer *et al.* 1993, Vignais *et al.* 2001). The α-subunit, which shares homology with the large subunit commonly found in [NiFe] hydrogenases, contains the binding site for the H_2-activating/splitting bimetallic [NiFe] center (Cammack 1995, Vignais *et al.* 2001).

The γ-subunit contains the FeS clusters that are characteristic of the small hydrogenase subunit, and may also confer electron acceptor specificity to the holoenzyme; the γ-subunit conducts electrons from the H_2-activating centre of the α-subunit to the physiological electron acceptor (Vignais *et al.* 2001). Mutation of the FeS clusters from the γ-subunit of the F_{420} H_2ase from *Mc. voltae* results in a 10-fold decrease in F_{420}-reduction, but has no effect on methyl viologen-reduction (Bingemann and Klein 2000).

The β-subunit, containing the FAD binding site, confers specificity for F_{420} to the F_{420} H_2ase (Figure 5.15A); absence or denaturation of the β-subunit eliminates the

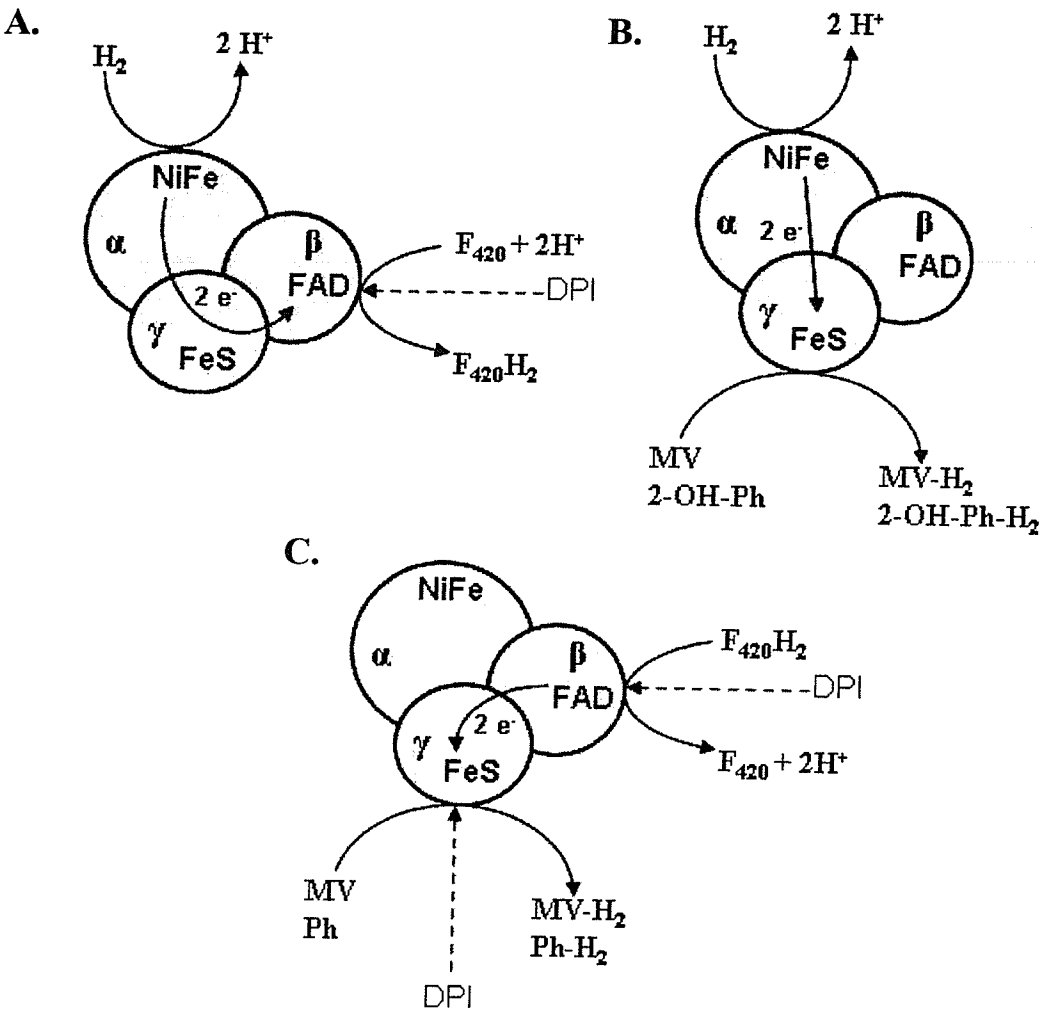

Figure 5.15. Models of electron shuttling with the F_{420}-reducing hydrogenase, using different substrates. A. H_2-dependent F_{420}-reduction. Electrons from the H_2-splitting [NiFe] center in the α-subunit flow through the FeS clusters in the γ-subunit to the β-subunit. Electrons are converted to a hydride ion *via* FAD for transfer to F_{420}. DPI may inhibit $F_{420}H_2$ reduction by binding to the FAD in the β-subunit. B. H_2-dependent reduction of methyl viologen and 2-OH-phenazine (in *Mtb. thermoautotrophicus* ΔH, Meuer *et al.* 1999). Electrons transferred from the α-subunit through the FeS clusters in the γ-subunit, to the single e^- acceptors methyl viologen or 2-OH-phenazine. C. $F_{420}H_2$-dependent reduction of methyl viologen or phenazine. Hydride ion from $F_{420}H_2$ converted to single electrons *via* FAD in β-subunit; electrons shuttled through FeS clusters in γ-subunit to methyl viologen or phenazine. DPI may inhibit phenazine reduction at different sites. MV, methyl viologen. 2-OH-Ph, 2-Oh-phenazine. Ph, phenazine. DPI, Diphenyleneiodonium chloride.

enzymes' ability to react with F_{420} (Thauer *et al.* 1993). FAD is essential as it allows the hydrogenase to use F_{420}, which is a hydride donor/acceptor. Theβ-subunits of the F_{420} H_2ase s from various methanoarchaea share homology with the FpoF subunit of the Fpo complex from *Ms. mazei* Gö1 (Bäumer *et al.* 2000). FpoF, which contains FAD and an FeS cluster, is expected to be the point of electron entry from $F_{420}H_2$ for the $F_{420}H_2$ dehydrogenases; overexpression of the *fpoF* gene in *E. coli* leads to the production of a protein that oxidizes $F_{420}H_2$ while reducing methyl viologen (Baümer *et al.* 2000). It is not known if the β-subunit of the F_{420} H_2ase, which contains FAD but no FeS clusters, can catalyze a similar reaction apart from the holoenzyme.

Based on available knowledge of electron transfer through the F_{420} H_2ase, a mechanism for $F_{420}H_2$-dependent phenazine reduction can be hypothesized. Frh and Mvh of *Mtb. thermoautotrophicus* both catalyze the H_2-dependent reduction of 2-OH-phenazine in the same manner as methyl viologen; electrons are transferred from the α-subunit through the FeS-containing γ-subunit to 2-OH-phenazine (Figure 5.15B) (Albracht 1994, Vignais *et al.* 2001, Meuer *et al.* 2002). $F_{420}H_2$-dependent reduction would not require the α-subunit, but would likely require the β- and γ-subunits (Figure 5.15C). Electrons from $F_{420}H_2$ (E° = -0.360 V) enter the F_{420} H_2ase by way of the FAD in the β-subunit, which converts the hydride ion into two single electrons. The electrons are then channeled through the γ-subunit *via* the 3 FeS clusters, shuttling each electron to phenazine (E° = -0.265 to -0.165 V), which accepts 2 electrons in single transfer steps (Abken *et al.* 1998).

DPI inhibits the $F_{420}H_2$ dehydrogenase of *Ms. mazei* Gö1, inhibiting the reduction of 2-OH-phenazine. At low concentrations of DPI (1 μM), the $F_{420}H_2$ dehydrogenase of

Ms. mazei Gö1 was competitively inhibited, increasing the apparent K_m for 2-OH-phenazine from 35 μM to 100 μM (Brodersen *et al.* 1999). At 10-fold higher concentrations of DPI, $F_{420}H_2$-dependent methyl viologen reduction was inhibited, indicating that there were two sites of DPI inhibition; at higher concentrations it was believed that the FAD component was being inhibited (Brodersen *et al.* 1999).

Addition of 25 μM DPI inhibited phenazine-dependent $F_{420}H_2$ dehydrogenation activity, but not the F_{420} H_2ase activity (Table 5.6 and 5.7); the K_m for phenazine increased from 288.3 μM to 370.0 μM, Vmax = 19.5 μmol $F_{420}H_2$ oxidized·min^{-1}·mg^{-1} (Michaelis Menten kinetics). The inhibition observed in the presence of 25 μM DPI appears to be competitive, due to competition with phenazine for the binding site at the γ-subunit. However, addition 50 μM DPI inhibited both the phenazine-dependent $F_{420}H_2$ dehydrogenation and F_{420}-reducing activities (Table 5.6 and 5.7). This may indicate that the observed inhibition at this concentration of DPI is due to inhibition of the FAD moiety, preventing the interaction of the β-subunit with $F_{420}/F_{420}H_2$.

Phenazine was used in our studies, but it is not clear whether methanophenazine is found in *Msp. hungatei* GP1. It is possible that the $F_{420}H_2$-dependent reduction of phenazine may be an artifact of the F_{420} H_2ase, similar to the H_2-dependent reduction of methyl viologen by this enzyme. The purified F_{420} H_2ase of *Mtb. thermoautotrophicus* ΔH also catalyzes the reduction of phenazine in place of F_{420}; methanophenazine is not found in this methanoarchaeon (Abken *et al.* 1998, Meuer *et al.* 1999, Beifuss and Tietze 2005).

5.4.4. Analyses of the genome of Methanospirillum hungatei *JF1*

The genes encoding for the Fpo complex were not observed in the genome of *Msp. hungatei* JF1 (NC_007796). The amino acid sequence of the FpoF subunit (AAF6574) from *Ms. mazei* Gö1 was most closely related to the FrhB (β) subunit of the F_{420} H_2ase of *Msp. hungatei* JF1 (found in the Frh operon), and to a homologue of the β-subunit outside of the operon (Table 5.8). The FpoF and Frhβ subunits contain the FAD component for the respective enzymes, while FpoF also contains an additional FeS cluster (Bäumer *et al.* 2000).

An F_{420}-nonreducing H_2ase was not detected in *Msp. hungatei* GP1 by Sprott *et al.* (1987), nor did we did detect this protein during our own biochemical studies. BLAST analyses of the genome of *Msp. hungatei* JF1 using the amino acid sequences encoding the subunits of the F_{420}-nonreducing H_2ases from various methanoarchaea (Tables 5.10-5.12) did not result in the location of putative genes encoding for an F_{420}-nonreducing H_2ase in *Msp. hungatei* JF1; only the genes sequences of subunits encoding the F_{420} H_2ase and Ech H_2ase were found during these searches. However, homologues for the sequences encoding the D/δ-subunits from the F_{420}-nonreducing H_2ases of *Mtb. thermoautotrophicus* ΔH and *Mc. voltae* were found in the genome of *Msp. hungatei* JF1.

An examination of Contig 65 (http://genome.ornl.gov.microbial/mhun/) at JGI indicates the presence of genes coding for the δ-subunits of the F_{420} H_2ase (Mhun 1839, 2073516-2073938), at the 3' end of the gene encoding the HdrA subunit (Mhun 1838, 2071501-2073516); this is in addition to the δ-subunit encoded within the Frh operon of *Msp. hungatei* JF1. The putative δ-subunit at the 3' end of *hdrA* also shares up to 55% identity (72% similarity) with the δ-/D-subunit of the F_{420}-nonreducing H_2ase of various

methanoarchaea, including *Mc. voltae* (E = 4e-40), *Mc. maripaludis* (E = 2e-38), and *Mtb. thermoautotrophicus* ΔH (E = 1e-37). BLAST analyses at NCBI identify putative subunit as being similar to MvhD and VhuD subunits of the F_{420}-nonreducing H_2ase of *Mtb. thermoautotrophicus* ΔH (Table 5.10) and *Mc. voltae* (Table 5.12), respectively, indicating a possible electronic link between the F_{420} H_2ase and Hdr of *Msp. hungatei* GP1.

A homologue of the *mvhD* gene, which encodes an FeS-containing subunit of the Mvh H_2ase, is fused to the 3' end of the *hdrA* genes of *Mtb. thermoautotrophicus* ΔH, *Mtb. marburgensis*, and *Msph. stadtmanae* (Stojanowic *et al.* 2002, Fricke *et al.* 2006), suggesting a functional link between the Mvh H_2ase and the Hdr in these methanoarchaea (Figure 1.15B, Chapter 1). It is suggested that electrons flow from the F_{420}-nonreducing H_2ase to the Hdr through contact formed between the MvhD and HdrA subunits of the respective enzymes, this has not been confirmed experimentally (Fricke *et al.* 2006). In contrast, *frhD* encodes for a peptidase involved in maturation of the F_{420} H_2ase; FrhD is not involved in electron transport, nor is it a subunit of the holoenzyme.

The F_{420}-nonreducing H_2ase plays a key role in the H_2-dependent reduction of CoM-S-S-CoB (Thauer *et al.* 1993); absence of this protein would require an alternate mechanism for shuttling of electrons to Hdr. A similar arrangement with the F_{420} H_2ase and the Hdr of *Msp. hungatei* GP1 may be possible. Braks *et al.* (1994) observed the presence of 10-20 kDa proteins linking the F_{420} H_2ase of *Mtb. marburgensis* to the inner face of the cell membrane *via* microscopic analyses. It is not known if these linkers are the D/δ-subunits fused to HdrA, or if these linkers are associated with electron transport

from the F_{420} H_2ase to proteins in the membrane that may be associated with energy conservation.

5.4.6. Physiological interpretations

It has been proposed that the F_{420}-nonreducing H_2ase of methanoarchaea outside of the *Methanosarcinaceae* docks directly with Hdr (Figure 1.15B, Chapter 1), with electron transfer directly from the δ-/D-subunit of the F_{420}-nonreducing H_2ase to HdrA (Stojanowic *et al.* 2003, Fricke *et al.* 2006). This is consistent with the findings of Setzke *et al.* (1994), who found that the F_{420}-nonreducing H_2ase (Mvh) and Hdr of *Mtb. thermoautotrophicus* ΔH copurified together as a tightly bound complex.

In the absence of an F_{420}-nonreducing H_2ase, a similar role for the F_{420} H_2ase of *Msp. hungatei* GP1 may be envisioned, as depicted in Figure 5.16. The $F_{420}H_2$ dehydrogenation activity, associated with the F_{420} H_2ase of *Msp. hungatei* GP1, may be an essential part of an $F_{420}H_2$-dependent CoM-S-S-CoB oxidoreductase system, of which the Hdr comprises the second major component of this proposed electron transport system. The F_{420} H_2ase of *Msp. hungatei* GP1 has hydrophobic character, with up to 10-20% of the activity associated with the cell membrane (Choquet and Sprott 1991, Sprott and Beveridge 1993, this study). The F_{420} H_2ases behave on hydrophobic column matrices as very hydrophobic proteins, suggesting a functional association with the cytoplasmic membrane (Sprott and Beveridge 1993). Lipids are also associated with the purified protein, and in fact stimulate the F_{420} H_2ase activity of *Msp. hungatei* (Choquet and Sprott1991); it has been suggested that the lipids may be essential for anchoring the F_{420} H_2ase to the inner face of the cell membrane.

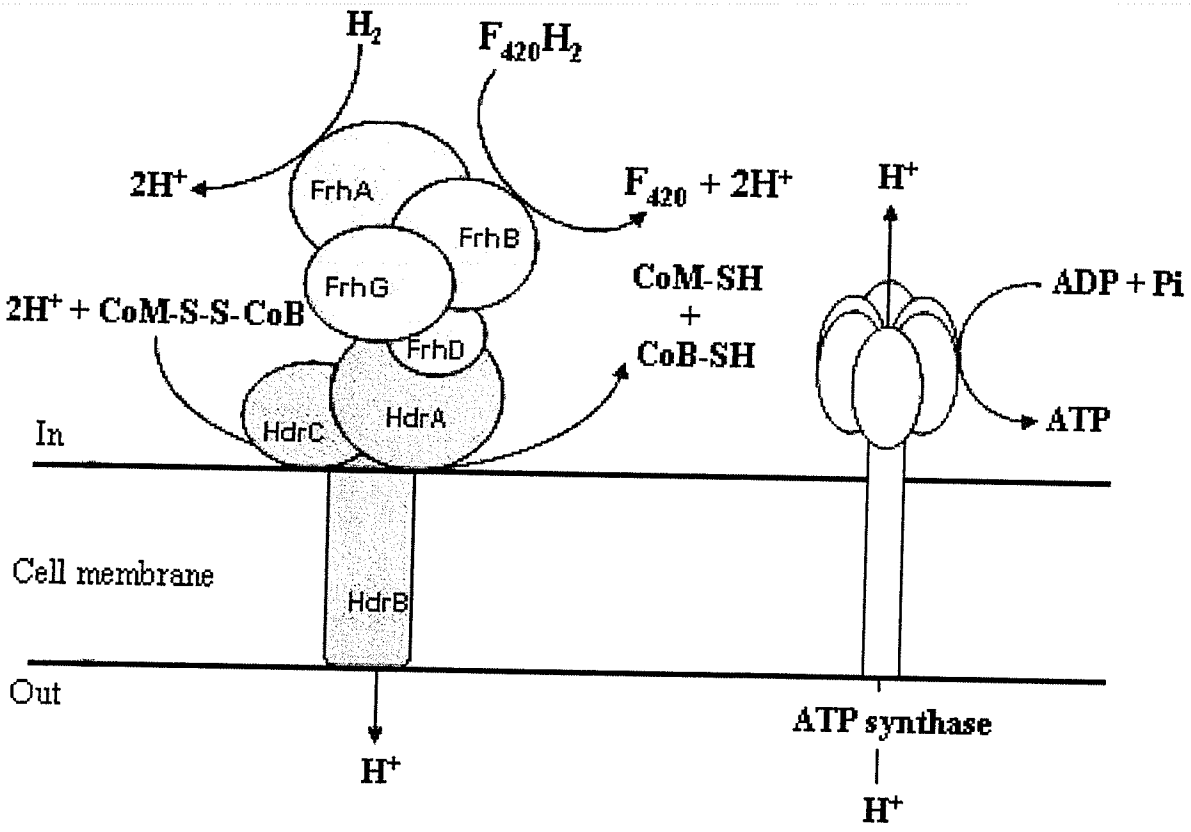

Figure 5.16. Hypothetical model of membrane-bound electron transport in *Methanospirillum hungatei* GP1 during growth on H_2 and CO_2. F_{420}-reducing hydrogenase (Frh) is docked onto the heterodisulfide reductase (Hdr). Electrons from $F_{420}H_2$ transferred from Frh to Hdr *via* contact between the δ/D-subunit of Frh, and HdrA.

Electrons derived from $F_{420}H_2$ could be shuttled through the F_{420} H_2ase and transferred to CoM-S-S-CoB *via* Hdr, to produce the free cofactors CoM-SH and CoB-SH. An energy conserving transmembrane proton gradient would be generated with CoM-S-S-CoB reduction, driving the formation of ATP *via* ATP synthase. H_2 may also be used as a source of electrons for the reduction of CoM-S-S-CoB (Figure 5.16).

H_2- and $F_{420}H_2$-dependent reduction of CoM-S-S-CoB *via* membrane vesicles of *Ms. mazei* Gö1 leads to the translocation of H^+ across the cytoplasmic membrane and generation of $\Delta\mu H^+$, which is used to drive the synthesis of ATP, indicating a requirement for integral membrane components (Peinemann *et al.*1990, Bäumer *et al.* 2000). The Hdr (*hdrDE*) of methanoarchaea from the *Methanosarcinales* is found integral to the membrane with several transmembrane helices anchoring the protein to the membrane (Deppenmeier *et al.* 1991, Ide *et al.* 1999, Deppenmeier *et al.* 2002). The electron carriers cytochromes and methanophenazine (putative), exclusive to the *Methanosarcinales*, are also found in the cell membranes (Fricke *et al.* 2006).

H_2-dependent CoM-S-S-CoB reduction also generates $\Delta\mu H^+$ in non-cytochrome containing methanoarchaea; cell suspensions of *Methanosphaera* (*Msph.*) *stadtmanae* generate $\Delta\mu H^+$ and ATP sythesis *via* H_2-dependent reduction of methanol (Sparling *et al.* 1993), while cell suspensions of *Mtb. thermoautotrophicus* couple H_2-dependent reduction of CoM-S-S-CoB with H^+ translocation (de Poorter *et al.* 2003). However, the Hdr (*hdrABC*) of *Mtb. thermoautotrophicus* has primarily been isolated from the soluble cytoplasmic fraction, although there is evidence that suggests that HdrB may be integral to the membrane (Hedderich and Thauer 1988, Setzke *et al.* 1994, Fricke *et al.* 2006).

While HdrB lacks transmembrane helical segments, Setzke *et al.* (1994) reported that 40% of the H_2:heterodisulfide oxidoreductase complex was found in the membranes of *Mtb. marburgensis*. Thus there may be alternate means for attachment to the cell membrane. The archaeon *Acidianus ambivalens* possesses a succinate:quinone oxidoreductase (*aka* succinate dehydrogenase), which catalyzes the oxidation of succinate to fumarate, with e^- transfer to quinones; HdrB of *Msph. stadtmanae* shares sequence similarity with the SdhC subunit (31% identity) (Lemos *et al.* 2001, Fricke *et al.* 2006). This enzyme is an integral membrane protein, but SdhC lacks the usual membrane-anchoring subunits (i.e. transmembrane helical segments). Instead, amphipathic α-helices are present in SdhC that may bind the succinate dehydrogenase to the membranes. A similar phenomenon is observed with mammalian proteins such as the RGS4, a protein that accelerates GTP hydrolysis on α protein (Bernstein *et al.* 2000).

Brodersen *et al.* (1999b) observed that formate-grown *Mc. voltae* cultures possess a membrane-bound $F_{420}H_2$ dehydrogenation-activity, similar to the $F_{420}H_2$ dehydrogenase activity isolated from *Ml. tindarius* and *Ms. mazei* Gö1, that was associated with CoM-S-S- CoB reduction. Further examination of the membrane-associated activity lead to the conclusion that the $F_{420}H_2$ dehydrogenation activity was associated with the membrane-bound F_{420} H_2ase, identical to the activity previously purified from the soluble cytoplasmic fraction of *Mc. voltae* by Muth *et al.* (1987). While $F_{420}H_2$ oxidation was measured using the combination of methyl viologen and metronidazole, our results have indicated that phenazine can be used as an electron acceptor for the $F_{420}H_2$ dehydrogenation activity of *Mc. voltae* (Chapter 4). It remains to be seen if the mechanism of $F_{420}H_2$-dependent CoM-S-S-CoB reduction in *Mc. voltae* is as proposed

for *Msp. hungatei* GP1. More research will have to be conducted to determine if the model shown in Figure 5.16 can be confirmed experimentally.

6. Purification of the phenazine-dependent $F_{420}H_2$ dehydrogenation activity from *Methanosarcina barkeri* strain Fusaro

6.1. Introduction

The $F_{420}H_2$ dehydrogenase (also referred to as the Fpo complex ($F_{420}H_2$:phenazine oxidoreductase) has only been isolated from *Methanolobus tindarius* and *Methanosarcina mazei* Gö1, methylotrophic methanoarchaea from the *Methanaosarcinaceae* family, and also from the hyperthermophilic sulfate-reducing archaeon *Archaeoglobus fulgidus* (Haase *et al.* 1992, Abken and Deppenmeier 1997, Brüggermann *et al.* 2000). Although this activity was initially assayed using methyl viologen, the physiological electron acceptor for the methanogenic $F_{420}H_2$ dehydrogenase activity is believed to be methanophenazine, while the acceptor for *A. fulgidus* is a menaquinone (Abken *et al.* 1998, Brüggermann *et al.* 2000).

Most of the present knowledge regarding the methanogenic $F_{420}H_2$ dehydrogenase has been derived from *Ms. mazei* Gö1. Using inverted cell membrane vesicles of *Ms. mazei* Gö1, Deppenmeier *et al.* (1990a, b) observed that $F_{420}H_2$ oxidation and CoM-S-S-CoB reduction was coupled to proton translocation into the lumen of the vesicles. Methanophenazine, which is isolated in small amounts from the cell membranes of *Ms. mazei* Gö1, is extremely hydrophobic, such that 2-OH-phenazine was synthesized as a water soluble alternative (Abken *et at.* 1998, Beifuss and Tietze 2005). Purified $F_{420}H_2$ dehydrogenase from *Ms. mazei* Gö1 catalyzed the reduction of 2-OH-phenazine; the reduced 2-OH-phenazine was then oxidized by heterodisulfide reductase (Hdr) for the reduction of CoM-S-S-CoB (Bäumer *et al.* 1998). Both reactions are coupled to the

generation of a transmembrane proton gradient ($\Delta\mu H^+$) and energy conservation (Bäumer *et al.* 2000, Deppenmeier 2002, 2004).

Comparisons with the gene sequences of the *nuo* operon from *E. coli* suggested that the $F_{420}H_2$ dehydrogenase of *Ms. mazei* Gö1 was an integral membrane-bound multisubunit protein, with a structure similar to NADH:ubiquinone oxidoreductase (NDH-1, complex I) of *E. coli* (Bäumer *et al.* 2000). Analysis of the *fpo* operon revealed that the organization of the gene cluster was ordered as in the *nuo* operon of *E. coli*, with the exception of the subunits required for oxidation of the respective electron carrier (*nuoEFG* for NDH-1 (NADH), *fpoF* for Fpo ($F_{420}H_2$)). The purified enzymes from the respective methanoarchaea were in fact only a portion of a much larger and more intricate complex, comprising the electron input module for the complex (Deppenmeier *et al.* 1999, Bäumer *et al.* 2000, Deppenmeier 2002).

Like *Ms. mazei* Gö1, *Methanosarcina* (*Ms.*) *barkeri* strain Fusaro is a nutritionally versatile methanoarchaeon from the family *Methanosarcinaceae* that can metabolize H_2/CO_2, acetate, and CH_3OH or methylamines as substrate for methanogenesis. Keltjens and Vogels (1993) noted that $F_{420}H_2$ dehydrogenase activity of *Ms. barkeri* Fusaro appeared to be co-purified along with F_{420}-reducing hydrogenase activity (F_{420} H_2ase). The F_{420} H_2ase has been purified (Fiebig and Friedrich 1989, Michel *et al.* 1995); it is a peripherally-bound membrane protein located on the cytoplasmic side of the cell membrane (Lünsdorf *et al.* 1991). Two phylogenetically closely related isoenzymes, Frh and Fre, are encoded in the genome (*frh* and *fre*) of *Ms. barkeri* Fusaro; both isoenzymes are synthesized when *Ms. barkeri* is grown on CH_3OH or H_2:CO_2, but not during growth on acetate (Vaupel and Thauer 1998).

Initial research in our laboratory also detected a MV-dependent $F_{420}H_2$ dehydrogenase activity in this methanoarchaeon; sucrose density gradient profiles demonstrated distinctly different elution patterns of the $F_{420}H_2$ dehydrogenation activities for *Ml. tindarius* and *Ms. barkeri* Fusaro (Wong, Ph.D thesis 1999). The $F_{420}H_2$ dehydrogenation activity of *Ms. barkeri* Fusaro appeared to consist of a larger protein mass relative to the respective activity of *Ml. tindarius*, and co-migrated with an F_{420} H_2ase activity. The purified $F_{420}H_2$ dehydrogenase activities from *Ml. tindarius* and *Ms. mazei* Gö1 do not possess F_{420} H_2ase activity (Abken and Deppenmeier 1997). Indeed, *Ml. tindarius* does not possess an F_{420} H_2ase (Deppenmeier *et al.*1989). BLAST analyses of the unpublished genome of *Ms. barkeri* Fusaro (circa. 2003), using the sequences coding for subunits of the Fpo complex from *Ms. mazei* Gö1, indicated the presence of open reading frames (ORFs) coding for a putative Fpo complex. It was not clear whether or not these genes were being expressed.

In this study we report the purification and characterization of a phenazine-dependent $F_{420}H_2$ dehydrogenation activity from *Ms. barkeri* Fusaro, grown on CH_3OH. N-terminus sequencing of the isolated subunits confirmed the identity of the protein as the F_{420} H_2ase of *Ms. barkeri* Fusaro. A possible role for the F_{420} H_2ase during energy conservation is discussed.

6.2. Materials and methods

For a comprehensive look at the materials and methods used for this chapter, the reader is referred to the following sections in Chapter 3:

3.2. Growth media

3.3. Cell lysis

6.3. Results

6.3.1 Preliminary results

The phenazine-dependent $F_{420}H_2$ dehydrogenation activity assayed using washed membranes of CH_3OH-grown *Ms. barkeri* Fusaro was similar to that observed using *Ml. tindarius*. When assayed in the presence of 3 and 9 μM DPI, the K_m for phenazine for *Ml. tindarius* increases from 238.9 to 965.6 and 1823.4 μM phenazine (Vmax = 0.41 μmol $F_{420}H_2$ oxid·min^{-1}·mg^{-1}), respectively (Figure 6.1). In contrast, the same concentration of DPI has negligible effect on the $F_{420}H_2$ dehydrogenation activity of *Ms. barkeri* Fusaro. Even when 50 and 100 μM DPI are added, which is greater than 10-fold the amount used for *Ml. tindarius*, the K_m only increases from 106.1 to 204.0 and 342.3 μM phenazine (Vmax = 0.32 μmol $F_{420}H_2$ oxid·min^{-1}·mg^{-1}), respectively.

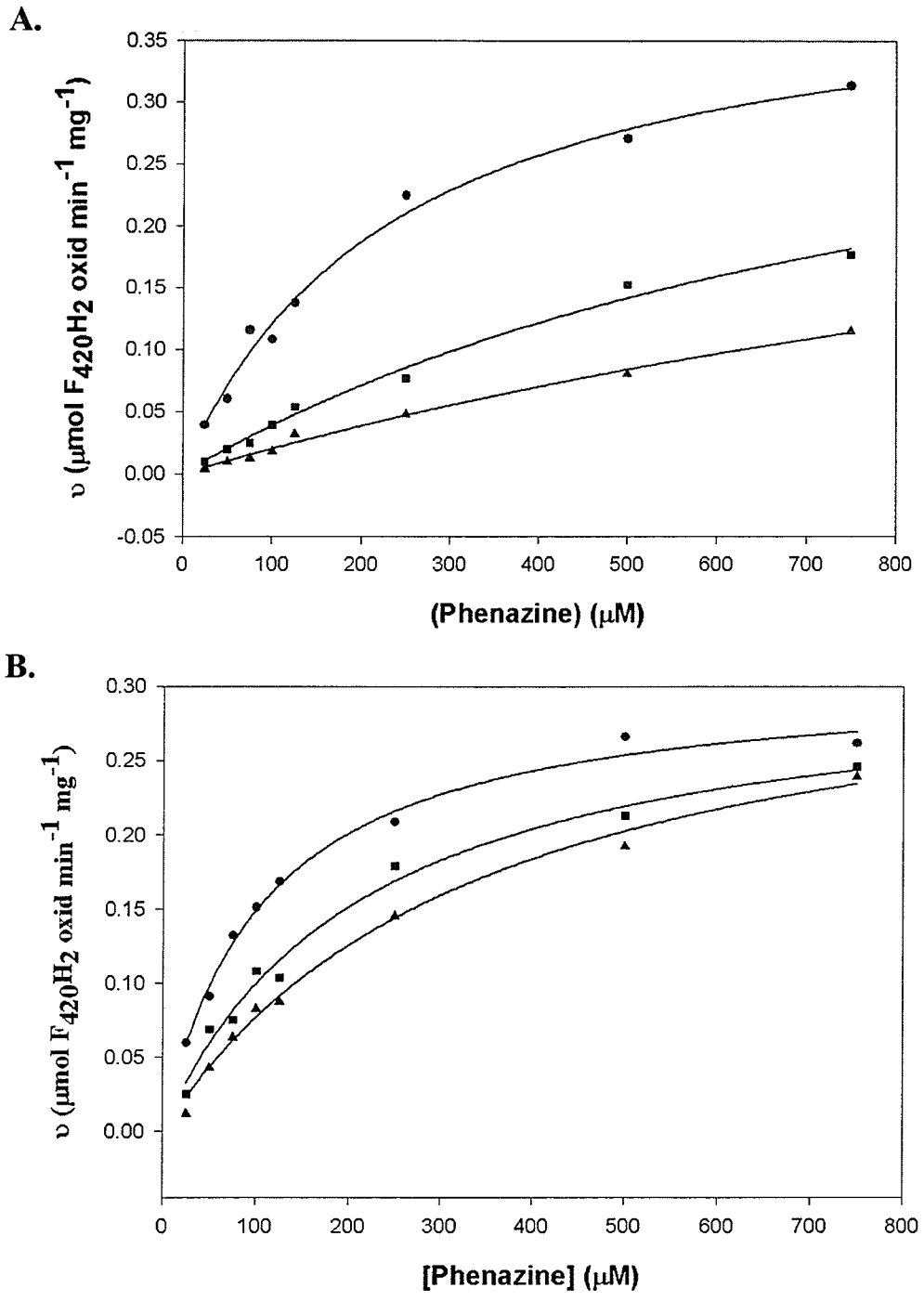

Figure 6.1. Michaelis menten kinetics of the membrane-bound phenazine-dependent $F_{420}H_2$ dehydrogenase activity of *Ml. tindarius* and *Ms. barkeri* Fusaro. A. *Ml. tindarius*. ●, no DPI. ■, + 3 μM DPI. ▲, + 9 μM DPI. B. *Ms. barkeri* Fusaro, grown on CH_3OH. ●, no DPI. ■, + 50 μM DPI. ▲, + 100 μM DPI.

The F_{420} H_2ase of *Methanospirillum* (*Msp.*) *hungatei* GPI also catalyzes a reaction similar to the $F_{420}H_2$ dehydrogenase of *Ms. mazei* Gö1 (Chapter 5). Thus, we could not discount the possibility that the phenazine-dependent $F_{420}H_2$ dehydrogenation activity of the Fpo complex was being masked by a similar activity catalyzed by the membrane-bound F_{420} H_2ase of *Ms. barkeri* Fusaro that is not found in *Ml. tindarius*.

Studies of the $F_{420}H_2$ dehydrogenation activity of *Ms. barkeri* Fusaro began with an examination of the membrane-bound proteins. The proteins were extracted from washed membranes (3x) solubilized with CHAPS (1.5 mg CHAPS/mg protein), followed by chromatography of the solubilized protein using various chromatographic matrices; the $F_{420}H_2$ dehydrogenation activity was assayed using phenazine at each stage of purification.

Ni^{2+} affinity chromatography was used as the initial enrichment step to remove the F_{420} H_2ase, since it is expected to have a high affinity for Ni^{2+} (Choquet and Sprott 1991, this thesis). Unexpectedly, the $F_{420}H_2$ dehydrogenation activity also bound to the column and was eluted along with the F_{420} H_2ase activity using a single step addition of 25 mM imidazole (Figure 6.2). The pooled fractions containing the $F_{420}H_2$ dehydrogenation activity also contained significant hydrogenase activity. Varying the concentration of imidazole or changing from a single step addition of imidazole to a continuous gradient did not resolve the $F_{420}H_2$ dehydrogenation and F_{420} H_2ase activities.

The pooled fractions were desalted, concentrated, and then applied to a 45-50% (10 ml·step^{-1}) sucrose density gradient, followed by ultracentrifugation for 48 hours at

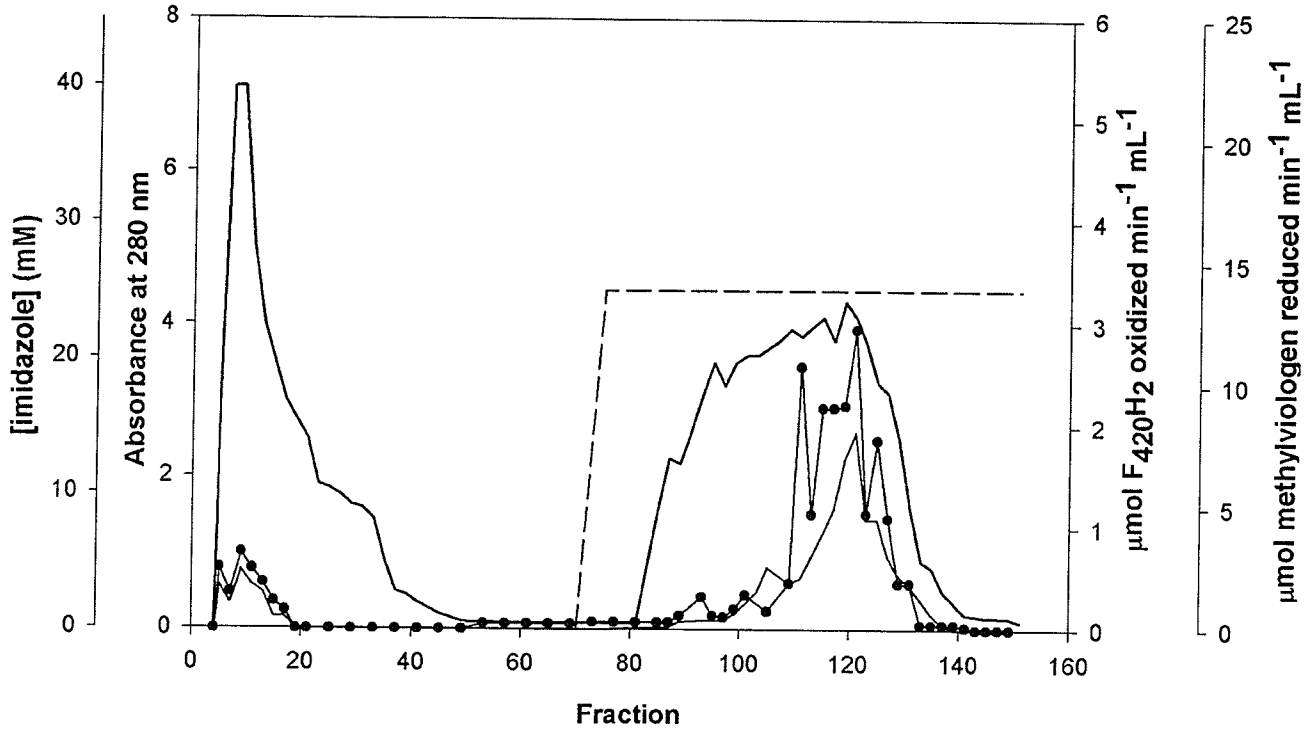

Figure 6.2. Protein and activity profile of fractions collected from a Ni^{2+} affinity column, from protein extracted from washed and solubilized cell membranes of *Methanosarcina barkeri* Fusaro. Elution of protein from the column as described under 'Materials and methods'. (—), A_{280}. (----), imidazole. ●, Phenazine-dependent $F_{420}H_2$ dehydrogenation activity. ■, Methyl viologen-reducing hydrogenase.

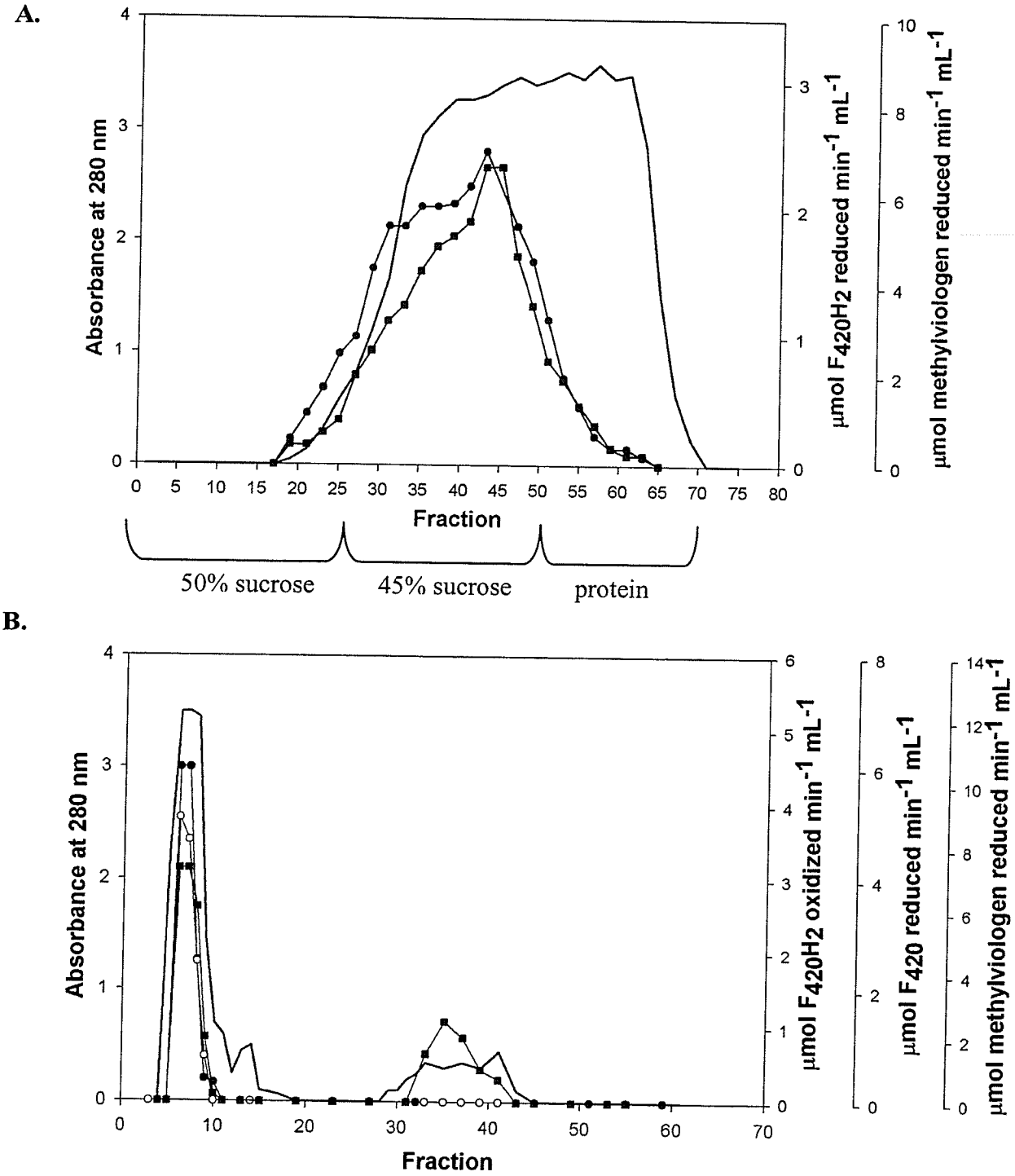

Figure 6.3. Protein and activity profile of fractions collected from: (A) 50-45% sucrose step gradient loaded with protein eluted from a Ni^{2+}-affinity column and (B) Sepharose 6B column loaded with protein collected from the 50-45% sucrose step gradient. Protein solubilized and extracted from washed cell membranes. (—), A_{280}. ●, Phenazine-dependent $F_{420}H_2$ dehydrogenation activity. ○, F_{420}-reducing hydrogenase activity. ■, Methyl viologen-reducing hydrogenase activity.

23,000 rpm. The sucrose fractions containing the$F_{420}H_2$ dehydrogenation activities (Figure 6.3A) were pooled, concentrated, and loaded onto a Sepharose 6B gel filtration column, where the $F_{420}H_2$ dehydrogenation activity eluted with an F_{420} H_2ase activity (Figure 6.3B). Sepharose 6B resolves proteins with molecular weights ranging from 10 to 4 $x10^3$ kDa; the $F_{420}H_2$ dehydrogenation activity would be expected to have a molecular weight of approximately 115-120 kDa, whereas the F_{420} H_2ase would have a molecular weight of approximately 845 kDa (Fiebig and Friedrich 1989, Abken and Deppenmeier 1997). While the $F_{420}H_2$ dehydrogenation activity had not been purified to apparent homogeneity, the $F_{420}H_2$ dehydrogenation and F_{420} H_2ase activities appeared to be closely associated through all the various chromatographic steps. The yield of $F_{420}H_2$ dehydrogenation activity remaining after the Sepharose 6B gel filtration step was too low to make further analyses feasible.

A possible conclusion was that the steps selected for the purification of the $F_{420}H_2$ dehydrogenase activity failed to separate it from the F_{420} H_2ase activity. Another possibility is that the observed $F_{420}H_2$ dehydrogenation activity in *Ms. barkeri* Fusaro might solely be the property of the F_{420} H_2ase. Therefore, the same protocol used to purify the $F_{420}H_2$ dehydrogenation activity from *Msp. hungatei* GP1 was used to try and separate the respective activity from *Ms. barkeri* Fusaro. The F_{420} H_2ase also catalyzes the oxidation of $F_{420}H_2$; by selecting for the purification of this protein, we expected to separate the expected Fpo from this "artifact" activity present in the protein extract.

6.3.2. Purification of the phenazine-dependent $F_{420}H_2$ dehydrogenation activity

Following cell lysis, and removal of the unlysed cells and debris, the cell-free extract was centrifuged at 180000xg for 6 hours. This resulted in the sedimentation of both the soluble and membrane-bound $F_{420}H_2$ dehydrogenation activities in a tight dark brown pellet, referred to as the high speed pellet (HSP).

Ni^{2+} affinity chromatography was used as the initial step in the enrichment of the $F_{420}H_2$ dehydrogenation activity from the homogenized HSP. The cell membranes, which contain 15-20% of the overall $F_{420}H_2$ dehydrogenation activity, eluted from the column without binding. The soluble $F_{420}H_2$ dehydrogenation activity bound to the Ni^{2+}-charged matrix and was eluted using a single step addition of 25 mM imidazole (Figure 6.4). As expected, the $F_{420}H_2$ dehydrogenation and F_{420} H_2ase activities elute together from the Ni^{2+}-charged column.

Fractions containing the $F_{420}H_2$ dehydrogenation activity were pooled, desalted and concentrated using an Amicon ultrafiltrator, loaded onto a 3-20% native gradient PAGE, and electrophoresed overnight at 4°C. Intense yellow-brown bands were observed in their respective lanes near the top of the gel; this is due to the presence of FAD and FeS clusters in the protein. Activity staining (as described under 'Materials and methods) indicated that these bands possess hydrogenase activity, suggesting the presence of the F_{420} H_2ase.

The high molecular weight bands were excised from the gel and cut into 1-2 mm^3 pieces, followed by elution of the protein from the gel pieces using the Bio-Rad Electro-Elutor (~8 hours). The eluted protein was then dissolved with 10 mM HEPES, pH 7.0, with 0.05% Triton-X-100 and 5% glycerol. Solutions of the purified $F_{420}H_2$

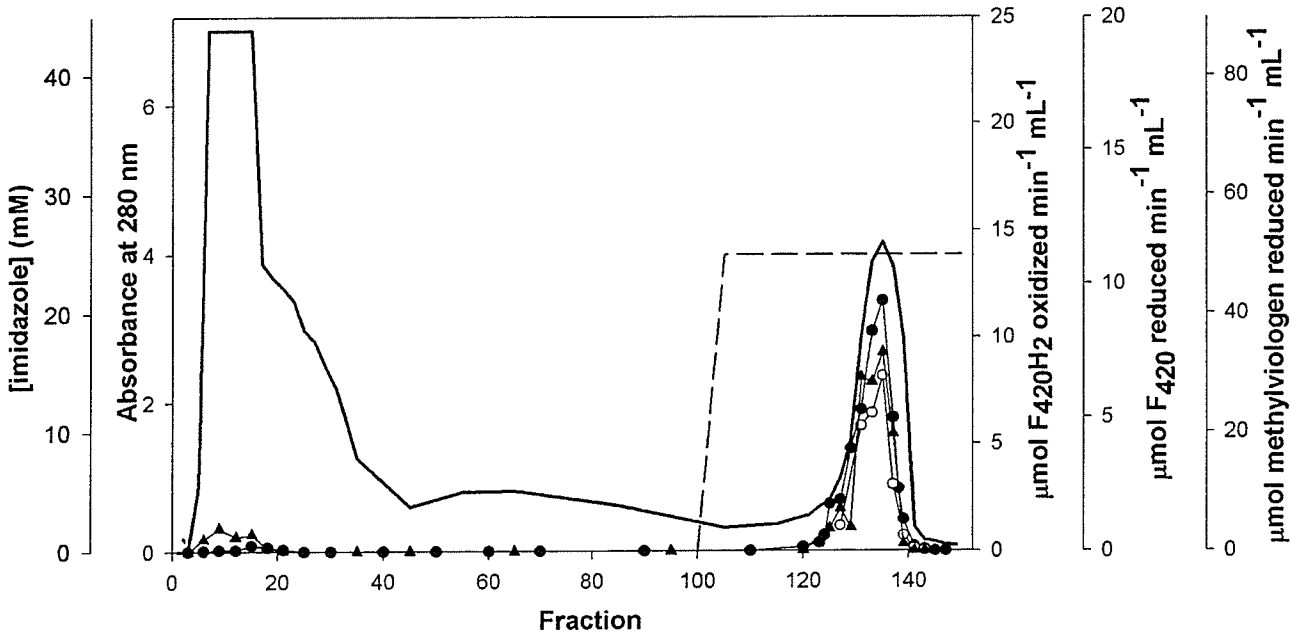

Figure 6.4. Protein and activity profile of fractions collected from a Ni^{2+} affinity column. Column loaded with homogenized HSP, which contains soluble and membrane-bound $F_{420}H_2$ dehydrogenation activity. Membrane-bound $F_{420}H_2$ dehdyrogenation activity did not bind to the Ni^{2+} column, while the soluble $F_{420}H_2$ dehydrogenation activity bound and was eluted from the column by the addition of 25 mM imidazole. (—), A_{280}. (----), imidazole. ●, $F_{420}H_2$ dehydrogenation activity. ○, F_{420}-reducing activity. ▲, Methyl viologen reducing activity.

Table 6.1. Purification of the soluble phenazine-dependent $F_{420}H_2$ dehydrogenation activity of methanol-grown *Methanosarcina barkeri* Fusaro. MCAC, metal chelate affinity chromatography.

Purification stage	Protein (mg)	Activity[†]	Yield (%)	Sp. activity[‡]	Purification
Cell-free extract	723.9	466.9	100	0.65	-
High speed pellet	264.3	345.4	74.0	1.31	2.0-fold
MCAC pool	78.8	158.8	34.0	2.02	3.1-fold
Eluted protein[‡‡]	2.9	55.4	11.9	19.10	29.4-fold

[†] μmol $F_{420}H_2$ oxidized·min^{-1}.
[‡] μmol $F_{420}H_2$ oxidized·min^{-1}·mg^{-1} protein
[‡‡]protein eluted from 3-20% native gradient PAGE

dehydrogenation activity were yellowish-brown in color, indicating the presence of flavins and iron-sulfur clusters. The purified enzyme was stored at 4°C under an atmosphere of N_2 for up to 3 months without significant loss of activity.

Excision and electrophoresis of lower molecular weight bands of similar color and/or molecular weight to the $F_{420}H_2$ dehydrogenase of *Ml. tindarius* and *Ms. mazei* Gö1 (~120 kDa) from the native PAGE did not reveal protein containing $F_{420}H_2$ dehydrogenation or F_{420} H_2ase activity. The purification of the $F_{420}H_2$ dehydrogenation activity is summarized in Table 6.1; this process was repeated three times, and representative data are presented here.

Concurrent with $F_{420}H_2$ dehydrogenation purification, the F_{420} H_2ase activity was also tracked and monitored. The ratio of $F_{420}H_2$ dehydrogenation:F_{420} hydrogenase activity throughout the enrichment process indicates that the F_{420} H_2ase was enriched at roughly the same rate as the $F_{420}H_2$ dehydrogenation activity, strengthening the argument

Table 6.2. Enrichment of the soluble F_{420} reducing hydrogenase activity during the purification of the phenazine-dependent $F_{420}H_2$ dehydrogenation activity of methanol-grown *Methanosarcina barkeri* Fusaro. MCAC, metal chelate affinity chromatography.

Purification stage	Protein (mg)	Activity†	Yield (%)	Sp. activity‡	Purification	DeH$_2$ase/ H$_2$ase
Cell-free extract	723.9	661.3	100	0.91	-	0.71
High speed pellet	264.3	547.8	82.8	2.07	2.3-fold	0.63
MCAC pool	78.8	287.1	43.4	3.64	4.0-fold	0.55
Eluted protein‡‡	2.9	46.5	7.0	16.03	17.6-fold	1.19

† μmol F_{420} reduced·min^{-1}.
‡ μmol F_{420} reduced·min^{-1}·mg^{-1} protein
‡‡protein eluted from 3-20% native gradient PAGE

for the association of the two enzyme activities.

When the HSP was loaded onto the Ni^{2+} affinity column, only the soluble $F_{420}H_2$ dehydrogenation activity binds to the column, while the membrane-bound activity flows through the column unhindered. Analyses of the unpublished and incompletely sequenced genome of *Ms. barkeri* Fusaro (circa. 2003-2004) indicated the presence of genes encoding for a putative Fpo complex. The electron transport apparatus of the *Methanosarcinaceae* is located in the cell membranes; to ensure that the activity of the Fpo complex was not being masked by the presence of a similar activity by the F_{420} H_2ase, the phenazine-dependent $F_{420}H_2$ dehydrogenation activity was also purified from membranes collected from the Ni^{2+} affinity column.

Protein was extracted from washed and CHAPS-solubilized membranes, and processed in the same manner as the soluble activity. The eluate from the Ni^{2+} affinity

column containing $F_{420}H_2$ dehydrogenation activity was desalted, concentrated and electrophoresed on a 3-20% native gradient PAGE. The high molecular weight bands were excised from the gel, minced into 1-2 mm^3 pieces, and the protein extracted from the minced gel pieces. The results are summarized in Tables 6.3 (phenazine-dependent $F_{420}H_2$ dehydrogenation) and 6.4 (F_{420} H_2ase). A constant ratio of $F_{420}H_2$ dehydrogenation: F_{420} H_2ase activity is maintained throughout the purification process. Electrophoresis of the protein on a native 3-20% gradient PAGE, followed by hydrogenase activity staining, indicates the presence of the F_{420} H_2ase, and not the presence of the $F_{420}H_2$ dehydrogenase (Figure 6.6). Protein was also extracted from

Table 6.3. Purification of the membrane-bound phenazine-dependent $F_{420}H_2$ dehydrogenation activity of methanol-grown *Methanosarcina barkeri* Fusaro. MCAC, metal chelate affinity chromatography.

Purification stage	Protein (mg)	Activity[†]	Yield (%)	Sp. activity[‡]	Purification
Cell-free extract	979.0	561.9	-	0.57	-
Membranes	385.2	129.2	100	0.34	-
Solubilized protein[††]	42.4	35.7	27.6	0.84	2.5-fold
MCAC pool	18.6	27.8	21.6	1.49	4.4-fold
Eluted protein[‡‡]	0.6	8.0	5.8	12.50	36.8-fold

[†] μmol $F_{420}H_2$ oxidized·min^{-1}.
[‡] μmol $F_{420}H_2$ oxidized·min^{-1}·mg^{-1} protein
[††]protein extracted from solubilized membranes
[‡‡]protein eluted from 3-20% native gradient PAGE

Table 6.4. Enrichment of the membrane-bound F_{420} reducing hydrogenase activity during the purification of the phenazine-dependent $F_{420}H_2$ dehydrogenation activity of methanol-grown *Methanosarcina barkeri* Fusaro. MCAC, metal chelate affinity chromatography.

Purification stage	Protein (mg)	Activity[†]	Yield (%)	Sp. activity[‡]	Purification	DeH_2ase/H_2ase
Cell-free extract	979.0	899.0	-	0.92	-	0.62
Membranes	385.2	233.7	100	0.61	-	0.56
Solubilized protein[††]	42.4	67.8	27.6	1.60	2.6-fold	0.53
MCAC pool	18.6	54.2	21.6	2.91	4.8-fold	0.51
Eluted protein[‡‡]	0.6	11.6	4.4	19.33	31.7-fold	0.64

[†] μmol F_{420} reduced·min^{-1}.
[‡] μmol F_{420} reduced·min^{-1}·mg^{-1} protein
[††]protein extracted from solubilized membranes
[‡‡]protein eluted from 3-20% native gradient PAGE

gel pieces excised from the native PAGE gel with MW in the range of the $F_{420}H_2$ dehydrogenase of *Ml. tindarius* and *Ms. mazei* Gö1 (~120 kDA); neither $F_{420}H_2$ dehydrogenation nor F_{420}-reducing activity was detected in these fractions.

6.3.3. Properties of the $F_{420}H_2$ dehydrogenation activity

6.3.3.1. Molecular properties

Electrophoresis of the purified $F_{420}H_2$ dehydrogenation activity on a nondenaturing 3-20% native PAGE (Figure 6.5) revealed the presence of two prominent bands. One band has a molecular mass greater than 669 kDa, while the second band has a mass of approximately 198 kDa; the profile is identical to the pattern observed during

the purification of the F_{420} H_2ase from *Ms. barkeri* Fusaro (Fiebig and Friedrich 1989, Michel *et al.* 1995).

Under an anaerobic atmosphere of 10% H_2 (balance N_2) and immersion in 50 mM Tris/Cl, pH 8.0, with 20 mM $MgCl_2 \cdot 6H_2O$, and 20 mM DTT, H_2 uptake-activity by the gel-bound protein was observed, using methyl viologen (2 mM) as electron acceptor (Figure 6.5A). The positions of the activity bands are identical with the bands on the coomassie blue-stained native PAGE gel (Figure 6.5B).

Purification of the membrane-bound $F_{420}H_2$ dehydrogenation activity alongside the soluble activity reveals that the F_{420} H_2ase catalyzes both activities, and that a distinct Fpo complex is not being detected under the growth conditions. The hydrogenase activity- and coomassie blue-stained native gradient PAGE gels show that the soluble and membrane-bound $F_{420}H_2$ dehydrogenation activities are identical (Figure 6.6).

A double stained (coomassie blue and silver-stained) SDS PAGE of the purified enzyme (Figure 6.7) indicates the presence of three major polypeptides, corresponding to apparent molecular masses of 48 (α), 33 (β), and 30 (γ) kDa as reported for the F_{420} H_2ase of *Ms. barkeri* Fusaro by Fiebig and Friedrich (1989).

N-terminus sequencing of the α- and β-subunits confirmed that the purified phenazine-dependent $F_{420}H_2$ dehydrogenation activity was the F_{420} H_2ase (Table 6.5); sequence information for the γ-subunit was inconclusive. No other source of $F_{420}H_2$ dehydrogenation activity could be detected over the course of this study, regardless of method of chromatography used to resolve the proteins. The sequences of the α- and β-subunits, excluding the mismatches, are identical to the sequences reported by Michel *et*

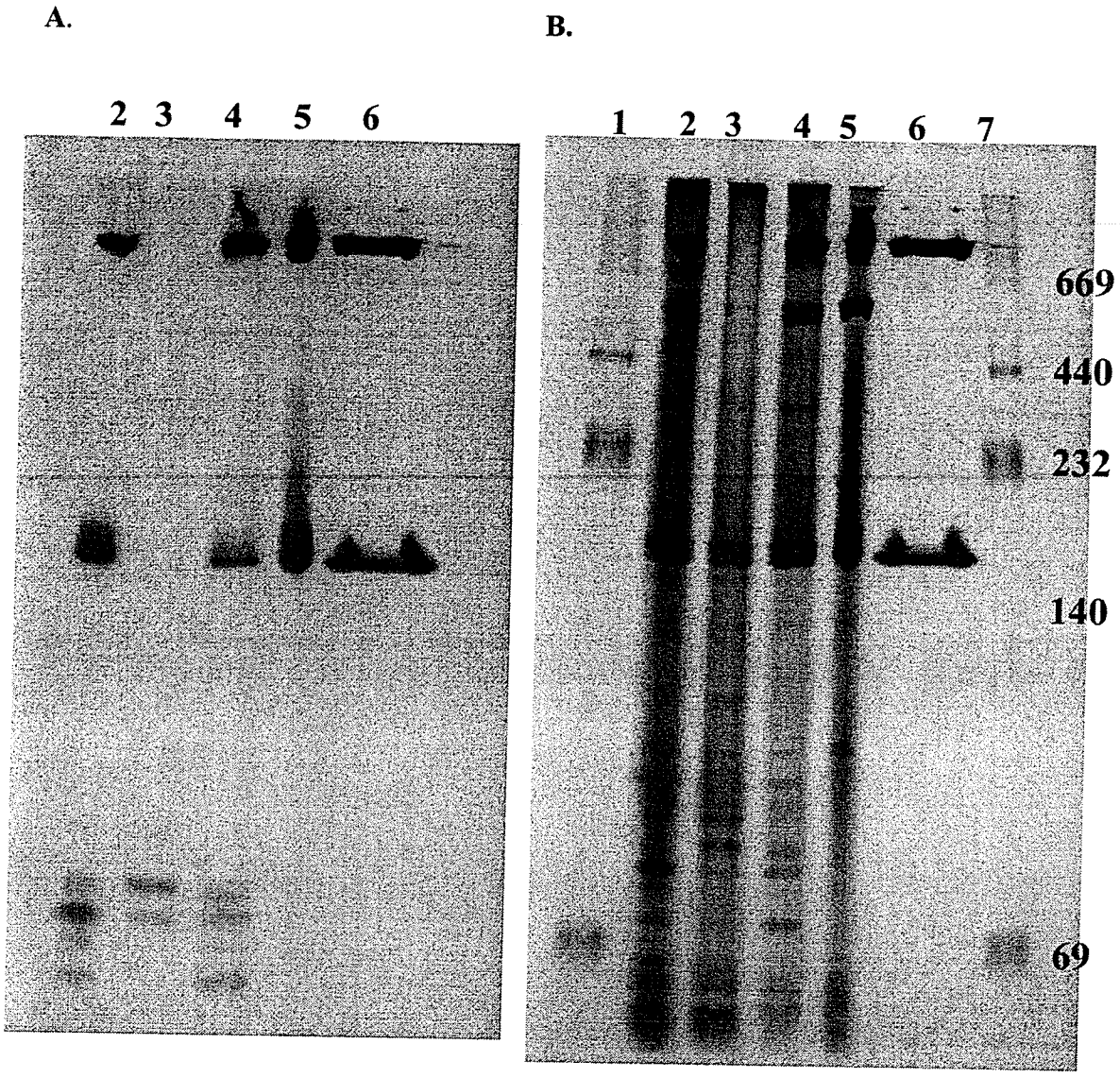

Figure 6.5. (A) Activity- and (B) coomassie blue-stained 3-20% native gradient PAGE showing progression of the purification of the soluble phenazine-dependent $F_{420}H_2$ dehydrogenation activity of CH_3OH-grown *Ms. barkeri* Fusaro. Pattern of protein bands observed suggests presence of F_{420}-reducing hydrogenase. Lanes 1 and 7, ladder, kDa. Lane 2. cell-free extract. Lane 3. clarified cell-free extract. Lane 4. high speed pellet. Lane 5. MCAC pooled protein. Lane 6. purified protein.

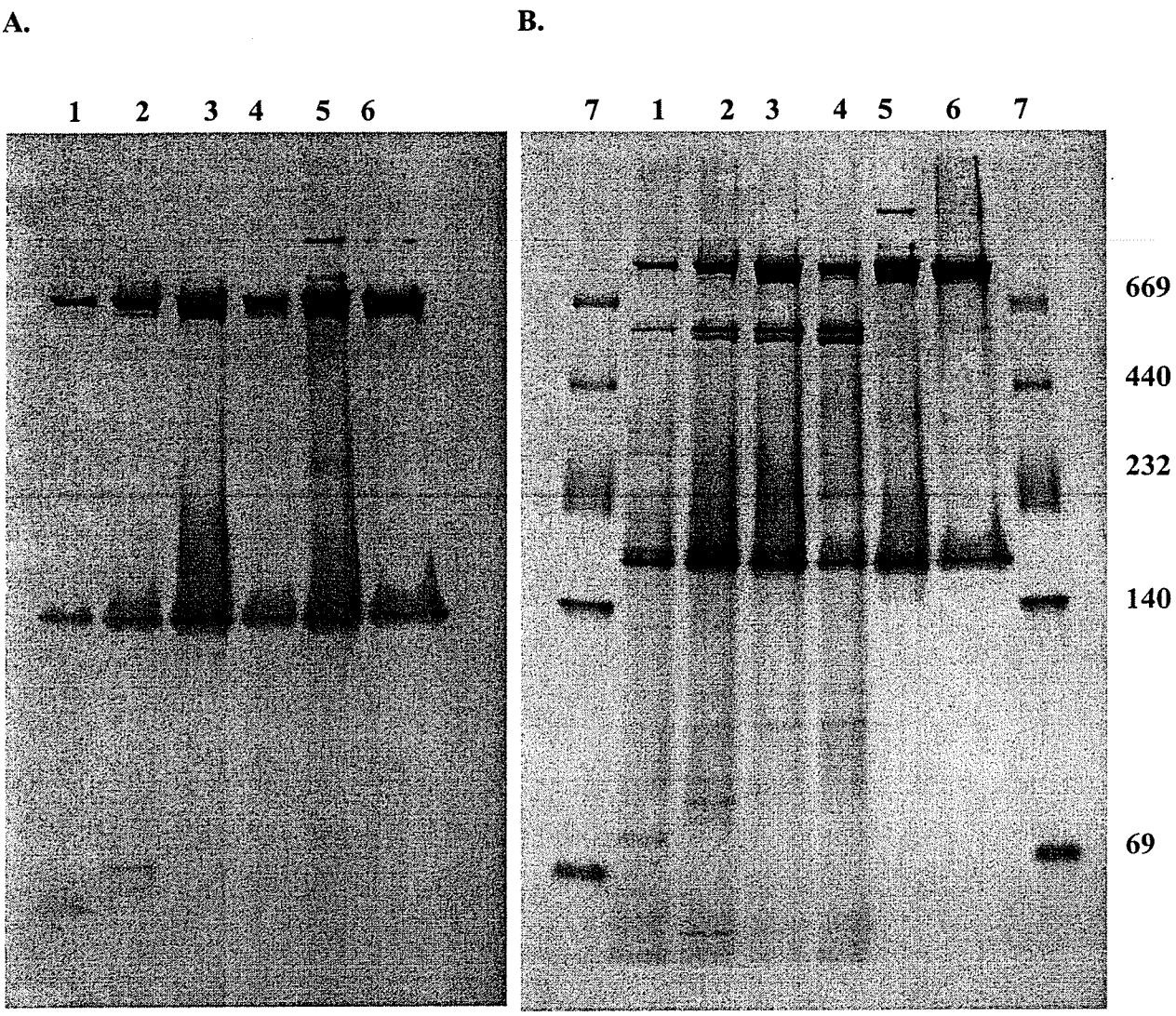

Figure 6.6. Electrophoresis of proteins at various stages of purification of the soluble and membrane-bound phenazine-dependent $F_{420}H_2$ dehydrogenation activity of CH_3OH-grown *Ms. barkeri* Fusaro, as visualized on: (A) Activity-stained, and (B) activity- and coomassie blue-stained native gradient 3-20% PAGE gel. Pattern of activity and protein bands observed suggests presence of F_{420}-reducing hydrogenase. 1. cell-free extract. 2. high speed pellet (HSP). 3. MCAC pooled protein from HSP (soluble fraction). 4. MCAC pooled protein from solubilized membranes. 5. purified soluble $F_{420}H_2$ dehydrogenation activity. 6. purified (eluted) membrane-bound $F_{420}H_2$ dehydrogenation activity. 7. molecular markers, kDa.

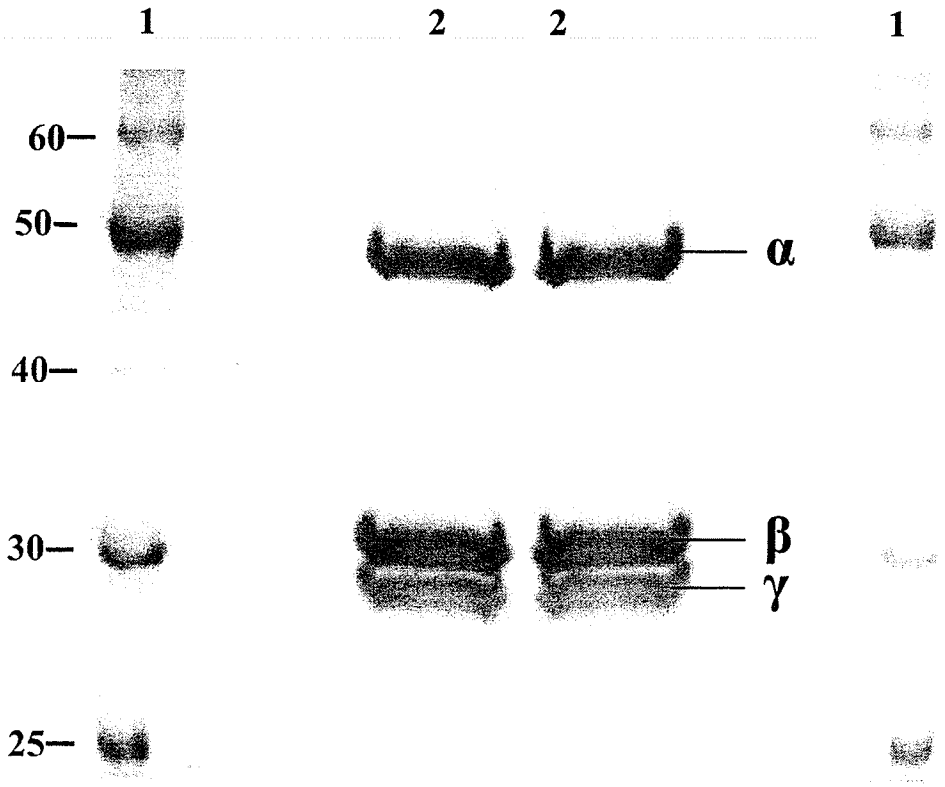

Figure 6.7. SDS PAGE profile of the purified soluble phenazine-dependent $F_{420}H_2$ dehydrogenation activity from CH_3OH-grown *Ms. barkeri* Fusaro. Pattern of subunits on coomassie- and silver-stained (12.8% acrylamide) gel suggests presence of F_{420}-reducing hydrogenase. 1. molecular markers (KDa). 2. purified protein.

al. 1995, and to the corresponding amino acid sequences predicted by the gene sequences of the *frh* and *fre* operons, encoding for iso-enzymes of F_{420} H_2ase in *Ms. barkeri* Fusaro.

Table 6.5. N-terminus sequences of the α- (48 kDa) and β- (33 kDa) subunits from the purified phenazine-dependent $F_{420}H_2$ dehydrogenation activity of *Methanosarcina barkeri* Fusaro (seen in Figure 7.7).

	A	β
This study	Thr-Lys-Val-Val-Glu-Ile-Ser-Pro-Thr-Thr	**Gly**[†]-Ile-Glu-Asp-Pro-Tyr-Leu-**Leu**[‡]-Lys-**Lys**[‡]
F_{420}-reducing hydrogenase of *Ms. barkeri* Fusaro (Michel *et al.* 1995)	Thr-Lys-Val-Val-Glu-Ile-Ser-Pro-Thr-Thr	Met-Ile-Glu-Asp-Pro-Tyr-Leu-Gly-Lys-Tyr

[†]mismatched amino acid.
[‡]ambiguous amino acid

6.3.3.2. Catalytic properties

The phenazine-dependent $F_{420}H_2$ dehydrogenation activity was purified 29.4-fold to apparent homogeneity with a yield of 11.9 % and a final specific activity of 19.1 μmol $F_{420}H_2$ oxidized·min^{-1}·mg^{-1} protein. The $F_{420}H_2$ dehydrogenation activity (500 μM phenazine, room temperature (~25°C)) was highest at pH 7.5 (Figure 6.8). The pH optimum for the purified $F_{420}H_2$ dehydrogenase activities of *Ml. tindarius* and *Ms. mazei* Gö1 are, respectively, 6.8 and 8.5. The pH optimum for the F_{420} H_2ase activity of *Ms. barkeri* Fusaro was reported as pH 6.5-7.25, measured at 55°C (Michel *et al.* 1995).

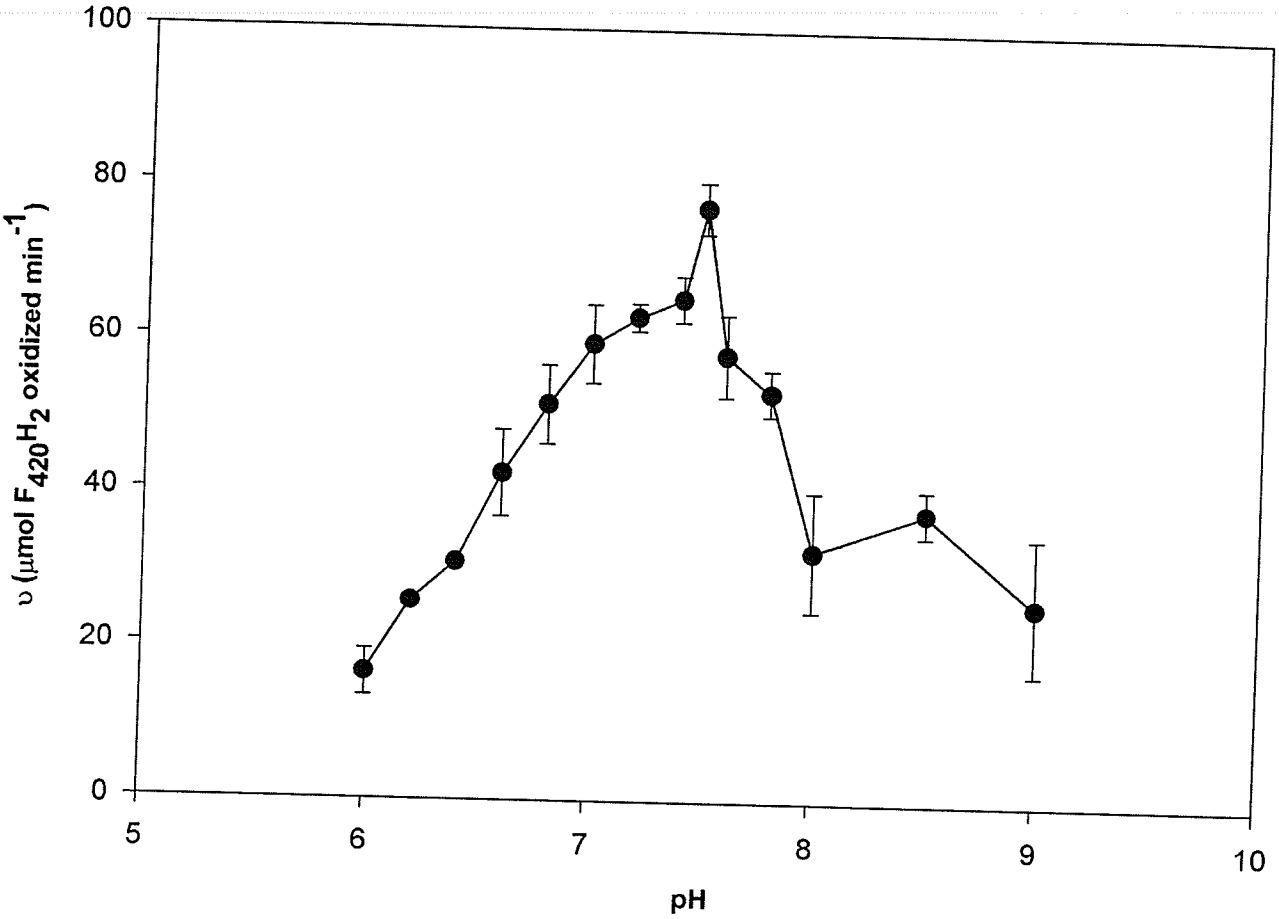

Figure 6.8. pH profile of the purified soluble phenazine-dependent $F_{420}H_2$ dehydrogenation activity of CH_3OH-grown *Ms. barkeri* Fusaro. Assay conditions as described under 'Materials and Methods'. All points represent experiments performed in triplicate. pH established using 40 mM KPO_4 (pH 6-8) and 50 mM Tris/Cl (pH 8-9), ambient room temperature (~25°C). 500 μM phenazine added per tube.

The $F_{420}H_2$ dehydrogenation activity of *Ms. barkeri* Fusaro was assayed primarily using phenazine ($E^{\circ\prime}$ = -0.265 to -0.165 V), but methyl viologen ($E^{\circ\prime}$ = -0.446 V) (with metronidazole) and FAD ($E^{\circ\prime}$ = -0.219 V) were also used to assay the $F_{420}H_2$ dehydrogenation activity (Table 6.6). $NADP^+$, NAD^+, and ferredoxin were not able to substitute for phenazine as electron acceptors. NADH and NADPH could not substitute for $F_{420}H_2$ as electron donor. The phenazine-dependent $F_{420}H_2$ dehydrogenation activity

Table 6.6. Electron acceptor specificities of the purified $F_{420}H_2$ dehydrogenation activity of *Methanosarcina barkeri* Fusaro. 10-15 μM $F_{420}H_2$ added per assay tube.

E^- acceptor / inhibitor (μM)	Activity (μmol $F_{420}H_2$ oxidized·min^{-1}·mg^{-1})
-	0.3 ± 0.05
Methylviologen (500) + Metronidazole (1000)	3.1 ± 0.4
Phenazine (500)	19.5 ± 1.2
Phenazine (500) + DMSO (100 μL)	18.0 ± 1.3
DPI (100)	0.3 ± 0.05
Phenazine (500) + DPI (50)	15.0 ± 1.2
Phenazine (500) + DPI (100)	12.4 ± 1.0
FAD (50)	15.2 ± 1.4
$NADP^+$ (300)	0.4 ± 0.05
NAD^+ (300)	0.3 ± 0.05
Ferredoxin (1 mg/ml)	0.3 ± 0.03

was inhibited by DPI, dissolved in Dimethyl sulfoxide (DMSO)), an inhibitor of mitochondrial and bacterial electron transport systems that also inhibits the $F_{420}H_2$ dehydrogenation activity of *Ms. mazei* Gö1 (Brodersen *et al.* 1999).

DPI was also tested for its inhibitory effect on the F_{420} H_2ase of *Ms. barkeri* Fusaro, since DPI is an inhibitor of flavoproteins. The F_{420} H_2ase was reductively activated prior to assay, incubated under H_2 with 10 μM FAD, 10 μM F_{420}, and 20 mM DTT. When using methyl viologen as electron acceptor, the protein was incubated in assay buffer containing 0.05 mM methyl viologen, under H_2; the protein was considered reactivated when the buffer turned light blue in color.

Using standard concentrations of F_{420} (~20 μM) or methyl viologen (2 mM), H_2-dependent F_{420}- or methyl viologen-reduction were not inhibited in the presence of DPI (Table 6.7). This would indicate that inhibition of the $F_{420}H_2$ dehydrogenation activity is due to competition with phenazine for the binding site, and not due to direct attack of DPI to the FAD; the concentrations of DPI used inhibited $F_{420}H_2$ dehydrogenation activity, but not F_{420} H_2ase activity (using equivalent amounts of protein). Reduction of methyl viologen was used as a negative control since the FAD component is not required for electron transfer to this substrate; inhibition of methyl viologen reduction was not observed (Table 6.7).

Hydrogenase activities were also assayed in the presence of phenazine (500 μM) (Table 6.7). Phenazine ($E^{\circ\prime}$ = -0.265 to -0.165 V) appeared to compete with F_{420} for electrons from H_2 ($E^{\circ\prime}$ = -0.420 V), since phenazine inhibited F_{420}-reduction 10-fold. Another explanation is that as F_{420} is reduced by the hydrogenase activity, the $F_{420}H_2$ formed may be used to reduce phenazine by the dehydrogenation activity in a competing

Table 6.7. Effect of DPI on the hydrogenase activities of *Methanosarcina barkeri* Fusaro. [F_{420}] = 20 μM. [methyl viologen] = 2 mM. Protein reductively reactivated prior to addition of DPI or phenazine.

Electron acceptor	Addition (μM)	Activity
F_{420}	-	44.0 ± 3.2[†]
F_{420}	100 μl DMSO	45.0 ± 2.2[†]
F_{420}	DPI (50)	44.0 ± 3.2[†]
F_{420}	DPI (100)	39.1 ± 1.1[†]
F_{420}	DPI (150)	41.0 ± 4.3[†]
F_{420}	Phenazine (500)	4.4 ± 0.4[†]
Methyl viologen	-	63.0 ± 6.1[‡]
Methyl viologen	100 μl DMSO	64.7 ± 7.4[‡]
Methyl viologen	DPI (100)	66.5 ± 4.9[‡]
Methyl viologen	Phenazine (500)	63.0 ± 3.1[‡, ††]

[†] μmol F_{420} reduced·min^{-1}·mg^{-1}
[‡]μmol methyl viologen reduced·min^{-1}·mg^{-1}
[††]full activity after 5-10 minute lag

reaction. Thus the apparent inhibition of the F_{420} H_2ase activity may be due to competition from the phenazine-dependent $F_{420}H_2$ dehydrogenation reaction.

Phenazine was also a substrate for the hydrogenase activity of the purified protein. Protein was incubated in $F_{420}H_2$ dehydrogenation assay buffer (40 mM KPO_4, pH 7.0) for 1 hour, under an H_2 atmosphere to insure that the protein was reductively reactivated; phenazine was reduced at a rate of 14.6 ± 1.3 μmol phenazine red·min^{-1}·mg^{-1}.

Phenazine was not reduced under an atmosphere of N_2 or in the absence of protein. The physiological relevance of this activity in *Ms. barkeri* Fusaro, if any, is unclear. In the presence of phenazine, methyl viologen ($E^{\circ\prime} = -0.446$ V) reduction lagged for several minutes (~5-10 minutes), before reaching full activity. This may be due to the preference of the hydrogenase activity for phenazine as substrate, or possibly to transfer of electrons from the reduced methyl viologen to phenazine (either chemical or enzymatic).

As with *Msp. hungatei* GP1 (Chapter 5), there are differences with respect to the requirement for activation of the $F_{420}H_2$ dehydrogenation and F_{420} H_2ase activities. The $F_{420}H_2$ dehydrogenation activity did not require a period of reactivation and was assayed immediately, even after aerobic manipulation. In contrast, the F_{420} H_2ase activity is reversibly inactivated in the presence of O_2, and must be reactivated under reducing conditions to prevent a lag in activity (Fiebig and Friedrich 1989). The reactivation process was modified from Choquet and Sprott (1991), with incubation of the protein in 10 μM FAD, 10 μM F_{420} and 20 mM DTT, under an atmosphere of H_2, prior to assay. This is essential for recovery of the hydrogenase activity, since the protein is purified under aerobic conditions.

6.3.3.3. Kinetic analyses

The apparent K_m for $F_{420}H_2$ was determined to be 2.8 μM $F_{420}H_2$, with Vmax = 23.7 μmol $F_{420}H_2$ oxidized·min^{-1}·mg^{-1} protein (Michaelis Menten kinetics) (Lineweaver Burk kinetics: K_m $F_{420}H_2$ = 3.0 μmol $F_{420}H_2$, Vmax = 23.9 μmol $F_{420}H_2$ oxidized· min^{-1}·mg^{-1}) (Figure 6.9). In contrast, the apparent K_m for $F_{420}H_2$ for *Ml. tindarius* and *Ms. mazei* Gö1 are 5.4 and 7 μM $F_{420}H_2$, respectively (Haase *et al.* 1992, Abken and

Deppenmeier 1997). The apparent K_m for phenazine was determined to be 112.4 μM (Figures 6.10 and 6.11; by contrast, the K_m of the phenazine-dependent activity of the $F_{420}H_2$ dehydrogenation from *Ms. mazei* Gö1 (pure enzyme) and *Ml. tindarius* (membrane-bound activity) was 250 and 238.9 μM, respectively (Abken *et al.* 1998, this thesis). The turnover number, kcat, was determined to be 416.9 s^{-1} ($k_{cat}/ K_m = 37.2x10^5 \cdot M^{-1} \cdot s^{-1}$).

Inhibition of the purified $F_{420}H_2$ dehydrogenation activity was similar to that observed with the membrane fraction. Additions of 50 and 100 μM DPI increased the K_m for phenazine from 112.4 μM to 238.7 and 299.4 μM, respectively, with Vmax = 29.5 μmol $F_{420}H_2$ oxidized$\cdot min^{-1} \cdot mg^{-1}$ protein (Lineweaver Burk kinetics: Additions of 50 and 100 μM DPI increased the K_m for phenazine from 105.0 μM to 195.0 and 268.0 μM, respectively, with Vmax = 24.6 μmol $F_{420}H_2$ oxidized$\cdot min^{-1} \cdot mg^{-1}$ protein) (Figures 6.10 and 6.11).

A.

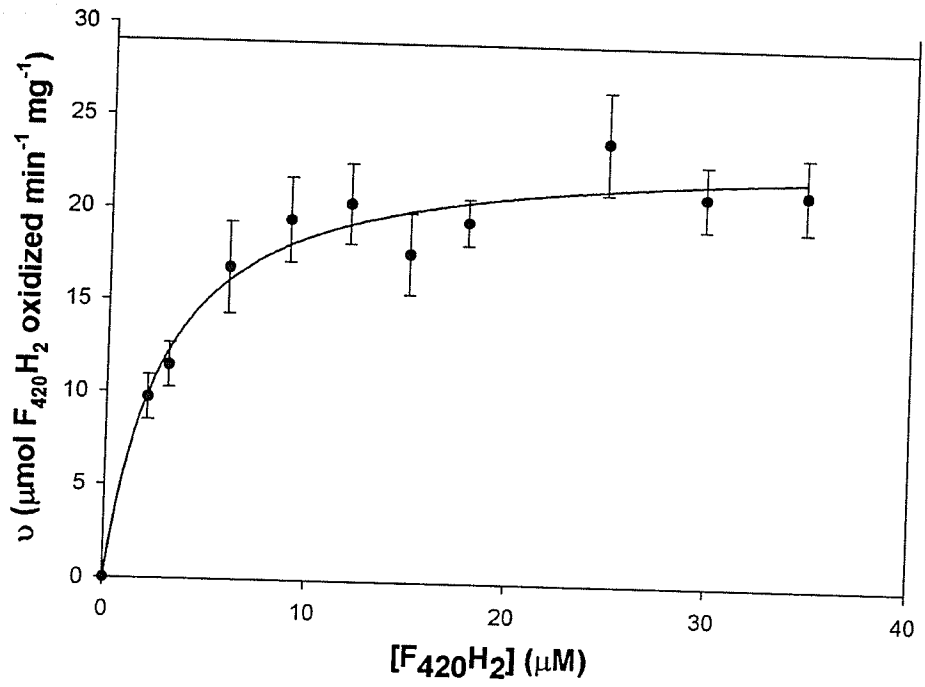

B.

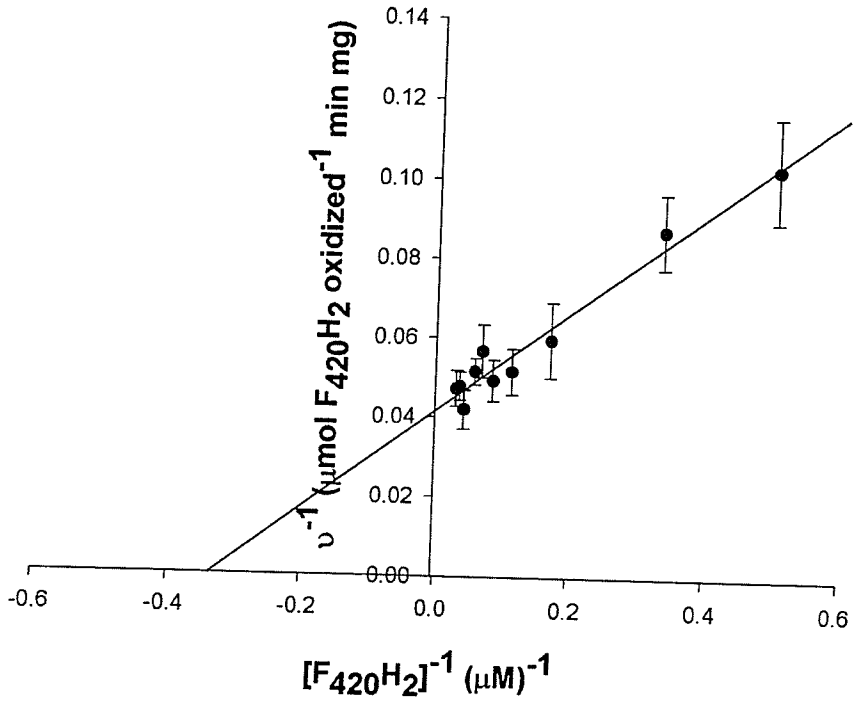

Figure 6.9. Michaelis Menten kinetics (A) and Lineweaver Burk plot (B) for the determination of KmF_{420} for the purified phenazine-dependent $F_{420}H_2$ dehydrogenation activity of *Methanosarcina barkeri* Fusaro. 500 μM phenazine added per tube.

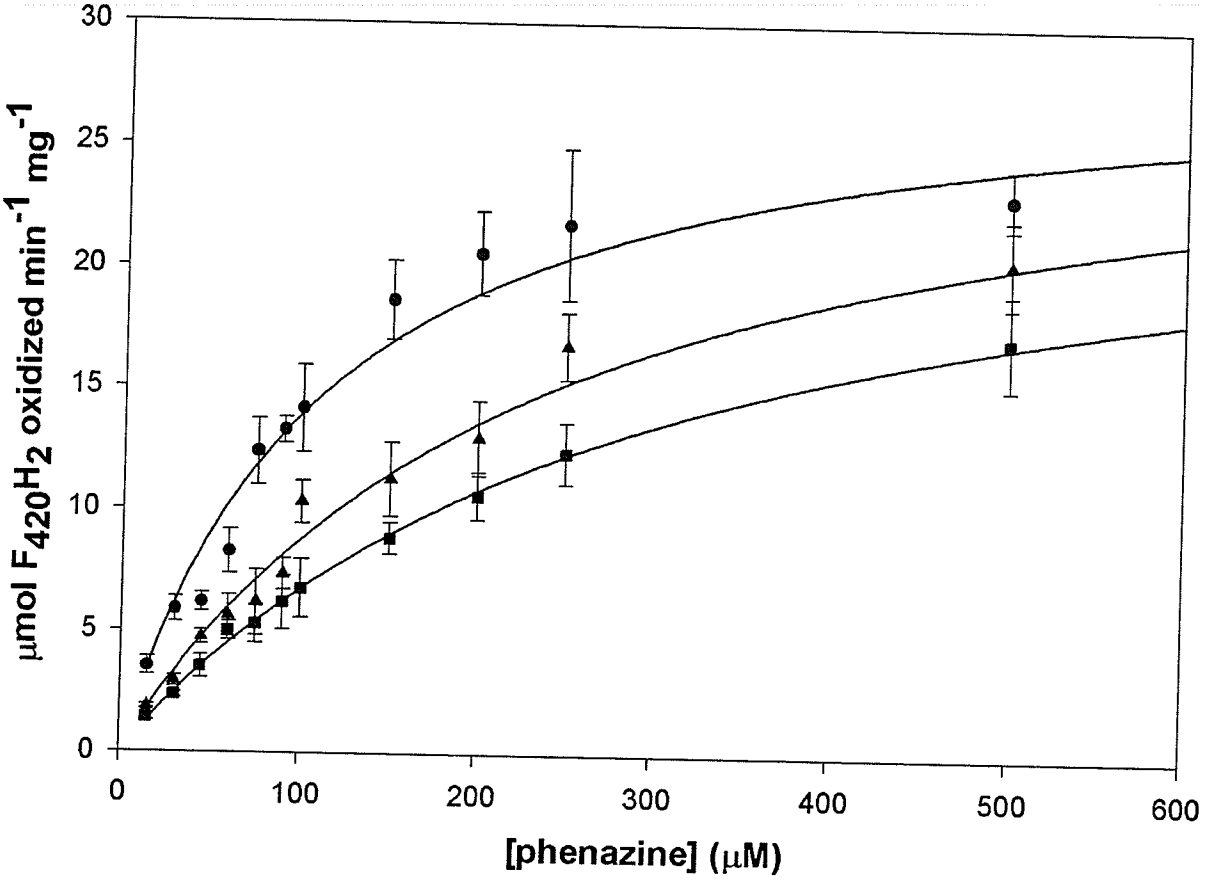

Figure 6.10. Michaelis Menten kinetics plot of the purified phenazine-dependent $F_{420}H_2$ dehydrogenation activity in the presence/absence of DPI. All points represent experiments performed in triplicate. Assay conditions as described under 'Materials and Methods'. No DPI, ●. 50 µM DPI, ▲. 100 µM DPI, ■. 10-15 µM $F_{420}H_2$ added per assay tube.

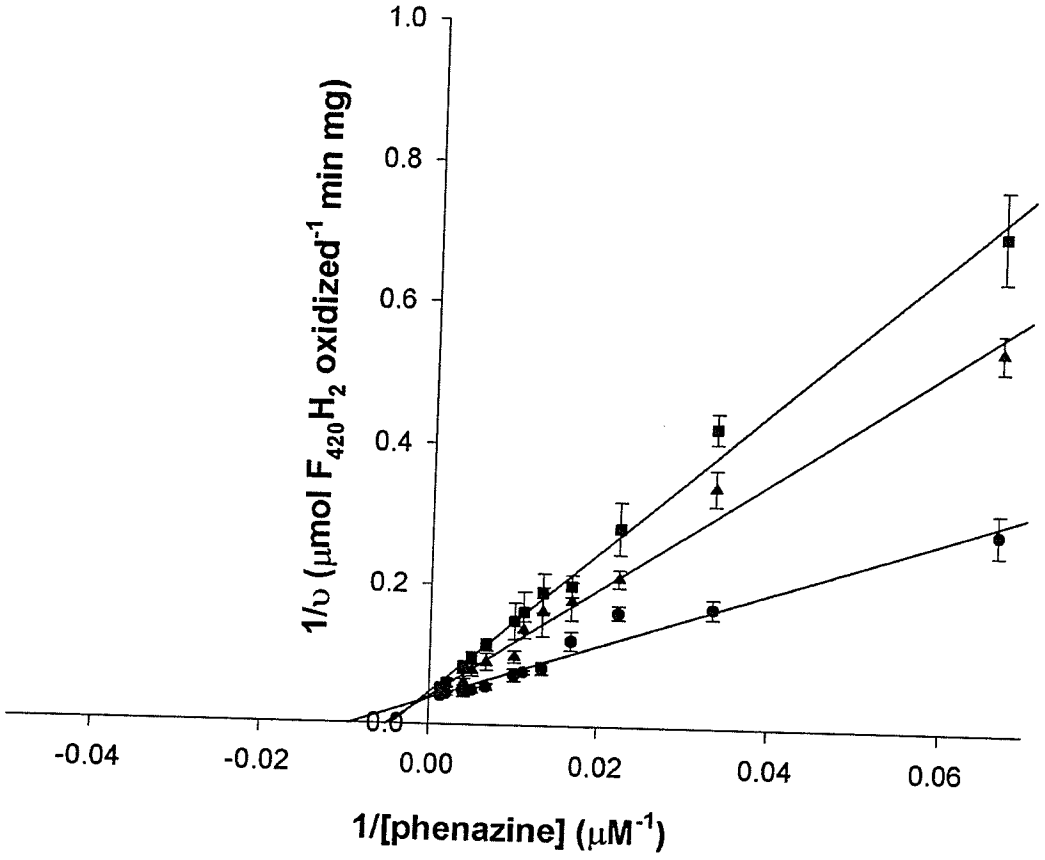

Figure 6.11. Lineweaver Burke kinetics plot of the purified phenazine-dependent $F_{420}H_2$ dehydrogenation activity in the presence/absence of DPI. All points represent experiments performed in triplicate. Assay conditions as described under 'Materials and Methods'. No DPI, ●. 50 μM DPI, ▲. 100 μM DPI, ■. 10-15 μM $F_{420}H_2$ added per assay tube.

6.4. Discussion

6.4.1. Comparing the $F_{420}H_2$ dehydrogenation activity of Methanosarcina barkeri Fusaro with Methanolobus tindarius and Methanosarcina mazei Gö1

Comparisons of the genome of *Ms. barkeri* Fusaro with the genomes of *Ms. mazei* Gö1 and *Ms. acetivorans* C2 indicate that this methanoarchaeon contains the full complement of enzymes necessary for the metabolism of the various substrates, with all biosynthetic and catabolic genes conserved, including *fpo* (Deppenmeier *et al.* 2002, Galagan *et al.* 2002, Maeder *et al.* 2006).

Studies were conducted examining the phenazine-dependent $F_{420}H_2$ dehydrogenase activities in the washed membranes of *Ml. tindarius* and *Ms. barkeri* Fusaro (Figure 6.1). The apparent K_m for phenazine of the $F_{420}H_2$ dehydrogenation activity of *Ml. tindarius* was 238.9 μM phenazine; the apparent K_m for phenazine for the homologous activity of *Ms. barkeri* Fusaro was 106.0 μM phenazine, indicating that the activity of *Ms. barkeri* has a higher affinity for phenazine.

Addition of DPI has a more severe effect on the activity of *Ml. tindarius*, comparable to the inhibition of the purified $F_{420}H_2$ dehydrogenase activity of *Ms. mazei* Gö1. The inhibition curve for *Ml. tindarius* (Ic_{50} = 3 μM DPI) shows a much steeper drop in dehydrogenation activity compared to *Ms. barkeri* Fusaro (Ic_{50} > 100 μM DPI) (Chapter 4).

Low concentrations of DPI significantly inhibit the membrane-bound $F_{420}H_2$ dehydrogenation activity of *Ml. tindarius*, increasing the K_m from 238.9 to 965.6 (3 μM DPI) and 1823.4 μM phenazine (9 μM DPI); this is consistent with the observations of DPI-mediated inhibition of the purified $F_{420}H_2$ dehydrogenase activity of *Ms. mazei* Gö1 (assayed with 2-OH-phenazine) (Brodersen *et al.* 1999).

The membrane-bound $F_{420}H_2$ dehydrogenation activity of *Ms. barkeri* Fusaro does not respond to DPI as expected under the growth conditions tested; the K_m increased from 106.0 to 204.0 (50 μM DPI) and 342.3 μM phenazine (100 μM DPI). The total phenazine-dependent $F_{420}H_2$ dehydrogenation activity measured should be due to the cumulative activity of the Fpo complex and F_{420} H_2ase. If the Fpo complex were located in the membranes of *Ms. barkeri* Fusaro, a more prominent effect on the overall $F_{420}H_2$ dehydrogenation activity would have been observed, as the activity of the Fpo complex should have been completely inhibited at the concentrations of DPI used. The remaining $F_{420}H_2$ dehydrogenation activity would be due to the F_{420} H_2ase, and simple Michaelis Menten kinetics would not be observed.

One conclusion that can be drawn from these results is that *Ms. barkeri* Fusaro apparently does not express the genes encoding the Fpo complex under the tested growth conditions; to confirm the apparent lack of expression of the Fpo complex, reverse transcriptase (RT)-PCR could be used to confirm the presence/absence of mRNA encoding for the Fpo complex in *Ms. barkeri* Fusaro under the growth conditions tested.

6.4.2. Purification of the phenazine-dependent $F_{420}H_2$ dehydrogenation activity

Various chromatographic techniques were used to enrich for the phenazine-dependent $F_{420}H_2$ dehydrogenation activity from proteins extracted from solubilized membranes, but in each case the $F_{420}H_2$ dehydrogenation activity was found to elute with an F_{420}-reducing activity (Figures 6.2 and 6.3); the purified $F_{420}H_2$ dehydrogenase activities from *Ml. tindarius* and *Ms. mazei* Gö1 are devoid of hydrogenase activity

(Abken and Deppenmeier 1997). The membranes of *Ml. tindarius* do not contain an F_{420} H_2ase (Deppenmeier *et al.* 1989).

Purification of the phenazine-dependent $F_{420}H_2$ dehydrogenation activity from the hydrogenotrophic methanoarchaea *Msp. hungatei* strain GP1 (Chapter 5) revealed that phenazine-dependent $F_{420}H_2$ dehydrogenation activity is located on the F_{420} H_2ase. In light of these findings, we believed that a phenazine-dependent $F_{420}H_2$ dehydrogenation activity in *Ms. barkeri* might also reside on its F_{420} H_2ase.

The use of metal chelate affinity chromatography, sucrose gradient ultracentrifugation, and gel filtration chromatography established that the membrane-associated $F_{420}H_2$ dehydrogenation activity was eluting with an F_{420} H_2ase activity (Figures 6.2 and 6.3). Other chromatographic techniques yielded similar results. The F_{420} H_2ase also catalyzes the oxidation of $F_{420}H_2$; by selecting for the purification of this protein, we expected to separate this "artifact" activity from any other source of $F_{420}H_2$ dehydrogenation present in the protein extract.

In an attempt to reduce the amount of time to purify the protein, and to increase the yield, the sucrose gradient ultracentrifugation and gel filtration steps were replaced with electrophoresis of the protein on a native gradient PAGE, followed by electro-elution of the bands of interest. Elution of protein from a 3-20% native gradient PAGE confirmed that the phenazine-dependent $F_{420}H_2$ dehydrogenation activity was indeed located on the F_{420} H_2ase. Other bands excised from the gel, including gel bands with similar MW as the $F_{420}H_2$ dehydrogenase of *Ml. tindarius* and *Ms. mazei* Gö1, did not contain $F_{420}H_2$ dehydrogenase or F_{420} H_2ase activity.

The results were the same whether the activity was isolated from the soluble fraction, or from the membranes of *Ms. barkeri* Fusaro. No other source of $F_{420}H_2$ dehydrogenation activity was observed in *Ms. barkeri* Fusaro. It is not clear whether this activity is an artifact of the F_{420} H_2ase, or if this activity holds any physiological significance.

6.4.3. Molecular properties

As with *Msp. hungatei* GP1 (Chapter 5), the purified phenazine-dependent $F_{420}H_2$ dehydrogenation activity of *Ms. barkeri* Fusaro was isolated on the F_{420} H_2ase. This was evident after electrophoresis of purified protein on native gradient PAGE (Figures 6.5 and 6.6) and SDS PAGE (Figure 6.7). The protein consists of three distinct subunits with molecular weights of 48, 33, and 30 kDa. The presence of the F_{420} H_2ase was confirmed with N-terminal sequencing of the 48 kDa (α-) and 33 kDa (β-) subunits (Table 6.5).

In contrast, the $F_{420}H_2$ dehydrogenase activity purified from *Ml. tindarius* and *Ms. mazei* Gö1 each consist of 5 distinct subunits with molecular weights ranging from of 45, 40, 22, 18, and 17 kDa (120 kDa overall, *Ml. tindarius*) and 40, 37, 22, 20, and 16 kDa (115 KDa overall, *Ms. mazei* Gö1) (Haase *et al.* 1992, Abken and Deppenmeier 1997).

Ms. barkeri Fusaro possesses two isoenzymes of F_{420} H_2ase, Frh and Fre (Vaupel and Thauer 1998), but is not known if which of the isoenzymes was isolated during our studies. The N-terminus sequences derived from the α- and β-subunits of the purified protein are identical to both isoenzymes. Whether Frh or Fre, or both, are the source of

the observed phenazine-dependent $F_{420}H_2$ dehydrogenation activity in *Ms. barkeri* Fusaro during growth on CH_3OH remains unclear.

The only significant difference found between the two isoenzymes are the FrhD (δ-) and FreE (ε-) subunits encoded by the *frhADGB* (F_{420} H_2ase II) and *freAEGB* (F_{420} H_2ase I), respectively. BLAST analyses confirm that FrhD (159 aa) is a hydrogenase maturation factor, while FreE (40 aa) does not show any similarity to any sequences found in the Eukarya, Bacteria, or Archaea databases. Further analyses using the Loctree (Nair and Rost 2005) and Subloc v1.0 (Hua and Sun 2001) software indicate that FreE is an extracellular or periplasmic protein, respectively; FrhD was designated a cytoplasmic protein as expected. Thus, neither the FrhD nor FreE subunits appear to be factors that influence the presence of the $F_{420}H_2$ dehydrogenation activity.

6.4.4. Catalytic and kinetic analyses

The $F_{420}H_2$ dehydrogenation activity of *Ms. barkeri* Fusaro is similar to the activity of the $F_{420}H_2$ dehydrogenase purified from *Ms. mazei* Gö1: both activities use $F_{420}H_2$ as electron donor; both activities can use phenazine as electron acceptor; and both activities are inhibited by the addition of DPI. Methyl viologen and FAD could substitute for phenazine as substrate for the $F_{420}H_2$ dehydrogenation activity, but NAD^+, $NADP^+$, and ferredoxin could not replace phenazine for use as electron acceptors.

The phenazine-dependent $F_{420}H_2$ dehydrogenation activity of *Ms. barkeri* Fusaro was competitively inhibited by DPI, but the degree of inhibition was not as great as observed in *Ms. mazei* Gö1 (Brodersen *et al.* 1999) or *Ml. tindarius*. DPI inhibition of the $F_{420}H_2$ dehydrogenation activity of *Ms. barkeri* Fusaro follows simple Michaelis-

Menten enzyme kinetics. Additions of 50 and 100 μM DPI increased the K_m for phenazine from 112.4 μM to 241.3 and 301.9 μM, respectively, and Vmax = 29.5 μmol $F_{420}H_2$ oxidized·min^{-1}·mg^{-1} protein.

The F_{420} H_2ase activity of *Ms. barkeri* Fusaro was not inhibited by the addition of DPI, indicating that DPI was not interacting directly with the FAD component. Phenazine could substitute for F_{420} as electron acceptor for the F_{420} H_2ase (Table 6.7). The physiological significance of this activity, if any, is unclear. Meuer *et al.* 1999 reported that the F_{420} H_2ase from *Mtb. thermoautotrophicus* ΔH also catalyzes the H_2-dependent reduction of phenazine, yet methanophenazine is not found in this methanoarchaeon. Phenazine may be functioning solely as an artificial electron acceptor, like methyl or benzyl viologen.

6.4.5. Location of the $F_{420}H_2$ dehydrogenation activity on the F_{420}-reducing hydrogenase – physiological ramifications

During growth on H_2 and CO_2, the F_{420} H_2ase of *Ms. barkeri* Fusaro catalyzes the reversible reduction of F_{420} with H_2 (Thauer *et al.* 1993, Shima *et al.* 2002, Deppenmeier 2004). Electrons from $F_{420}H_2$ are transferred to H_4MPT-bound C_1 intermediates in order to reduce CO_2 to CH_3-H_4MPT (Thauer *et al.* 1993):

(1) $F_{420}H_2$ + N^5,N^{10}-methenyl-H_4MPT → N^5,N^{10}-methylene-H_4MPT + F_{420}

(2) $F_{420}H_2$ + N^5,N^{10}-methylene-H_4MPT → N^5-methyl-H_4MPT + F_{420}

However, when grown on CH_3OH there is no apparent need for H_2-dependent reduction of F_{420}, as $F_{420}H_2$ is synthesized through the course of CH_3OH dis-proportionation to CH_4, using the same reactions as in CO_2 reduction, but in the reverse direction. 1 mol of CH_3OH is oxidized to CO_2 to produce $F_{420}H_2$ for the reduction of

CoM-S-S-CoB generated by the remaining 3 mol of CH_3OH (Deppenmeier *et al.* 1996, Bäumer *et al.* 1998).

$F_{420}H_2$-dependent CoM-S-S-CoB reduction is catalyzed by the Fpo complex and Hdr in the membranes of *Ms. mazei* Gö1; methanophenazine is the purported electronic link between Fpo and Hdr (Deppenmeier 2002, 2004). We did not detect the presence of a similar complex in *Ms. barkeri* Fusaro, despite the presence of genes encoding for an Fpo complex in the genome of this methanoarchaeon. The membrane-bound $F_{420}H_2$ dehydrogenation activity was found solely on the F_{420} H_2ase, and no other source of $F_{420}H_2$ dehydrogenation activity was detected. Furthermore, the $F_{420}H_2$ dehydrogenation activity was phenazine-dependent; the cytoplasmic portion of the Fpo complex of *Ms. mazei* Gö1 was also assayed using phenazine (Abken *et al.* 1998).

Our studies indicate that $F_{420}H_2$ dehydrogenation activity is highest when *Ms. barkeri* Fusaro is grown with CH_3OH (Table 4.1, Chapter 4); this is consistent with the findings of Mukhopadhyay *et al.* (1993), who reported differential expression of the F_{420} H_2ase of *Ms. barkeri* when grown using different methanogenic substrates. Production of the F_{420} H_2ase was highest when grown on CH_3OH (0.437 ± 0.0507 μmol F_{420}-reduced·min^{-1}·mg^{-1} protein), compared to growth on H_2/CO_2 (0.340 ± 0.0386 μmol F_{420}-reduced·min^{-1}·mg^{-1} protein) and acetate (0.080 ± 0.0131 μmol F_{420}-reduced·min^{-1}·mg^{-1} protein) (cultures grown to mid-log phase, Mukhopadhyay *et al.* (1993)).

Brodersen *et al.* (1999b) discovered that the membrane-bound F_{420} H_2ase of the hydrogenotrophic methanoarchaeon *Mc. voltae* was the source of an $F_{420}H_2$ dehydrogenation activity coupled to membrane-bound CoM-S-S-CoB reduction.

Mc. voltae can grow either on H_2/CO_2 or on formate as substrate for methanogenesis. During growth on H_2/CO_2 $F_{420}H_2$ is not required as an electron donor for CoM-S-S-CoB reduction, since H_2 can be used directly by the F_{420}-nonreducing H_2ase: however, when growing on formate, $F_{420}H_2$, generated from formate dehydrogenation, is the source of reductant (Brodersen *et al.* 1999b). The identity of the intermediate electron carrier linking the passage of electrons from $F_{420}H_2$-oxidizing activity (of the F_{420} H_2ase) and the Hdr in *Mc. voltae* is currently not known.

It has been suggested that the F_{420} H_2ase or F_{420}-nonreducing H_2ase of *Ms. barkeri* Fusaro could be involved in energy conservation (Lünsdorf *et al.* 1991). From the results of our studies, it is plausible that electrons may be transferred from $F_{420}H_2$ to an electron acceptor such as methanophenazine *via* the $F_{420}H_2$ dehydrogenation activity associated with the F_{420} H_2ase (Figure 6.12A). Methanophenazine, which would act as the electronic link between the F_{420} H_2ase and Hdr; Hdr would then transfer the electrons from reduced methanophenazine to CoM-S-S-COB. In contrast to the Fpo complex, the F_{420} H_2ase does not act as a proton pump, as it lacks a transmembrane proton channel (Lünsdorf *et al.* 1991). It is not known whether the F_{420} H_2ase may be attached to another integral membrane protein that may function as a proton pump. Protons would be pumped out of the cell during the reduction of CoM-S-S-COB, with electrons derived from reduced methanophenazine; the $\Delta\tilde{u}H^+$ generated would drive the synthesis of ATP from ADP and Pi, *via* the A_1A_0 ATP synthase (Bäumer *et al.* 1998, Ide *et al.* 1999, Deppenmeier 2002, 2004).

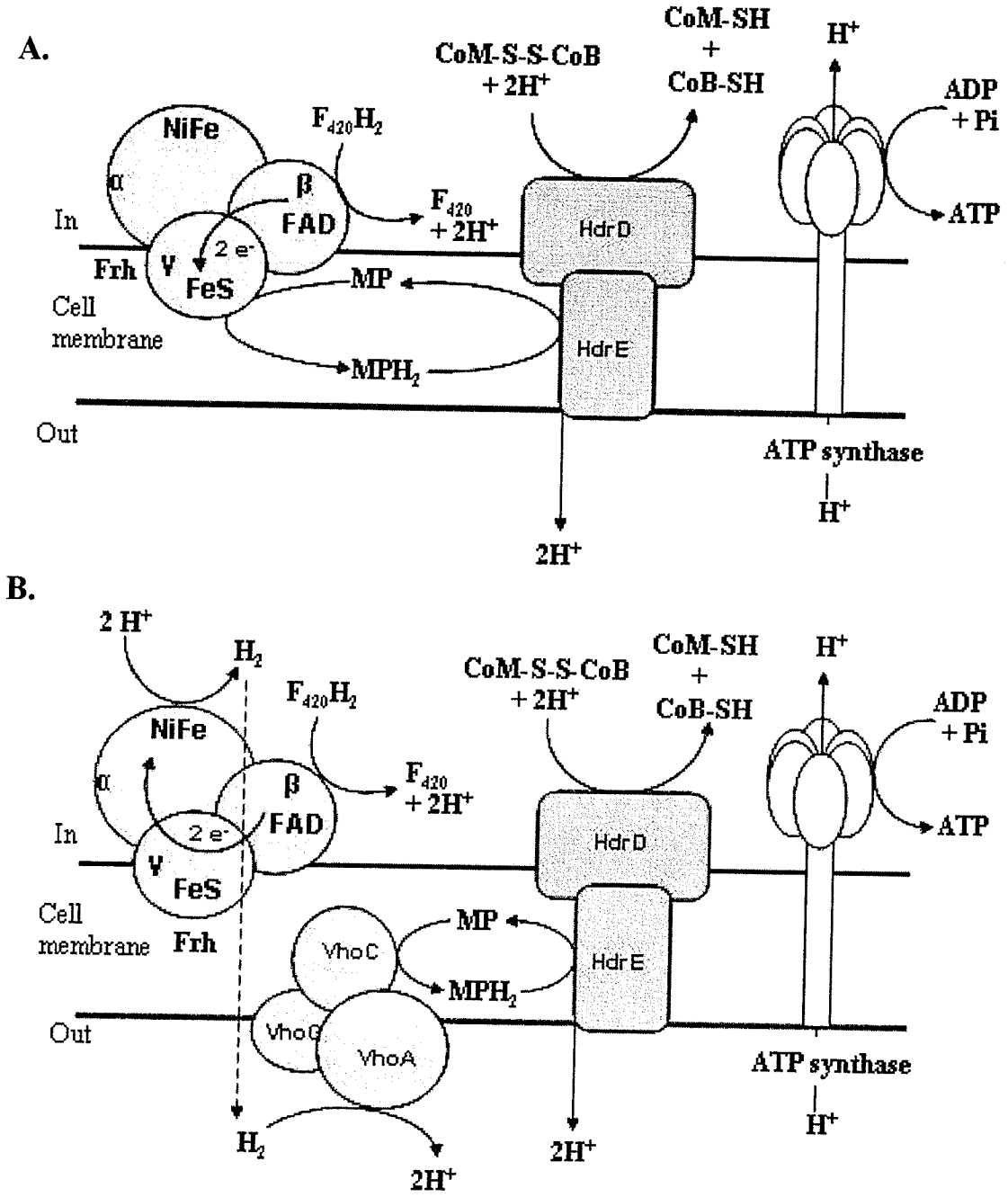

Figure 6.12. Possible models of $F_{420}H_2$-dependent CoM-S-S-CoB reduction in CH_3OH-grown *Methanosarcina barkeri* Fusaro. A. Model 1: F_{420}-reducing hydrogenase (Frh) catalyzes the $F_{420}H_2$-dependent reduction of methanophenazine (MP). MPH_2 used to reduce CoM-S-S-CoB *via* Hdr. $\Delta\tilde{u}H^+$ generated used to synthesize ATP. B. Model 2: $F_{420}H_2$ oxidized to H_2 *via* Frh, which diffuses through cell membrane. H_2 is then oxidized *via* the F_{420}-nonreducing hydrogenase (Vho), and electrons are transferred to MP. MPH_2 used to reduce CoM-S-S-CoB *via* Hdr.

It has been suggested that the F_{420} H_2ase, during growth on CH_3OH, may be a redox valve to regulate the levels of $F_{420}H_2$ and H_2 in cultures of *Ms. barkeri* Fusaro (Keltjens and Vogels 1993, de Poorter *et al.* 2005). With respect to energy conservation, the F_{420} H_2ase may oxidize $F_{420}H_2$ to F_{420} and H_2, producing a source of electrons used by the F_{420}-nonreducing H_2ase (Vho) to reduce methanophenazine (Figure 6.12B). The F_{420}-nonreducing H_2ase is produced when *Ms. barkeri* Fusaro is grown on CH_3OH (Figure 6.5); the homologous membrane-bound extra-cytoplasmic enzyme in *Ms. mazei* Gö1 is also expressed during growth on CH_3OH (Deppenmeier 1995, Deppenmeier *et al.* 1996). Vho catalyzes the reduction of 2-OH-phenazine, which generates an energy conserving $\Delta\mu H^+$; the reduced methanophenazine is then used for the reduction of CoM-S-S-CoB *via* Hdr, also generating an energy conserving $\Delta\mu H^+$ (Ide *et al.* 1999, Deppenmeier 2002, 2004).

A model was suggested for *Msp. hungatei* GP1 (Chapter 5), where electrons are shuttled from the F_{420} H_2ase directly to the Hdr, and then to CoM-S-S-CoB (Figure 5.16, Chapter 5); this is likely not the case for *Ms. barkeri* Fusaro. Electron transport in the *Methanosarcinaceae* is dependent on cytochromes (VhoC and HdrE) and methanophenazine, electron carriers found within the membranes; these electron carriers are not found in methanoarchaea outside of the *Methanosarcinaceae* (Ide *et al.* 1999, Deppenmeier 2002, 2004).

It should be noted that in our studies, using a protocol derived from Abken *et al.* (1998), we have not detected the presence of methanophenazine from lyophilized membranes of *Ms. barkeri* Fusaro or *Ml. tindarius*; it is possible that the technique used to isolate the compound from the membranes of *Ms. barkeri* Fusaro or *Ml. tindarius* was

not sensitive enough detect to the low amounts of methanophenazine present; Beifuss and Tietze (2005) reported that there were very low amounts of methanophenazine isolated from the membranes of *Ms. mazei* Gö1.

Further studies are required to conclusively resolve the mechanism of $F_{420}H_2$-dependent CoM-S-S-CoB reduction in *Ms. barkeri* Fusaro, as well as the implications with respect to bioenergetics in this methanoarchaeon.

7. Phenazine-dependent $F_{420}H_2$ dehydrogenation activity in *Methanosphaera stadtmanae*

7.1. Introduction

Methanosphaera stadtmanae is a coccoid methanoarchaeon that resides in the human large intestine (Miller and Wolin 1983, 1985). Along with *Methanosphaera cuniculi*, a closely related methanoarchaeon isolated from the intestinal tract of rabbits (Biavati *et al.* 1988), *Msph. stadtmanae* belongs to the order *Methanobacteriales* (Miller and Wolin 1985). *Msph. stadtmanae* has strict growth requirements for acetate, CO_2, isoleucine, and thiamin, and can only produce methane (CH_4) in the presence of H_2 and methanol (CH_3OH); this is in contrast to other members of the *Methanobacteriales*, which metabolize H_2 and CO_2 as methanogenic substrate (van de Wijngaard *et al.* 1991). *Msph. stadtmanae* can also produce CH_4 using H_2 and serine as methanogenic precursors, although the amount of CH_4 produced is approximately 50-fold lower compared to cells grown on H_2 and CH_3OH (Lin and Sparling 1995, 1998).

H_2 and CH_3OH are both metabolic waste products produced by other microorganisms indigenous to the large intestine: H_2 is a common byproduct of fermentation by the intestinal microbial community, and CH_3OH is obtained in the gut *via* degradation of pectin by *Bacteroides thetaiotaomicron* (Miller and Wolin 1983, Dongowski *et al.* 2000). Reduction of CH_3OH to CH_4 is coupled to energy conservation and ATP synthesis (Sparling *et al.* 1993).

7.1.1. Msph. stadtmanae and the Methanosarcinales: key differences

Msph. stadtmanae produces CH_4 when growing on CH_3OH and H_2 in a manner similar to *Methanosarcina barkeri*, a member of the order *Methanosarcinales*, according to the following equation (van de Wijngaard *et al.* 1991):

$$H_2 + CH_3OH \rightarrow CH_4 + H_2O,\ \Delta G^{\circ\prime} = -113\ kJ/mol$$

Unlike the CH_3OH-metabolizing methanoarchaea from the order *Methanosarcinales*, *Msph. stadtmanae* cannot disproportionate CH_3OH or metabolise methylamines (Miller and Wolin 1983, 85). *Msph. stadtmanae* also does not possess cytochromes, which are characteristic of most CH_3OH-metabolizing methanoarchaea (Miller and Wolin 1985).

In some members of the *Methanosarcinales* capable of CH_3OH disproportionation, the $F_{420}H_2$ dehydrogenase (Fpo complex, $F_{420}H_2$ phenazine oxidoreductase) is expected to be an essential component of the $F_{420}H_2$:heterodisulfide oxidoreductase system (Deppenmeier *et al.* 1999, Deppenmeier 2002). Electrons from $F_{420}H_2$ are transferred to the putative electron carrier methanophenazine *via* the $F_{420}H_2$ dehydrogenase; the electrons are then transferred from reduced methanophenazine to the heterodisulfide reductase (Hdr) and ultimately to the heterodisulfide complex (CoM-S-S-CoB), generating an energy conserving transmembrane proton gradient ($\Delta\mu H^+$) (Deppenmeier 2002, 2004).

Msph. stadtmanae possesses an F_{420}-nonreducing hydrogenase (MV H_2ase, MvhADG), which is found in most hydrogenotrophic methanoarchaea and is an essential component of the H_2:heterodisulfide oxidoreductase complex, transferring electrons from H_2 to Hdr for the reduction of CoM-S-S-CoB and generation of $\Delta\mu H^+$ (Thauer *et al.*

1993, Wong Ph.D thesis 1999, Shima *et al.* 2002). As such, neither $F_{420}H_2$ nor $F_{420}H_2$ dehydrogenase would be necessary during growth on H_2 and CH_3OH. However, low levels of $F_{420}H_2$ dehydrogenation activity have been detected in the cell-free extract of *Msph. stadtmanae* (Wong *et al.* 1994). The $F_{420}H_2$ dehydrogenation activity of *Msph. stadtmanae* was studied primarily using the synthetic electron acceptor methyl viologen (with metronidazole) (Wong, Ph.D thesis 1999). Unlike the $F_{420}H_2$ dehydrogenase purified from *Ml. tindarius* and *Ms. mazei* Gö1, the $F_{420}H_2$ dehydrogenation activity in *Msph. stadtmanae* is aerobically unstable (Wong *et al.* 1994).

7.1.2. $F_{420}H_2$ Dehydrogenation activity of Methanosphaera stadtmanae

It has been proposed that the role of the $F_{420}H_2$ dehydrogenation activity in *Msph. stadtmanae* is actually to couple the transfer of electrons from H_2 to the reduction of F_{420}, as the presence of a H_2-dependent F_{420}-reducing activity had not been detected in cell-free extract (Deppenmeier *et al.* 1989, van de Wijngaard *et al.* 1991, Wong *et al.* 1994). F_{420} has been detected in very low amounts in *Msph. stadtmanae* (0.16 nmol $F_{420}{\cdot}mg^{-1}$ protein); while $F_{420}H_2$ is not required for methanogenesis from H_2 and CH_3OH, $F_{420}H_2$ is required for methanogenesis from H_2 and L-serine, or 2-propanol and CH_3OH, and for cellular biosynthesis (Wong *et al.* 1994, Lin and Sparling 1995). One of the objectives of this thesis was to purify this activity, and to determine if this activity is could be linked to F_{420}-reduction in *Msph. stadtmanae* as proposed. Studies of the $F_{420}H_2$ dehydrogenation activity of *Msph. stadtmanae* focused on the use of phenazine as the electron acceptor, since methanophenazine is the putative physiological electron acceptor for the $F_{420}H_2$ dehydrogenase activity in the *Methanosarcinaceae* (Abken *et al.* 1998).

7.2. Materials and methods

For a comprehensive look at the materials and methods used for this chapter, the reader is referred to the following sections in Chapter 3:

3.2. Growth media

3.3. Cell lysis

3.6. Enzyme assays

3.6.1. $F_{420}H_2$ dehydrogenation assays

3.6.2. Hydrogenase assays

3.6.2.1. F_{420}-reducing hydrogenase activity

3.6.2.2. Methyl viologen reducing hydrogenase activity

3.6.2.3. H_2-dependent phenazine reduction

3.6.3. $F_{420}H_2$ oxidase activity of *Methanosphaera stadtmanae*

3.7. Gel electrophoresis

3.7.2. Native gradient PAGE gel electrophoresis

In addition, several column chromatography techniques used to study the $F_{420}H_2$ dehydrogenation activity of *Msph. stadtmanae* are described in Appendix E.

7.3. Results

7.3.1. Catalytic properties of the $F_{420}H_2$ dehydrogenation activity in cell-free extract

The vast majority of the phenazine-dependent $F_{420}H_2$ dehydrogenation activity was found in the soluble cytoplasmic fraction (clarified cell-free extract, membranes removed *via* ultracentrifugation) of *Msph. stadtmanae*, with approximately 10-15% of the overall activity located in the membrane (Table 7.1). Therefore, the experimental work

in this chapter was performed using either clarified cell-free extract or cell-free extract (where noted), under anaerobic conditions.

Table 7.1. Location of the phenazine-dependent $F_{420}H_2$ dehydrogenation activity of *Methanosphaera stadtmanae*. Activity measured using 500 μM phenazine, 10 μM $F_{420}H_2$.

Cell fraction	Total activity (nmol $F_{420}H_2$ oxid·min^{-1})	% activity
Cell-free extract	4164.4 (3.2)†	100
Clarified cell-free extract	3446.2 (3.5)†	82.7
Membranes	518.2 (1.6)†	12.4

† specific activity: nmol $F_{420}H_2$ oxid·min^{-1}·mg^{-1}

Several different substrates were tested in comparison to phenazine as electron acceptors for the $F_{420}H_2$ dehydrogenation activity in cell-free extract. The results are summarized in Table 7.2. Phenazine is not the optimal electron acceptor in the reaction buffer used, as greater $F_{420}H_2$ dehydrogenation activity is observed when using methyl viologen or FAD. The rate of $F_{420}H_2$ oxidation using methyl viologen in place of phenazine is up to 3-fold higher compared to the activity when the same concentration of phenazine is used. FAD can also substitute for phenazine as electron acceptor; FAD catalyzes the chemical oxidation of $F_{420}H_2$, this amount is subtracted from the activity observed in the presence of clarified cell-free extract.

Table 7.2. Electron acceptor specificity of the $F_{420}H_2$ dehydrogenation activity of *Msph.stadtmanae* in clarified cell-free extract. All values represent the average of three separate assays, each performed in triplicate. 10-12 μM $F_{420}H_2$ added per assay tube.

Electron acceptor (μM)	**Activity (nmol $F_{420}H_2$ oxidized·min^{-1}·mg^{-1})**
Phenazine (25)	1.22 ± 0.5
Phenazine (500)	3.82 ± 0.2
Phenazine (500)[†]	1.24 ± 0.2
Methyl viologen (500)	7.3 ± 0.4
Ferredoxin (1.0 mg/ml)	No activity detected
FAD (40)	5.69 ± 0.6
NAD^+ (300)	No activity detected
O_2 (25)[‡]	3.5 ± 0.3

[†] 40 mM KPO_4 dehydrogenation assay buffer
[‡] breathing grade air-saturated MilliQ H_2O ([O_2] = ~250 μM), 200 μL added per tube

NADH could not substitute for $F_{420}H_2$ as electron donor; similarly, NAD^+ could not substitute for phenazine as an electron acceptor. $NADP^+$ was not tested, but it is expected that $F_{420}H_2$ oxidation would occur, as *Msph. stadtmanae* possesses an $F_{420}H_2$:$NADP^+$ oxidoreductase (Elias *et al.* 2000). Ferredoxin (from *Clostridium pasteuranium*) was also tested for its effectiveness as an electron acceptor, but $F_{420}H_2$ dehydrogenation activity was not detected with this substrate. O_2 (breathing grade air dissolved in Milli-Q H_20, ~250 μM) was also tested as an electron acceptor and was found to be an effective electron acceptor; the Km for O_2 was approximately 10-fold

lower than that of phenazine, indicating a higher affinity for O_2 as an electron acceptor for the $F_{420}H_2$ dehydrogenation activity (See section 7.3.10). In the absence of protein, $F_{420}H_2$ oxidation was not observed upon addition of O_2. O_2 and the possible physiological function of the $F_{420}H_2$ dehydrogenation activity will be discussed at the conclusion of this chapter.

7.3.2. pH Profile of the $F_{420}H_2$ Dehydrogenation of Msph.stadtmanae

A pH profile had been compiled for the $F_{420}H_2$ dehydrogenation activity in cell-free extract, using methyl viologen as electron acceptor; the $F_{420}H_2$ dehydrogenation activity was greatest at pH 7.0 (Denny Wong, PhD thesis, 1999). A similar pH profile was observed when using phenazine as electron acceptor, with the optimum activity found between pH 6.8-7.3 (Figure 7.1). This is similar to the pH optimum of the purified $F_{420}H_2$ dehydrogenase activity of *Ml. tindarius*, whose activity was highest at pH 6.8 (Haase *et al.* 1992), and of the phenazine-dependent $F_{420}H_2$ dehydrogenation activity of *Ms. barkeri* Fusaro (pH 7.5, this thesis). In contrast, the pH optimum for the purified $F_{420}H_2$ dehydrogenase activities from *Ms. mazei* Gö1 and sulfate-reducing archaeon *Archaeoglobus fulgidus* were pH 8.5 and pH 8.0, respectively (Kunow *et al.* 1994, Abken and Deppenmeier 1997). In the case of *Ml. tindarius*, *Ms. mazei* Gö1, and *A. fulgidus*, the pH profiles of the respective $F_{420}H_2$ dehydrogenation activities were determined using methyl viologen as electron acceptor.

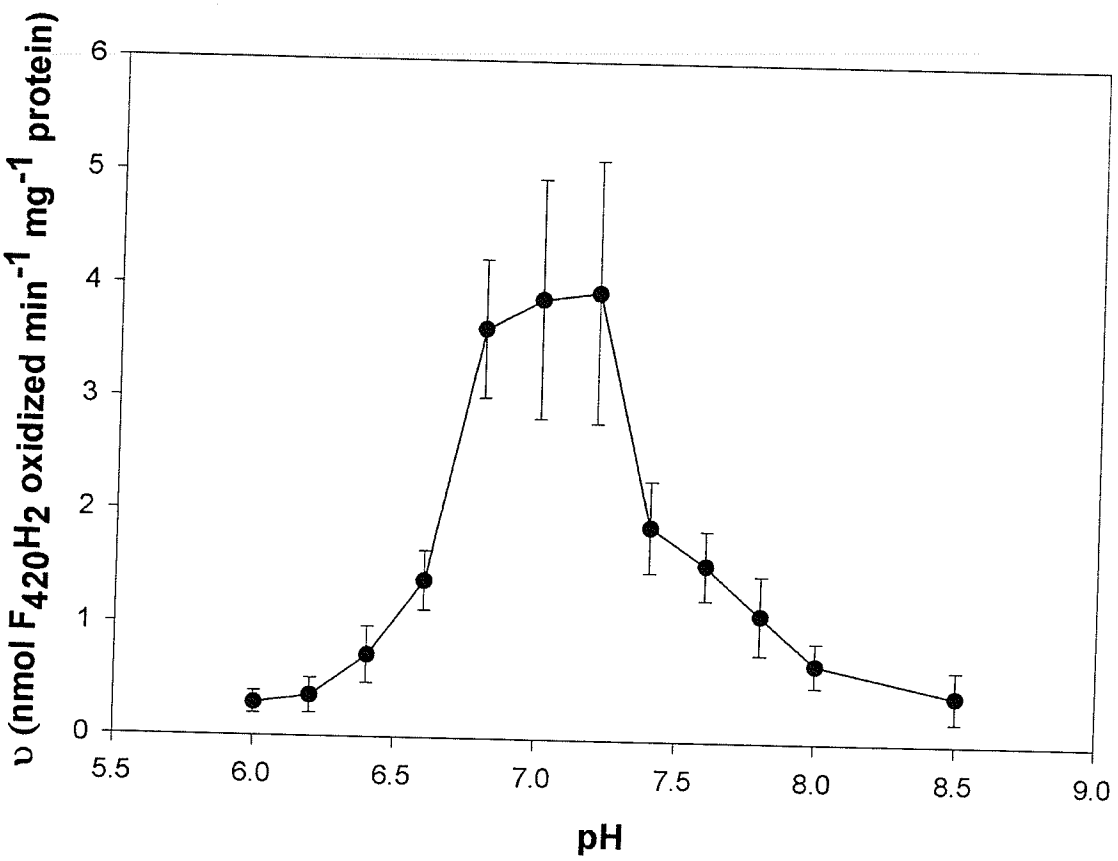

Figure 7.1. pH profile of the phenazine-dependent $F_{420}H_2$ dehydrogenation activity in clarified cell-free extract. pH of assay buffer established by varying concentration of K_2HPO_4 and KH_2PO_4. Final $[KPO_4]$ = 200 mM. $[F_{420}]$ = 10-15 μM

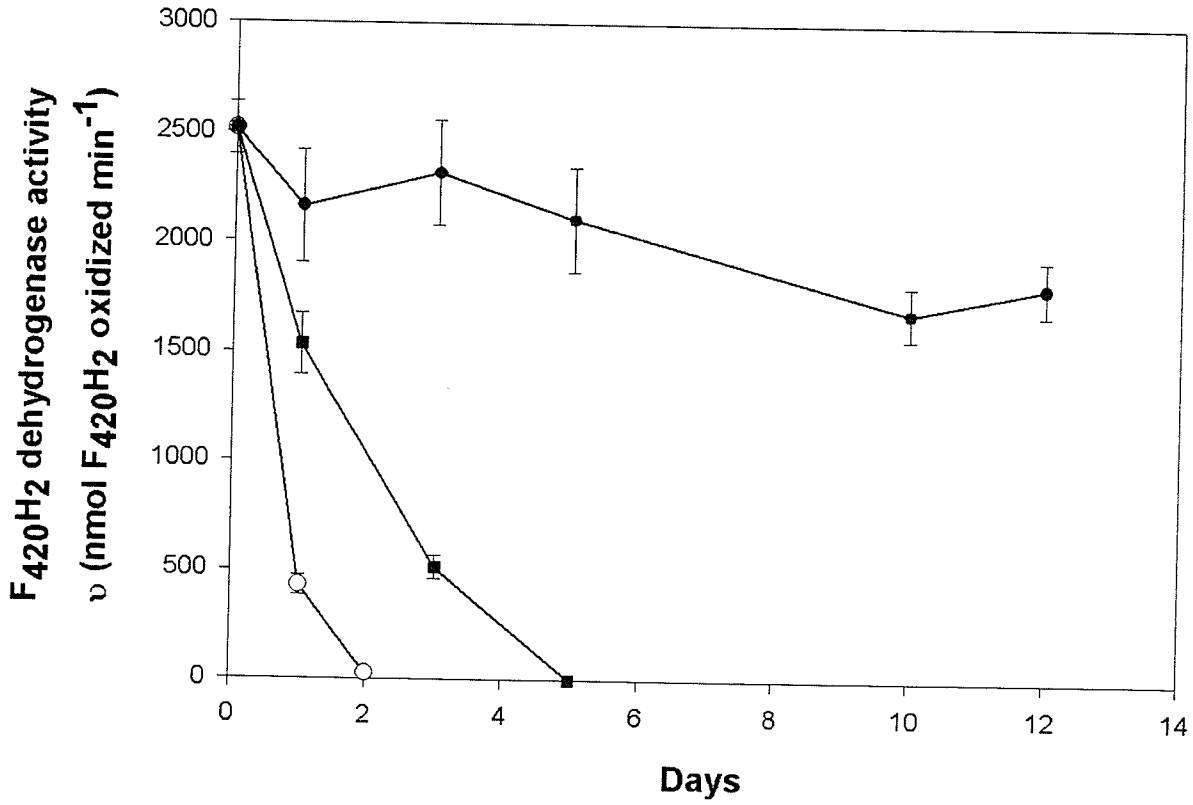

Figure 7.2. Stability of the phenazine-dependent $F_{420}H_2$ dehydrogenation activity in clarified cell-free extract (CCFE). (○), aerobic, 4°C. (●), anaerobic, 4°C. (■), anerobic, ambient room temperature. O_2 in aerobic sample purged with N_2 prior to assay.

7.3.3. Stability of the $F_{420}H_2$ Dehydrogenation activity

The $F_{420}H_2$ dehydrogenation activity was stable under refrigerated, anaerobic conditions, in unprocessed clarified cell-free extract (Figure 7.2). The activity was stable for up to two weeks, with or without the presence of $(NH_4)_2SO_4$. This is in contrast to the stability of the activity under aerobic conditions, where the enzyme activity was greatly diminished after one day; assay of the $F_{420}H_2$ dehydrogenation activity after incubation for 24 hour under aerobic conditions (4°C) resulted in approximately 80 to 85% loss of activity, and inactivity after 48 hours. Storage of the CCFE at ambient room temperature (25°C) results in rapid loss of activity, with the protein rendered inactive after 4-5 days.

By comparison, the phenazine-dependent $F_{420}H_2$ dehydrogenation activities of *Ms. barkeri* Fusaro and *Msp. hungatei* GP1, associated with the respective F_{420} H_2ase, were stable under aerobic conditions, stored at 4°C (chapters 5 and 6).

7.3.4. Kinetic analyses of the phenazine-dependent $F_{420}H_2$ dehydrogenation activity

The $F_{420}H_2$ dehydrogenation activity as catalyzed by clarified cell-free extract follows simple Michaelis-Menten kinetics. The apparent K_m for $F_{420}H_2$ was determined to be 18.4 μM, with Vmax = 9.7 nmol $F_{420}H_2$ oxidized·min^{-1}·mg^{-1} (Lineweaver Burk: K_m $F_{420}H_2$ = 14.5 μM, Vmax = 8.5 nmol $F_{420}H_2$ oxid·min^{-1}·mg^{-1}) (Figure 7.3).

The apparent K_m for phenazine was calculated to be 138 μM, with Vmax = 3.0 nmol $F_{420}H_2$ oxidized· min^{-1}·mg^{-1} (Lineweaver Burk: $K_{m\ phenazine}$ = 156 μM, Vmax = 3.2 nmol $F_{420}H_2$ oxid·min^{-1}·mg^{-1}) (Figures 7.4 and 7.5). This value is lower than the K_m determined for the $F_{420}H_2$ dehydrogenase of *Ml. tindarius* (cell-free extract) (266 μM phenazine, Chapter 4).

A.

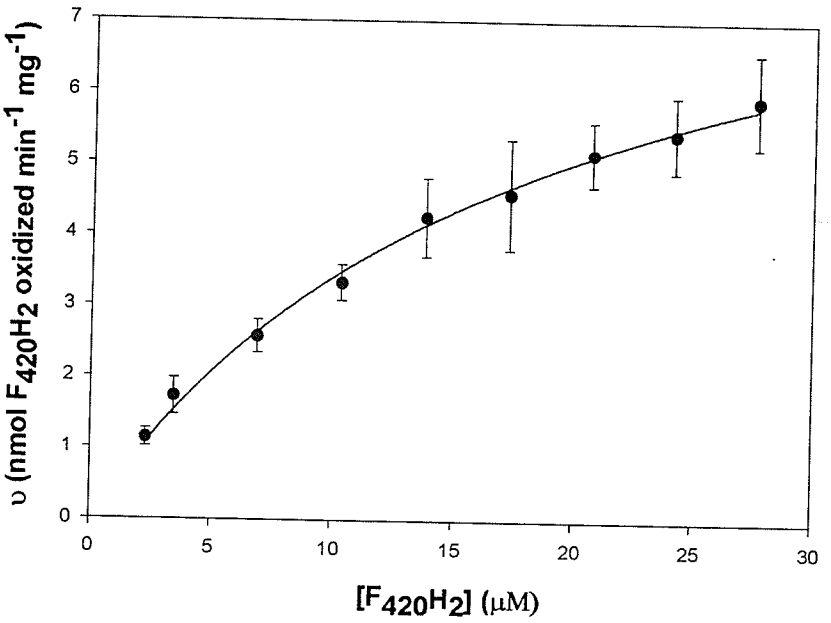

B.

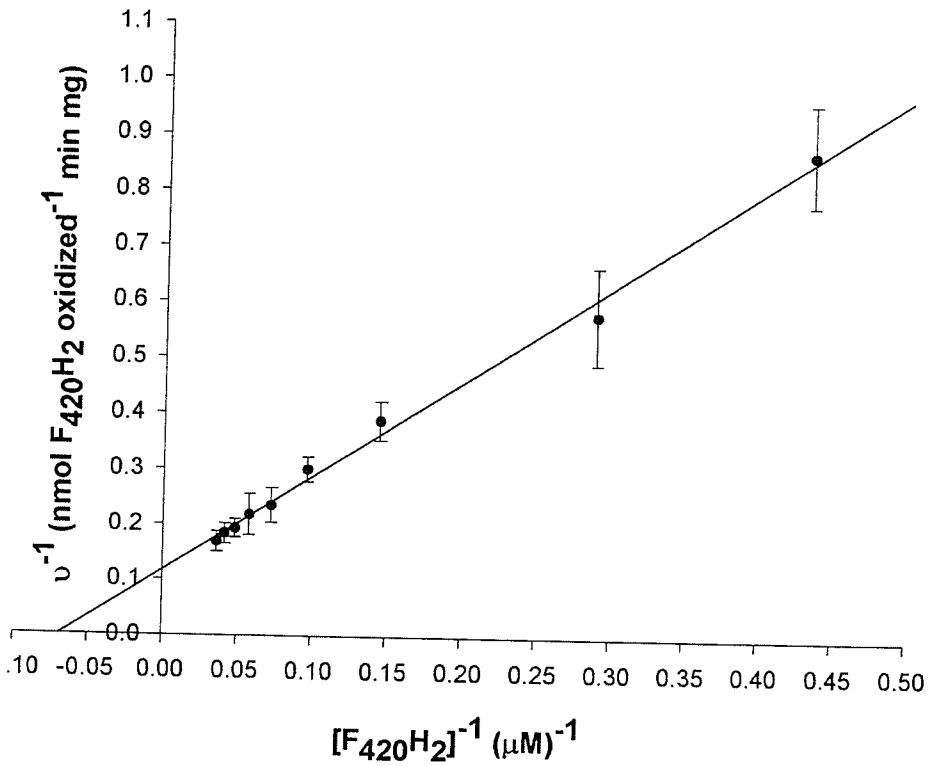

Figure 7.3. Determination of Km_{F420H2} for the phenazine-dependent $F_{420}H_2$ dehydrogenation activity in clarified cell-free extract of *Methanosphaera stadtmanae*. (A) Michaelis Menten kinetics plot. (B) Lineweaver Burk kinetics plot. Activity measured using 500μM phenazine.

Diphenyleneiodonium (DPI) chloride (1 μM) was found to be a competitive inhibitor of the purified $F_{420}H_2$ dehydrogenase activity of *Ms. mazei* Gö1(Brodersen *et al.* 1999). Our studies also show that the phenazine-dependent $F_{420}H_2$ dehydrogenation activity of *Ml. tindarius* (in cell-free extract) is also inhibited in the presence of DPI, as are the respective activities of *Ms. barkeri* Fusaro and *Msp. hungatei* GP1 (Chapters 5 and 6).

The $F_{420}H_2$ dehydrogenation activity of *Msph. stadtmanae* is also inhibited by DPI, but the nature of inhibition is unclear. Addition of 5 μM resulted in an increase in the apparent K_m from 138.0 to 170.0 μM, but the apparent Vmax decreases from 3.0 to 1.2 nmol $F_{420}H_2$ oxidized·min^{-1}·mg^{-1} (Lineweaver Burk kinetics: Addition of 5 μM resulted in an increase in the apparent K_m from 156.0 to 166.5 μM phenazine, apparent Vmax decreases from 3.2 to 1.1 nmol $F_{420}H_2$ oxidized·min^{-1}·mg^{-1}) (Figures 7.4 and 7.5). This would appear to indicate non-competitive inhibition of the phenazine-dependent $F_{420}H_2$ dehydrogenation activity of *Msph. stadtmanae*.

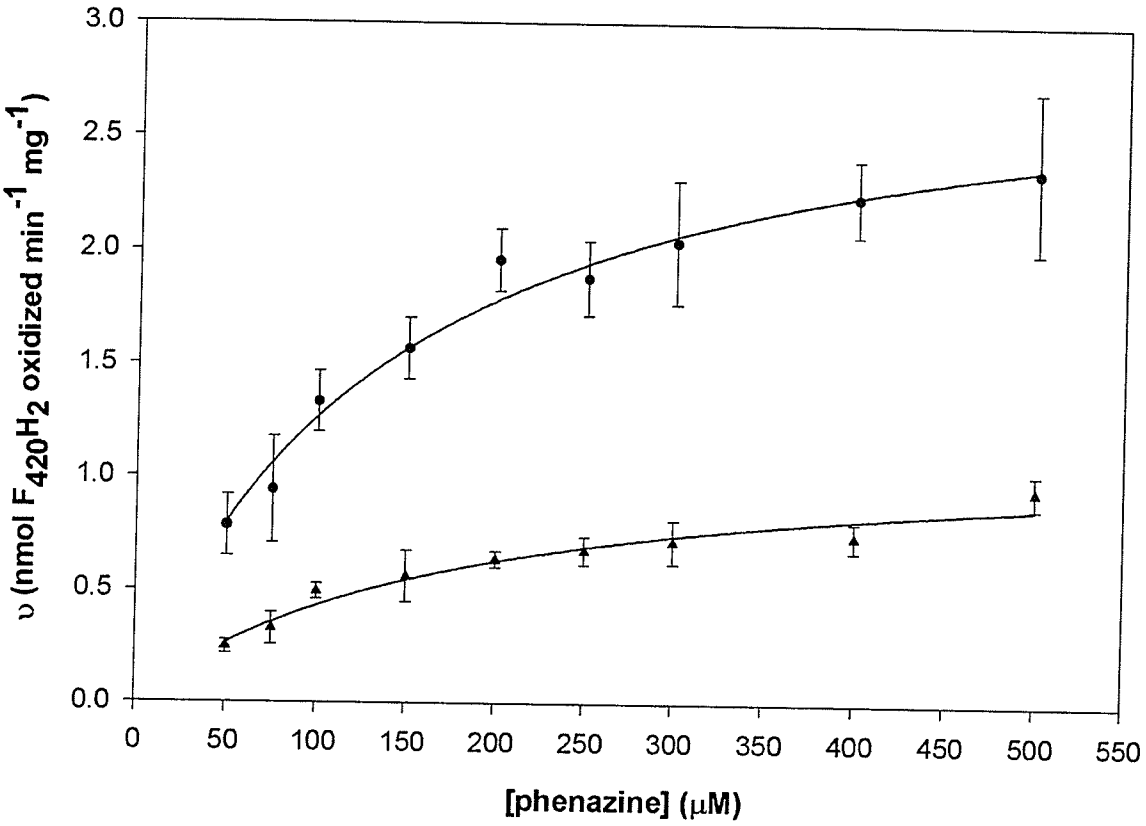

Figure 7.4. Michaelis Menten kinetics plot of the phenazine-dependent $F_{420}H_2$ dehydrogenation activity in clarified cell-free extract of *Methanosphaera stadtmanae*, in the presence/absence of DPI. All points represent experiments performed in triplicate. Assay conditions as described under 'Materials and Methods'. ●, No DPI. ▲, 5 μM DPI.

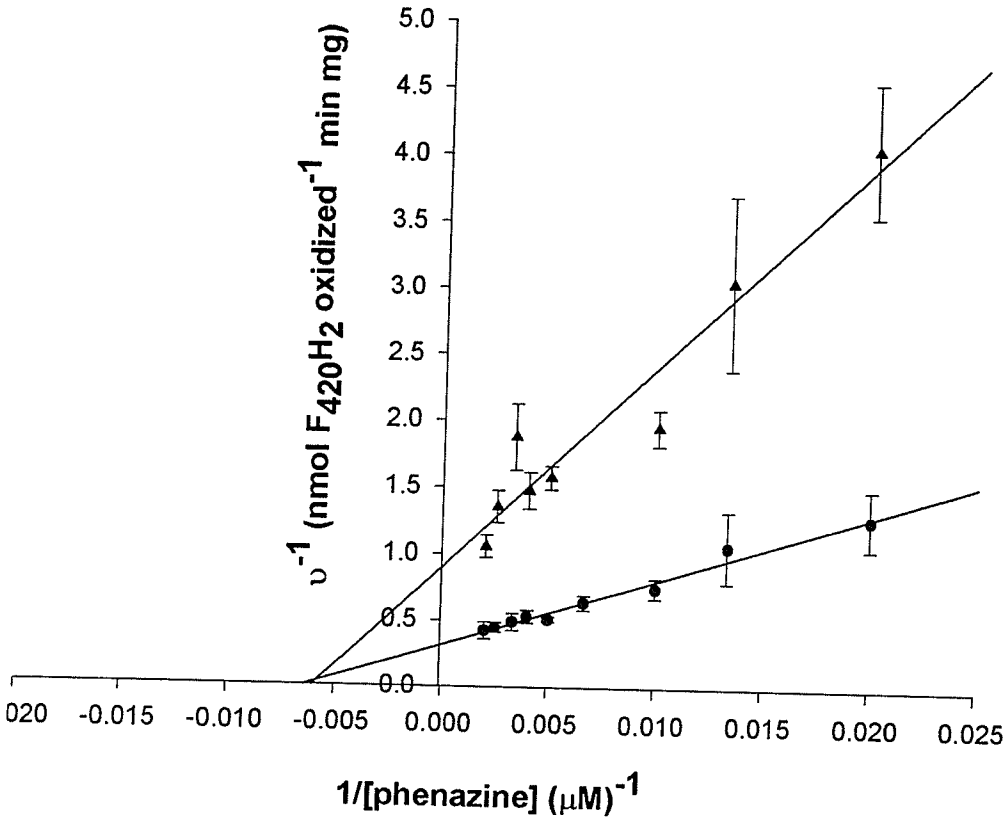

Figure 7.5. Lineweaver Burke kinetics plot of the phenazine-dependent $F_{420}H_2$ dehydrogenation activity in clarified cell-free extract of *Methanosphaera stadtmanae*, in the presence/absence of diphenyleneiodonium (DPI)chloride. All points represent experiments performed in triplicate. Assay conditions as described under 'Materials and Methods'. ●, No DPI. ▲, 5 μM DPI.

7.3.5. Comparison of the phenazine-dependent $F_{420}H_2$ dehydrogenation activity with other methanoarchaea

The phenazine-dependent $F_{420}H_2$ dehydrogenation activity of *Msph. stadtmanae*, in cell-free extract, is significantly lower when compared to the activities from a number of methanoarchaea, ranging from 30- to 140-fold difference in activity (Table 7.3). This is not surprising, since the amount of F_{420} found in *Msph. stadtmanae* is also low (0.16 nmol $F_{420} \cdot mg^{-1}$ protein, (Wong *et al.* 1994)), consistent with a role in biosynthetic pathways or O_2-detoxification.

The phenazine-dependent $F_{420}H_2$ dehydrogenation activity of *Msph. stadtmanae* is over 100-fold lower than the activity of *Ml. tindarius*, a methanoarchaeon containing the Fpo complex (Haase *et al.* 1992), and *Ms. barkeri* Fusaro (grown on CH_3OH).

The activity from *Msph. stadtmanae* is also 65- to 100-fold lower than the phenazine-dependent $F_{420}H_2$ dehydrogenation activities measured from other hydrogenotrophic methanoarchaea from the order *Methanobacteriales*, and from the orders *Methanococcales* and *Methanomicrobiales*.

Table 7.3. Comparison of the $F_{420}H_2$ dehydrogenation ($F_{420}H_2$ deH_2ase) activity in cell-free extract of various methanoarchaea. [phenazine] = 500 μM. [methyl viologen (mv)] = 500 μM (note – 1 mM metronidazole added to assay tubes using methyl viologen as electron acceptor). [F_{420}] = 10-15 μM. Values are the average of triplicate assays. (Reprinted from Chapter 4).

Methanoarchaeon	**Order**	**Growth substrate**	**$F_{420}H_2$ deH_2ase[†] (phenazine)**	**$F_{420}H_2$ deH_2ase[†] (mv)**
Ml. tindarius	*Methanosarcinales*	CH_3OH	0.379	0.2
***Ms. barkeri* Fusaro**	*Methanosarcinales*	CH_3OH	0.421	0.048
		H_2:CO_2	0.225	0.019
		Acetate	0.116	0.047
Mst. concilli	*Methanosarcinales*	Acetate	0.087	0.042
***Msp. hungatei* GP1**	*Methanomicrobiales*	H_2:CO_2	0.129	0.123
Mc. voltae	*Methanococcales*	H_2:CO_2	0.212	0.067
Mtb. marburgensis	*Methanobacteriales*	H_2:CO_2	0.270	0.070
Mb. bryantii	*Methanobacteriales*	H_2:CO_2	0.296	0.091
Msph. stadtmanae	*Methanobacteriales*	H_2: CH_3OH	0.002	0.005

[†] μmol $F_{420}H_2$ oxidized·min^{-1}·mg^{-1}

7.3.6. Development of a protocol for the enrichment of the $F_{420}H_2$ dehydrogenation activity of Methanosphaera stadtmanae

Various column chromatography techniques were tested in order to enrich the phenazine-dependent $F_{420}H_2$ dehydrogenation activity of *Msph. stadtmanae*, some with very mitigated success. All steps were performed under anaerobic conditions, at ambient room temperature. The results of some of these steps are summarized in Appendix E.

Since the activity is best preserved under high salt conditions after $(NH_4)_2SO_4$ precipitation, a strategy had to be developed that could be used under high salt conditions, at least during the initial enrichment step. A protocol utilizing several column chromatography techniques in tandem was devised to purify the $F_{420}H_2$ dehydrogenation activity. All steps were performed under anaerobic conditions at ambient room temperature. Ice gel packs were used to keep the protein cool when possible. Purification of the activity was not successful, but the end results appeared to be promising, suggesting that the potential for purification of this activity exists. The results are summarized in Table 7.4.

7.3.6.1. Ammonium sulfate ($(NH_4)_2SO_4$) precipitation

$F_{420}H_2$ dehydrogenation activity was enriched *via* 75% $(NH_4)_2SO_4$ saturation of the clarified cell-free extract (Figure 7.6). A methyl viologen reducing hydrogenase activity was also enriched along with the $F_{420}H_2$ dehydrogenation activity.

7.3.6.2. Phenyl Sepharose CL-4B

Crystals of anaerobic $(NH_4)_2SO_4$ were added to the resuspended 75% $(NH_4)_2SO_4$ pellet to insure a final saturation of 60%; the concentration of $(NH_4)_2SO_4$ remaining in

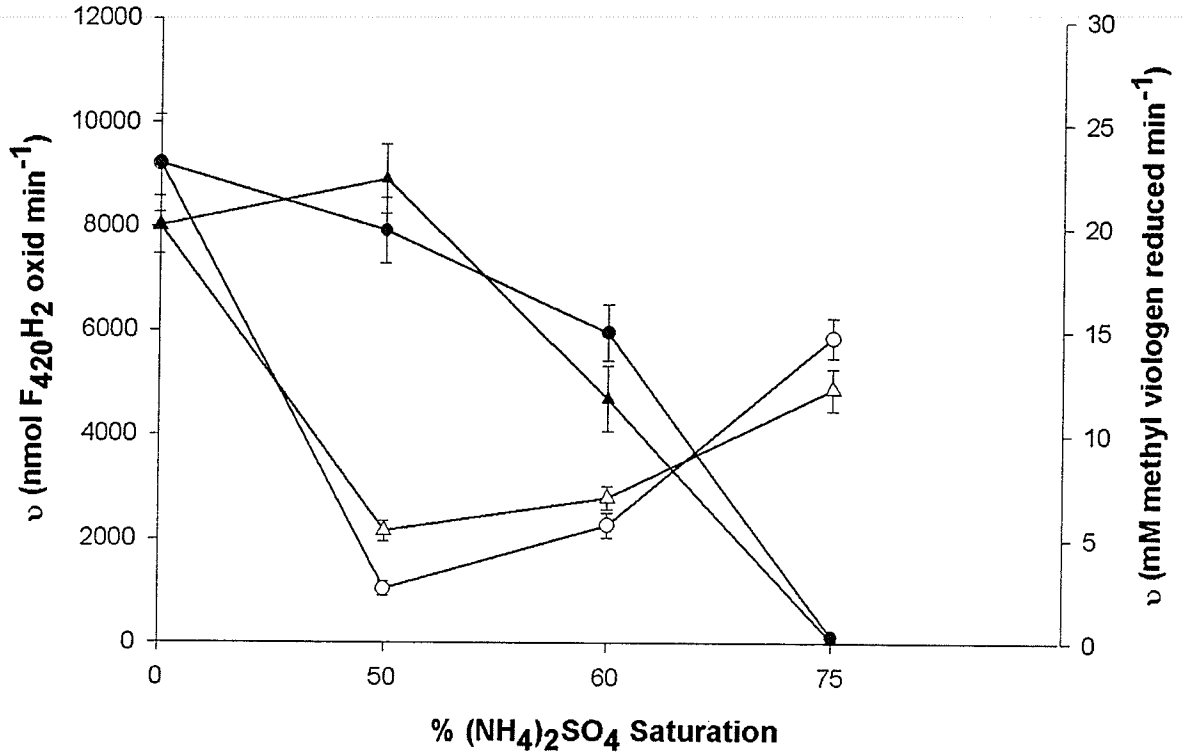

Figure 7.6. Ammonium sulfate precipitation profile of the $F_{420}H_2$ dehydrogenation activity from clarified cell-free extract.
●, $F_{420}H_2$ dehydrogenation activity of $(NH_4)_2SO_4$ supernatant.
○, $F_{420}H_2$ dehydrogenation activity of $(NH_4)_2SO_4$ pellet.
▲, methyl viologen-reducing hydrogenase activity of $(NH_4)_2SO_4$ supernatant. Δ, methyl viologen reducing hydrogenase activity of $(NH_4)_2SO_4$ pellet.

the protein pellet would be approximately 0.01 M. The protein solution was then diluted ½ with 60% $(NH_4)_2SO_4$ saturated 50 mM HEPES, pH 7.0, containing 5% glycerol and 10 mM DTT (buffer A) and applied to a 45 mL Phenyl Sepharose CL-4B column equilibrated with buffer A; the protein and activity profile is shown in Figure 7.7A.

3 mL aliquots were collected in 4 inch glass tubes, using a Bio-Rad fraction collector. Filled tubes were removed from the fraction collector, sealed with rubber stoppers, and cooled on ice prior to removal from the anaerobic chamber for activity assay. Once the protein was fully loaded, the column was washed with two bed volumes of buffer A + 0.05% Triton-X-100, followed by a continuous 60%-0% $(NH_4)_2SO_4$ gradient (3 bed volumes). At the end of the gradient, the column was washed with 2 bed volumes of 50 mM HEPES, pH 7.0, containing 5% glycerol, 0.05% Triton-X-100, and 10 mM DTT.

The fractions containing the $F_{420}H_2$ dehydrogenation activity were pooled and tested for activity. Two peaks of activity were observed; only the activity eluted in the absence of $(NH_4)_2SO_4$ (fractions 95-110) were processed further. When dialysis or gel filtration was employed to desalt the $(NH_4)_2SO_4$–containing fractions the activity was lost upon desalting. Therefore, only the salt free fractions could be saved for further processing.

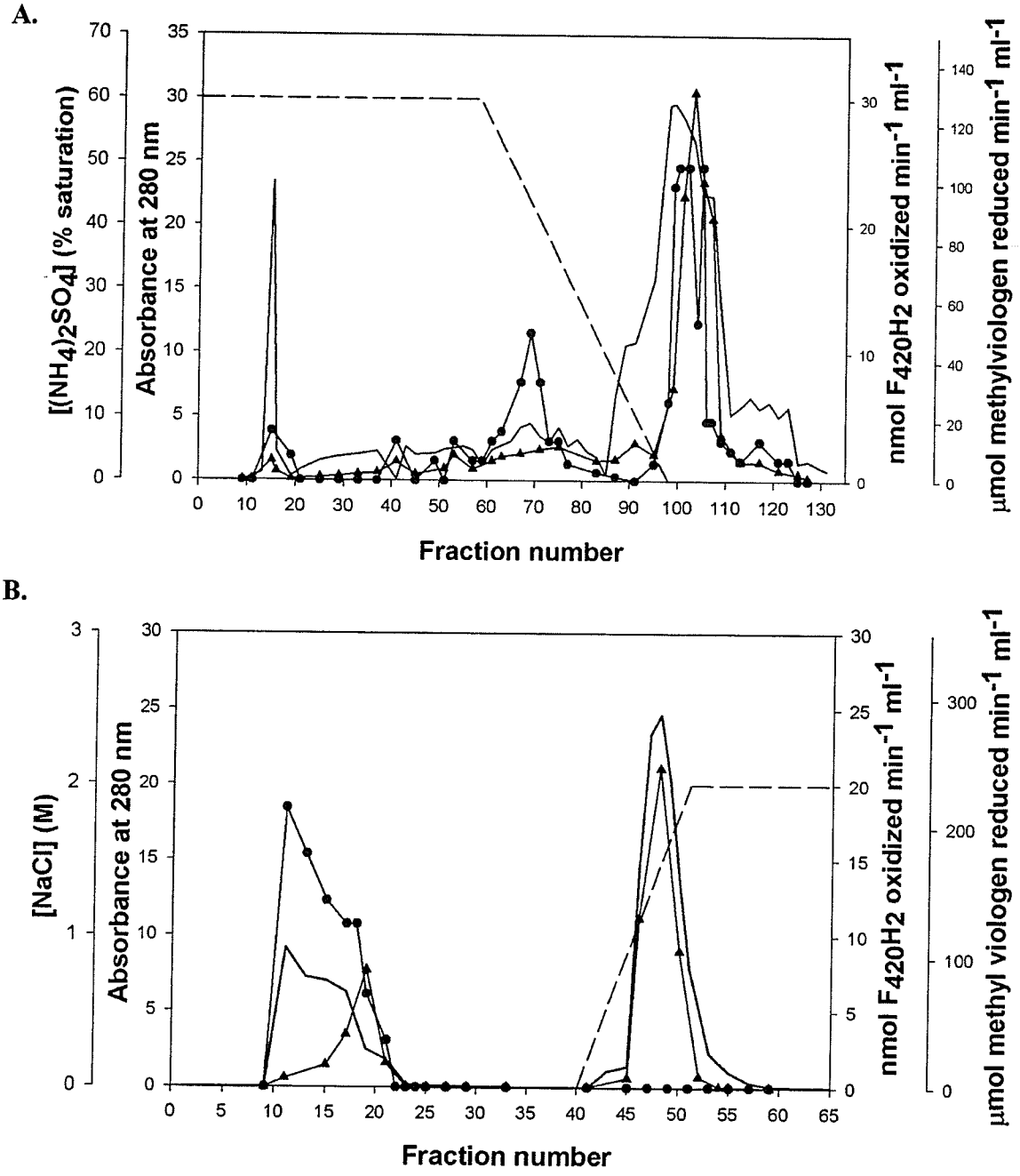

Figure 7.7. A. Protein and activity profile of fractions eluted from a Phenyl Sepharose CL 4B chromatography column. (—), A_{280}. (---) 60-0% $(NH_4)_2SO_4$. ●, $F_{420}H_2$ dehydrogenation activity. ▲, Methyl viologen reducing hydrogenase activity. B. Protein and activity profile of fractions eluted from a DEAE Sephacel chromatography column. (—), A_{280}. (---) 0-2 M NaCl. ●, $F_{420}H_2$ dehydrogenation activity. ▲, Methyl viologen reducing hydrogenase activity. Conditions for elution as described in text. $F_{420}H_2$ dehydrogenation activity assayed using 500 μM phenazine.

7.3.6.3. DEAE Sephacel

The salt-free eluted protein collected from the Phenyl Sepharose CL-4B column was then applied to DEAE Sephacel column equilibrated with 50 mM HEPES, pH 7.0, containing 5% glycerol, 0.05% Triton-X-100, and 10 mM DTT (buffer B). The column was then washed with 2 bed volumes of buffer B before a gradient of 0-2 M NaCl was applied (3 bed volumes). The elution and activity profile of the DEAE Sephacel column is shown in Figure 7.7B. Only one peak of $F_{420}H_2$ dehydrogenation activity was observed; the $F_{420}H_2$ dehydrogenation did not have an affinity for the DEAE Sephacel and passed through the column without binding to the matrix (fractions 15-25).

7.3.6.4. F_{420}-Affinity Column

The F_{420}-affinity chromatography steps were completed in diffuse light (i.e. ambient light only) to prevent the bound F_{420} from photolysing. The protein was loaded onto F_{420}-bound EAH sepharose (8 mL) equilibrated with buffer B (50 mM HEPES, pH 7.0, with 5% glycerol, 0.05% Triton-X-100, and 10 mM DTT). After the protein was loaded onto the column, the column was washed with 2 bed volumes of buffer B, followed by a continuous 0-2 M NaCl gradient (made using buffer B). The protein and activity profile is shown in Figure 7.8. The $F_{420}H_2$ dehydrogenation activity did not appear to have any affinity for the bound F_{420} and eluted from the column with the buffer front. The fractions containing $F_{420}H_2$ dehydrogenation activity (fractions 5-11) were collected, pooled and tested for activity. Surprisingly, a significant H_2-dependent methyl viologen reducing activity devoid of $F_{420}H_2$ dehydrogenation activity was eluted from the

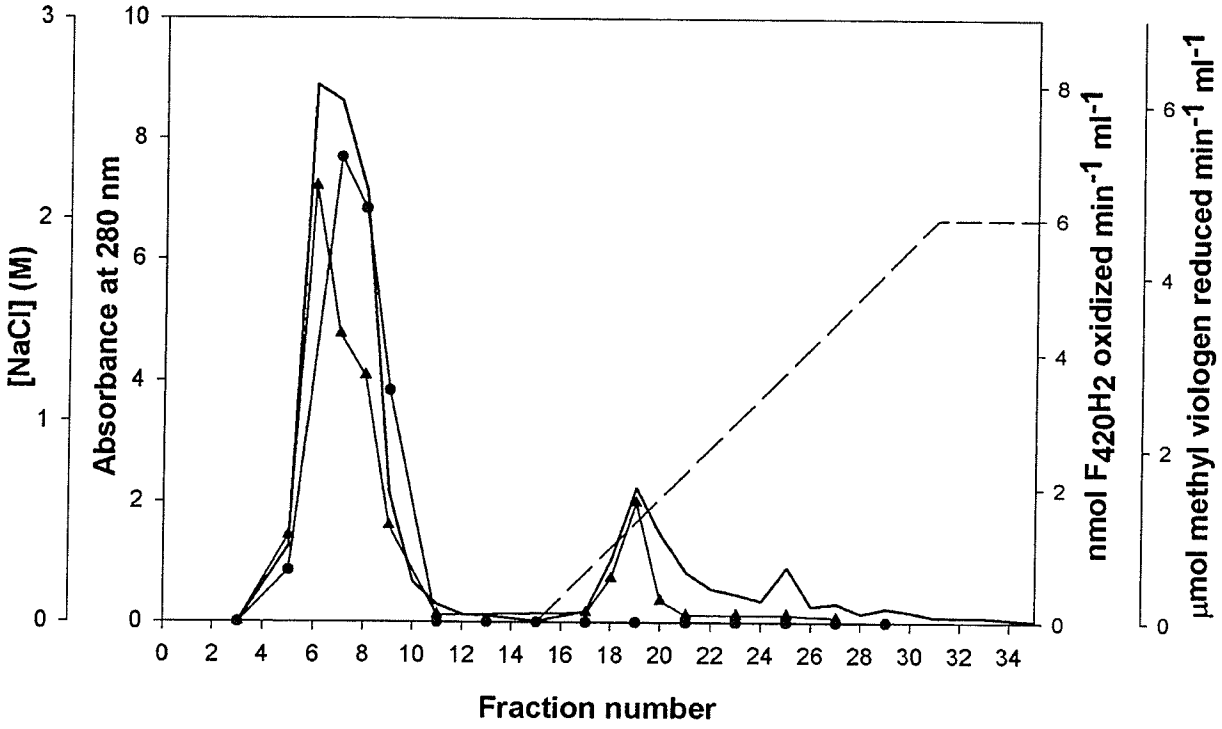

Figure 7.8. Protein and activity profile of fractions collected from an F_{420}-affinity column. (—), A_{280}. (---), linear 0-2 M NaCl.. ●, $F_{420}H_2$ dehydrogenation activity. ▲, Methyl viologen reducing hydrogenase activity. $F_{420}H_2$ dehydrogenation activity assayed with 500 μM phenazine.

column during the 0-2 M NaCl gradient – no further analyses were performed on these fractions.

A summary of the attempted purification of the $F_{420}H_2$ dehydrogenation is shown in Table 7.4. The highest degree of purification occurred at the Phenyl-Sepharose CL-4B stage. Further purification attempts beyond this stage did not yield satisfactory results, as the stability of the $F_{420}H_2$ dehydrogenation activity decreased quickly as the purification process progressed. This is in contrast to the cell-free extract (stored at 4°C), which was stable throughout the length of the enrichment procedure. As the $F_{420}H_2$ dehydrogenation activity is O_2 labile, the chromatography steps were performed in the anaerobic chamber,

Table 7.4. Summary of the enrichment process for the $F_{420}H_2$ dehydrogenation activity of *Methanosphaera stadtmanae*. Process was repeated three times, with representative data presented here. $[F_{420}H_2]$ = 10-15 μM. [phenazine] = 500 μM.

Stage	Protein (mg)	Activity[†]	Yield (%)	Specific activity[‡]	Purification (-fold)
CCFE	929.3	3235.2	100	3.5	-
75% $(NH_4)_2SO_4$ pellet	583.2	4125.6	127.5	7.1	2.0
Phenyl-Sepharose CL-4B	20.4	456.7	14.1	22.1	6.3
DEAE-Sephacel[††]	6.1	86.5	2.7	14.3	4.1
F_{420}-affinity[††]	2.1	14.3	0.4	6.8	1.9

[†] nmol $F_{420}H_2$ oxidized·min^{-1}
[‡] nmol $F_{420}H_2$ oxidized·min^{-1}·mg^{-1}
[††] activity measured from pooled non-binding fractions

at room temperature, but the protein extracts were kept cool using cold gel packs, and fractions were kept on ice prior to removal from the anaerobic chamber; pooled extracts were refrigerated between chromatographic steps, such that temperature should not have been an issue.

A coomassie blue- and silver-stained linear 0-20% native PAGE gel is shown in Figure 9.9. As the protein passes through the various column chromatography steps it is evident that certain protein bands are being enriched, while others are lost, indicating that the $F_{420}H_2$ dehydrogenation activity is being enriched.

7.3.7. Reactivation of the $F_{420}H_2$ Dehydrogenation activity of Methanosphaera stadtmanae

As the phenazine-dependent $F_{420}H_2$ dehydrogenation activity of *Msph. stadtmanae* goes through the various chromatographic steps, the activity yield at each stage drops, ultimately to a point where further chromatographic steps/analyses were not feasible. Furthermore, the $F_{420}H_2$ dehydrogenation activity was inactive after 3-4 days storage at 4°C, under reduced, anaerobic conditions. Several assays were performed to determine if the $F_{420}H_2$ dehydrogenation activity could be restored after apparent loss of this activity. The protein was mixed with one of the following: $(NH_4)_2SO_4$ (60% saturation); 200 mM KPO_4 $F_{420}H_2$ dehydrogenation assay buffer; 20 μM FAD.

The results are summarized in Table 7.5. The addition of solid $(NH_4)_2SO_4$ crystals to protein extract to yield 60% saturation did not restore $F_{420}H_2$ dehydrogenation activity. While $(NH_4)_2SO_4$ is apparently able to maintain/enhance the $F_{420}H_2$ dehydrogenation activity (in cell-free extract), it cannot reactivate the activity after it is lost. The addition of KPO_4 buffer (200 mM KPO_4, with 0.5 M sucrose, 10 mM DTT, pH

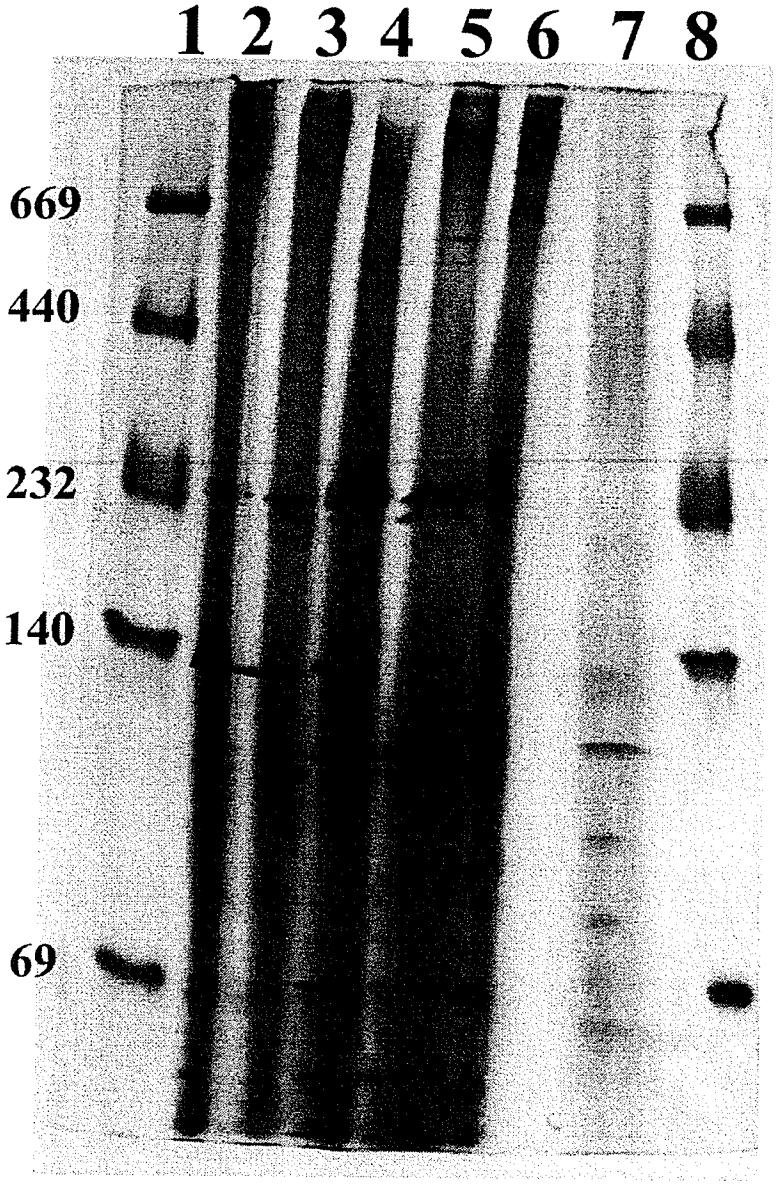

Figure 7.9. Double-stained 3-20% native gradient PAGE detailing the enrichment of the $F_{420}H_2$ dehydrogenation activity from the clarified cell-free extract of *Methanosphaera stadtmanae*. 1, 8. Molecular markers, kDa. 2. Clarified cell-free extract. 3. re-suspended 75% $(NH_4)_2SO_4$ pellet. 4. Phenyl Sepharose CL-4B pool. 5. DEAE Sephacel pool 1. 6. DEAE Sephacel pool 2. 7. F_{420}-affinity column pool.

7.0, final concentration), the standard buffer system used to assay the phenazine-dependent $F_{420}H_2$ dehydrogenation activity of *Msph. stadtmanae*, did not have any noticeable effect on the inactive $F_{420}H_2$ dehydrogenation activity.

Since FAD appears to be essential for the reactivation of the F_{420} H_2ase activity of *Msph. stadtmanae*, the use of this compound is a logical step for reactivation of the $F_{420}H_2$ dehydrogenation activity, which would also require FAD. Incubation of the protein with 20 μM FAD for 3-4 hours at 4°C lead to reactivation of the phenazine-dependent $F_{420}H_2$ dehydrogenation activity. Moreover, in the presence of 20 μM FAD, the phenazine-dependent $F_{420}H_2$ dehydrogenation activity increased almost 3-fold (2.6x) higher as compared to the initial activity of the non reactivated protein.

Table 7.5. Reactivation of the phenazine-dependent $F_{420}H_2$ dehydrogenation activity under different conditions. Protein reactivated approximately 3 days after initial measurement after collection from F_{420}-affinity column.

Incubation condition (all at 4°C)	**Activity (nmol $F_{420}H_2$ oxidized min^{-1} mg^{-1})**
Initial activity (no addition)	6.8 ± 0.8
No addition (3 days later)	No activity detected
+ 20 μM FAD	19.0 ± 0.1
+ 200 mM KPO_4, 0.5 mM sucrose, 10 mM DTT	No activity detected
+ 60% $(NH_4)_2SO_4$	No activity detected

7.3.8. Enrichment of an H_2-dependent F_{420}-reducing activity

Early attempts to detect H_2-dependent F_{420}-reduction in cell-free extracts of *Msph. stadtmanae* indicated that this activity appeared to be absent (< 0.01 μmol F_{420} reduced·min^{-1}·mg^{-1}), although a methyl viologen-dependent $F_{420}H_2$ dehydrogenation activity was present in this methanoarchaeon (Wong *et al.* 1994, Wong, Ph.D thesis 1999). With the discovery of methanophenazine as an intermediate in F_{420} recycling in *Ms. mazei* Gö1 (Abken *et al.* 1998), it was believed that a similar compound might be present in *Msph. stadtmanae*. Indeed, F_{420}-reduction with H_2 was observed when phenazine was included in the reaction buffer: a 2 step mechanism for F_{420} reduction was suggested, involving (1) H_2-dependent reduction of an unknown intermediate, followed by (2) F_{420}-dependent oxidation of this intermediate (Wong, Ph.D thesis 1999). As such, it had been proposed (Wong, Ph.D thesis 1999) that the phenazine-dependent $F_{420}H_2$ dehydrogenation activity observed in the cell-free extract of *Msph. stadtmanae* may be operating in the reverse direction *in vivo*, with F_{420} being reduced using electrons

Table 7.6. H_2-dependent F_{420}-reducing activity using cell-free extract of *Msph. stadtmanae*. Activity assayed using 200 mM KPO_4, 0.5 M sucrose, 10 mM DTT, under H_2 (except where noted). [F_{420}] = 20 μM. Note – results from one assay, in triplicate.

Mediator	**μmol F_{420} reduced·min^{-1}·mg^{-1}**
none	0.003 ± 0.0001
none (under N_2)	0.0004
Phenazine (10 μM)	0.003 ± 0.0001
Ferredoxin (25 μg/ml)	0.002 ± 0.001

extracted from an alternate electron donor, potentially reduced-methanophenazine, *via* the $F_{420}H_2$ dehydrogenation activity (Wong, Ph.D thesis 1999).

H_2-dependent F_{420}-reduction in cell-free extract, using redox mediators such as phenazine and ferredoxin, was also studied simultaneously with the ongoing enrichment experiments of the $F_{420}H_2$ dehydrogenation activity. These assays indicated that H_2-dependent F_{420}-reducing activity was not dependent on the presence of phenazine or ferredoxin (Table 7.6). Subsequent assays demonstrated a requirement for incubation under reducing conditions, with the inclusion of FAD, for optimal activity (Chapter 8).

The F_{420} H_2ases from *Msp. hungatei* GP1 (Chapter 5) and *Ms. barkeri* Fusaro (Chapter 6) were the sole source of a phenazine-dependent $F_{420}H_2$ dehydrogenation activity in the respective methanoarchaeon. In order to elucidate whether the $F_{420}H_2$ dehydrogenation activity of *Msph. stadtmanae* might also be associated with its putative F_{420} H_2ase, F_{420}-reducing activity of was also monitored after each chromatographic step. The F_{420}-reducing activity (Table 7.7) follows a similar pattern of purification comparable to the $F_{420}H_2$ dehydrogenation (Table 7.4), indicating possible association of the phenazine-dependent $F_{420}H_2$ dehydrogenation activity with the F_{420} H_2ase activity.

Table 7.7. Summary of the enrichment process for the F_{420}-reducing hydrogenase activity of *Methanosphaera stadtmanae*. F_{420} H_2ase activated with 10 μM FAD and 10 μM F_{420} prior to assay. [F_{420}] = 25-30 μM.

Stage	Protein (mg)	Activity[†]	Yield (%)	Specific[‡] activity	Purification (-fold)
CCFE	929.2	193.9	100	0.21[‡‡]	-
75% $(NH_4)_2SO_4$ pellet	583.2	235.2	121.3	0.40	1.9
Phenyl-Sepharose	20.4	41.4	21.4	2.03	9.7
DEAE Sephacel[††]	6.1	13.5	7.0	2.21	10.6
F_{420}-affinity[††]	2.1	2.1	1.1	1.00	4.8

[†] μmol F_{420} reduced·min^{-1}
[‡] μmol F_{420} reduced·min^{-1}·mg^{-1}
[††] activity measured from pooled non-binding fractions
[‡‡] in the absence of FAD,
$F_{420}H_2$ase activity of CCFE = 0.005 μmol F_{420} reduced·min^{-1}·mg^{-1}

7.3.9. $F_{420}H_2$ oxidase – source of a phenazine-dependent $F_{420}H_2$ dehydrogenation activity?

The recently published genome of *Msph. stadtmanae* indicates the presence of a putative $F_{420}H_2$ oxidase (FprA), which catalyzes the $F_{420}H_2$-dependent reduction of O_2 (Seedorf *et al.* 2004, Fricke *et al.* 2006). As seen in Table 7.3 (section 7.3.1.), O_2 is able to substitute for phenazine as substrate for the $F_{420}H_2$ dehydrogenation activity. This activity is primarily located in the soluble cytoplasmic fraction (i.e. clarified cell-free extract, CCFE) (>95% of the activity), with only 2-5% of the activity measured using

washed membranes (Table 7.8). This is similar to the $F_{420}H_2$ oxidase isolated from *Methanobrevibacter arboriphilus*, which is a cytoplasmic protein (Seedorf *et al.* 2004). Similarly, 85-90% of the phenazine-dependent $F_{420}H_2$ dehydrogenation activity is detected in the CCFE (10-15% from the washed membranes); this is comparable to the level of F_{420} H_2ase activity detected in *Msph. stadtmanae* (Table 7.8).

Table 7.8. Comparison of the phenazine- and O_2-dependent $F_{420}H_2$ dehydrogenation, and H_2-dependent F_{420}-reducing hydrogenase activities of *Methanosphaera stadtmanae*. Activities measured from cell-free extract, clarified cell-free extract, and washed membranes. F_{420} H_2ase activated with 10 μM FAD and 10 μM F_{420} prior to assay. 18-20 μM F_{420} added to $F_{420}H_2$ deH_2ase or $F_{420}H_2$ oxidase assay tubes.

Fraction	$F_{420}H_2$ deH_2ase† [phenazine] = 500 μM†	$F_{420}H_2$ oxidase [O_2] = 25 μM†	F_{420} H_2ase‡ [F_{420}] = 20-25 μM
Cell-free extract	1.4 ± 0.2	1.1 ± 0.2	93.6 ± 9.5
Clarified cell-free extract	1.2 ± 0.1	1.1 ± 0.1	81.5 ± 3.3
Washed membranes	0.2 ± 0.02	0.02 ± 0.005	9.2 ± 2.2

† nmol $F_{420}H_2$ oxidized·min^{-1}
‡ μmol F_{420} reduced·min^{-1}; O_2 added as aliquot from air-saturated H_20, ~250 μM

The apparent K_m for O_2 was determined to be 11 μM O_2, with Vmax = 5.1 nmol $F_{420}H_2$ oxidized·min^{-1}·mg^{-1} (Figure 7.10). O_2-dependent $F_{420}H_2$ oxidation was observed with the addition of clarified cell-free extract; this activity was not observed in the absence of added protein, indicating that the activity is enzymatic in nature. O_2-dependent $F_{420}H_2$ oxidation activity is aerobically unstable, with only 23 % activity remaining after 24 hours storage under aerobic conditions at 4°C, and 2.3% activity

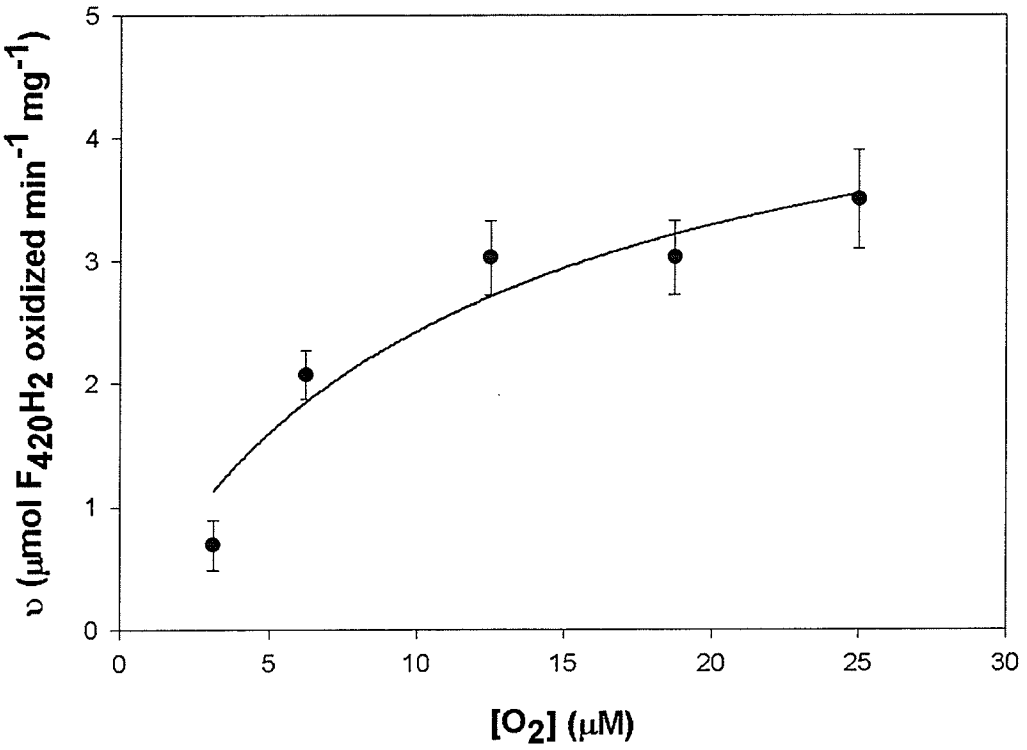

Figure 7.10. Michaelis Menten kinetics plot for the $F_{420}H_2$ oxidase activity in clarified cell-free extract. O_2 added to anaerobic assay tubes as air-saturated MilliQ H_2O. $[F_{420}H_2]$ = 18-20 μM.

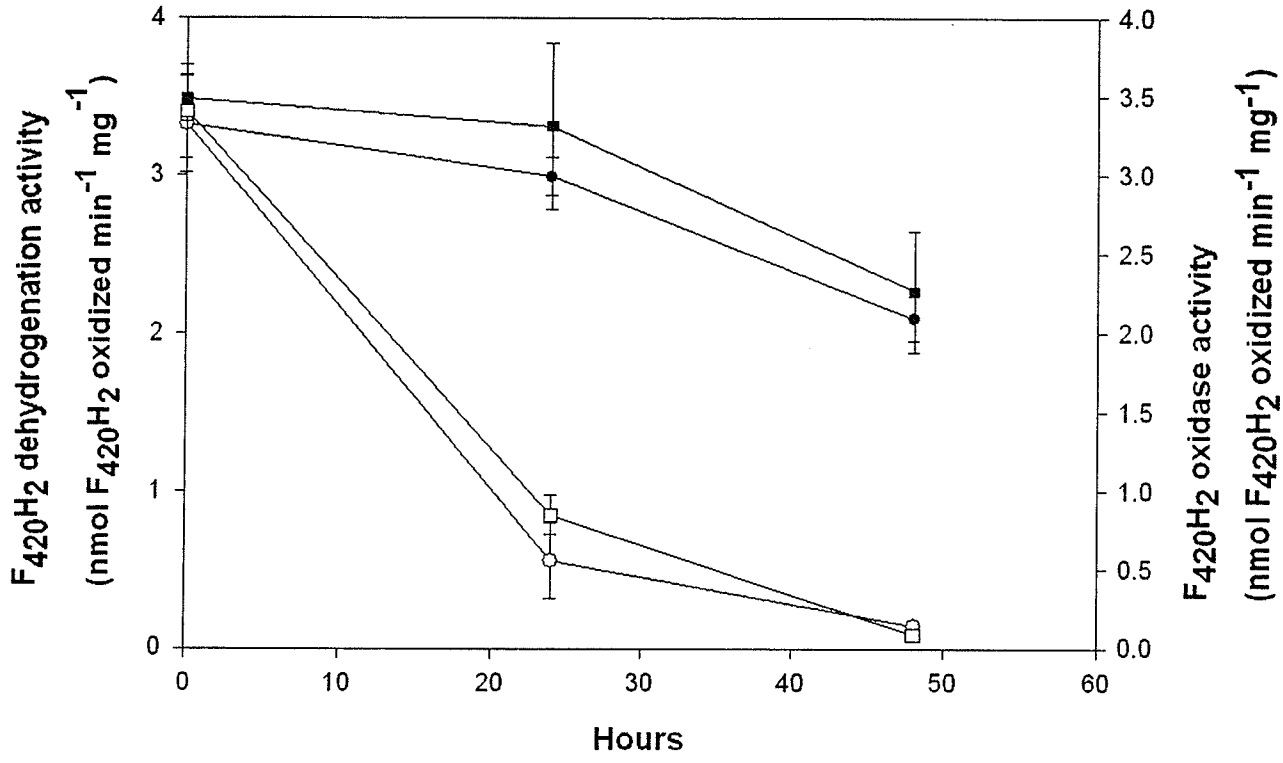

Figure 7.11. Comparison of the stability of the phenazine-dependent $F_{420}H_2$ dehydrogenation activity and the $F_{420}H_2$ oxidase activity in the cell-free extract of *Methanosphaera stadtmanae*. Activities were assayed over a 48 hour period. Aerobically stored extract purged with N_2 prior to assay. $[F_{420}H_2] = 15\ \mu M$. [phenazine] = 500 μM. $[O_2] = 18.75\ \mu M$
●, $F_{420}H_2$ dehydrogenation activity (anaerobic). ○, $F_{420}H_2$ dehydrogenation activity (aerobic). ■, $F_{420}H_2$ oxidase activity (anaerobic). □, $F_{420}H_2$ oxidase activity (aerobic).

detected after 48 hours. The decrease in $F_{420}H_2$ oxidase activity is comparable to the loss of activity observed with the phenazine-dependent $F_{420}H_2$ dehydrogenation activity when stored under aerobic conditions; only 17% of the phenazine-dependent $F_{420}H_2$ dehydrogenation activity was remaining after 24 hours, and 4% of the activity after 48 hours (Figure 7.11).

7.4. Discussion

7.4.1. $F_{420}H_2$ dehydrogenation activity in Methanosphaera stadtmanae

In methylotrophic members of the *Methanosarcinales*, such as *Ms. mazei* Gö1, the $F_{420}H_2$ dehydrogenase (Fpo complex, $\underline{F}_{420}H_2$ $\underline{p}$henazine $\underline{o}$xidoreductase), in tandem with the heterodisulfide reductase (Hdr) is an essential component of the $F_{420}H_2$: heterodisulfide oxidoreductase complex, catalyzing the reduction of CoM-S-S-CoB and generating an energy conserving transmembrane proton gradient (Deppenmeier 2002, 2004). Methanophenazine is believed to be the physiological electron acceptor for the $F_{420}H_2$ dehydrogenation activity; this compound has not been isolated in methanoarchaea.

A similar activity is observed in the cell free extract of *Msph. stadtmanae,* a member of the *Methanobacteriales* that grows solely on H_2 and CH_3OH (Miller and Wolin 1983, 1985). However, the Fpo complex is not encoded in the recently published genome of *Msph. stadtmanae*, nor does it appear to be essential for methanogenesis on H_2 and CH_3OH as *Msph. stadtmanae* possesses an MV H_2ase (Mvh) (Fricke *et al.* 2006). For most hydrogenotrophic methanoarchaea, the MV H_2ase is part of the H_2:CoM-S-S-CoB oxidoreductase complex, catalyzing the H_2-dependent reduction of CoM-S-S-CoB

(Thauer *et al.* 1993, Shima *et al.* 2002). In the absence of the Fpo complex, what is the source of the $F_{420}H_2$ dehydrogenation activity in *Msph. stadtmanae*?

The recently published genome of *Msph. stadtmanae* indicates the presence of several different putative genes encoding for $F_{420}H_2$-dependent enzymes. These include methylene-H_4MPT dehydrogenase and methylene-H_4MPT reductase, the $F_{420}H_2$:NADP oxidoreductase (Fno), and a putative $F_{420}H_2$ oxidase (FprA) (Fricke *et al.* 2006). The genome also indicates the presence of genes encoding for a putative F_{420} H_2ase; our studies have demonstrated that the purified F_{420} H_2ase from various methanoarchaea possess phenazine-dependent $F_{420}H_2$ dehydrogenation activity. A natural question to ask would be whether the observed phenazine-dependent $F_{420}H_2$ dehydrogenation activity in *Msph. stadtmanae* is associated with any of the above mentioned proteins as potential candidates for this activity, or if it is a distinct protein on its own?

Methylene-H_4MPT dehydrogenase catalyzes the reversible reduction of N^5,N^{10}-methenyl-H_4MPT to N^5,N^{10}-methylene-H_4MPT, while methylene-H_4MPT reductase catalyzes the reduction of N^5,N^{10}-methylene-H_4MPT to N^5-methyl-H_4MPT (Shima *et al.* 2002). Both reactions proceed *via* stereospecific hydride transfer, with a ternary complex kinetic mechanism (Ma and Thauer 1990, Thauer *et al.* 1993). As such, these enzymes cannot be the source of the $F_{420}H_2$ dehydrogenation activity, since reduction of methyl viologen and phenazine both occur *via* single electron transfers.

The $F_{420}H_2$:NADP oxidoreductase (Fno) was purified and characterized by Elias *et al.* (2000); this enzyme catalyzes the reversible $F_{420}H_2$-dependent reduction of NADP to NADPH. Several properties appear to rule out this protein as a source of the $F_{420}H_2$ dehydrogenation activity. The Fno is aerobically stable, whereas the $F_{420}H_2$

dehydrogenation activity rapidly diminishes under aerobic conditions. The bulk of the Fno activity precipitates at 95% $(NH_4)_2SO_4$ saturation, while the $F_{420}H_2$ dehydrogenation activity precipitates at 75% $(NH_4)_2SO_4$ (Wong *et al.* 1994, this thesis). Fno reduces $NADP^+$ with $F_{420}H_2$ using a ternary sequential reaction, *via* direct hydride transfer (Warkentin *et al.* 2001); the $F_{420}H_2$ dehydrogenation activity catalyzes the reduction of substrates such as methyl viologen or phenazine *via* single e^- transfers (Wong *et al.* 1994, this thesis).

The putative proteins $F_{420}H_2$ oxidase and F_{420} H_2ase are both potential candidates for sources of phenazine-dependent $F_{420}H_2$ dehydrogenation activity. Both are flavoproteins: $F_{420}H_2$ oxidase contains FMN, while the F_{420} H_2ase contains FAD. $F_{420}H_2$ is a hydride donor, such that 2 electrons are transferred to the protein in a single step (Jacobson and Walsh 1984). Reduction of phenazine occurs in two single electron transfer steps (Abken *et al.* 1998), such that a 2 e^- /1 e^- switch is necessary for the transit of electrons from $F_{420}H_2$ through the protein, and then to phenazine. Finally, both enzymes can use the low potential electron donor coenzyme $F_{420}H_2$ to reduce higher potential substrates such as O_2 or phenazine.

7.4.2. Electron acceptor specificity and kinetics studies of the $F_{420}H_2$ dehydrogenation activity

NADH ($E^{\circ\prime}$= -0.320 V) could not substitute for $F_{420}H_2$ ($E^{\circ\prime}$= -0.360 V) as electron donor for the $F_{420}H_2$ dehydrogenation activity, although both are hydride donors with similar midpoint potentials. Several substrates were able to substitute for phenazine ($E^{\circ\prime}$= -0.265 to -0.165 V) as electron acceptor for the $F_{420}H_2$ dehydrogenation activity, including FAD ($E^{\circ\prime}$ = -0.219 V), methyl viologen ($E^{\circ\prime}$= -0.446 V), and O_2 (added as

breathing grade air-saturated H_2O, E°'= +1.229 V) (Table 7.2). The use of O_2 as electron acceptor is particularly interesting as a putative $F_{420}H_2$ oxidase is encoded by the genome of *Msph. stadtmanae* (Fricke *et al.* 2006). The presence of $F_{420}H_2$-dependent O_2-reduction is not necessarily indicative of the presence of an $F_{420}H_2$ oxidase; the F_{420} H_2ase of *Mtb. thermoautotrophicus* ΔH also catalyzes the $F_{420}H_2$-dependent reduction of O_2 to H_2O_2 (Jacobson *et al.* 1982). Neither NAD^+ nor ferredoxin could replace phenazine as electron acceptor.

The phenazine-dependent $F_{420}H_2$ dehydrogenation activity, in cell-free extract, of *Msph. stadtmanae* appears to follow simple Michaels Menten kinetics, similar to what has been reported for *Ms. mazei* Gö1 (Abken *et al.* 1998), and for other methanoarchaea possessing this activity (Chapter 4). The $K_{mphenazine}$ for the $F_{420}H_2$ dehydrogenation activity of *Msph. stadtmanae* was 138 μM, indicating a higher affinity for phenazine relative to the *Ml. tindarius* (266 μM, cell-free extract) and *Ms. mazei* Gö1 (250 μM, purified enzyme, Brodersen *et al.* 1999) $F_{420}H_2$ dehydrogenase activities. By comparison, the $K_{mphenazine}$ values determined for the purified phenazine-dependent $F_{420}H_2$ dehydrogenation activity (associated with the F_{420} H_2ase) in *Msp. hungatei* GP1 and *Ms. barkeri* Fusaro were determined to be approximately 290 μM and 95 μM, respectively (Chapters 5 and 6).

DPI has been shown to be a competitive inhibitor for the purified $F_{420}H_2$ dehydrogenase of *Ms. mazei* Gö1, with low concentrations of DPI (1 μM) increasing the apparent K_m from 35 to 100 μM 2-OH-phenazine (Brodersen *et al.* 1999). In contrast, DPI does not appear to act as a competitive inhibitor of the $F_{420}H_2$ dehydrogenation activity of *Msph. stadtmanae*. While there is a small increase in the apparent K_m for

phenazine upon addition of 5 μM DPI (138 μM → 170 μM), the apparent Vmax decreases from 3.0 to 1.2 nmol $F_{420}H_2$ oxidized·min^{-1}·mg^{-1}, indicating noncompetitive inhibition. This is likely due to DPI binding to the FAD component of the protein bearing $F_{420}H_2$ dehydrogenation activity; the F_{420} H_2ase activity is also inhibited when 5μM DPI is included in the reaction mixture, which would suggest noncompetitive inhibition (see Chapter 8).

Another explanation for the observed non-competitive inhibition may have to do with the presence of two sources of phenazine-dependent $F_{420}H_2$ dehydrogenation activities in the cell-free extract: the F_{420} H_2ase and $F_{420}H_2$ oxidase. One of the activities may be inhibited more strongly by the addition of DPI, likely the F_{420} H_2ase, leaving the $F_{420}H_2$ oxidase as the major source of $F_{420}H_2$ dehydrogenation activity remaining. Initial studies indicated that addition of DPI greater than 10 μM did not have further effect on the $F_{420}H_2$ dehydrogenation activity, which remained constant (~0.6 nmol $F_{420}H_2$ oxidized·min^{-1}·mg^{-1}) without a significant decrease in activity as the [DPI] increases up to 40 μM (Figure 6A, Chapter 4). This would indicate that one of the phenazine-dependent $F_{420}H_2$ dehydrogenation activities in the cell-free extract is less susceptible to inhibition by DPI.

7.4.3. Attempts at purification of the $F_{420}H_2$ dehydrogenation activity of Methanosphaera stadtmanae

The strategies used to enrich for the $F_{420}H_2$ dehydrogenation activity from *Msp. hungatei* GP1 and *Ms. barkeri* Fusaro could not be applied here, for several reasons. The $F_{420}H_2$ dehydrogenation activity of *Msph. stadtmanae* is aerobically unstable, in contrast

to the respective activity of *Msp. hungatei* GP1 and *Ms. barkeri* Fusaro, and must be handled under anaerobic conditions at all times. The protocols used in *Msp. hungatei* GP1 and *Ms. barkeri* Fusaro either did not enrich for the dehydrogenation activity of *Msph. stadtmanae*, or destroyed it. This resulted in a "trial and error" approach to the purification, using chromatographic matrices with different binding properties.

The majority of the $F_{420}H_2$ dehydrogenation activity of *Msph. stadtmanae* is located in the soluble cytoplasmic fraction (85-90%). To get an initial enrichment of the activity, $(NH_4)_2SO_4$, to 75% saturation, was used to precipitate the activity. Removal of $(NH_4)_2SO_4$ from the resuspended protein pellet, *via* gel filtration or dialysis, resulted in loss of activity up to 60-75% (or greater). However, in the absence of a desalting step, the resuspended protein pellet (~0.01 M $(NH_4)_2SO_4$) did not have affinity for matrices requiring low salt concentrations for binding. At this point it was clearly beneficial to find a chromatographic technique that could take advantage of the high salt content.

Enrichment of the $F_{420}H_2$ dehydrogenation activity was observed with the hydrophobic matrix Phenyl Sepharose CL-4B. The use of Phenyl Sepharose CL-4B makes sense as it makes use of the high salt content of the homogenized 75% $(NH_4)_2SO_4$ pellet, which contains the bulk of the $F_{420}H_2$ dehydrogenation activity. Interestingly, there were two separate peaks of $F_{420}H_2$ dehydrogenation activity, with one peak eluting within the linear 60-0% $(NH_4)_2SO_4$ gradient, and the other displaced when the column was washed with $(NH_4)_2SO_4$-free buffer, which desalted the protein and allowed for the use of chromatographic matrices that require low salt conditions. Once it became available, the genome of *Msph. stadtmanae* indicated that there were potentially two proteins that could be the source of the observed phenazine-dependent $F_{420}H_2$

dehydrogenation activity: the F_{420} H_2ase and the $F_{420}H_2$ oxidase (Fricke *et al.* 2006). Thus, the observations of two peaks of dehydrogenation activity are consistent with the findings in the genome of *Msph. stadtmanae.*

Initial chromatography results using DEAE Sephacel loaded with cell-free extract of *Msph. stadtmanae* also indicated the presence of 2 distinct $F_{420}H_2$ dehydrogenation activity peaks, one with no apparent affinity for the DEAE Sephacel matrix, and another that elutes within the 0-2 M NaCl gradient (Figure 3A, Appendix E). When the pooled fractions collected from the Phenyl Sepharose CL-4B column are loaded onto the DEAE Sephacel column (Figure 7.7B), only one activity peak is observed, the non-binding activity. This particular $F_{420}H_2$ dehydrogenation activity of *Msph. stadtmanae* did not have an affinity for the DEAE matrix material, but other extraneous proteins did bind, thereby reducing the protein content of the $F_{420}H_2$ dehydrogenation activity eluate.

The $F_{420}H_2$ dehydrogenation activity is enriched after elution from the Phenyl Sepharose column, but the specific activity decreases after passing through the DEAE Sephacel column. An F_{420} H_2ase activity is also enriched in the pooled fractions collected from the Phenyl Sepharose CL-4B and DEAE Sephacel chromatography steps (Table 7.7). Taken together, the results indicate an enrichment of the F_{420} H_2ase, accounting for one of the observed phenazine-dependent $F_{420}H_2$ dehydrogenation activities. Further discussion of the F_{420} H_2ase continues in Chapter 8.

The pooled fractions collected from the DEAE Sephacel column were then loaded onto an F_{420}-affinity column (Figure 8), the results of which are rather puzzling. The inability of the $F_{420}H_2$ dehydrogenation activity to bind to the coenzyme F_{420}-affinity column came as an unexpected surprise, since this column was expected to be one of the

more potent steps in the purification; this step had been used in the purification of the $F_{420}H_2$ dehydrogenation activity of *Ml. tindarius* by Haase *et al.* (1992). One possible explanation for the apparent non-affinity of the $F_{420}H_2$ dehydrogenation activity for F_{420} may be that the protein does not have an affinity for oxidized F_{420}, since the primary substrate would be the reduced form, $F_{420}H_2$. Since the oxidized form would in effect be a product of the reaction, the protein would not be expected to have a high affinity for F_{420} relative to $F_{420}H_2$. On the other hand, if the F_{420} H_2ase is the source of the $F_{420}H_2$ dehydrogenation activity, it would be expected to bind to the F_{420}-affinity column, yet the F_{420} H_2ase activity is also collected in the non-binding fractions.

While the $F_{420}H_2$ dehydrogenation activity did not bind to the F_{420}-bound matrix, a portion of the MV H_2ase activity did have apparent affinity for the matrix. Interestingly, passage of the protein through the column led to the reduction of the F_{420} bound on the matrix; the MV H_2ase does not use F_{420} as substrate. The eluted protein did not possess $F_{420}H_2$ dehydrogenation or F_{420} H_2ase activity. It is possible that by the time the protein was collected from the column it emerged in a destabilized form that could not be reactivated in the presence of FAD or F_{420}. During the enrichment process, extended exposure of the protein extract to the reducing conditions in the anaerobic chamber (filled with 10% H_2, balance N_2) may have lead to destabilization of the protein. In contrast, the unprocessed cell-free extract still retains greater than 70% activity after 48 hours (Figures 7.2 and 7.11). It has been suggested that storage of the F_{420} H_2ase under reduced, anaerobic conditions may lead to the reduction of FAD to $FADH_2$, which may be less tightly bound and lost from the holoprotein (Fox *et al.* 1987). Sprott *et al.* (1987) found that the purified F_{420} H_2ase activity of *Msp. hungatei* GP1 decreased sharply

after 2 hours incubation under reducing conditions. Fiebig and Friedrich (1989) reported that when the F_{420} H_2ase of *Ms. barkeri* Fusaro was maintained under reducing conditions, the activity was unstable with 15% loss of activity after 50 minutes, and could not be stablilized.

The results are also similar to the findings of Schink and Probst (1980), who reported that storage of solubilized or purified hydrogenase from *Alcaligenes eutrophus* under O_2-free H_2 or N_2, or prolonged exposure to reducing agents, such as β-mercapto-ethanol or DTT, leads to rapid and complete loss of activity. The F_{420}-dependent formate dehydrogenase of *Mb. formicicum* is a FAD-dependent enzyme which is susceptible to loss of the FAD component when stored with reducing agents such as dithionite; incubation of the protein with excess FAD restores activity (Schauer and Ferry 1985).

The purification process was not successful, but the native gradient PAGE (Figure 7.11) indicates that there is potential for Enrichment of this activity. Purification of the $F_{420}H_2$ dehydrogenation activity was greatly hampered by the instability of the protein(s) through the various stages.

7.4.4. Reactivation of the $F_{420}H_2$ dehydrogenation activity

A significant problem with respect to the enrichment of the $F_{420}H_2$ dehydrogenation activity of *Msph. stadtmanae* was the instability of the activity during the various column chromatography steps. While the unprocessed cell-free extract was stable for at least two weeks, or in $(NH_4)_2SO_4$, the activity was rapidly lost during the process of enrichment through the various column chromatography steps. Several additives were tested to try and stabilize/restore the $F_{420}H_2$ dehydrogenation activity.

Reactivation of the $F_{420}H_2$ dehydrogenation activity *via* the addition of crystals of $(NH_4)_2SO_4$ to 60% saturation appeared to be plausible, since the activity of the $(NH_4)_2SO_4$ precipitated (75% saturation) $F_{420}H_2$ dehydrogenation activity appeared to be enhanced on a consistent basis (from 130-150%) compared to the activity of the cell-free extract from which it was precipitated (Table 7.4); the activity of the resuspended protein pellet was also stable for 2 weeks or more. This is comparable to observations of the activity of the Fno, which was enhanced and stable after $(NH_4)_2SO_4$ precipitation (Wong *et al.* 1994). Addition of $(NH_4)_2SO_4$ to 60 or 75% saturation did not restore activity to the inactive $F_{420}H_2$ dehydrogenation activity to any degree.

High concentrations of KPO_4 (200 mM) have been shown to increase the stability and activity of the methyl viologen-dependent $F_{420}H_2$ dehydrogenation activity of *Msph. stadtmanae* (Wong, Ph.D thesis 1999). However, incubation of the inactive $F_{420}H_2$ dehydrogenation activity in 200 mM KPO_4 (final concentration) also did not restore activity.

The inactive $F_{420}H_2$ dehydrogenation activity of *Msph. stadtmanae* was reactivated when the protein was incubated with 20 μM FAD. The protein might also have been destabilized over time, with loss of FAD, resulting in the loss of $F_{420}H_2$ dehydrogenation activity. Indeed, part of the reactivation process for the F_{420} H_2ase activity of *Msph. stadtmanae* requires the addition of FAD, under reducing conditions, prior to assay; in the absence of added FAD, the observed F_{420} H_2ase activity is 40- to 50-fold lower, compared to protein reactivated with FAD (Chapter 8).

In contrast, addition of FAD did not lead to an increase in the specific activity of the purified $F_{420}H_2$ dehydrogenase of *Ms. mazei* Gö1 (Abken and Deppenmeier 1997).

The purified $F_{420}H_2$ dehydrogenation activities (located on the F_{420} H_2ase) of *Msp. hungatei* GP1 and *Ms. barkeri* Fusaro did not require addition of FAD; incubation of the $F_{420}H_2$ dehydrogenation activity of *Msp. hungatei* GP1 with FAD did not increase the yield or specific activity of the $F_{420}H_2$ dehydrogenation activity.

However, there are several examples of proteins requiring reactivation with FAD. Nelson *et al.* (1984) reported that the loss of activity of the F_{420} H_2ase of *Methanobacterium formicicum* during its purification *via* anaerobic hydrophobic column chromatography was due to loss of FAD; addition of FAD restored the F_{420} H_2ase activity. Addition of FAD is not typically used in the reactivation of the F_{420} H_2ase activity of *Mc. voltae*, but FAD is essential for reactivation after passage of the F_{420} H_2ase through hydrophobic chromatography matrices, and also after inactivation *via* heat treatment (Muth *et al.* 1987). The F_{420} H_2ase of *Msp. hungatei* GP1 was routinely reactivated in the presence of FAD by Choquet and Sprott (1991).

Incubation of protein extract of *Msph. stadtmanae* with FAD, under reducing conditions, may allow for reintegration of FAD into the protein and activation of the F_{420} H_2ase activity. A similar step may be necessary to fully activate the $F_{420}H_2$ dehydrogenation activity of *Msph. stadtmanae*, particularly as the activity progresses through various chromatography steps.

7.4.5. Resolution of the phenazine-dependent $F_{420}H_2$ dehydrogenation activity in Methanosphaera stadtmanae

Negligible F_{420} H_2ase activity had been detected in cell-free extract (< 0.01 μmol F_{420} reduced·min^{-1}·mg^{-1}), such that the means for F_{420}-reduction in *Msph. stadtmanae*

were unclear (van de Wijngaard *et al.* 1991, Wong *et al.* 1994, Wong, Ph.D thesis 1999). It had been suggested that the role of the $F_{420}H_2$ dehydrogenation activity in *Msph. stadtmanae* may be associated with methanophenazine-dependent F_{420} reduction, since F_{420}-reduction was observed in the presence of phenazine, F_{420}, and cell-free extract, under an atmosphere of H_2 (Wong, Ph.D thesis 1999). A mechanism for F_{420}-reduction was proposed for *Msph. stadtmanae*.

In the initial step, MV H_2ase (Mvh), which is typically associated with CoM-S-S-CoB reduction, would catalyze the reduction of methanophenazine (MP) to MPH_2 (Wong, Ph.D thesis 1999). The F_{420}-nonreducing hydrogenase (Vho) of *Ms. mazei* Gö1, which is part of the H_2:CoM-S-S-CoB oxidoreductase complex, catalyzes the reduction of 2-OH-phenazine (Abken *et al.* 1998, Ide *et al.* 1999). The purified F_{420} H_2ase and MV H_2ase of *Mtb. thermoautotrophicus* ΔH are both able to catalyze the H_2-dependent reduction of 2-OH-phenazine (Meuer *et al.* 1999). Finally, MP-H_2 would become the source of electrons for the reduction of F_{420} *via* the phenazine-dependent $F_{420}H_2$ dehydrogenase activity detected in the cell-free extract of *Msph. stadtmanae* (Wong PhD thesis 1999).

Neither the $F_{420}H_2$ dehydrogenase (Fpo complex) or methanophenazine are found in *Msph. stadtmanae* (Fricke *et al.* 2006). The question remains, what is the source of the phenazine-dependent $F_{420}H_2$ dehydrogenation activity in *Msph. stadtmanae*? The results from our studies indicate the presence of two possible sources of phenazine-dependent $F_{420}H_2$ dehydrogenation activities.

One source of $F_{420}H_2$ dehydrogenation activity appears to be consistent with the presence of an F_{420} H_2ase: enzymatic analyses indicate the presence of this activity in

Msph. stadtmanae. The recently published genome also indicates the presence of genes (*frhADGB*) encoding for a putative F_{420} H_2ase in *Msph. stadtmanae* (Fricke *et al.* 2006). This activity has been detected in the cell-free extract and co-elutes with an $F_{420}H_2$ dehydrogenation activity throughout the chromatographic steps (Table 7.6). The F_{420} H_2ase of *Mc. voltae* also possesses an $F_{420}H_2$ dehydrogenation activity linked to CoM-S-S-CoB reduction (Brodersen *et al.* 1999). Our studies have shown that the respective F_{420} H_2ases from *Msp. hungatei* GP1 (Chapter 5) and *Ms. barkeri* Fusaro (Chapter 6) both possess phenazine-dependent $F_{420}H_2$ dehydrogenation activity. However, analyses of the F_{420} H_2ase and $F_{420}H_2$ dehydrogenation activities of *Msph. stadtmanae* show some striking differences.

When incubated under anaerobic and optimal conditions, the F_{420} H_2ase activity of *Msph. stadtmanae* (in cell-free extract) is approximately 60-fold greater than the phenazine-dependent $F_{420}H_2$ dehydrogenation activity (Chapter 8); with respect to *Msp. hungatei* GP1 and *Ms. barkeri* Fusaro, under identical conditions there is less than a four-fold difference in the anaerobic F_{420} H_2ase:$F_{420}H_2$ dehydrogenation activity ratios (F_{420} H_2ase/ $F_{420}H_2$ DeH_2ase = 3.5 for *Msp. hungatei* GP1, *Ms. barkeri* Fusaro). The F_{420} H_2ase:$F_{420}H_2$ dehydrogenation activity ratio for *Methanobacterium bryantii*, a member of the *Methanobacteriales*, is 3.93 (See Chapter 4 and 8).

In contrast to the homologous activities in *Msp. hungatei* GP1 and *Ms. barkeri* Fusaro, the phenazine-dependent $F_{420}H_2$ dehydrogenation activity of *Msph. stadtmanae* is aerobically unstable. However, although the F_{420} H_2ase activity was enriched under anaerobic conditions, the activity was stable when stored under aerobic conditions (Chapter 8); on this basis, it would seem that the phenazine-dependent $F_{420}H_2$

dehydrogenation activity is not associated with the F_{420} H_2ase activity in *Msph. stadtmanae*, although the activities appeared to co-migrate. Whether this is an anomaly specific for the F_{420} H_2ase of *Msph. stadtmanae* has yet to be resolved. Further study of the F_{420} H_2ase activity of *Msph. stadtmanae* is required to elucidate the nature of $F_{420}H_2$ dehydrogenation activity associated with this putative protein.

Genomic data of *Msph. stadtmanae* indicates the presence of a gene encoding a putative $F_{420}H_2$ oxidase (Fricke *et al.* 2006). An $F_{420}H_2$ oxidase (FprA, 45 kDa), which contains FMN, was purified from the cell-free extract of *Methanobrevibacter arboriphilus*, a methano-archaeon found in the intestinal tract of termites (Seedorf *et al.* 2004). $F_{420}H_2$ oxidase catalyzes the $F_{420}H_2$-dependent reduction of O_2 to form 2 H_2O and 2 F_{420} (Seedorf *et al.* 2004). The presence of an $F_{420}H_2$ oxidase in *Msph. stadtmanae* would not be surprising, as the large intestine contains enough oxygen (PO_2 = ~15 mm Hg) to inhibit the growth of strictly anaerobic microorganisms, and this methanoarchaeon does not possess a superoxide dismutase or a catalase (Levitt 1970, Fricke *et al.* 2006).

The $F_{420}H_2$ oxidase is a possible source of the observed phenazine-dependent $F_{420}H_2$ dehydrogenation activity. Like the $F_{420}H_2$ dehydrogenation activity, the $F_{420}H_2$ oxidase activity is also aerobically unstable, with activity declining at a similar rate as the $F_{420}H_2$ dehydrogenation activity when stored under aerobic conditions (Figure 7.11). The phenazine-dependent $F_{420}H_2$ dehydrogenation activity was restored/enhanced when the protein was incubated with FAD, under reducing conditions. As the $F_{420}H_2$ oxidase contains FMN instead of FAD, one way to determine whether the $F_{420}H_2$ oxidase is a source of the observed phenazine-dependent $F_{420}H_2$ dehydrogenation activity would be to see if the activity is enhanced when the protein is incubated with FMN.

It should be noted that the F_{420} H_2ase of *Mtb. thermoautotrophicus* ΔH is also capable of catalyzing the $F_{420}H_2$ dependent reduction of O_2 (Jacobson *et al.* 1982, Livingston *et al.* 1987), so we cannot conclude that the $F_{420}H_2$ oxidase is being expressed without further enrichment of this activity in *Msph. stadtmanae*.

Reverse transcription polymerase chain reaction (RT PCR) may be one method to elucidate whether the F_{420} H_2ase or $F_{420}H_2$ oxidase are being expressed. RT PCR can also be used to quantify transcription and determine the levels at which *frh* and *fprA* are expressed. Once it has become clear that the genes encoding for the respective proteins are being expressed, strategies can be developed for purification of the specific protein.

8. F_{420}-reducing hydrogenase activity in *Methanosphaera stadtmanae*

8.1. Introduction

According to recently published genomic information, *Methanosphaera* (*Msph.*) *stadtmanae* possesses the genes encoding several distinct putative hydrogenases; an F_{420}-nonreducing hydrogenase (MV H_2ase, *mvhADG*); an Ech-type hydrogenase (*ehb*); and an F_{420}-reducing hydrogenase (F_{420} H_2ase, *frhADGB*) (Fricke *et al.* 2006).

The MV H_2ase from *Msph. stadtmanae* has been characterized (Wong, PhD thesis 1999); as with most hydrogenotrophic methanoarchaea, the expected function of the MV H_2ase, in conjuction with Hdr, is to catalyze the H_2-dependent reduction of CoM-S-S-CoB to the free cofactors CoM-SH and CoB-SH (Fricke *et al.* 2006). The *mvh* operon of *Mtb. thermoautotrophicus* also encodes the electron carrier polyferredoxin (*mvhB*) (Reeve *et al.* 1989); this is apparently not the case for *Msph. stadtmanae*, where *mvhB* is not found in the genome (Fricke *et al.* 2006). The significance of this gene is unclear, as polyferredoxin is not a substrate for the Mvh hydrogenase of *Mtb. thermoautotrophicus*, nor does it seem to be essential for its activity.

The genome of *Msph. stadtmanae* reveals the presence of a single Ech hydrogenase (Ehb), which is expected to catalyze the reduction of Fd for the reductive carboxylation of acetyl-CoA to pyruvate (Hedderich 2004, Fricke *et al.* 2006):

$$H_2 + Fd \rightarrow Fd\text{-}H_2$$

$$\text{Acetyl-CoA} + CO_2 + Fd\text{-}H_2 \rightarrow \text{pyruvate} + CoA + Fd$$

The appearance of an F_{420} H_2ase has not been detected in *Msph. stadtmanae*, and the hypothesis was that this activity did not exist in this methanoarchaeon (Deppenmeier *et al.* 1989, van de Wijngaard *et al.* 1991, Wong *et al.* 1994). Recent observations

indicate the presence of an F_{420}-reducing H_2ase activity in the cell-free extract of *Msph. stadtmanae*; this activity was enriched during studies of the phenazine-dependent $F_{420}H_2$ dehydrogenation activity (Chapter 7). The recently sequenced genome of *Msph. stadtmanae* also indicates the presence of genes encoding sequences consistent with the F_{420} H_2ase (*frhADBG*); however it was unclear to Fricke *et al.* (2006) whether the genes were silent, or if the activity itself was just very low, since this activity was not reported from 3 different laboratories (Deppenmeier *et al.* 1989, van de Wijngaard *et al.* 1991, Wong *et al.* 1994).

While there is no apparent need for this activity during methanogenesis when grown on H_2 and methanol (CH_3OH), *Msph. stadtmanae* can produce limited quantities of CH_4 in the presence of H_2 and L-serine (Lin and Sparling 1995, 1998), and 2-propanol and CH_3OH (Wong *et al.* 1994). During methanogenesis from H_2 and L-serine, the hydroxymethyl group from serine is transferred to H_4MPT, catalyzed by H_4MPT-dependent serine hydroxymethyl transferase. N^5N^{10}-methylene-H_4MPT is then reduced to CH_3-H_4MPT, a step requiring $F_{420}H_2$. 2-propanol can be used as the source of electrons for methanogenesis with methanol. 2-propanol is oxidized to acetone *via* 2-propanol ADH, with the electrons transferred to $NADP^+$. Electrons from NADPH are then transferred to F_{420} *via* $F_{420}H_2$:$NADP^+$ oxidoreductase (Fno); $F_{420}H_2$ is then used to reduce CoM-S-S-CoB (Wong *et al.* 1994).

$F_{420}H_2$ is also required for cellular biosynthesis, specifically the reduction of $NADP^+$ to NADPH (Wong *et al.* 1994). Fno catalyzes the $F_{420}H_2$-dependent reduction of $NADP^+$ (Elias *et al.* 2000):

$$F_{420}H_2 + NADP^+ \rightarrow F_{420} + NADPH + H^+$$

The low cellular concentration of F_{420} (0.16 nmol F_{420}·mg^{-1} protein) supports the biosynthetic role of $F_{420}H_2$ in *Msph. stadtmanae* (Wong *et al.* 1994).

Previous studies of the F_{420}-reducing activity of *Msph. stadtmanae* indicated extremely low F_{420}-reducing activity (<0.01 μmol F_{420} reduced·min^{-1}·mg^{-1} protein) in this methanoarchaeon (Wong *et al.* 1994). Slow H_2-dependent reduction of F_{420} using cell-free extract had been observed, but appeared to be dependent on the presence of phenazine in a high phosphate (200 mM KPO_4, pH 7.0) buffer. It was suggested that phenazine may act as an intermediate between H_2 and F_{420}; the observed F_{420}-reducing activity under these conditions was reportedly very low (Wong, PhD thesis 1999).

Subsequent studies indicated that the F_{420} H_2ase activity was not dependent on the presence of mediators such as phenazine or Fd (Table 7.5, Chapter 7). In this chapter we present an initial description and characterization of an F_{420} H_2ase activity in the cell-free extract of *Msph. stadtmanae*.

8.2. Materials and methods

For a comprehensive look at the materials and methods used for this chapter, the reader is referred to the following sections in Chapter 3:

3.2. Growth media
3.3. Cell lysis
3.6. Enzyme assays
    3.6.1. $F_{420}H_2$ dehydrogenation assays
    3.6.2. Hydrogenase assays
        3.6.2.1. F_{420}-reducing hydrogenase activity
        3.6.2.2. Methyl viologen reducing hydrogenase activity

Several buffer systems were tested to determine optimal conditions for assay of the F_{420}-reducing activity: 50 mM Tris/Cl, pH 8.0, containing 20 mM $MgCl_2 \cdot 6H_20$ and 20 mM DTT; 200 mM potassium phosphate, pH 7.0, with 0.5 M sucrose and 20 mM DTT; and 100 mM HEPES, pH 7.0, with 200 mM KCl, 20 mM $MgCl_2$ $6H_20$ and 20 mM DTT. All manipulations of the cell-free extract were conducted under anaerobic conditions, with the extract being stored at 4°C under an atmosphere of N_2.

3.7. Gel electrophoresis

3.7.2. Native gradient PAGE gel electrophoresis

3.8. Genome sequence analysis

Clustal W software (Chenna et al. 2003) was used to generate a phylogenetic tree of the amino acid sequences coding for the α-subunit (FrhA) from various methanoarchaea.

8.3. Results

8.3.1. Reactivation of the F_{420}-reducing hydrogenase activity

Preliminary analyses of the F_{420} H_2ase activity were initiated with an examination of several buffers to determine optimal conditions for assay of the F_{420}-reducing activity; the results are shown in Table 8.1. The highest levels of F_{420}-reducing activity were observed when using 100 mM HEPES or 200 mM KPO_4 buffer; the former was used by Choquet and Sprott (1991) to assay the F_{420} H_2ase activity of *Msp. hungatei* GP1, and the latter is typically used to assay the $F_{420}H_2$ dehydrogenation activity of *Msph. stadtmanae*, with N_2 in place of H_2 (Chapter 7). When measurement of the F_{420} H_2ase activity was preceded by incubation of the protein extract under reducing conditions (in either 100 mM HEPES or 200 mM KPO_4 assay buffer), with 10 μM F_{420} and 10 μM FAD at room

Table 8.1. Assay of the F_{420}-reducing hydrogenase activity of *Msph. stadtmanae* in different buffers, with or without incubation with 10 μM FAD and 10 μM F_{420}.

Assay buffer	Activity (μmol F_{420} reduced min^{-1} mg^{-1})
100 mM HEPES, pH 7.0	0.26 ± 0.02
100 mM HEPES, pH 7.0†	0.005 ± 0.0005
200 mM KPO_4, pH 7.0	0.21 ± 0.01
200 mM KPO_4, pH 7.0†	0.005 ± 0.001
50 mM Tris/Cl, pH 8.0†	< 0.0004

† no reactivation with FAD or F_{420}

temperature, a 40- to 50-fold increase in activity was observed relative to those tubes without prior reactivation with FAD.

50 mM Tris/Cl buffer, pH 8.0, had initially been used to survey the membrane-bound F_{420} H_2ase activity of a variety of methanoarchaea, including *Msph. stadtmanae*; F_{420}-reduction in cell-free extract of all tested methanoarchaea was observed, with the exceptions of *Methanolobus tindarius* and *Msph. stadtmanae* using this buffer (Deppenmeier *et al.* 1989); our results using 50 mM Tris/Cl, pH 8.0 are consistent with previous results.. It should be noted, however, that the optimal pH for measurement of F_{420}-reduction is typically lower, from pH 7.0 – 7.5 (Fox *et al.* 1987, Muth *et al.* 1987, Fiebig and Friedrich 1989, Choquet and Sprott 1991). In contrast, significant levels of the F_{420}- reducing H_2ase activities of *Msp. hungatei* GP1 and *Ms. barkeri* Fusaro (in cell-free extract or purified enzyme, non-reactivated) could be observed using 50 mM Tris/Cl, pH 8.0, buffer with little loss of activity.

From this point forward, the F_{420} H_2ase activity of *Msph. stadtmanae* was assayed in 100 mM HEPES, pH 7.0, with 200 mM KCl, 20 mM $MgCl_2 \cdot 6H_20$ and 20 mM DTT, with protein preincubated in the reaction buffer-filled assay tubes with 10 μM FAD and 10 μM F_{420} at room temperature prior to assay; measurement of activity began with the addition of F_{420} (final concentration 25-30 μM).

8.3.2. Detection of the F_{420}-reducing hydrogenase activity via native PAGE electrophoresis

Studies of the F_{420} H_2ase activity of *Msph. stadtmanae* were also conducted *via* native gel electrophoresis simultaneously with the enzyme activity assays in the different buffers. Activity staining was performed using methyl viologen, a synthetic electron acceptor also used as substrate by F_{420} H_2ases.

On initial analysis, the results following electrophoresis of cell-free extract on activity-stained native PAGE gels appeared to be consistent with previous reports of low or no expression of the F_{420} H_2ase in *Msph. stadtmanae*. High molecular weight (MW) bands (600–1300 kDa) possessing hydrogenase activity, attributed to the presence of the F_{420} H_2ase, are not found in the expected positions on activity-stained 3- 20% native gradient PAGE gels (Figure 8.1). However, a single band with an approximate molecular weight of 232 kDa can be observed (Figure 1); this band has a higher apparent MW than the MV H_2ase (> 100 kDa), yet a lower MW than the high MW F_{420} H_2ase band (< 600 kDa). For comparison, the MW of the MV H_2ase described by Wong (Ph.D thesis, 1999) was 49 kDa.

The F_{420} H_2ase was not expected to comprise a major portion of the overall protein in *Msph. stadtmanae*, since this activity was likely associated with anabolic

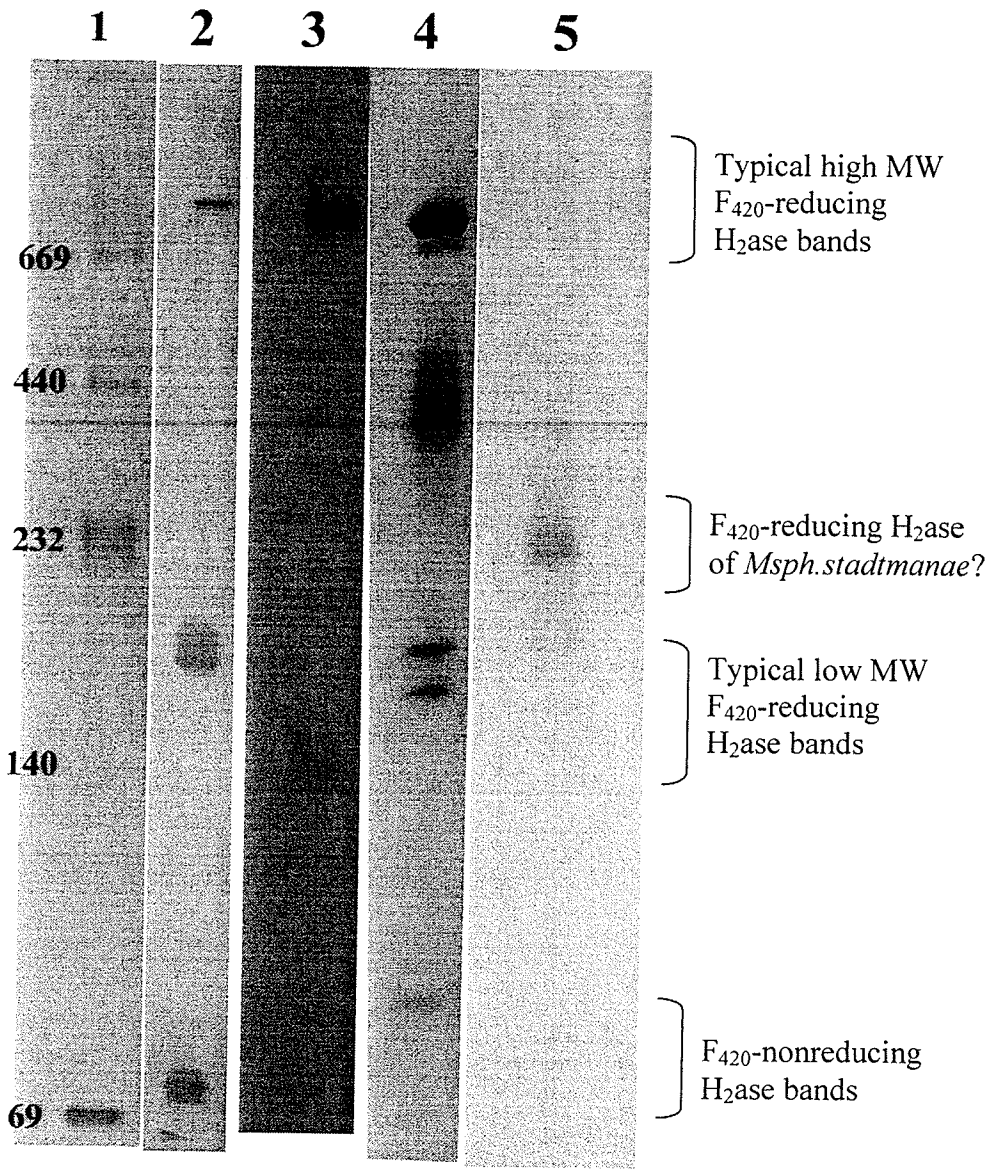

Figure 8.1. A comparison of the hydrogenase activities from the cell-free extract (CFE) of several methanoarchaea on activity-stained 3-20% native gradient PAGE gels. 140 μg of CFE protein added per lane. Gel incubated in 50 mM Tris/Cl, pH 8.0, with 20 mM $MgCl_2 \cdot 6H_20$, 2 mM methyl viologen. 1. Molecular markers, kDa. 2. *Methanosarcina barkeri* Fusaro (grown on CH_3OH). 3. *Methanospirillum hungatei* GP1. 4. *Methanococcus voltae*. 5. *Methanosphaera stadtmanae*.

functions rather than methanogenesis. As such, the protein loaded (~140 μg) may not have contained detectable amounts of the F_{420} H_2ase. To determine the minimal amount of protein necessary to produce detectable hydrogenase activity in the gel, a series of dilutions were made of the clarified cell-free extract (membranes removed) (final protein content loaded: 1100, 552, 276, and 138 μg) and loaded onto a 3-20% native gradient PAGE (Figures 8.2 and 8.3).

Based on the banding patterns, two observations were made of these gels. First, the typical high molecular weight F_{420} H_2ase activity bands were not visualized on the activity-stained gel, regardless of the amount of protein loaded onto the gel (Figure 8.2). The coomassie blue-stained gel indicates the presence of a high molecular weight protein band that typically displays hydrogenase activity (from methanoarchaea that possess the F_{420} H_2ase) (Figure 8.3). One can speculate that this band may represent the F_{420} H_2ase of *Msph. stadtmanae*, as this band lies at a position typically occupied by the F_{420} H_2ase of methanoarchaea such as *Mtb. thermoautotrophicus*, *Ms. barkeri* Fusaro, *Msp. hungatei*, *Mc. voltae*, etc, when electrophoresed on native PAGE gels. However, there is no evidence to suggest that this is the F_{420} H_2ase, since this band does not stain for hydrogenase activity. Potential loss of FAD is not expected to be a factor here, as methyl viologen reduction is not dependent on the presence of FAD (Muth *et al.* 1987, Fox *et al.* 1987, Thauer *et al.* 1993)

The second observation was the appearance of an activity stained band with a molecular weight of approximately 232 kDa (Figure 8.2). This band was faint when the standard amount of protein (140 μg) was electrophoresed. The molecular weight of the band would seem to disqualify it as the MV H_2ase (Mvh), which has a molecular weight

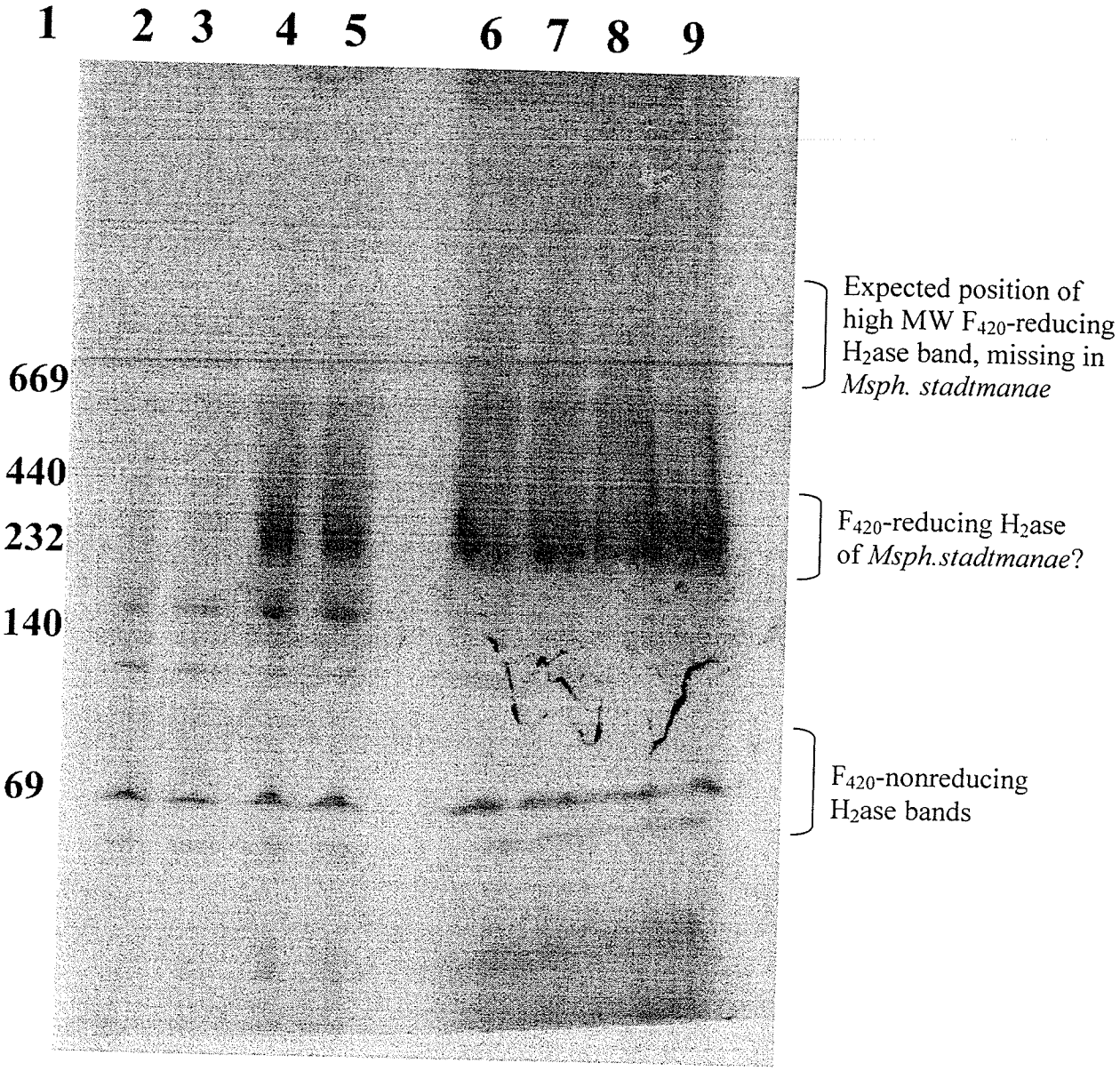

Figure 8.2. A comparison of the hydrogenase activities from the clarified cell-free extract of *Methanosphaera stadtmanae*, with varying amounts of protein, as observed on activity-stained 3-20% native gradient PAGE gels. 1. Molecular markers, kDa. 2,3. 138 μg. 4,5, 276 μg . 6,7. 552 μg. 8,9. 1100 μg.

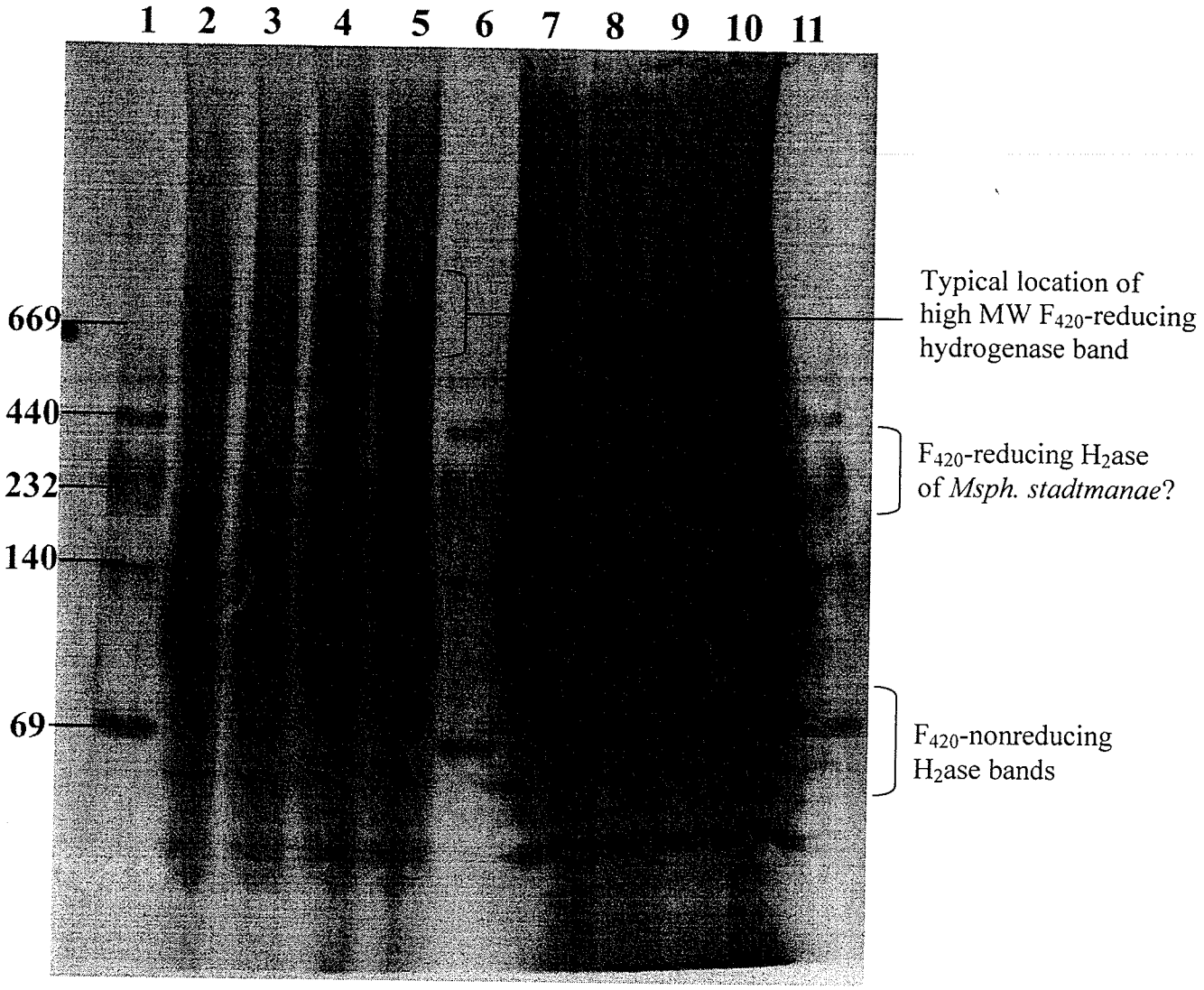

Figure 8.3. Activity (red)- and coomassie blue-stained 3-20% native gradient PAGE comparison of the hydrogenase activities from the clarified cell-free extract of *Methanosphaera stadtmanae*, with varying amounts of protein. 1,6,11. Molecular markers, kDa. 2,3. 138 µg. 4,5. 276 µg . 7,8. 552 µg. 9,10. 1100 µg.

of approximately 49 kDa when electrophoresed on a native gradient PAGE (Wong, PhD thesis 1999). However, the apparent molecular weight of the band is also much lower than the typical high molecular weight band typically observed for the F_{420} H_2ase (600–1300 kDa) (Michel *et al.* 1995).

8.3.3. Catalytic and kinetic properties of the F_{420}-reducing hydrogenase activity in the cell-free extract of Methanosphaera stadtmanae

The F_{420} H_2ase activity of *Msph. stadtmanae*, in clarified cell-free extract, appears to be highest at pH 6.8 (Figure 8.4). NAD^+ and $NADP^+$, both hydride donors/acceptors, were also tested for use as electron acceptors but could not substitute for coenzyme F_{420}. H_2-dependent phenazine reduction was observed using cell-free extract of *Msph. stadtmanae*; phenazine is reduced at a rate of 0.16 μmol phenazine·min^{-1}·mg^{-1}. Phenazine is also reduced by cell-free extract under an atmosphere of N_2, presumably using reducing equivalents remaining in the cell-free extract; this value was taken into account when calculating the H_2-dependent activity. The significance of this activity is unclear, as methanophenazine is apparently not present in *Msph. stadtmanae*.

A kinetic profile of the F_{420}-reducing activity in cell-free extract is shown in Figure 8.5. The activity follows simple Michaelis Menten kinetics, with an apparent Km for F_{420} = 53 μM, and Vmax = 0.8 μmol F_{420} reduced·min^{-1}·mg^{-1} (Lineweaver Burk: apparent Km= 89 μM $F_{420}H_2$, Vmax = 1.2 μmol F_{420} reduced·min^{-1}·mg^{-1}).

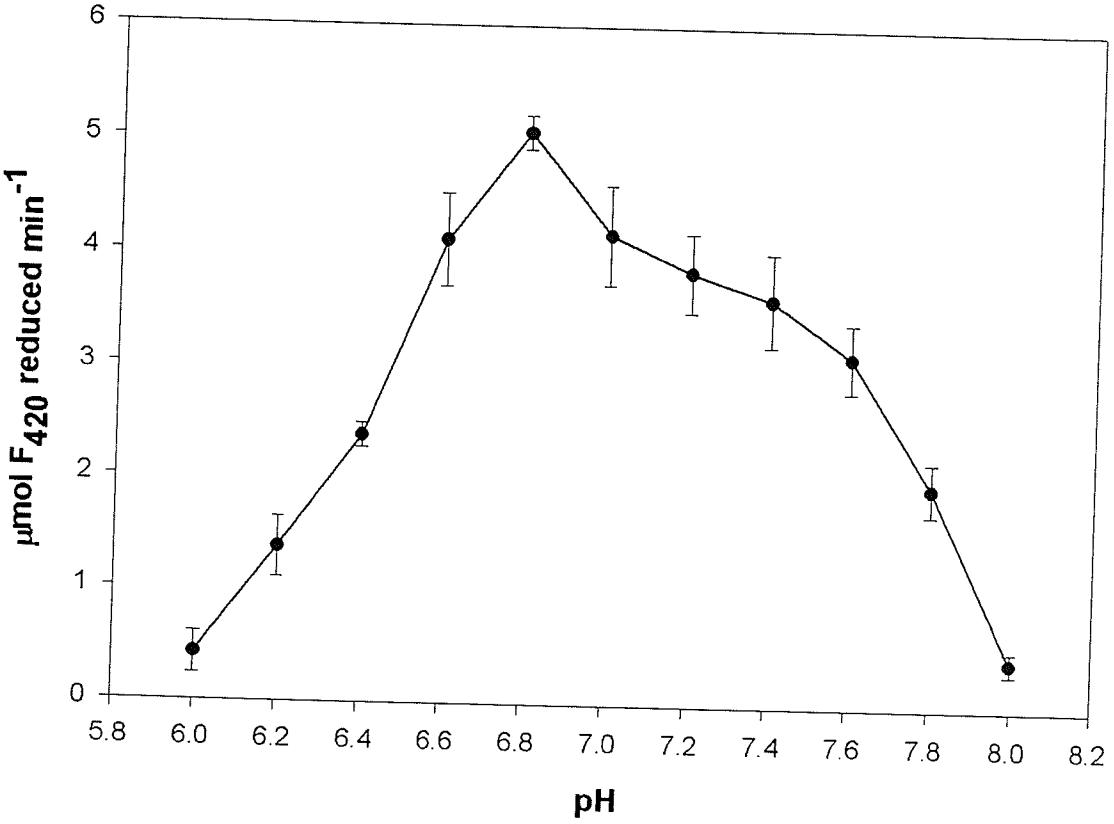

Figure 8.4. pH profile of the F_{420}-reducing hydrogenase activity in clarified cell-free extract. CCFE reactivated with FAD and F_{420} prior to assay. pH of assay buffer established by varying concentration of K_2HPO_4 and KH_2PO_4. Final $[KPO_4]$ = 200 mM. $[F_{420}]$ = 20-25 µM.

A.

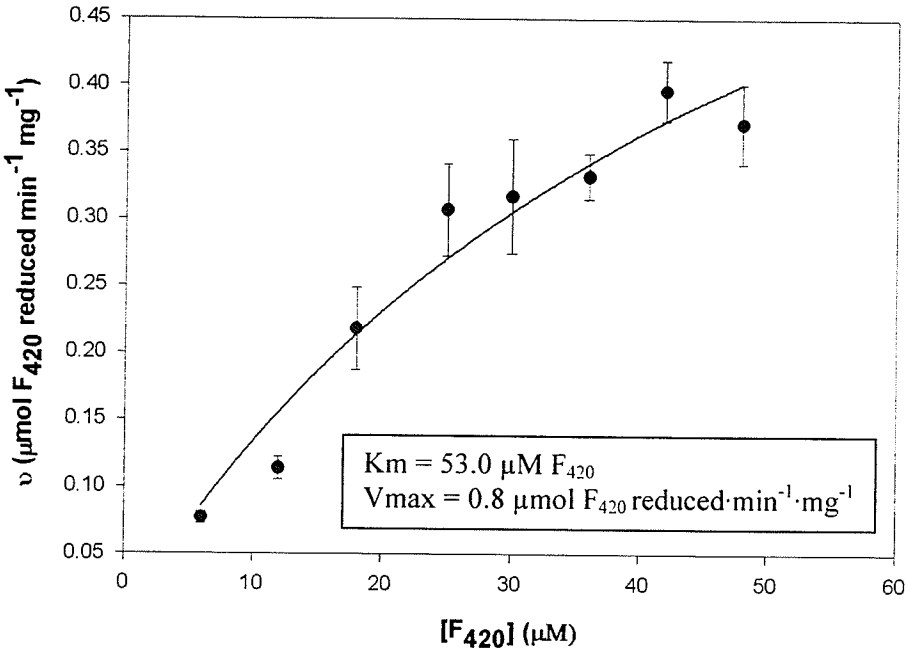

B.

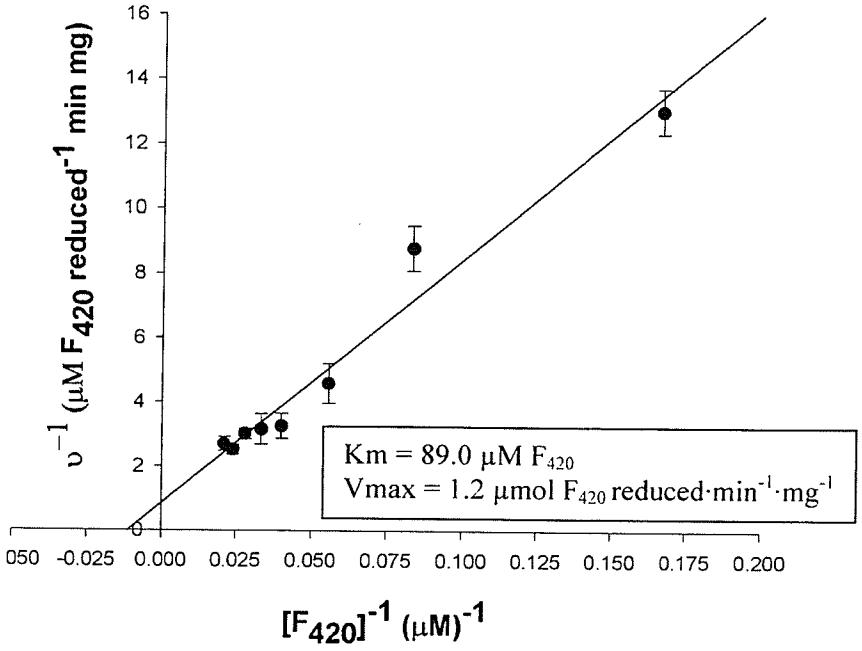

Figure 8.5. Kinetics plots of the F_{420}-reducing hydrogenase activity in the cell-free extract of *Methanosphaera stadtmanae*. (A) Michaelis Menten kinetics plot (B) Lineweaver Burk kinetics plot. $[F_{420}]$ = 20-25 μM

8.3.4. Inhibitor analyses of the F_{420}-reducing hydrogenase activity

Prior to publication of the genome of *Msph. stadtmanae*, it was not clear whether the F_{420}-reducing activity in the cell-free extract was due to the presence of a distinct F_{420} H_2ase, or if the observed activity was the coupled reaction of two or more proteins, as suggested by Wong 1999 (PhD thesis). A study had been conducted examining the effect of various compounds on the MV H_2ase activity by Denny Wong (PhD thesis, 1999). Various metals (Ni^{2+}, Hg^{2+}, etc), toxic anions (CN^-, N_3^-), and chemicals such as the metal chelator EDTA, were tested for their ability to inhibit the MV H_2ase activity.

To help determine whether the F_{420}-reduction was indeed the activity of a distinct F_{420} H_2ase, a similar study was performed to determine the extent, if any, of inhibition by these chemicals on the F_{420} H_2ase activity in cell-free extract. The potentially inhibitory substances were added to the assay tubes after reactivation of the F_{420} H_2ase activity.

The results are shown in Table 8.2. Heavy metal ions inhibit the F_{420} H_2ase activity, the most inhibitory being Cu^{2+} (17.9% activity remaining). CN^- and N_3^- stimulated the F_{420} H_2ase activity, as did EDTA and the methanogenic inhibitor 2-bromoethanesulfonic acid (2-BES), a structural analog of CoM-SH. Diphenyleneiodonium (DPI) chloride also inhibits F_{420} reduction; in contrast, the methylviologen-reducing hydrogenase activity of the cell-free extract was not inhibited in the presence of DPI.

Table 8.2. Inhibition of the F_{420}-reducing hydrogenase activity of the clarified cell-free extract of *Methanosphaera stadtmanae*. Hydrogenase activity was reactivated with 10 μM FAD and 10 μM F_{420} prior to addition of inhibitor. [F_{420}] = 25-30 μM.

Inhibitor (mM)	Activity (μmol F_{420} reduced min^{-1} mg^{-1})	% activity
-	0.28 ± 0.03	100.0
CN^- (1)	0.31 ± 0.04	109.4
N_3^- (3)	0.35 ± 0.09	124.5
2-BES (4)	0.31 ± 0.01	111.3
EDTA (10)	0.36 ± 0.01	128.3
Cd^{2+} (1)	0.07 ± 0.02	24.5
Cu^{2+} (1)	0.05 ± 0.01	17.9
Zn^{2+} (1)	0.07 ± 0.01	26.4
DPI (0.005)	0.18 ± 0.04	66.0
DPI (0.010)	0.06 ± 0.02	22.6

8.3.5. Comparison of the F_{420}-reducing hydrogenase activity of **Methanosphaera stadtmanae** *in cell-free extract with the homologous activity from various methanoarchaea.*

For comparison purposes, the F_{420} H_2ase activities (in cell-free extract) from several methanoarchaea were measured. F_{420} H_2ase activity from each methanoarchaeon was assayed under conditions modified from Choquet and Sprott (1991): protein extract was reactivated and assayed in 'standard buffer' of 100 mM HEPES, pH 7.0, with 10 μM FAD, 10 μM F_{420}, 20 mM $MgCl_2 \cdot 6H_2O$ and 200 mM KCl, at room temperature (~25°C). The results of this brief survey are shown in Table 8.3. *Methanolobus tindarius* was also

included as a negative control, as this methanoarchaeon apparently does not possess an F_{420} H_2ase (Deppenmeier *et al.* 1989).

Table 8.3. Comparison of the F_{420}-reducing hydrogenase activities in the clarified cell-free extract of various methanoarchaea. All assays performed at room temperature as described in text except where noted, following activation as described, with modification, by Choquet and Sprott (1991). Values determined using Michaelis Menten kinetics.

Methanoarchaeon	Order	Growth substrate	Km (μM F_{420})	Vmax[†]
Ml. tindarius	*Methanosarcinales*	CH_3OH	-	-
***Ms. barkeri* Fusaro**	*Methanosarcinales*	CH_3OH	26.3 ± 3.0	2.1 ± 0.1
***Msp. hungatei* GP1**	*Methanomicrobiales*	H_2:CO_2	73.5 ± 18.5	1.8 ± 0.3
Mc. voltae	*Methanococcales*	H_2:CO_2	50.0 ± 9.3	1.3 ± 0.1
Mtb. marburgensis[‡]	*Methanobacteriales*	H_2:CO_2	$2.4x10^6$	$2.5x10^4$
Mtb. marburgensis[‡‡]	*Methanobacteriales*	H_2:CO_2	36.5 ± 9.1	1.6 ± 0.1
Mb. bryantii	*Methanobacteriales*	H_2:CO_2	59.4 ± 23.5	5.6 ± 1.4
Msph. stadtmanae	*Methanobacteriales*	H_2:CH_3OH	53.2 ± 22.6	0.8 ± 0.2

[†] μmol F_{420} reduced·min^{-1}·mg $protein^{-1}$
[‡]activity of *Mtb. marburgensis* could not be fully activated using the modified method of Choquet and Sprott when incubated at room temperature
[‡‡] activity of *Mtb. marburgensis* reactivated using the modified method of Choquet and Sprott at 45°C for 30 minutes prior to assay

The apparent Km for F_{420} of the F_{420} H_2ase activity of *Msph. stadtmanae* is similar to the values (with the exception of *Mtb. marburgensis*) obtained for the homologous activity from the other methanoarchaea in the survey (at room temperature). Excluding *Mtb. marburgensis*, the maximum F_{420} H_2ase activity in the cell-free extract of *Msph. stadtmanae* is less than 2- to 7-fold lower than the corresponding activity from the cell-free extract of a number of methanoarchaea (Figures 8.6-8.10). Comparisons of F_{420} H_2ase activity could not be accurately made with the F_{420} H_2ase activity of *Mtb. marburgensis* when using the reactivation procedure of Choquet and Sprott (1991); this is likely due to the different requirements for reactivation of the F_{420} H_2ase activity of *Mtb. marburgensis.*

According to Jacobson *et al.* (1981), the F_{420} H_2ase activity of *Mtb. thermoautotrophicus* ΔH is reactivated *via* incubation of protein extract or purified enzyme at 45°C for 1 hour, in 1M salt (K^+ or Na^+); under these conditions, the apparent Km was reported as 19 μM F_{420}. Using our standard reaction buffer, at room temperature, the apparent Km was determined to be 2.4×10^6 μM; when the cell-free extract was incubated in standard reaction buffer at 45°C for ½ hour, the apparent Km_{F420} was 36.5 μM, considerably closer to the Km value reported by Jacobson *et al.* (1981).

A.

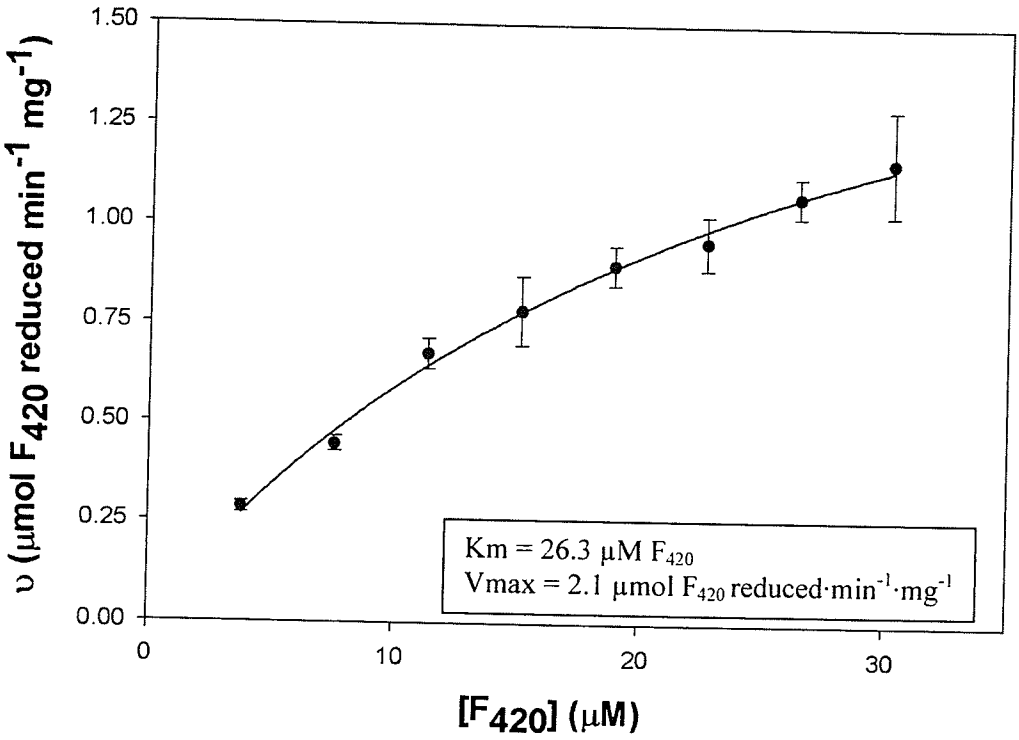

B.

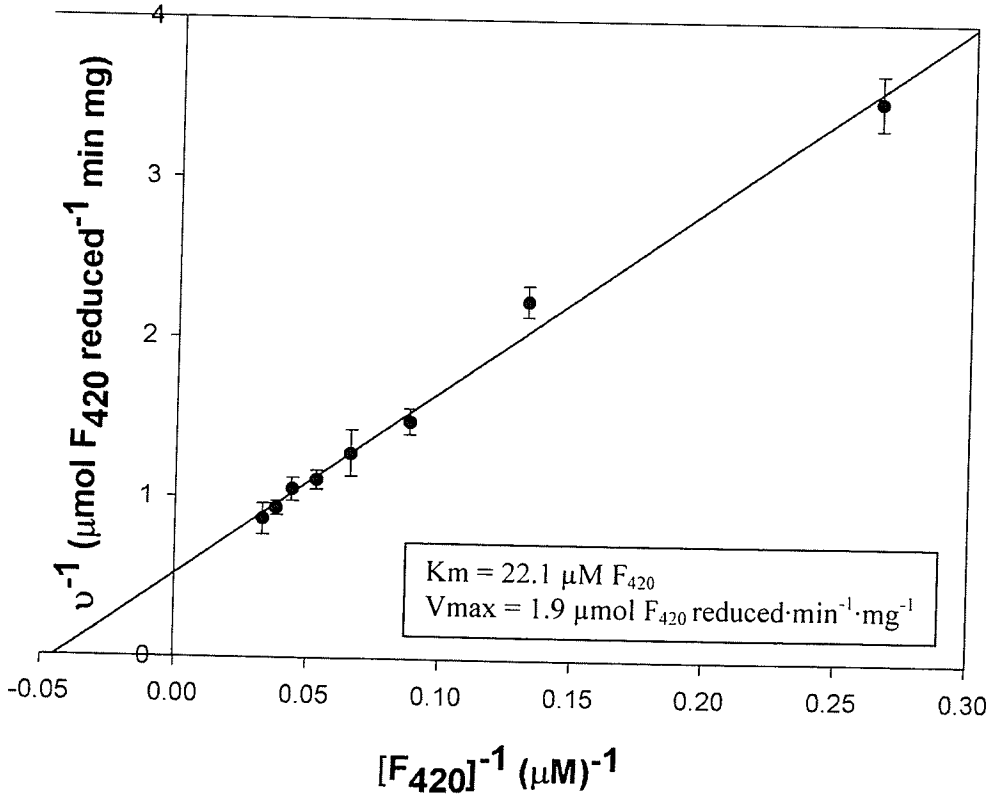

Figure 8.6. Kinetics plots of the F_{420}-reducing hydrogenase activity in the cell-free extract of *Methanosarcina barkeri* Fusaro. (A) Michaelis Menten kinetics plot (B) Lineweaver Burk kinetics plot. $[F_{420}]$ = 20-25 μM

A.

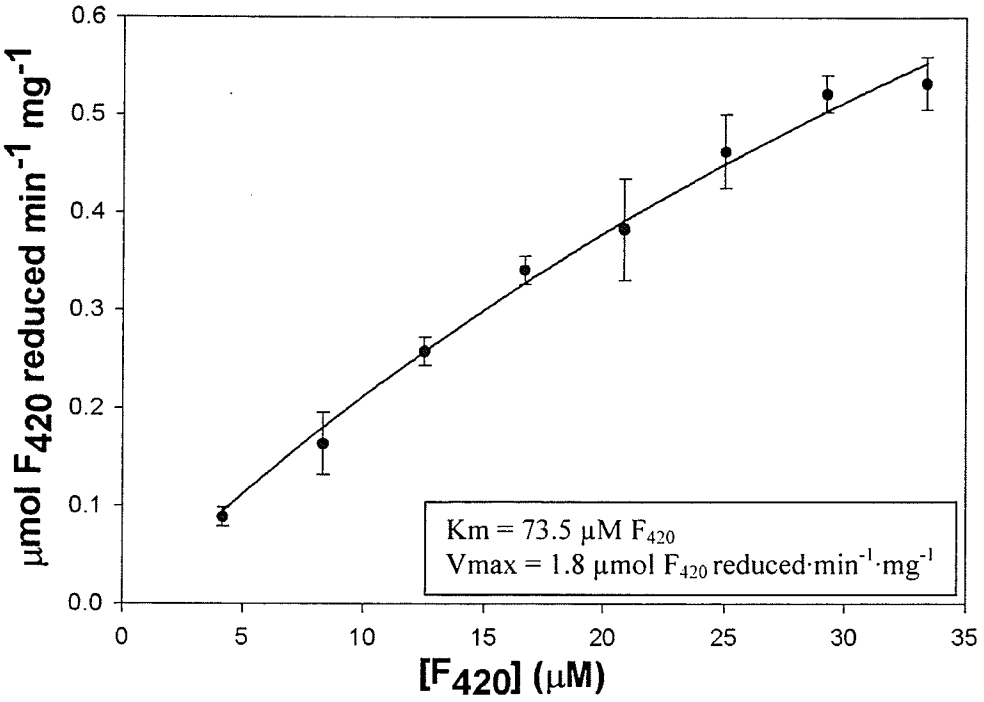

B.

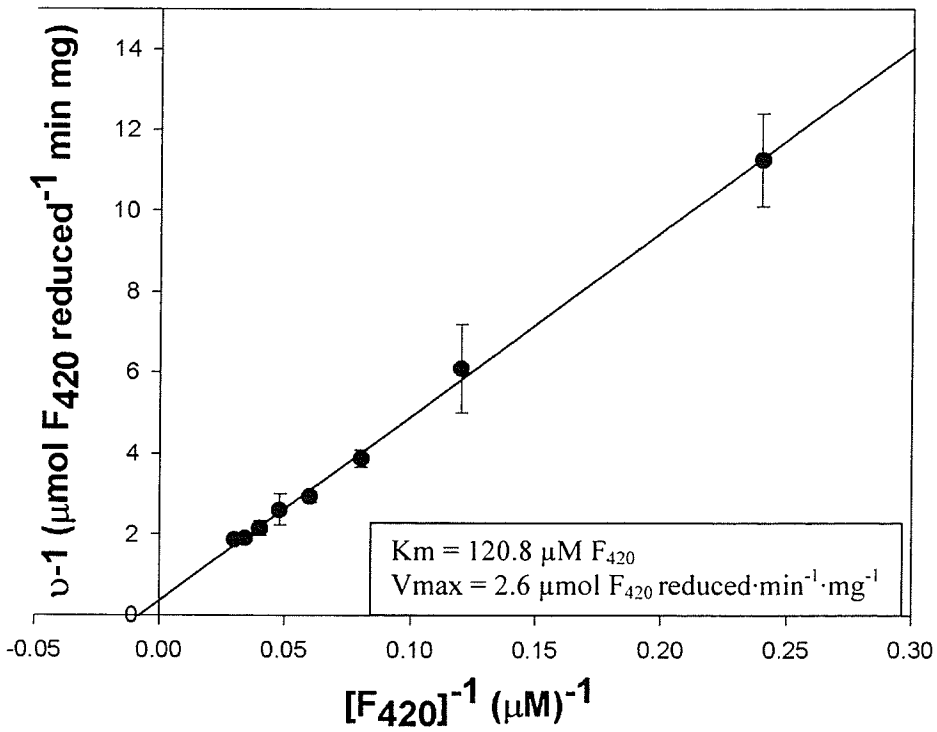

Figure 8.7. Kinetics plots of the F_{420}-reducing hydrogenase activity in the cell-free extract of *Methanospirillum hungatei GP1*. (A) Michaelis Menten kinetics plot (B) Lineweaver Burk kinetics plot. [F_{420}] = 20-25 µM

A.

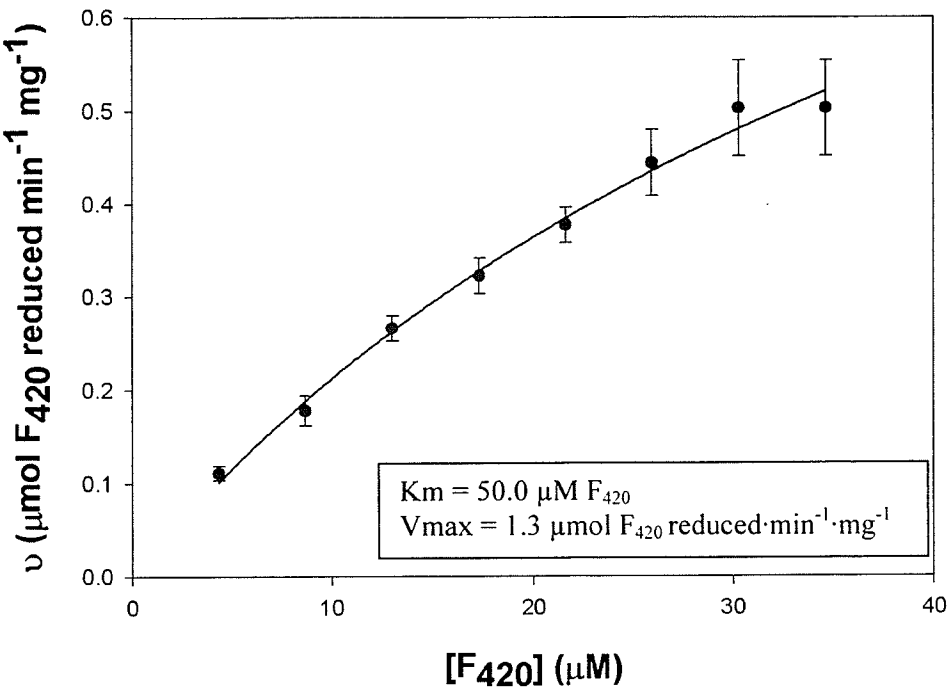

B.

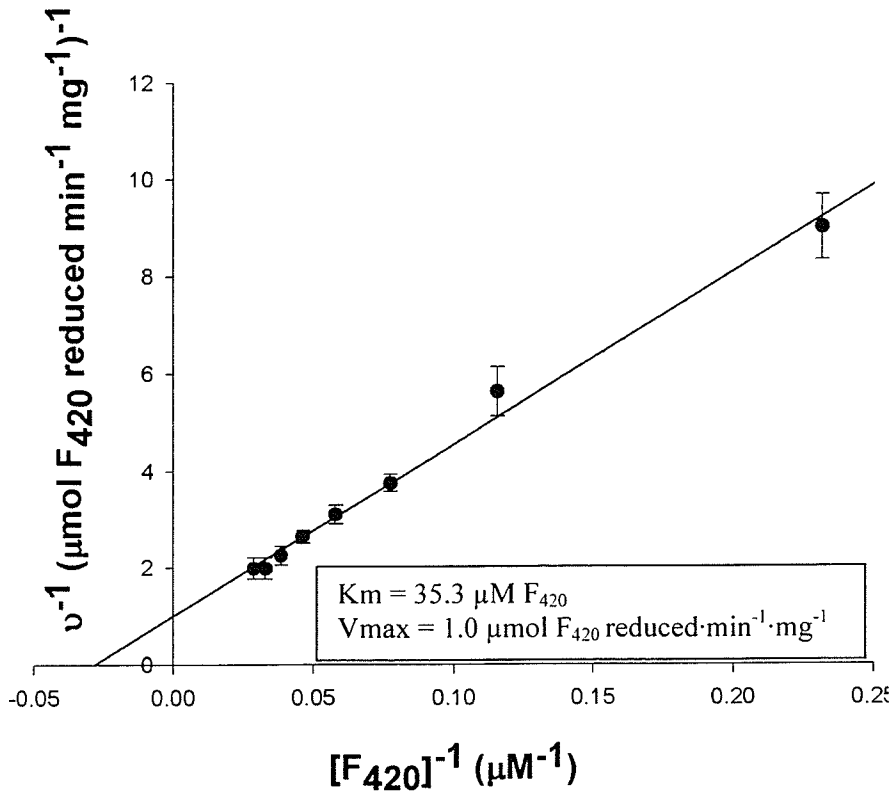

Figure 8.8. Kinetics plots of the F_{420}-reducing hydrogenase activity in the cell-free extract of *Methanococcus voltae*. (A) Michaelis Menten kinetics plot (B) Lineweaver Burk kinetics plot. $[F_{420}]$ = 20-25 μM

A.

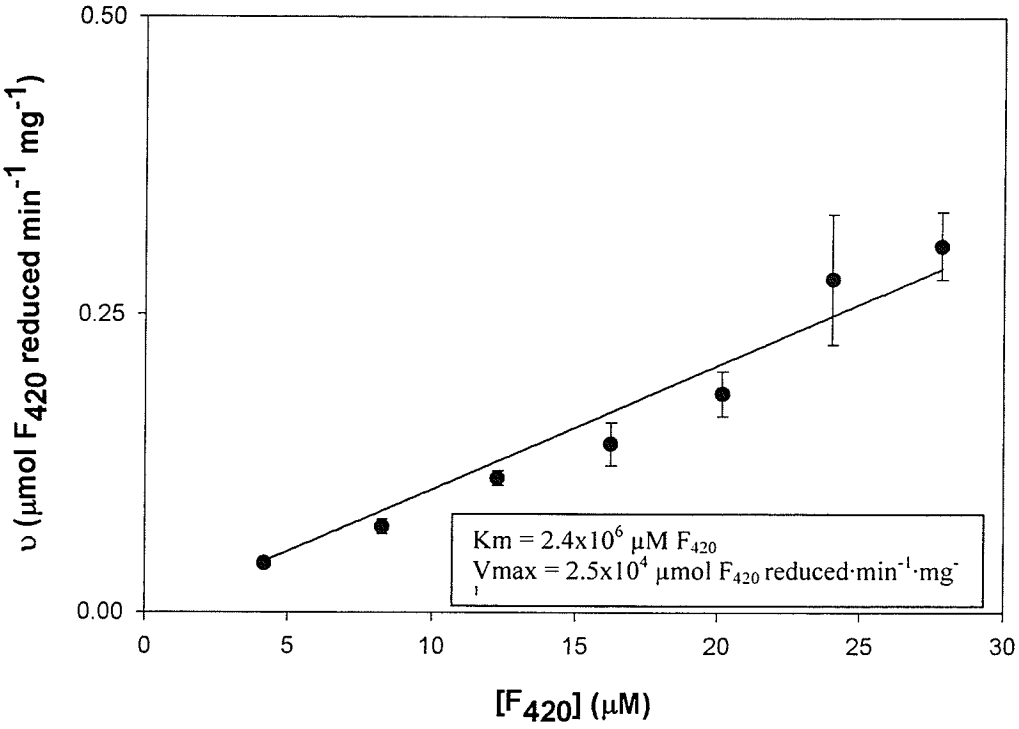

B.

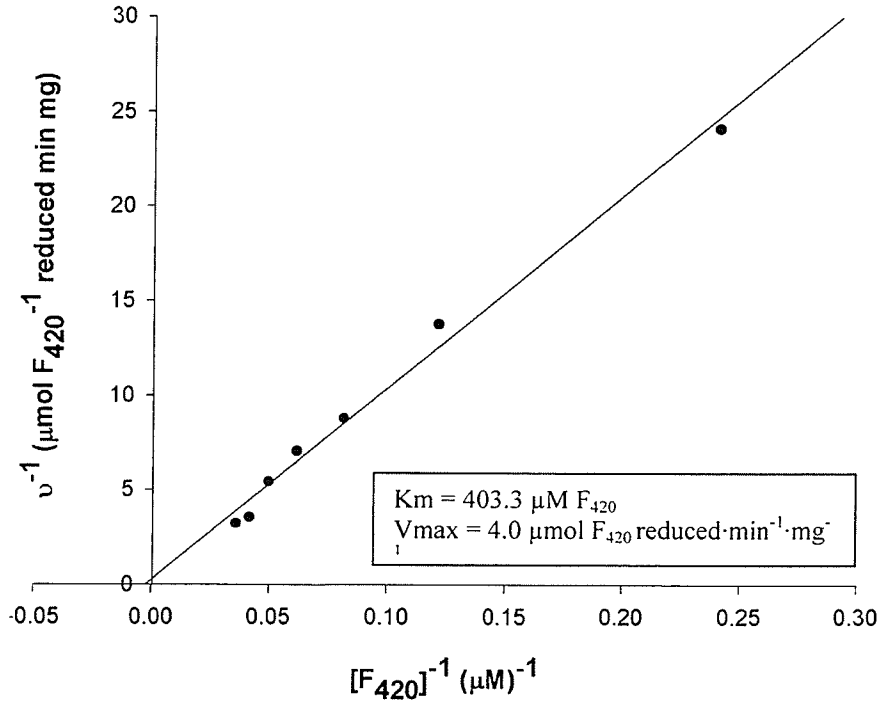

Figure 8.9. Kinetics plots of the F_{420}-reducing hydrogenase activity in the cell-free extract of *Methanothermobacter marburgensis*. (A) Michaelis Menten kinetics plot (B) Lineweaver Burk kinetics plot. $[F_{420}]$ = 20-25 μM

A.

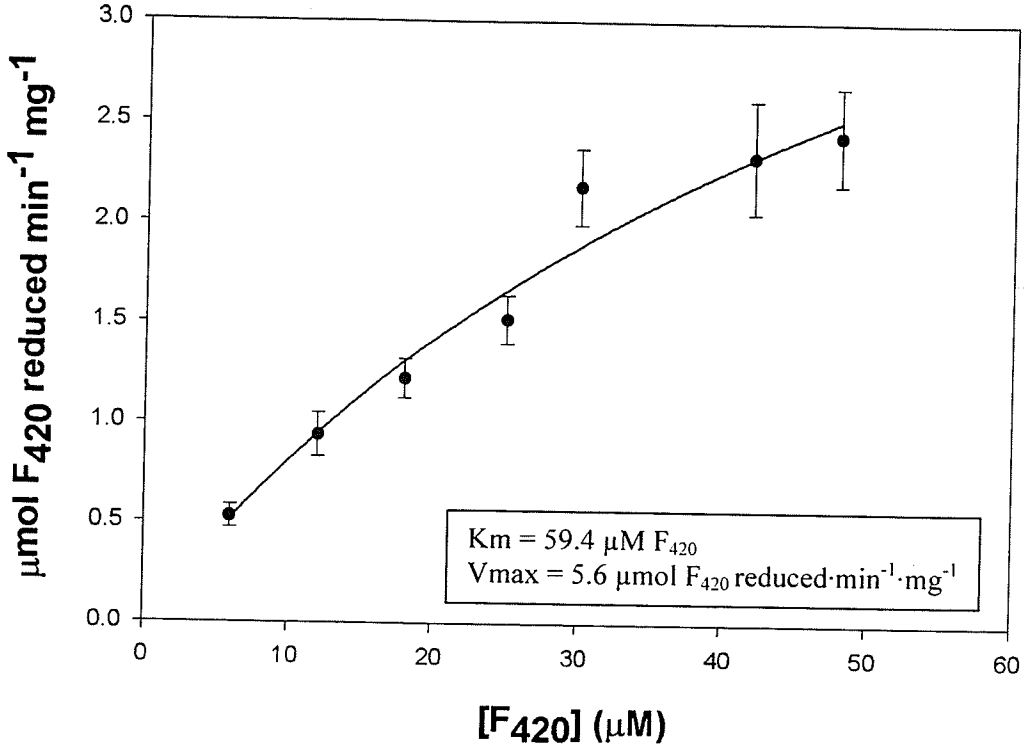

B.

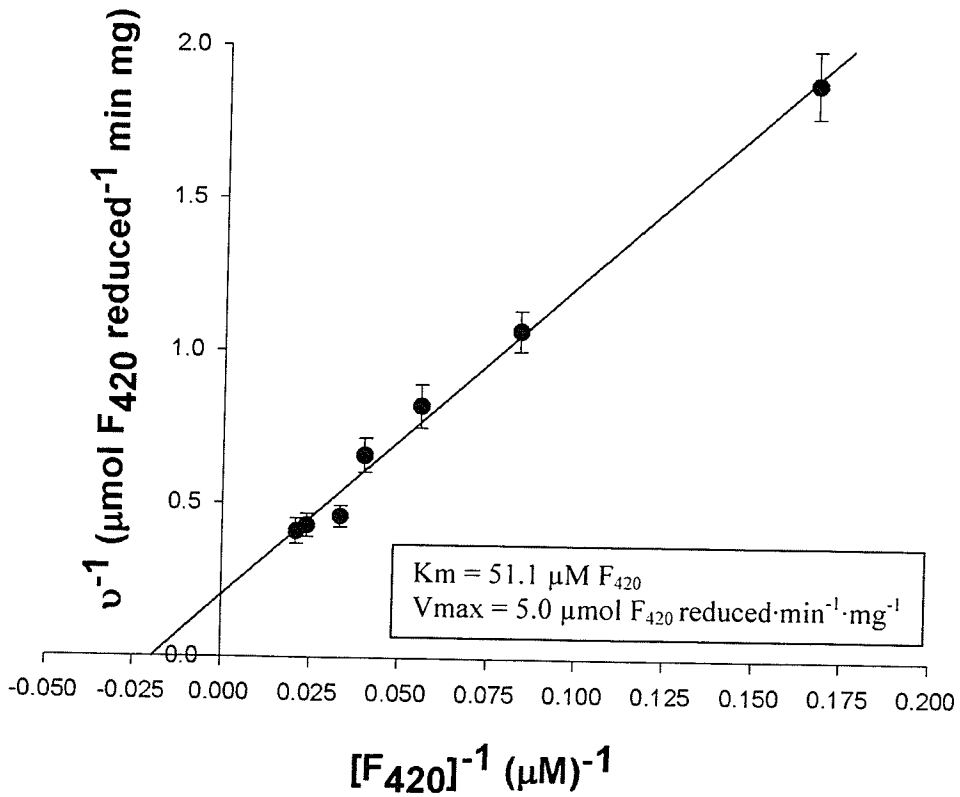

Figure 8.10. Kinetics plots of the F_{420}-reducing hydrogenase activity in the cell-free extract of *Methanobacterium bryantii*. (A) Michaelis Menten kinetics plot (B) Lineweaver Burk kinetics plot. $[F_{420}]$ = 20-25 µM

8.3.6. Genetic relatedness to known methanogenic F_{420}-reducing hydrogenases

BLAST analyses, using the tblastn program, of existing methanogenic genome sequences in the Archaea database, using the amino acid sequences coding for the α-, β-, γ-, and δ-subunits of the putative F_{420} H_2ase of *Msph. stadtmanae* (NC_007681), were performed through the National Center for Biotechnology Information website (NCBI, http://www.ncbi.nlm.nih.gov/). The results indicate that the F_{420} H_2ase of *Msph. stadtmanae* is most closely related to the homologous enzyme of *Mtb. thermoautotrophicus* ΔH, with identity ranging from 36-60%, depending on the subunit. As with *Mtb. thermoautotrophicus* ΔH, a thermophilic member of the *Methanobacteriales*, the putative holoenzyme of F_{420} H_2ase from *Msph. stadtmanae* is also composed of three distinct subunits, FrhAGB; FrhD is a peptidase involved in hydrogenase maturation that does not purify with the F_{420} H_2ase (Fricke *et al.* 2006).

The [NiFe]-containing subunit, FrhA (α), is 60% identical (240/406) and 78% similar (317/406) with the homologous subunit from *Mtb. thermoautotrophicus* ΔH (E = 5e-153). FrhG (γ), the subunit containing the e^- transporting iron-sulfur (FeS) clusters, is 53% identical (123/229) (78% (164/229) similar) to the corresponding subunit of an F_{420} H_2ase from an uncultured methanoarcheon (E = 2e-69). The FAD-containing subunit FrhB (β) is 55% identical (154/280) (72% (202/280) similar) with the subunit from *Mtb. thermoautotrophicus* ΔH (E = 6e-86). FrhD (δ), the hydrogenase maturation peptidase protein, is only 36% identical (55/152) (67% (102/152) similar) to the homologous subunit in *Mtb. thermoautotrophicus* ΔH (E = 3e-28).

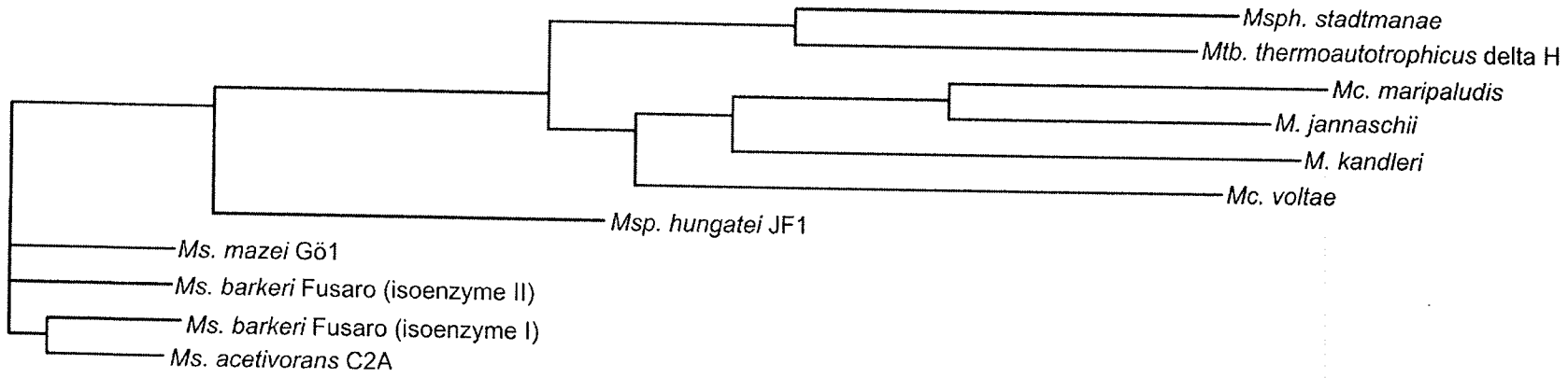

Figure 8.11. Phylogenetic tree showing the evolutionary relationships of the F_{420}-reducing hydrogenase from various methanoarchaea, including the putative F_{420} H_2ase of *Msph. stadtmanae*. ClustalW software (Chenna *et al.* 2003) was used to produce a multiple sequence alignment from the amino acid sequences encoding the α-subunit from the F_{420} H_2ase of various methanoarchaea. The sequence alignment was then used to produce the phylogenetic tree with ClustalW, in the Phylip output format.

Multiple sequence alignments of the amino acid sequences coding for the α-subunit (FrhA) from various methanoarchaea were also used to generate a phylogenetic tree that indicates the close evolutionary relationship between the F_{420} H_2ase of *Mtb. thermoautotrophicus* ΔH (Figure 8.11).

8.3.7. Enrichment of the F_{420}-reducing hydrogenase

F_{420}-reducing activity was monitored during the enrichment of the phenazine-dependent $F_{420}H_2$ dehydrogenation activity of *Msph. stadtmanae* using various column chromatography steps (Chapter 7); the results are summarized in Table 8.4. There are some signs indicating the enrichment of the F_{420}-reducing activity. The specific activity of the F_{420} H_2ase activity increased, as did the degree of purification, during progression from the homogenized 75% $(NH_4)_2SO_4$ pellet through the Phenyl Sepharose CL-4B and DEAE Sephacel column chromatography steps.

Hydrogenase and $F_{420}H_2$ dehydrogenation activities co-eluted from the Phenyl Sepharose CL-4B column when washed with $(NH_4)_2SO_4$-free buffer (Figure 7.7A); at this point, the F_{420} H_2ase activity was enriched 5-fold compared to the 75% $(NH_4)_2SO_4$ saturated protein pellet activity. An examination of lane 5 of the activity- stained native PAGE (Figure 8.12B) indicates the presence of a band containing hydrogenase activity with a molecular weight of approximately 232 kDa; this band displays greater activity staining intensity than the clarified cell-free extract (lane 3) or the re-suspended 75% $(NH_4)_2SO_4$ pellet (lane 4); the corresponding lane of the coomassie blue-stained native PAGE also indicates the presence of a protein band that similarly

Table 8.4. Progression of the F_{420}-reducing hydrogenase activity from *Methanosphaera stadtmanae* through various column chromatography steps (reprinted from Chapter 7). Protein reactivated with 10 μM FAD and 10 μM F_{420} prior to assay. [F_{420}] = 25-30 μM.

Purification stage	Protein (mg)	Activity[†]	Yield (%)	Specific[‡] activity	Purification (-fold)
Clarified cell-free extract	929.2	193.9	100	0.21	-
75% $(NH_4)_2SO_4$ pellet	583.2	235.2	121.3	0.40	1.9
Phenyl-Sepharose CL-4B	20.4	41.4	21.4	2.03	9.7
DEAE Sephacel[‡‡]	6.1	13.5	7.0	2.21	10.6
F_{420}-affinity[‡‡]	2.1	2.1	1.1	1.00	4.8

[†] μmol F_{420} reduced·min^{-1}
[‡] μmol F_{420} reduced·min^{-1}·mg^{-1}
[‡‡] protein pooled from non-binding fractions

shows a greater stained intensity relative to the previous purification stage (Figure 8.12A).

The pooled fractions collected from the Phenyl Sepharose CL-4B column were then loaded onto a DEAE Sephacel column; the $F_{420}H_2$ dehydrogenation activity did not have any apparent affinity for the matrix and flowed through the column uninhibited (Figure 7.7B, Chapter 7). A significant portion of the hydrogenase activity remained bound to the DEAE Sephacel column, while a fraction (~30%) of the hydrogenase activity passed through the column without binding to the column. The protein content of the non-binding hydrogenase activity decreased approximately 3.5-fold from the

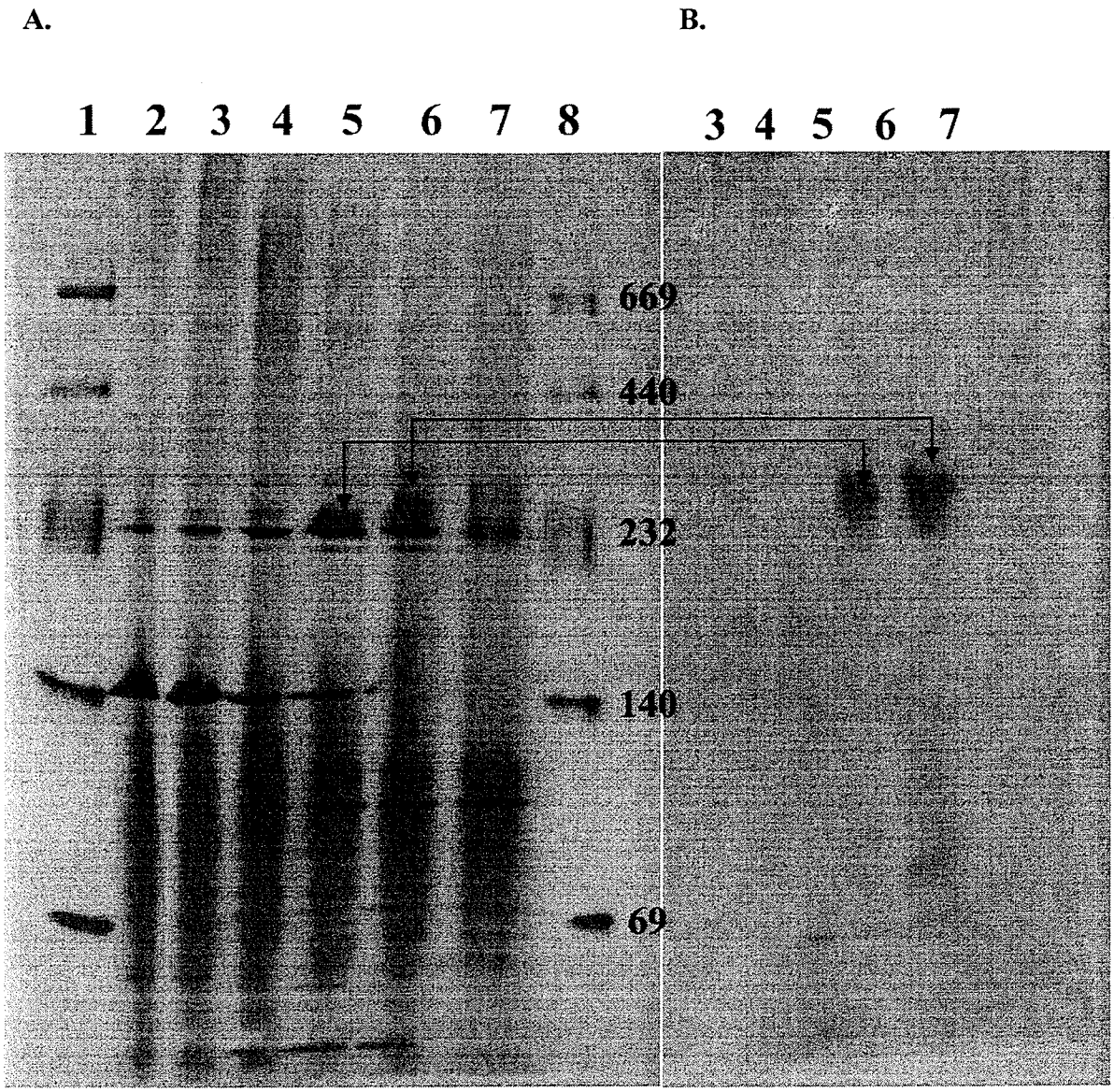

Figure 8.12. (A.) Coomassie blue- and (B.) activity stained (using methyl viologen) 3-20% native gradient PAGE showing enrichment of hydrogenase activity at ~232 kDa at various purification stages of the phenazine-dependent $F_{420}H_2$ dehydrogenase activity of *Methanosphaera stadtmanae*. 1, 8. Molecular markers, kDa. 2. Cell-free extract (CFE). 3. Clarified CFE . 4. Re-suspended $(NH_4)_2SO_4$ pellet. 5. Phenyl Sepharose CL-4B pool. 6. DEAE Sephacel pool. 7. F_{420}-affinity column pool. Approximately 90 μg of protein loaded per lane.

amount loaded onto the column, with a 10% increase in the specific activity of the F_{420} H_2ase activity (Table 8.4). The 232 kDa band (lane 6, Figure 8.12A) displays greater coomassie blue-staining intensity compared to the Phenyl Sepharose CL-4B band; the corresponding hydrogenase activity-stained native PAGE also shows an increase in staining intensity at ~232 kDa (Figure 8.12B).

Finally, the pooled non-binding protein collected from the DEAE Sephacel column was loaded onto an F_{420}-affinity column, where neither the $F_{420}H_2$ dehydrogenation activity nor the hydrogenase activity had any significant affinity for the matrix-bound F_{420}, and co-elute from the column in the non-binding fractions (Figure 7.8, Chapter 7); F_{420} H_2ase activity was also detected in the pooled fractions. Approximately 10-20% of the hydrogenase activity remained bound to the F_{420}-affinity column and was eluted using the 0-2M NaCl gradient, although no F_{420}-reducing activity was detected in the eluate. The amount of protein isolated at this step, (measured from the pooled, non-binding fractions) decreases 3-fold, but the specific activity of the F_{420} H_2ase activity decreases by more than 50%. Furthermore, activity- and coomassie blue-staining of the 232 kDa bands is greatly reduced, with a significant loss in staining intensity (Figure 8.12, lane 7).

8.3.7.1. F_{420}-reducing hydrogenase activity vs F_{420}-nonreducing hydrogenase activity

Table 8.5 summarizes the enrichment of the MV H_2ase activity of *Msph. stadtmanae*. The F_{420} H_2ase can reduce F_{420} as well as artificial electron acceptors such as methyl or benzyl viologen; the MV H_2ase can not reduce F_{420}, but is assayed using methyl or benzyl viologen. Based on genomic evidence, *Msph. stadtmanae* is expected

Table 8.5. Progression of the F_{420}-nonreducing hydrogenase activity from *Methanosphaera stadtmanae* through various column chromatography steps. [methyl viologen] = 2 mM

Stage	Protein (mg)	Activity[†]	Yield (%)	Sp. activity[‡]	Purification
Clarified cell-free extract	929.2	4181.4	100	4.5	-
75% $(NH_4)_2SO_4$ pellet	583.2	2755.2	65.9	4.7	1.0
PhenylSepharose CL-4B	20.4	663.8	15.8	32.5	7.2
DEAE Sephacel[‡‡]	6.1	52.2	1.2	8.6	1.9
F_{420}-affinity[‡‡]	2.1	2.4	0.06	1.1	0.3

[†] µmol methyl viologen reduced·min^{-1}
[‡] µmol methyl viologen reduced·min^{-1}·mg^{-1}
[‡‡] protein pooled from non-binding fractions

to possess the F_{420} H_2ase and MV H_2ase as separate and distinct enzyme activities (Fricke *et al.* 2006).

Enrichment of the MV H_2ase activity did not progress at the same rate as the F_{420} H_2ase activity. Figure 7.7B (Chapter 7) shows there are two peaks of methyl viologen-reducing activity that elute from the DEAE Sephacel column; the first peak, collected with the $F_{420}H_2$ dehydrogenation activity, elutes in the void volume, before commencement of the linear NaCl gradient; the pooled fractions contain F_{420} H_2ase activity. The second peak of methyl viologen-reducing activity elutes during the application of the linear 0-2M NaCl gradient, without apparent $F_{420}H_2$ dehydrogenation or F_{420} H_2ase activity. The yield of the MV H_2ase hydrogenase activity (MV H_2ase + F_{420}

H_2ase) measured from the pooled non-binding fractions dropped nearly 12-fold; by comparison, the F_{420} H_2ase activity decreased ~3-fold relative to the activity loaded onto the column.

The MV H_2ase activity of the pooled non-binding fractions collected from the F_{420}-affinity column decreased 22-fold, whereas the F_{420}-reducing activity decreased 6-fold. The protein and activity profile of fractions collected from the F_{420}-affinity column (Figure 7.8, Chapter 7) shows that there are two separate peaks of methyl viologen-reducing hydrogenase activity. The major hydrogenase activity peak (80-90%) elutes in the void volume (i.e. non-binding fractions) along with the $F_{420}H_2$ dehydrogenation activity, while the other MV H_2ase activity peak elutes from the F_{420}-affinity column within the linear NaCl gradient. The non-binding protein fractions contained F_{420} H_2ase activity along with $F_{420}H_2$ dehydrogenation activity, while the NaCl-eluted fractions from the F_{420}-affinity column contained MV H_2ase activity only. Table 8.6 highlights the change in ratio of the methyl viologen-reducing hydrogenase activity to F_{420} H_2ase activity as the protein extract progresses through the column chromatography steps described above, indicating the enrichment of the F_{420} H_2ase activity relative to the methyl viologen-reducing activity.

The results indicate a consistently observed trend, a steady increase in the F_{420} H_2ase activity relative to the MV H_2ase activity, demonstrating an enrichment of the F_{420} H_2ase, and separation of the MV H_2ase throughout the various chromatographic stages.

Table 8.6. Ratio of the F_{420} H_2ase activity to the MV H_2ase activity and $F_{420}H_2$ dehydrogenation activity of *Methanosphaera stadtmanae* after various column chromatographic stages. F_{420}-H_2ase activated with 10 μM FAD and 10 μM F_{420} prior to assay. MV H_2ase activated with 0.05 mM MV prior to assay. All assays performed at room temperature.

Purification stage	F_{420} H_2ase/MV H_2ase	F_{420} H_2ase/$F_{420}H_2$ DeH_2ase
Cell-free extract	0.046	58.8
75% $(NH_4)_2SO_4$ pellet	0.085	55.6
Phenyl Sepharose CL-4B	0.062	90.9
DEAE Sephacel	0.259	166.7
F_{420}-affinity	0.875	142.9

8.3.7.2. F_{420}-reducing hydrogenase vs $F_{420}H_2$ dehydrogenation activity

In cell-free extract, the F_{420} H_2ase activity is ~60-fold greater than the phenazine-dependent $F_{420}H_2$ dehydrogenation activity, and the ratio of F_{420} H_2ase activity to $F_{420}H_2$ dehydrogenation activity increases as the protein progresses through the column chromatography steps, although not at the same pace as the F_{420} H_2ase:MV H_2ase ratio (Table 8.6). This may suggest partial separation of the F_{420} H_2ase activity from the $F_{420}H_2$ dehydrogenation activity, which was not observed during the purification of the $F_{420}H_2$ dehydrogenation activity from *Msp. hungatei* GP1 and *Ms. barkeri* Fusaro, where a constant F_{420} H_2ase:$F_{420}H_2$ dehydrogenation ratio was maintained throughout the process.

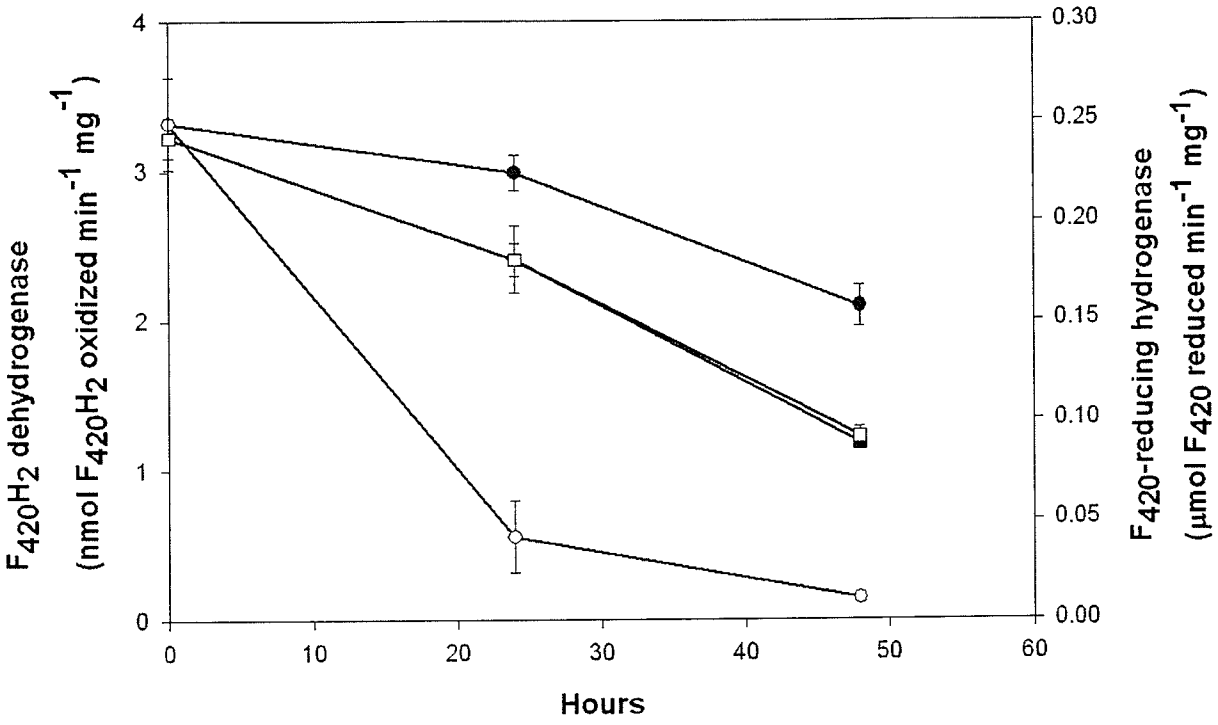

Figure 8.13. Comparison of the stability of the phenazine-dependent $F_{420}H_2$ dehydrogenation activity and the F_{420}-reducing hydrogenase activity in the cell-free extract of *Methanosphaera stadtmanae*, under aerobic and anaerobic conditions. Activities were assayed over a 48 hour period. Aerobic extract was made anaerobic with N_2 prior to assay. F_{420} H_2ase activity reactivated with 10 μM FAD and 10 μM F_{420} in reaction buffer prior to assay. ●, $F_{420}H_2$ dehydrogenation activity (anaerobic). ○, $F_{420}H_2$ dehydrogenation activity (aerobic). ■, F_{420}-reducing hydrogenase activity (anaerobic). □, F_{420}-reducing hydrogenase activity (aerobic).

As with other methanogenic F_{420} H_2ases, the F_{420} H_2ase activity of *Msph. stadtmanae* is stable under aerobic or anaerobic conditions (Figure 8.13); aerobic samples are flushed with N_2, and then incubated in the reaction buffer, under reducing conditions with FAD, prior to assay. In contrast, and unexpectedly, the $F_{420}H_2$ dehydrogenation activity is O_2 labile, with approximately 75-95% lost after 24 hours (Figure 8.13); the enriched F_{420} H_2ase is more air stable, losing only 50% of its activity after 48 hours, which is also observed for the anaerobically stored activity.

These observations differ from the observations with *Msp. hungatei* GP1 and *Ms. barkeri* Fusaro, where both the F_{420} H_2ase and phenazine-dependent $F_{420}H_2$ dehydrogenation activities are aerobically stable.

8.4. Discussion

8.4.1. Discovery of an F_{420}-reducing hydrogenase activity in Methanosphaera stadtmanae

As a methanoarchaeon growing solely on H_2 and CH_3OH, *Msph. stadtmanae* does not metabolize CH_3OH in the same manner as the methylotrophic members of the *Methanosarcinales* are able to do, such that $F_{420}H_2$ cannot be produced using the methylotrophic pathway. There is no apparent need for $F_{420}H_2$ during methanogenesis on CH_3OH and H_2, and unlike most members of the *Methanobacteriales*, *Msph. stadtmanae* does not metabolize CO_2 as substrate for methanogenesis: metabolism of CO_2 requires $F_{420}H_2$ for the reduction of C_1-bound H_4MPT intermediates to the level of CH_3-H_4MPT (Miller and Wolin 1985, Thauer *et al.* 1993, Shima *et al.* 2002).

Msph. stadtmanae is also capable of producing CH_4 from H_2 and L-serine, although attempts to grow *Msph. stadtmanae* on H_2 and serine were unsuccessful (Lin

and Sparling 1995, 1998). The hydroxymethyl group of L-serine forms N^5,N^{10}-methylene-H_4MPT; this would imply that $F_{420}H_2$ would be required for the reduction of N^5,N^{10}-methylene-H_4MPT to methyl-H_4MPT as in other hydrogenotrophic methanoarchaea growing on H_2 and CO_2 (Thauer *et al.* 1993, Lin and Sparling 1995). In the absence of H_2, 2-propanol can be used as a source of electrons for the reduction of CH_3OH; 2-propanol is oxidized to provide electrons for the reduction of $NADP^+$ to NADPH. Fno then catalyzes the NADPH-dependent reduction of F_{420}, with the $F_{420}H_2$ formed expected to be used for the reduction of CoM-S-S-CoB (Wong *et al.* 1994).

The low levels of $F_{420}H_2$ found in *Msph. stadtmanae* (0.16 nmol $F_{420}\cdot mg^{-1}$ protein) would indicate that the cofactor is likely used for biosynthetic purposes, in conjunction with the Fno, and possibly for the detoxification of O_2 (Wong *et al.*1994, Elias *et al.* 2000, Fricke *et al.* 2006).

Until recently, the means of F_{420}-reduction in *Msph. stadtmanae* were largely unknown, since the F_{420} H_2ase had not been detected in this methanoarchaeon (Deppenmeier *et al.* 1989, van de Wijngaard *et al.* 1991, Wong *et al.* 1994). *Msph. stadtmanae* possesses formate dehydrogenase (Lin and Sparling 1995), but this activity is not F_{420}-dependent as it is in some methanoarchaea such as *Methanobacterium* (*Mb.*) *formicicum* (Schauer and Ferry 1985). Interest in the process of H_2-dependent F_{420}-reduction in *Msph. stadtmanae* was reinvigorated by the observation of a phenazine-dependent $F_{420}H_2$ dehydrogenation activity in the cell-free extract of *Msph. stadtmanae*, albeit at low levels of activity (Wong, Ph.D thesis 1999).

As part of the enrichment protocol for the $F_{420}H_2$ dehydrogenation activity (Chapter 7), passage of cell-free extract through an F_{420}-affinity column (in an anaerobic

chamber containing 10% H_2, 90% N_2) resulted in reduction of the F_{420} bound to the matrix material. In the absence of protein, the matrix-bound F_{420} is not reduced in the anaerobic chamber. It was not clear if F_{420} was being reduced directly from H_2, or if there was another electron carrier acting as an intermediate between H_2 and F_{420}. Follow up studies demonstrated that F_{420}-reduction occurred at the same rate in the presence/absence of mediators such as phenazine or ferredoxin (Table 7.5, Chapter 7).

8.4.2. Reactivation of the F_{420}-reducing hydrogenase activity of Methanosphaera stadtmanae

The F_{420} H_2ase activity of *Msph. stadtmanae*, located primarily in the clarified cell-free extract (85-90%), required reactivation under reducing conditions, with the addition of FAD and F_{420}, to achieve optimal activity. Addition of FAD appears to be particularly important in the activation of the F_{420} H_2ase (and $F_{420}H_2$ dehydrogenation) activity of *Msph. stadtmanae*; in the absence of incubation with FAD and F_{420}, the F_{420} H_2ase activity was approximately 40- to 50-fold lower compared to the reactivated activity (Table 8.1). The low F_{420}-reducing activity observed in the absence of reactivation is consistent with the observations made by Wong *et al.* (1994).

The need for exogenous FAD for stability is not unique to the putative F_{420} H_2ase of *Msph. stadtmanae*, but appears to be required at a level that is distinctive for this methanoarchaeon relative to F_{420} H_2ase from other methanoarchaea. FAD is not typically used in the reductive reactivation protocols for the F_{420} H_2ase activities of *Mtb. thermoautotrophicus*, *Mc. voltae*, or *Ms. barkeri* Fusaro (Fox *et al.* 1987, Muth *et al.* 1987, Fiebig and Friedrich 1989, Michel *et al.* 1995), but is included for the F_{420} H_2ase activity of *Msp. hungatei* GP1 (Choquet and Sprott 1991).

FAD is included under some conditions. Nelson *et al.* (1984) reported that the FAD moiety dissociated from the F_{420} H_2ase of *Mb. formicicum* during anaerobic hydrophobic column chromatography, resulting in loss of F_{420}-reducing activity that was restored when the protein was incubated with FAD. Addition of FAD also prevents loss of activity from heat treated F_{420} H_2ase of *Mc. voltae*; in the absence of added FAD, only the methyl viologen-reducing activity remained (Muth *et al.* 1987).

The pH of the assay medium also appears to be important, as F_{420} H_2ase activity is not detected using 50 mM Tris/Cl buffer, pH 8.0; while this pH is often used to assay methyl viologen-dependent F_{420} H_2ase and MV H_2ase activity (Fiebig and Friedrich 1989, Wong PhD thesis 1999), the pH for measurement of F_{420}-reduction is typically lower, from pH 7.0–7.5 (Fox *et al.* 1987, Muth *et al.* 1987, Fiebig and Friedrich 1989, Choquet and Sprott 1991). Our results indicate a pH optimum of approximately 6.8, with low activity at pH 8.0 (Figure 4). Ultimately, the buffer modified from Choquet and Sprott (1991), consisting of 100 mM HEPES, pH 7.0, with 200 mM KCl, 20 mM $MgCl_2 \cdot 6H_2O$, 10 μM FAD, 10 μM F_{420}, and 20 mM DTT, was used to assay the F_{420} H_2ase activity of *Msph. stadtmanae*.

8.4.3. Electrophoretic properties of the F_{420}-reducing hydrogenase

The F_{420} H_2ases typically exhibit at least two distinct F_{420}-reducing forms on activity-stained native PAGE gels (small form: 89–115 kDa, large form(s): 600-1300 kDa); the small forms aggregate to form the larger macromolecular complexes (Michel *et al.* 1995). The F_{420} H_2ase of *Msp. hungatei* GP1 has a MW of 720 kDa (Figure 5.8, Sprott *et al.* 1987), while *Ms. barkeri* Fusaro exhibits a large heteromultimeric form at

845 kDa, and a smaller band at 198 kDa (Figure 6.5, Fiebig and Friedrich 1989). Electrophoresis of clarified cell free extract of *Msph. stadtmanae* on native PAGE gels did not yield the expected activity patterns as observed with other methanoarchaea (Figure 1). It seems unusual that the pattern formed by the F_{420} H_2ase activity from *Msph. stadtmanae* would deviate so drastically from the pattern observed from other methanoarchaea.

Lower MW bands containing hydrogenase activity are routinely seen at approximately 69 kDa; this is consistent with the presence of the MV H_2ase described by Denny Wong (PhD thesis 1999). However, a distinct activity-stained band, with a molecular weight of approximately 232 kDa, is also observed on the same gels.

The aerobically purified F_{420} H_2ase from *Mtb. thermoautotrophicus* ΔH is heterotrimeric flavoprotein with an overall MW of 800 kDa, consisting of three subunits; α (47 kDa), β (31 kDa), and γ (26 kDa) (Fox *et al.* 1987, Braks *et al.* 1994). In addition to the 800 kDa band, which contains the majority of the F_{420}-reducing activity, activity-staining also reveals the presence of a minor band at 115 kDa which also contained F_{420}-reducing activity; a similar profile was observed when the activity was purified under anaerobic conditions (Fox *et al.* 1987). Based on the presence of the 115 kDa form, it was suggested that the subunit stoichiometry (α:β:γ) was a 1:1:1 ratio, with an overall MW of 105 kDa (Fox *et al.* 1987). A fourth subunit, FrhD (δ-, 17 kDa), is encoded by the genome, but is not found with the purified holoenzyme after separation of the subunits on SDS PAGE (Fox *et al.* 1987). Proteins (10-20 kDa) that link the F_{420} H_2ase to the cell membrane have been observed in a related methanoarchaeon, *Mtb. marburgensis*, but have not been isolated (Braks *et al.* 1994).

BLAST analyses of the Archaea database, using the sequences encoding the putative F_{420} H_2ase of *Msph. stadtmanae*, and multiple sequence alignments of the sequences encoding the α-subunit of the F_{420} H_2ase from various methanoarchaea, indicate that the putative F_{420} H_2ase of *Msph. stadtmanae* is most closely related to the homologous enzyme from *Mtb. thermoautotrophicus* ΔH (see section 8.3.5). The MW of the α-, β-, and γ-subunits of the putative F_{420} H_2ase from *Msph. stadtmanae*, estimated using the Compute pI/MW software (Bjellqvist *et al.* 1993, 1994), are, respectively, 45, 33, and 28 kDa (overall MW: 106 kDa). As the F_{420} H_2ase of *Msph. stadtmanae* is most closely related to the enzyme from *Mtb. thermoautotrophicus* ΔH (section 8.3.5.), the observed 232 kDa band may be representative of a dimer of two ~115 kDa F_{420} H_2ases in *Msph. stadtmanae*.

It is interesting to note that the yellow-brown colored bands typically associated with the F_{420} H_2ase cannot be observed on the unstained gel. One explanation is that the protein may be more susceptible to loss of FAD relative to other F_{420} H_2ases from other methanoarchaea. Indeed, our findings reveal a requirement for FAD during reactivation of the F_{420} H_2ase activity of *Msph. stadtmanae* (Table 8.1).

8.4.4. Inhibitor analysis of the F_{420}-reducing hydrogenase activity

Several known inhibitors of hydrogenase activity were used to help elucidate whether the observed F_{420}-reduction in cell-free extract was associated with a distinct hydrogenase (Table 8.2).

Divalent metal ions are strong inhibitors of hydrogenase activity in various microorganisms (Woo *et al.* 1993). F_{420}-reducing activity in cell-free extract of *Msph.*

stadtmanae was inhibited by the addition of various metal ions, most significantly by Cu^{2+}. Cu^{2+}, when used as a potential ligand for MCAC, rendered the F_{420} H_2ase of *Msp. hungatei* GP1 inactive (Choquet and Sprott 1991); inhibition was also observed after the $F_{420}H_2$ dehydrogenation activity of *Msph. stadtmanae* was passed through a Cu^{2+}-charged column (Appendix E).

F_{420}-reduction was stimulated in the presence of the anionic metabolic inhibitors N_3^- and CN^-, as well as in the presence of the metal chelating agent EDTA. Azide (N_3^-) and cyanide (CN^-) are both electron transport inhibitors that also inhibit hydrogenases (Seefeldt and Arp 1989), while EDTA chelates divalent cations, including Ni^{2+} which is an essential component of [NiFe] hydrogenases (Friedrich *et al.* 1981).

2-Bromoethanesulfonate (2-BES), a methanogenic inhibitor with a similar structure to CoM-SH, was used as a negative control, and does not have any significant impact on the F_{420}-reducing activity. 2-BES inhibits the methylreductase, which catalyzes the reductive demethylation of CH_3-S-CoM with CoB-SH, forming CoM-S-S-CoB and CH_4 (DiMarco *et al.* 1990). These results are consistent with the inhibition/ stimulation observed when measuring methyl viologen-reducing activity in the cell-free extract of *Msph. stadtmanae* (Wong, Ph.D thesis 1999).

Addition of DPI also inhibits F_{420}-reduction from the cell-free extract of *Msph. stadtmanae*. DPI likely binds to the FAD component of the β-subunit, preventing access of F_{420} to the active site. Inhibition of F_{420} H_2ase activity is consistent with the observed inhibition of the phenazine-dependent $F_{420}H_2$ dehydrogenation activity of *Msph. stadtmanae*, indicating that attack of the FAD component by DPI is the likely basis for

inhibition of both activities in *Msph. stadtmanae*, suggesting non-competitive inhibition. DPI is an inhibitor of flavoproteins such as mitochondrial and bacterial NADH: ubiquinone oxidoreductase and NADH oxidase (O'Donnell *et al.* 1993, Majander *et al.* 1994), as well as the 2-OH-phenazine-dependent $F_{420}H_2$ dehydrogenase activity of *Ms. mazei* Gö1 (Brodersen *et al.* 1999). DPI acts as a competitive inhibitor to the 2-OH-phenazine-dependent $F_{420}H_2$ dehydrogenase activity of *Ms. mazei* Gö1, due to its planar structure which is similar to phenazine (Figure 1.15) (Brodersen *et al.* 1999). Methyl viologen-reduction in *Msph. stadtmanae* is not affected by the presence of DPI, as FAD is not necessary for methyl viologen-reduction by the F_{420} H_2ase (Thauer *et al.* 1993). This is consistent with our observations with the corresponding activity of *Msp. hungatei* GP1 (Table 5.7, Chapter 5) and *Ms. barkeri* Fusaro (Table 6.7, Chapter 6)

For comparison, the purified $F_{420}H_2$ dehydrogenation activity (associated with the F_{420} H_2ase) of *Msp. hungatei* GP1 was inhibited by DPI (25 and 50 μM), while the F_{420} H_2ase was inhibited by 50 μM DPI (Chapter 5), indicating competitive inhibition at lower [DPI] (25 μM), but non-competitive at higher [DPI] (50 μM). The purified $F_{420}H_2$ dehydrogenation activity (associated with the F_{420} H_2ase) of *Ms. barkeri* Fusaro was competitively inhibited by additions of 50 and 100 μM DPI, while the purified F_{420} H_2ase activity of *Ms. barkeri* Fusaro was not inhibited (Chapter 6).

8.4.5. Comparison of the F_{420}-reducing hydrogenase activity of Methanosphaera stadtmanae *with homologous activities in other methanoarchaea*

The catalytic/kinetic properties of the F_{420} H_2ase activity were examined from clarified cell-free extract of *Msph. stadtmanae*, and compared with the F_{420} H_2ase activity from other methanoarchaea (Table 8.3). Using an F_{420} H_2ase assay protocol modified

from Choquet and Sprott (1991) (described in section 8.3.4), the apparent K_m for F_{420} of the F_{420} H_2ase activity of *Msph. stadtmanae* was found to be similar to the activities observed in other methanogenic archaea, with the exception of *Mtb. marburgensis* (discussed further below). Once reactivated in the presence of FAD, the level of activity was similar to the F_{420} H_2ase activities in the clarified cell-free extracts of the methanoarchaea tested. It should be noted that assay conditions for the respective F_{420} H_2ase activities, particularly with respect to reactivation, vary from one methanoarchaeon to the next, such that the conditions may not have been optimal for each activity. Standardized conditions (i.e. the activation/assay conditions used for *Msph. stadtmanae*) were used to provide a means for comparison between the F_{420}-reducing activities of *Msph. stadtmanae* and other methanoarchaea.

While the putative F_{420} H_2ase of *Msph. stadtmanae* is most closely related to the enzyme of *Mtb. thermoautotrophicus* ΔH, the observed activities of a closely related methanoarchaeon, *Mtb. marburgensis*, and *Msph. stadtmanae* were quite distinct. This is due to the conditions under which the activities were assayed. As described by Jacobson *et al.* (1981), the F_{420} H_2ase activity of *Mtb. thermoautotrophicus* ΔH, at various stages of purification, is optimized *via* incubation at 45°C for 1 hour, in buffer containing 1M salt (K^+ or Na^+). The apparent K_m for F_{420} of the F_{420} H_2ase of *Mtb. thermoautotrophicus* ΔH was determined to be 19 μM F_{420} by Jacobson *et al.* (1981).

Under our standardized conditions (incubation of protein under H_2, in 100 mM HEPES, pH 7.0, with 200 mM KCl, 20 mM $MgCl_2 \cdot 6H_2O$, 10 μM FAD, 10 μM F_{420}, and 20 mM DTT , room temperature), the apparent K_m for F_{420} for *Mtb. marburgensis* was determined to be 2.4×10^6 μM (Michaelis Menten kinetics); however, when the clarified

cell-free extract was incubated at 45°C for ½ hour, the apparent K_m was determined to be 36.5 μM F_{420}, which is considerably closer to the value reported for *Mtb. thermoautotrophicus* ΔH by Jacobson *et al.* (1981). Thus, despite the phylogenetic similarities between the F_{420} H_2ase of *Msph. stadtmanae* and *Mtb. thermoautotrophicus* ΔH, there are clearly differences in requirements for activation of the respective F_{420} H_2ase activities.

8.4.6. Partial enrichment of the F_{420}-reducing hydrogenase activity

The F_{420} H_2ase activity of *Msph. stadtmanae* was only recently observed in our laboratory. It is apparent that the protocol used to isolate the F_{420} H_2ase from *Ms. barkeri* Fusaro, *Msp. hungatei* GP1, and *Mc. voltae* cannot be directly applied without some modification. The protocol (described in greater detail in Chapters 5 and 6) involved: enrichment of the $F_{420}H_2$ dehydrogenation/ F_{420} H_2ase activity from a Ni^{2+}-affinity column; electrophoresis of the pooled desalted/concentrated protein on a 3-20% native gradient PAGE; and electro-elution of the protein from gel bands excised from the native PAGE.

There is no significant affinity for the $F_{420}H_2$ dehydrogenation activity of *Msph. stadtmanae* to the Ni^{2+}-charged sepharose fast-flow resin (i.e. metal chelate affinity chromatography), such that the F_{420}-reducing activity cannot be enriched using this step. A distinct, high MW band consistent with the presence of F_{420} H_2ase is not visualized on the native gradient PAGE gel after electrophoresis of protein (over 1 mg of protein loaded) from *Msph. stadtmanae*, in the absence or presence of activity stain. This was an important step in the isolation of the F_{420} H_2ases of methanoarchaea studied in this

thesis, since the F_{420} H_2ase can be visualized (without staining) as a distinct, high MW, yellow-brown protein band separated from most other proteins. A protein band of similar high MW can only be visualized after coomassie blue-staining of the native PAGE, this band does not stain for hydrogenase activity (Figures 8.2 and 8.3).

Phenazine-dependent $F_{420}H_2$ dehydrogenation activity is associated with the F_{420} H_2ase of *Msp. hungatei* GP1 and *Ms. barkeri* Fusaro; it is possible that a similar association could be observed in *Msph. stadtmanae*. F_{420} H_2ase activity was monitored during the enrichment of the phenazine-dependent $F_{420}H_2$ dehydrogenation activity of *Msph. stadtmanae*. The F_{420} H_2ase activity was enriched after several chromatographic steps (Table 8.4); this is corroborated by the enrichment of hydrogenase activity- and coomassie blue-stained bands of approximately 232 kDa on a 3-20% native gradient PAGE (Figure 8.12). The F_{420} H_2ase activity appeared to be distinct from the MV H_2ase activity, since the ratio of MV H_2ase to F_{420} H_2ase activity increased throughout the chromatographic progression (Table 8.6). However, the F_{420} H_2ase also appeared to be distinct from the $F_{420}H_2$ dehydrogenation activity, since the ratio of F_{420} H_2ase to $F_{420}H_2$ dehydrogenation activity increased throughout the chromatographic progression (Table 8.6).

Present research indicates that there is an F_{420} H_2ase activity in the cell-free extract of *Msph. stadtmanae*; activity at similar levels as other methanoarchaea was observed when the cell-free extract was incubated, under reducing conditions, with 10 μM FAD and 10 μM F_{420}, at neutral pH (pH 7.0) and ambient room temperature (~25°C) (Table 8.4). Table 8.7 highlights some of the similarities and differences of the putative

Table 8.7. Comparison of properties of the putative F_{420}-reducing hydrogenase of *Methanosphaera stadtmanae* with the F_{420}-reducing hydrogenase of various methanoarchaea.

Methanoarchaeon	**Order**	**FAD requirement**	**pH optimum**	**Km (μM F_{420})**	**Molecular mass (kDa)**	**Subunit composition (kDa)**	**Reference**
Ms. barkeri Fusaro	*Methanosarcinales*	No	6.5-7.25	25	845, 198	48, 33, 30	Fiebig and Friedrich 1989, Michel *et al.* 1995
Msp. hungatei GP1	*Methanomicrobiales*	No[a]	7.0	N.D.	720	50.7, 32.9, 30.7	Sprott *et al.* 1987, Choquet and Sprott 1991
Mc. voltae	*Methanococcales*	No[b]	7.0	16	1300, 745, 105	55[c], 45, 37, 27	Muth *et al.* 1987
Mtb. thermoautotrophicus ΔH	*Methanobacteriales*	No	6.5-7.5	26	800, 115	47, 31, 26	Fox *et al.* 1987, Livingston *et al.* 1987
Msph. stadtmanae[d]	*Methanobacteriales*	Yes[e]	6.8[f]	53	232[d]	(45,33,28)[g]	This thesis

[a] FAD used but not needed, according to Sprott *et al.* 1987, Choquet and Sprott 1991
[b] FAD added after hydrophobic chromatography
[c] dimer of 27 kDa subunits
[d] putative F_{420} H_2ase
[e] 50- to 60-fold lower activity in the absence of FAD
[f] no activity detected in Tris/Cl pH 8.0, absence of FAD
[g] estimated *via* analysis of *frhAGB* using Compute pI/MW software
N.D., not determined in original references

F_{420} H_2ase of *Msph. stadtmanae* with the corresponding enzyme from various methanoarchaea.

In summary, the $F_{420}H_2$ dehydrogenation activity of *Msph. stadtmanae* was investigated as a possible source of phenazine-dependent F_{420}-reducing activity, in the apparent absence of an F_{420} H_2ase. The relationship between the $F_{420}H_2$ dehydrogenation activity and the F_{420} H_2ase activity of *Msph. stadtmanae* has yet to be resolved. While more work is required to isolate and to characterize this putative enzyme, the observation of an F_{420} H_2ase activity in *Msph. stadtmanae* is significant.

8.4.7. Resolution of the $F_{420}H_2$ dehydrogenation, F_{420}-reducing hydrogenase, and F_{420}-nonreducing hydrogenase activities

While the F_{420} H_2ase was not initially believed to be present in *Msph. stadtmanae*, our enrichment of this activity from cell-free extract led to some interesting observations. Table 8.6 indicates that as the cell-free extract of *Msph. stadtmanae* progresses through the various column chromatography stages, the ratio of F_{420} H_2ase activity to MV H_2ase activity increases, indicating a decrease in methyl viologen-reducing activity with a concurrent enrichment of F_{420}-reducing activity. This is consistent with the presence of genes encoding for the both hydrogenases in the genome of *Msph. stadtmanae* (Fricke *et al.* 2006).

Is the putative F_{420} H_2ase of *Msph. stadtmanae* a source of the $F_{420}H_2$ dehydrogenation activity? Resolution of the F_{420} H_2ase and $F_{420}H_2$ dehydrogenation activities is more difficult. As the cell-free extract passes through various column chromatography steps, the F_{420} H_2ase activity is enriched, while the $F_{420}H_2$ dehydrogenation activity decreases (Table 8.6). The observed $F_{420}H_2$ dehydrogenation

activity of *Msph. stadtmanae* (in cell-free extract) is O_2 labile, and activity declines rapidly; the F_{420} H_2ase activity is itself aerobically stable (Figure 8.13). Based on these results, it appears that the F_{420} H_2ase of *Msph. stadtmanae* is not the sole source of the phenazine-dependent $F_{420}H_2$ dehydrogenation activity, if at all. In contrast, the phenazine-dependent $F_{420}H_2$ dehydrogenation activity purified from *Msp. hungatei* GP1 and *Ms. barkeri Fusaro* is directly associated with the respective F_{420}-reducing hydrogenases, and is also aerobically stable (Chapter 5 and 6, respectively). However, we also must consider that the differences in the F_{420} H_2ase:$F_{420}H_2$ dehydrogenation activity ratios could also be due to loss of the FAD component during the column chromatography process, which was not taken into account during assays of the $F_{420}H_2$ dehydrogenation activity. Incubation of the $F_{420}H_2$ dehydrogenation activity with FAD was not a typical step during our studies, as the addition of FAD did not increase the specific activity of the $F_{420}H_2$ dehydrogenase activity of *Ml. tindarius* or *Ms. mazei* Gö1 (Haase *et al.* 1992, Abken and Deppenmeier 1997). Our results indicate that incubation of protein of *Msph. stadtmanae* with FAD can stimulate the $F_{420}H_2$ dehydrogenation activity after apparent loss of activity (Table 7.6). In the absence of further analysis, one cannot discount the possibility that the aerobic instability of the $F_{420}H_2$ dehydrogenation activity may be an anomaly of the F_{420} H_2ase of *Msph. stadtmanae*.

A putative $F_{420}H_2$ oxidase (FprA) is encoded in the genome of *Msph. stadtmanae* (Fricke *et al.* 2006). Similar to the phenazine-dependent $F_{420}H_2$ dehydrogenation activity, the $F_{420}H_2$ oxidase activity is also O_2 labile, and $F_{420}H_2$-dependent O_2-reduction declines at a similar pace as the phenazine-dependent $F_{420}H_2$ dehydrogenation activity when stored under aerobic conditions (Figure 7.11). These results should be interpreted with

caution, as the F_{420} H_2ase of *Mtb. thermoautotrophicus* ΔH also catalyzes the $F_{420}H_2$-dependent reduction of O_2 (Jacobson *et al.* 1982).

Recent biochemical and genomic studies in our laboratory have lead to new insights into the electron transport pathway of *Msph. stadtmanae*, in particular to reactions involving the reduction of $F_{420}H_2$. A model highlighting the findings of our recent studies on electron transport in *Msph. stadtmanae* are shown in Figure 8.14.

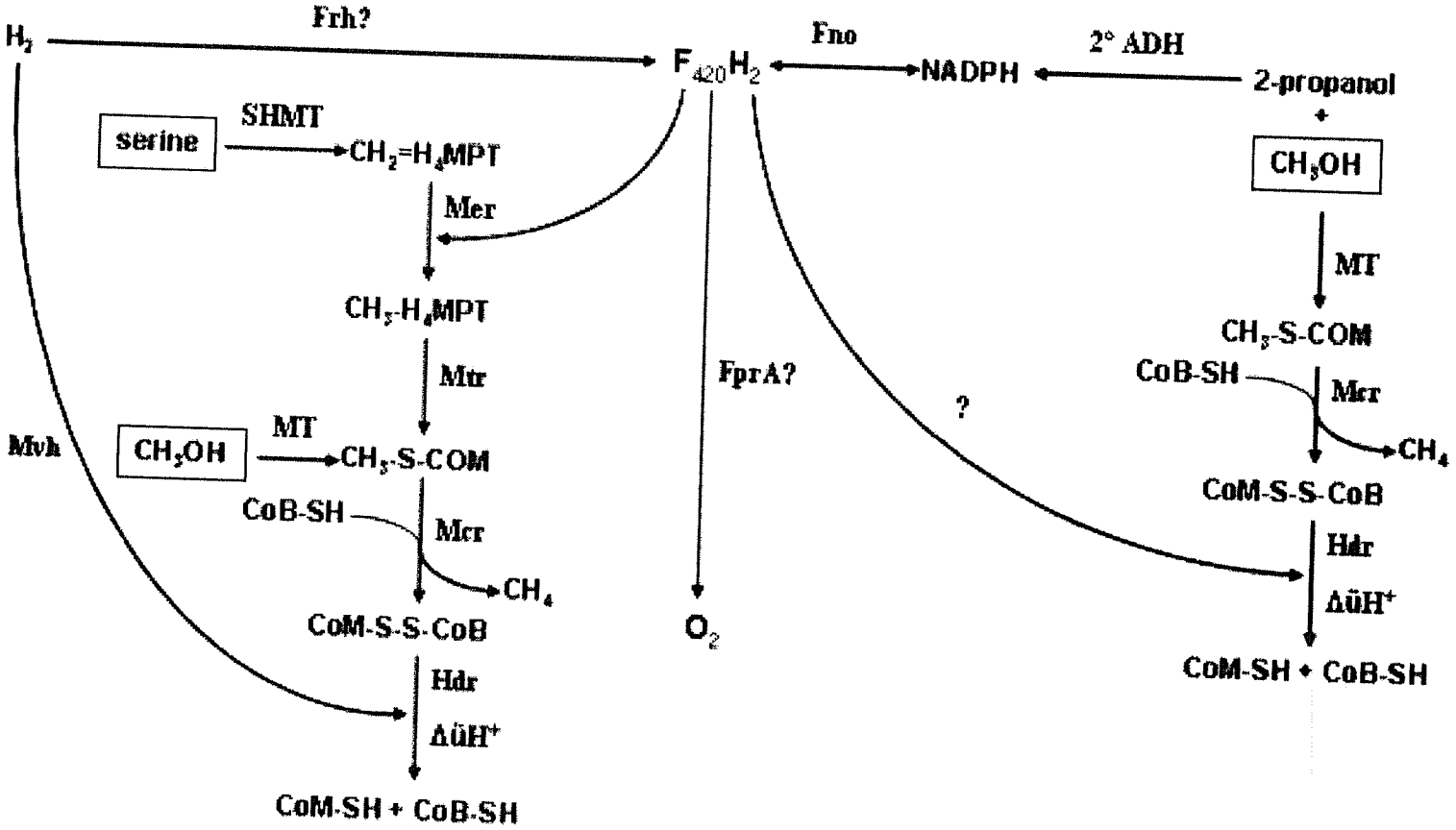

Figure 8.14. Elements of electron transport in *Methanosphaera stadtmanae*. CH_3OH, methanol; H_4MPT, tetrahydromethanopterin; CoM-SH, coenzyme M; CoB-SH, coenzyme B; CoM-S-S-CoB, heterodisulfide complex; Mer, methylene-H_4MPT reductase; Mtr, methyl-H_4MPT:coenzyme M methyltransferase; Mt, methyltransferase; Mcr, methyl-coenzyme M reductase; Hdr, heterodisulfide reductase; Mvh, methyl viologen-reducing hydrogenase; Frh, F_{420}-reducing hydrogenase (putative); Fno, $F_{420}H_2$:$NADP^+$ oxididoreductase; 2° ADH, secondary alcohol dehydrogenase; SHMT, serine hydroxymethyl transferase; FprA, flavoprotein A ($F_{420}H_2$ oxidase, putative).

9. Conclusions and Future Considerations

9.1. Introduction

The $F_{420}H_2$ dehydrogenase (Fpo ($F_{420}H_2$:phenazine oxidoreductase complex) has been purified from the methylotrophic methanoarchaea *Methanolobus tindarius* and *Methanosarcina mazei* Gö1; this enzyme is expected to be an essential component of the $F_{420}H_2$:heterodisulfide oxidoreductase complex (Haase *et al.* 1992, Abken and Deppenmeier 1997). Studies with *Ms. mazei* Gö1 indicate that methanophenazine is the purported electron carrier for this activity, but this activity is can also be assayed using various phenazine-containing compounds (Abken *et al.* 1998). While the Fpo complex has only been isolated from methylotrophic members of the *Methanosarcinaceae*, phenazine-dependent $F_{420}H_2$ dehydrogenation activity appeared to be ubiquitous amongst the methanoarchaea, independent of growth substrate or phylogeny. This activity was further examined in *Methanospirillum hungatei* GP1, CH_3OH-grown *Methanosarcina barkeri* Fusaro, and *Methanosphaera stadtmanae*.

Some of the differences and similarities of the methanogenic $F_{420}H_2$ dehydrogenation activity studied during the course of this thesis are summarized in Table 9.1 (from Chapters 4, 5, 6, and 7). Unlike the activity purified from *Ml. tindarius* (Haase *et al.* 1992), the $F_{420}H_2$ dehydrogenation activities of *Msp. hungatei* GP1 and *Ms. barkeri Fusaro* are both located on the respective F_{420} H_2ase; these activities are further distinguished from the activity of Fpo complex of *Ms. mazei* Gö1 (Abken *et al.* 1998) and *Ml. tindarius* (this thesis) by the low sensitivity to DPI. The $F_{420}H_2$ dehydrogenation activity of *Msph. stadtmanae* is among the lowest of all the activities observed. Unlike

the activity measured from other methanoarchaea, this activity was anaerobically unstable. The source of this activity is not immediately clear.

Table 9.1. Properties of the phenazine-dependent $F_{420}H_2$ dehydrogenation activity of methanoarchaea studied in this thesis.

Methano-archaeon	Substrate	Source of activity	$Km_{phenazine}$ ‡	Vmax‡‡	Ic_{50} (μM DPI)†	Reference
Ml. tindarius	CH_3OH	Fpo complex	266	0.5†	3	Haase *et al.* 1992, This thesis
Msp. hungatei GP1	H_2/CO_2	F_{420} H_2ase	288.3	19.5††	25	This thesis
Ms. barkeri Fusaro	CH_3OH	F_{420}-H_2ase	112.4	29.5††	>100	This thesis
Msph. stadtmanae	H_2/ CH_3OH	F_{420}-H_2ase† or $F_{420}H_2$ oxidase†	138.2	0.003†	2.5	Fricke *et al.* 2007, This thesis

†measured from cell-free or clarified cell-free extract
††purified activity
‡μM phenazine
‡‡μmol $F_{420}H_2$ oxidized·min^{-1}·mg^{-1}

9.2. Phenazine-dependent $F_{420}H_2$ dehydrogenation activity in Methanospirillum hungatei *GP1*

An F_{420}-nonreducing hydrogenase (MV H_2ase) was not detected in *Msp. hungatei* GP1 (Sprott *et al.* 1987); this enzyme is an essential component of H_2:CoM-S-S-CoB oxidoreductase complex in hydrogenotrophic methanoarchaea, catalyzing the H_2-dependent reduction of CoM-S-S-CoB (Figure 1.16) (Thauer *et al.* 1993, Shima *et al.* 2002). In the absence of MV H_2ase, alternate means for CoM-S-S-CoB reduction were investigated. Phenazine-dependent $F_{420}H_2$ dehydrogenation activity detected in the

soluble and membrane fractions was isolated and found associated with the F_{420}-reducing hydrogenase (F_{420} H_2ase), and not with an $F_{420}H_2$ dehydrogenase. Biochemical and genomic analyses during the course of this thesis confirmed the absence of an $F_{420}H_2$ dehydrogenase and MV H_2ase in *Msp. hungatei* JF1. The F_{420} H_2ase may provide an alternate means for CoM-S-S-CoB reduction in *Msp. hungatei* GP1, using $F_{420}H_2$; a similar mechanism has been suggested for *Methanococcus voltae*, grown on formate (Brodersen *et al.* 1999). Genomic analyses of *Msp. hungatei* JF1 indicate the presence of noncatalytic MV H_2ase subunits (MvhD) that may allow for direct transfer of electrons from H_2 or $F_{420}H_2$ to the heterodisulfide reductase (Hdr) (Figure 5.16).

More studies must be conducted to determine if the F_{420} H_2ase is associated with CoM-S-S-CoB reduction. This could be accomplished using membrane vesicle preparations of *Msp. hungatei* GP1, which would contain both the F_{420} H_2ase and Hdr. Spheroplasts of *Msp. hungatei* GP1 can be formed according to Sprott *et al.* (1987); gentle lysing of these cells would allow for study of the F_{420} H_2ase and Hdr in the cell membrane vesicles. Peinemann *et al.* (1990) were able to demonstrate ATP synthesis using H_2-dependent reduction of CoM-S-S-CoB using membrane vesicles of *Ms. mazei* Gö1. H_2 or $F_{420}H_2$-dependent CoM-S-S-CoB reduction, using vesicle preparations of *Msp. hungatei* GP1, could be monitored, as well as H^+ translocation and ATP synthesis.

9.3 Phenazine-dependent $F_{420}H_2$ dehydrogenation activity in methanol-grown Methanosarcina barkeri *Fusaro*

BLAST analyses of the unpublished genome of *Ms. barkeri* Fusaro indicated the presence of genes coding for a putative Fpo complex. However, kinetic profiles of the membrane-bound phenazine-dependent $F_{420}H_2$ dehydrogenation activities of CH_3OH-

grown *Ms. barkeri* Fusaro and *Ml. tindarius* are significantly different, indicating that the respective enzymes are likely dissimilar. Purification of the soluble and membrane-bound $F_{420}H_2$ dehydrogenation activity of *Ms. barkeri* Fusaro did not result in the isolation of the $F_{420}H_2$ dehydrogenase, but instead produced the F_{420} H_2ase. Our results indicate that the $F_{420}H_2$ dehydrogenation activity is highest when *Ms. barkeri* Fusaro is grown with CH_3OH as methanogenic substrate (Table 4.1), consistent with the findings of Mukhopadhyay *et al.* (1993), who reported that F_{420} H_2ase activity was highest in CH_3OH-grown cultures. The $F_{420}H_2$ dehydrogenation activity of *Ms. barkeri* Fusaro, associated with the F_{420} H_2ase, shares some similarities with the respective $F_{420}H_2$ dehydrogenase from *Ml. tindarius* and *Ms. mazei* Gö1.

While F_{420} H_2ase activity is comparable in *Ms. barkeri* Fusaro (0.034 μmol F_{420} reduced·min^{-1}) and *Ms. mazei* Gö1 (0.027 μmol F_{420} reduced·min^{-1}), neither *Ml. tindarius* nor *Methanosarcina acetivorans* have detectable F_{420} H_2ase activity (Deppenmeier *et al.* 1989, Galagan *et al.* 2002). It is not clear why significant levels of F_{420} H_2ase activity would be required in *Ms. barkeri* Fusaro during growth on CH_3OH, as $F_{420}H_2$ is produced during CH_3OH disproportionation (Deppenmeier *et al.* 1996). H_2 is produced during methanogenesis of CH_3OH-grown *Ms. barkeri* Fusaro (Ranalli *et al.* 1986), and it has been suggested that the function of F_{420} H_2ase in *Ms. barkeri* Fusaro may be to regulate levels of $F_{420}H_2$ and H_2 in CH_3OH-grown cultures, by acting as a redox valve (de Poorter *et al.* 2005). As one of the possible means for CoM-S-S-CoB-reduction during growth of *Ms. barkeri* Fusaro on CH_3OH, the H_2 produced *via* the F_{420} H_2ase could be obtained by the F_{420}-nonreducing hydrogenase (Vho) for CoM-S-S-CoB reduction (Figure 6.12B, Chapter 6), such that an $F_{420}H_2$ dehydrogenase would not be required.

It is not clear why a distinct $F_{420}H_2$ dehydrogenase is not produced under the growth conditions tested. It's possible that the H_2 produced during growth of CH_3OH-grown *Ms. barkeri* Fusaro may repress the expression of the *fpo* operon; since the cultures are grown in sealed bottles, H_2 would accumulate in the bottles and may be used as an electron source. Reverse transcriptase (RT) PCR could be used to confirm the absence of the Fpo complex in *Ms. barkeri* Fusaro. It is also possible that Fpo is being produced at levels to low for detection by our methods; RT PCR could be used to quantify the level of transcripts produced from the *fpo* operon.

9.4. The phenazine-dependent $F_{420}H_2$ dehydrogenation activity and electron transport in Methanosphaera stadtmanae

Our studies with *Msph. stadtmanae* focused on a phenazine-dependent $F_{420}H_2$ dehydrogenation activity, in the apparent absence of an F_{420} H_2ase (Deppenmeier *et al.* 1989, Wong *et al.* 1994, this thesis). This $F_{420}H_2$ dehydrogenation activity was distinct from similar activities in other methanoarchaea, in that the $F_{420}H_2$ dehydrogenation activity of *Msph. stadtmanae* is aerobically unstable, and much lower compared to other methanoarchaea (Table 4.1).

Due to its instability, the proteins involved in $F_{420}H_2$ dehydrogenation activity of *Msph. stadtmanae* could not be fully purified. In cell-free extract, the activity is stable for up to two weeks under anaerobic conditions, but rapidly declines during enrichment *via* column chromatography. The phenazine-dependent $F_{420}H_2$ dehydrogenation activity was partially characterized during the course of study, and sources for this activity in cell-free extract may have been revealed.

An F_{420} H_2ase activity was observed using the cell-free extract of *Msph. stadtmanae*, independent of the requirement for phenazine as coupling agent, as previously suggested (Table 7.6) (Wong, PhD thesis 1999). This activity required incubation under reducing conditions in the presence of FAD, at neutral pH. the putative F_{420} H_2ase could be a source of phenazine-dependent $F_{420}H_2$ dehydrogenation activity; the corresponding enzyme in *Msp. hungatei* GP1 and *Ms. barkeri* Fusaro contain phenazine-dependent $F_{420}H_2$ dehydrogenation activity. However, in contrast to similar activities in other methanoarchaea, the $F_{420}H_2$ dehydrogenation activity of *Msph. stadtmanae* is O_2 labile; this brings into question whether the observed $F_{420}H_2$ dehydrogenation activity is truly associated with the putative F_{420} H_2ase of *Msph. stadtmanae*.

Another source of phenazine-dependent $F_{420}H_2$ dehydrogenation activity may be the putative $F_{420}H_2$ oxidase. The genome of *Msph. stadtmanae* contains a gene encoding for $F_{420}H_2$ oxidase, an FMN-containing protein that detoxifies O_2 using $F_{420}H_2$ (Seedorf *et al.* 2004, Fricke *et al.* 2006); our studies have demonstrated O_2-dependent $F_{420}H_2$ oxidation using cell-free extract of *Msph. stadtmanae*. The proteins catalyzing $F_{420}H_2$-dependent phenazine-reduction or O_2-reduction, in cell-free extract, are aerobically unstable, and the respective activities decline at similar rates. While the activity is consistent with the presence of an $F_{420}H_2$ oxidase, these results must be interpreted with caution; the F_{420} H_2ase (from *Mtb. thermoautotrophicus* ΔH) also catalyzes the reduction of O_2 with $F_{420}H_2$ (Jacobson *et al.* 1982). Without further analysis, we cannot conclude that the observed $F_{420}H_2$-dependent O_2-reduction is the property of an $F_{420}H_2$ oxidase; RT

PCR could be a means to confirm and to quantify the presence of an $F_{420}H_2$ oxidase in *Msph. stadtmanae*.

The F_{420} H_2ase activity of *Msph. stadtmanae* was further examined. The properties of the F_{420} H_2ase activity, in cell-free extract, are similar to the corresponding activities of other methanoarchaea (Table 8.2); genomic analyses indicates that the genes encoding the putative F_{420} H_2ase are most closely related to the *frhAGDB* operon of *Mtb. thermoautotrophicus* ΔH. There are several features of the F_{420}-reducing activity that distinguish it from the activities of other methanoarchaea. Electrophoresis of protein extracts of *Msph. stadtmanae* on native PAGE gels do not indicate the presence of bands typical of an F_{420} H_2ase, as observed with other methano-archaea (Figure 8.1, Chaper 8).

The recently published genome of *Msph. stadtmanae* contains the gene sequences consistent with the presence of a putative F_{420} H_2ase (Fricke *et al.* (2006). It is not immediately clear if the observed F_{420}-reduction is due to the presence of the putative F_{420} H_2ase; RT PCR could be used to identify and to quantify the presence of transcripts coding for the F_{420} H_2ase in *Msph. stadtmanae*. Given the unexpected appearance of the F_{420} H_2ase activity in *Msph. stadtmanae*, it may also be worthwhile to use RT PCR to confirm the absence of F_{420} H_2ase in the *Methanosphaera cuniculi*, a closely related methanoarchaeon that also lacks F_{420} H_2ase activity (Biavati *et al.* 1988). There are other methanoarchaea that are not expected to possess an F_{420} H_2ase, including *Methanobacterium* strain G2R (McKellar and Sprott 1987), and *Ml. tindarius* (Deppenmeier *et al.* 1989); RT PCR could potentially be used to screen for the presence of transcripts encoding for a putative F_{420} H_2ase.

The results of this thesis show that while much of the methanogenic and electron transport pathways of the methanoarchaea have been elucidated, there may still be variations that arise in these pathways. After all, the five methanogenic orders contain widely diverse taxa with vast differences in morphology, physiological characteristics, and adaptations to different ecological niches (Bapteste *et al.* 2005). It should come as no surprise that a group as diverse as the methanoarchaea would have differences that may be unseen when information is derived from limited numbers of model organisms. The advent of increasingly sophisticated biochemical and genomic techniques through the years has aided in the study of these microorganisms and their unique physiologies, and will very likely lead to more interesting discoveries in the years to come.

References Cited

Abken, H-J. and U. Deppenmeier. 1997. Purification and properties of an $F_{420}H_2$ dehydrogenase from *Methanosarcina mazei* Gö1. FEMS Micro. Lett. 154:231-237

Abken, H-J., M. Tietze, J. Brodersen, S. Bäumer, U. Beifuss, and U. Deppenmeier. 1998. Isolation and characterization of methanophenazine and function of phenazines in membrane-bound electron transport of *Methanosarcina mazei* Gö1. J. Bacteriol. 180:2027-2032.

Adams, M.W.W., L.E. Mortenson, and J-S. Chen. 1981. Hydrogenase. Biochim. Biophys. Acta. 594:105-176

Adams, M.W.W., S.-L. C. Jin, J.-S. Chen, and L.E. Mortenson. 1986. The redox properties and activation of the F_{420}-non-reactive hydrogenase of *Methanobacterium formicicum*. Biochim. Biophys. Acta. 869:37-47

Afting, C., A. Hochheimer, and R.K. Thauer. 1998. Function of H_2-forming methylenetetrahydromethanopterin dehydrogenase from *Methanobacterium thermoautotrophicum* in coenzyme F_{420} reduction with H_2. Arch. Microbiol. 169:206-210.

Albracht, S.P.J. 1993. Intimate relationships of the large and the small subunits of all nickel hydrogenases with two nuclear-encoded subunits of mitochondrial NADH:ubiquinone oxidoreductase. Biochim. Biophys. Acta. 1144:221-224

Alex, L.A., J.N. Reeve, W.H. Orme-Johnson, and C.T. Walsh. 1990. Cloning, sequence determination, and expression of the genes encoding the subunits of the nickel-containing 8-hydroxy-5-deazaflavin reducing hydrogenase from *Methanobacterium thermoautotrophicum* ΔH. Biochemistry. 29:7237-7244

Allen, J.R., D.D. Clark, J.G. Krum, and S.A. Ensign. 1999. A role for coenzyme M (2-mercaptoethanesulfonic acid) in a bacterial pathway of aliphatic epoxide carboxylation. Proc. Natl. Acad. Sci. USA. 96:8432-8437

Altschul, S.F., W. Gish, W. Miller, E.W. Myers, and D.J. Lipman. 1990. Basic local alignment search tool. J. Mol. Biol. 215:403-410

Anthony, C. 1986. Bacterial oxidation of methane and methanol. Adv. Micro. Phys. 27:113-210

Aravalli, R.N., Q. She, and R.A. Garrett. 1998. Archaea and the new age or microorganisms. Trends in Ecology and Evolution. 13:190-194

Barker, H.A. 1956. *Bacterial Fermentations*. Wiley, New York.

Balch, W.E. and R.S. Wolfe. 1976. New approach to the cultivation of methanogenic bacteria: 2-mercaptoethanesulfonic acid (HS-CoM)-dependent growth of *Methanonbacterium ruminatium* in a pressurized atmosphere. Appl. Env. Micro. 32:781-791

Balch, W.E., G.E. Fox, L.J. Magrum, C.R. Woese, and R.S. Wolfe. 1979. Methanogens: Reevaluation of a Unique Biological Group. Microbiol. Rev. 43:260-296

Bapteste, É., C. Brochier, and Y. Boucher. 2005. Higher-level classification of the Archaea: evolution of methanogenesis and methanogens. Archaea. 1:353-363

Baron, S.F. and J.G. Ferry. 1989. Purification and properties of the membrane-associated coenzyme F_{420}-reducing hydrogenase from *Methanobacterium formicicum*. J. Bacteriol. 171:3846-3853

Baron, S.F., D.S. Williams, H.D. May, P.S. Patel, H.C. Aldrich, and J.G. Ferry. 1989b. Immunogold localization of coenzyme F_{420}-reducing formate dehydrogenase and coenzyme F_{420}-reducing hydrogenase in *Methanobacterium formicicum*. Arch. Microbiol. 151:307-313

Baross, J.A. and J.W. Deming. 1983. Growth of 'black smoker' bacteria at temperatures of at least 250°C. Nature. 303:423-426

Bartoschek, S., J.A. Vorholt, R.K. Thauer, B.H. Geierstanger, and C. Griesinger. 2000. *N*-Carboxymethanofuran (carbamate) formation from methanofuran and CO_2 in methanogenic archaea – Thermodynamics and kinetics of the spontaneous reaction. Eur. J. Biochem. 267:3130-3138

Bäumer, S., E. Murakami, J. Brodersen, G. Gottschalk, S.W. Ragsdale, and U. Deppenmeier. 1998. The $F_{420}H_2$:heterodisulfide oxidoreductase system from *Methanosarcina* species – 2-Hydroxyphenazine mediates electron transfer from $F_{420}H_2$ dehydrogenase to heterodisulfide reductase. FEBS Lett. 428:295-298

Bäumer, S., T. Ide, C. Jacobi, A. Johann, G. Gottschalk, and U. Deppenmeier. 2000. The $F_{420}H_2$ dehydrogenase is a redox-driven proton pump closely related to NADH dehydrogenases. J. Biol. Chem. 275:17968-17973

Baumgarten, A., I. Redenius, J. Kranczoch, and H. Cypionka. 2001. Periplasmic oxygen reduction by *Desulfovibrio* species. Arch. Microbiol. 176:306-309

Becher, B., V. Müller, and G. Gottschalk. 1992a. The methyltetrahydromethanopterin:coenzyme M methyltransferase of *Methanosarcina strain* Gö1 is a primary sodium pump. FEMS Microbiol. Lett. 91:239-244

Becher, B., V. Müller, and G. Gottschalk. 1992b. N^5-methyl-tetrahydromethanopterin:coenzyme M methyltransferase of *Methanosarcina* strain Gö1 is an Na^+-translocating membrane

protein. J. Bacteriol. 174:7656-7660

Becher, B. and V. Müller. 1994. $\Delta\mu_{Na}^{+}$ drives the synthesis of ATP *via* an $\Delta\mu_{Na}^{+}$-translocating F_1F_0-ATP synthase in membrane vesicles of the archaeon *Methanosarcina mazei* Gö1. J. Bact. 176:2543-2550

Beeder, J., R.K. Nilsen, J.T. Rosies, T. Torsvik, and T. Lien. 1994. *Archaeoglobus fulgidus* isolated from hot North Sea oil field waters. Appl. Environ. Microbiol. 60:1227-1231

Beifuss, U., M. Tietze, S. Bäumer, and U. Deppenmeier. 2000. Methanophenazine: Structure, total synthesis, and function of a new cofactor from methanogenic Archaea. Angew. Chem. Int. Ed. 39:2470-2472

Beifuss, U. and M.Tietze. 2005. Methanophenazine and other natural biologically active phenazines. Top. Curr. Chem. 244:77-113

Belay, Negash, R. Johnson, B.S. Rajagopal, E.C. De Macario, and L. Daniels. 1988. Methanogenic bacteria from human dental plaque. Appl. Environ. Microbiol. 54:600-603

Berk, H. and R.K. Thauer. 1997. Function of coenzyme F_{420}-dependent NADP reductase in methanogenic archaea containing an NADP-dependent alcohol dehydrogenase. Arch. Microbiol. 168:396-402

Bernstein, L.S., A.A.Grillo, S.S.Loranger, and M.E.Lindor. 2000. RGS4 binds to membranes through an amphipathic α-helix. J. Biol. Chem. 275:18520-18526

Biavati, B., M. Vasta, and J.G. Ferry. 1988. Isolation and characterization of "*Methanosphaera cuniculi*" sp. nov. Appl. Env. Microbiol. 54:768-771

Bingemann, R. and A. Klein. 2000. Conversion of the central [4Fe-4S] cluster into a [3Fe-4S] cluster leads to reduced hydrogen-uptake activity of the F_{420}-reducing hydrogenase of *Methanococcus voltae*. 267:6612-6618

Blaut, M., V. Müller, and G. Gottschalk. 1987. Proton translocation coupled to methanogenesis from methanol + hydrogen in *Methanosarcina barkeri*. FEBS Lett. 215:53-57

Bobik, T.A. and R.S. Wolfe. 1988. Physiological importance of the heterodisulfide of coenzyme M and 7-mercaptoheptanoylthreonine phosphate in the reduction of carbon dioxide to methane in Methanobacterium. Proc. Natl. Acad. Sci. USA. 85:60-63

Bobik, T.A. and R.S. Wolfe. 1989. J. Biol. Chem. 264:18714-18718

Bodelier, P.L., P. Rosiev, T. Henckel, and P.Frenzel. 2000. Stimulation by ammonium-based fertilizers of methane oxidation in soil around rice roots. Nature. 403:421-424

Boetius, A. K. Ravenschlag, C.J. Schubert, D. Rickert, F. Widdel, A. Gieseke, R. Amann, B.B. Jørgensen, U. Witte, and O. Pfannkuche. 2000. A marine microbial consortium apparently mediating oxidation of methane. Nature. 407:623-626

Bonacker, L.G., S. Baudner, E. Mörschel, R. Böcher, and R.K. Thauer. 1993. Properties of the two isoenzymes of methyl-coenzyme M reductase in *Methanobacterium thermoautotrophicum*. Eur. J. Biochem. 217:587-595

Boone, D.R., W.B. Whitman, and P. Rouvière. 1993. Diversity and taxonomy of methanogens. In *Methanogenesis. Ecology, physiology, biochemistry and genetics*. J.G. Ferry (ed.). Chapman and Hall, Inc. New York, pp. 35-80

Bradford, M. 1976. A rapid and sensitive method for the quantitation of microgram quantities of protein utilizing the principles of protein dye binding. Anal. Biochem. 72:248-254

Braks, I.J., M. Hoppert, S. Roge, and F.Mayer. 1994. Structural aspects and immunolocalization of the F_{420}-reducing and non-F_{420}-reducing hydrogenases from *Methanobacterium thermoautotrophicum* Marburg. J. Bacteriol. 176:7677-7687

Breitung, J. and R.K. Thauer. 1990. Formylmethanofuran:tetrahydromethanopterin formyl transferase from *Methanosarcina barkeri* – Identification of N5-formyltetrahydro-methanopterin as the product. FEBS Lett. 1,2:226-230

Brioukhanov, A., A. Netrusov, M. Sordel, R.K. Thauer, and S. Shima. Protection of *Methanosarcina barkeri* against oxidative stress: identification and characterization of an iron superoxide dismutase. Arch. Microbiol. 174:213-216

Brodersen, J., S. Bäumer, H-J. Abken, G. Gottschalk, and U. Deppenmeier. 1999. Inhibition of membrane-bound electron transport of the methanogenic archaeon *Methanosarcina mazei* Gö1 by diphenyleneiodonium. Eur. J. Biochem. 259:218-224.

Brodersen, J., G. Gottschalk, and U. Deppenmeier. 1999b. Membrane-bound $F_{420}H_2$ dependent heterodisulfide reduction in *Methanococcus voltae*. Arch Microbiol. 171:115-121

Brüggermann, H., F. Falinski, and U. Deppenmeier. 2000. Structure of the $F_{420}H_2$:quinone oxidoreductase of *Archaeoglobus fulgidus* - identification and overproduction of the $F_{420}H_2$-oxidizing subunit. Eur. J. Biochem. 267:5810-5814

Bult, C.J., O. White, G.J. Olsen, L. Zhou, R.D. Fleichmann, G.G. Sutton, J.A. Blake, L.M. Fitzgerald, R.A. Clayton, J.D. Gocayne, A.R. Kerlavage, B.A. Dougherty, J.F. Tomb, M.D. Adams, C.I. Reich, R. Overbeek, E.F. Kirkness, K.G. Weinstock, J.M. Merrick, A. Glodek, J.L. Scott, N.S.M. Geoghagen, and J.C. Venter. 1996. Complete genome sequence of the methanogenic archaeon, *Methanococcus jannaschii*. Science. 273:1058-1073

Buurman, G., S. Shima, and R.K. Thauer. 2000. The metal-free hydrogenase from methanogenic archaea: evidence for a bound cofactor. FEBS Lett. 200-204

Cammack, R. 1995. Splitting molecular hydrogen. Nature. 373:556-557

Cheeseman, P., A. Toms-Wood, and R.S. Wolfe. 1972. Isolation and properties of a fluorescent compound, Factor 420, from *Methanobacterium* strain M.o.H. J. Bacteriol. 112:527-531

Chen, Wei and J. Konisky. 1993. Characterization of a membrane-associated ATPase from *Methanococcus voltae*, a methanogenic member of the archaea. J. Bacteriol. 175:5677-5682

Chenna, R., H. Sugawara, T. Koike, R. Lopez, G. Rodrigo, J. Toby, D. Higgins, G. Desmond, J.D. Thompson. 2003. Multiple sequence alignment with the Clustal series of programs. Nucleic Acids Res. 31:3497-3500

Choquet, C.G. and G.D. Sprott. 1991. Metal chelate affinity chromatography for the purification of the F_{420}-reducing (Ni, Fe) hydrogenase of *Methanospirillum hungatei*. J. Microbiological Methods. 13:161-169

Cowan, D.A. 1992. Biotechnology of the archaea. TIBTECH. 10:315-323

Daniels, L. 1984. Biological methanogenesis: physiological and practical aspects. Trends in Biotech. 4:91-98

Daniels, L. and D. Wessels. 1984. A method for the spectrophotometeric assay of anaerobic enzymes. Anal. Biochem. 141:232-237

Daniels, L., N. Bakhiet, and K. Harmon. 1985. Widespread distribution of a 5-deazaflavin cofactor in Actinomyces and related bacteria. System. Appl. Microbiol. 6:12-17

Danson, M.J. 1988. Archaebacteria: The comparative enzymology of their central metabolic pathways. Adv. Microbial. Phys. 29:165-231

Das, A., J. Hugenholtz, H. van Halbeek, and L.G. Ljungdahl. 1989. Structure and function of a menaquinone involved in electron transport in membranes of *Clostridium thermoautotrophicum* and *Clostridium thermoaceticum*. J. Bact. 171:5823-5829

de Poorter, L.M., W.G. Geerts, A.P.R. Theuvenet, and J.T. Keltjens. 2003. Bioenergetics of the formyl-methanofuran dehydrogenase and heterodisulfide reductase reactions in *Methanothermobacter thermoautotrophicus*. Eur. J. Biochem. 270:66-75

de Poorter, L.M., W.J. Geerts, and J.T. Keltjens. 2005. Hydrogen concentrations in methane-forming cells probed by the ratios of reduced and oxidized coenzyme F_{420}. Microbiology. 151:1697-1705

Deppenmeier, U., M. Blaut, and G. Gottschalk. 1989. Dependence on membrane components of methanogenesis from methyl-CoM with formaldehyde or molecular hydrogen as electron donors. Eur. J. Biochem. 186:317-323

Deppenmeier, U., M. Blaut, A. Mahlmann, and G. Gottschalk. 1990a. Membrane-bound $F_{420}H_2$-dependent heterodisulfide reductase in methanogenic bacterium strain Gö1 and *Methanolobus tindarius*. FEBS Lett. 261:199-203

Deppenmeier, U., M. Blaut, A. Mahlmann, and G. Gottschalk. 1990b. Reduced coenzyme F_{420}:heterodisulfide oxidoreductase, a proton-translocating redox system in a methanogenic bacteria. Proc. Natl. Acad. Sci. USA. 87:9449-9453

Deppenmeier, U., M. Blaut, and G. Gottschalk. 1991. H_2:heterodisulfide oxidoreductase, a second energy-conserving system in the methanogenic strain Gö1. Arch. Microbiol. 155:272-277

Deppenmeier, U., M. Blaut, B. Schmidt, and G. Gottschalk. 1992. Purification and properties of a F_{420}-nonreactive, membrane-bound hydrogenase from *Methanosarcina* strain Gö1. Arch. Microbiol. 157:505-511

Deppenmeier, U. 1995. Different structure and expression of the operons encoding the membrane-bound hydrogenases from *Methanosarcina mazei* Gö1. Arch. Microbiol. 164:370-376

Deppenmeier, U., V. Müller, and G. Gottschalk. 1996. Pathways of Energy Conservation in Methanogenic Archaea. Arch. Microbiol. 165:149-163

Deppenmeier, U., T. Lienard, and G. Gottschalk, 1999. Novel reactions involved in energy conservation by methanogenic archaea. FEBS Lett. 457:291-297

Deppenmeier, U. A. Johann, T. Hartsch, R. Merkl, R.A. Schmitz, R. Martinez-Arias, A. Henne, A. Wiezer, S. Bäumer, C. Jacobi, H. Brüggermann, T. Lienard, A. Christmann, M. Bömeke, S. Steckel, A. Bhattacharyya, R. Overbeek, H.-P. Klenk, R.P. Gunsulus, H.-J. Fritz, and G. Gottschalk. 2002. The genome of *Methanosarcina mazei*: evidence for lateral gene transfer between bacteria and Archaea. J. Mol. Microbiol. Biotechnol. 4:453-461

Deppenmeier, U. 2002. Redox-driven Proton Translocation in Methanogenic Archaea. Cell. Mol. Life. Sci. 59:1513-1533

Deppenmeier, U. 2004. The membrane-bound electron transport system of Methanosarcina species. J. Bioenerg. Biomem. 36:55-64

Dickinson, R.E. and R.J. Cicerone. 1986. Future global warming from atmospheric trace gases.

Nature. 319:109-115

DiMarco, A.A., T.A. Bobik, and R.S. Wolfe. 1990. Unusual coenzymes of methanogenesis. Annu. Rev. Biochem. 59:355-94

Ding, Y-H. R. and J.G. Ferry. 2004. Flavin mononucleotide-binding flavoprotein family in the domain *Archaea*. J. Bacteriol. 186:90-97

Dongowski, G., A. Lorenz, and H. Anger. 2000. Degradation of pectins with different degrees of esterification by *Bacteroides thetaiotaomicron* isolated from human gut flora. Appl. Environ. Micro. 66:1321-1327

Donnelly, M.I. and S. Dagley. 1980. Production of methanol from aromatic acids by *Pseudomonas putida*. J. Bacteriol. 142:916-924

Dybas, M. and J. Konisky. 1992. Energy transduction in the methanogen *Methanococcus voltae* is based on a sodium current. J. Bacteriol. 174:5575-5583

Edward, B. and H. Maden. 2000. Tetrahydrofolate and tetrahydromethanopterin compared: functionally distinct carriers in C1 metabolism. Biochem. J. 350: 609-629

Eirich, L.D., G.D. Vogels, and R.S. Wolfe. 1978. Proposed structure for coenzyme F_{420} from *Methanobacterium*. Biochemistry. 17:4583-4593

Eirich, L.D., G.D. Vogels, and R.S. Wolfe. 1979. Distribution of coenzyme F_{420} and properties of its hydrolytic fragments. J. Bacteriol. 140:20-27

Elias, D.A., D.F. Juck, K.A. Berry, and R. Sparling. 2000. Purification of the $NADP^+$:F_{420} oxidoreductase of *Methanosphaera stadtmanae*. Can. J. Microbiol. 46:998-1003

Ellefson, W.L., W.B. Whitman, and R.S. Wolfe. 1982. Nickel-containing F_{430}: chromophore of the methylreductase of *Methanobacterium*. Proc. Natl. Acad. Sci. USA. 79:3707-3710

Ellermann, J., A. Kobelt, A. Pfaltz, and R.K. Thauer. 1987. On the role of *N*-7-mercaptoheptanoyl-*O*-phospho-L-threonine (component B) in the enzymatic reduction of methyl-coenzyme M to methane. FEBS Lett. 220:358-362

Ellermann, J., R. Hedderich, R. Böcher, R.K. Thauer. 1988. The final step in methane formation. Investigations with highly purified methyl-CoM reductase (Component C) from *Methanobacterium thermoautotrophicum* (strain Marburg). Eur. J. Biochem. 172:669-677

Ermler, U., W. Grabase, S. Shima, M. Goubeaud, and R.K. Thauer. 1997. Crystal structure of methyl-coenzyme M reductase: The key enzyme of biological methane production. Science. 278:1457-1462

Escalante-Semerena, J.C., J. A. Leigh, K.L. Rinehart, JR, and R.S. Wolfe. 1984a. Formaldehyde activation factor, tetrahydromethanopterin, a coenzyme of methanogenesis. Proc. Natl. Acad. Sci. USA. 81:1976-1980

Escalante-Semerena, J.C., K.L. Rinehart, JR, and R.S. Wolfe. 1984b. Tetrahydromethanopterin, a carbon carrier in methanogenesis. J. Biol. Chem. 259:9447-9455

Fauque, G., M. Teixeira, I. Moura, P.A. Lespinat, A.V. Xavier, D.V. der Vertaian, H.D. Peck Jr, J. LeGall, and J.G. Moura. 1984. Purification, characterization, and redox properties of hydrogenase from *Methanosarcina barkeri* (DSM 800). Eur. J. Biochem. 142:21-28

Ferry, J.G., P.H. Smith, and R.S. Wolfe. 1974. *Methanospirillum*, a new genus of methanogenic bacteria, and characterization of *Methanospirillum hungatii*, sp. nov. Int. J. Sys. Bac. 24:465-469

Ferry, J.G. 1990. Formate dehydrogenase. FEMS Microbiol. Rev. 87:377-382

Ferry, J.G. 1993. Fermentation of acetate. In *Methanogenesis. Ecology, physiology, biochemistry and genetics*. J.G. Ferry (ed.). Chapman and Hall, Inc. New York, pp. 304-334

Ferry, J.G. 1997. Methane: Small molecule, big impact. Science. 278:1413-1414

Ferry, J.G. 1999. Enzymology of one-carbon metabolism in methanogenic pathways. FEMS Microbiol. Rev. 23:13-38

Fetzer, S., F. Bak, and R. Conrad. 1993. Sensitivity of methanogenic bacteria from paddy soil to oxygen and dessication. FEMS Microbiol Ecol. 12:107-115

Fiebig, K. and B. Friedrich. 1989. Purification of the F_{420}-reducing hydrogenase from *Methanosarcina barkeri* (strain Fusaro). Eur. J. Biochem. 184:79-88

Fox, J.A., D.J. Livingston, W.H. Orme-Johnson, and C.T. Walsh. 1987. 8-hydroxy-5-deazaflavin-reducing hydrogenase from *Methanobacterium thermoautotrophicum*: 1. Purification and characterization. Biochemistry. 26:4219-4227

Fox, J.D., R.L. Kerby, G.P. Roberts, and P.W. Ludden. 1996a. Characterization of the CO-induced, CO-tolerant hydrogenase from *Rhodospirillum rubrum* and the gene encoding the large subunit of the enzyme. J. Bacteriol. 178:1515-1524

Fox, J.D., Y. He, D. Shelver, G.P. Roberts, and P.W. Ludden. 1996b. Characterization of the region encoding the CO-induced hydrogenase of *Rhodospirillum rubrum*. J. Bacteriol. 178:6200-6208

Fricke, W.F., S. Henning, A. Henne, M. Krüer, H. Liesegang, R. Hedderich, G. Gottschalk, and R.K. Thauer. 2006. The genome sequence of *Methanosphaera stadtmanae* reveals why this human intestinal archaeon is restricted to methanol and H_2 for methane formation and ATP synthesis. J. Bacteriol. 188:642-658

Friedrich, B., E. Heine, A. Finck, and C.G. Friedrich. 1981. Nickel requirement for active hydrogenase formation in *Alcaligenes eutrophus*. J. Bacteriol. 145:1449

Friedrich, T. and H. Weiss. 1997. Modular evolution of the respiratory NADH:ubiquinone oxidoreductase and the origin of its modules. J. Theor. Biol. 187:529-540

Friedrich, T. 1998. The NADH:ubiquinone oxidoreductase (complex I) from *Escherichia coli*. Biochim. Biophys. Acta. 1364:134-146

Friedrich, T. and D. Scheide. 2000. The Respiratory complex I of bacteria, archaea and eukarya and its module common with membrane-bound multisubunit hydrogenases. Febs Lett. 479:1-5

Fuchs, G., E. Stupperich, and R.K. Thauer. 1978. Acetate assimilation and the synthesis of alanine, aspartate, and glutamate in *Methanobacterium thermoautotrophicum*. Arch. Microbiol. 117:61-66

Galagan, J.E., C. Nusbaum, A. Roy, M.G. Endrizzi, P. Macdonald, W. FitzHugh, S. Calvo, R. Engels, S. Smirnov, D. Atnoor, A. Brown, N. Allen, J. Naylor, N. Stange-Thomann, K. DeArellano, R. Johnson, L. Linton, P. McEwan, K. McKernan, J. Talamas, A. Tirrell, W. Ye, A. Zimmer, R.D. Barber, I. Cann, D.E. Graham, D.A. Grahame, A.M. Guss, R. Hedderich, C. Ingram-Smith, H.C. Kuettner, J.A. Krycki, J.A. Leigh, W. Li, J. Liu, B. Mukhopadhyay, J.N. Reeve, K. Smith, T.A. Springer, L.A. Umayam, O. White, R.H. White, E. Conway de Macario, J.G. Ferry, K.F. Jarrell, H. Jing, A.J.L. Macario, I. Paulsen, M. Pritchett, K.R. Sowers, R.V. Swanson, S.H. Zinder, E. Lander, W.W. Metcalf, and B. Birren. 2002. The genome of *M.acetivorans* reveals extensive metabolic and physiological diversity. Genome.Res. 12:532-542

Garcia, J-L. 1998. Les bactèries méthanogènes (The methanogenic archaea). C.R. Acad. Fr. 84:23-33

Garcia, J.-L., B.K.C. Patel, and B. Ollivier. 2000. Taxonomic, phylogenetic, and ecological diversity of methanogenic *archaea*. Anaerobe. 6:205-226

Gärtner, P., A. Ecker, R. Fischer, D. Linder, G. Fuchs, and R.K. Thauer. 1993. Purification and properties of N^5-methyltetrahydromethanopterin:coenzyme M methyltransferase from *Methanobacterium thermoautotrophicum*. Eur. J. Biochem. 213:537-545

Gärtner, P., D.S. Weiss, U. Harms, and R.K. Thauer. 1994. N^5-methyltetrahydro-methanopterin:coenzyme M methyltransferase from *Methanobacterium*

thermoautotrophicum- Catalytic mechanism and sodium ion dependence. Eur. J. Biochem. 226:465-472

Gloss, L.M. and R.P. Hausinger. 1988. Methanogen factor 390 formation: species distribution, reversibility and effects of non-oxidative cellular stresses. Biofactors. 1:237-40
Gribbin, J. 1988. The greenhouse effect. New Scientist. October 22:1-4

Grahame, D.A. 1989. Different isoenzymes of methylcobalamin:2-mercaptoethanesulfonate methyltransferase predominate in methanol- versus acetate-grown *Methanosarcina barkeri*. J. Biol. Chem. 264:12890-12894

Gunsalus, R.P. and R.S. Wolfe. 1977. Stimulation of CO2 reduction to methane by methyl-coenzyme M in extracts of *Methanobacterium*. Biochem. Biophys. Res. Commun. 76:790-795

Gunsalus, R., J.A. Romesser, and R.S. Wolfe. 1978. Preparation of coenzyme M analogues and their activity in the methyl coenzyme M reductase system of *Methanobacterium thermoautotrophicum*. Biochemistry. 17:2374-2377

Haase, P., U. Deppenmeier, M. Blaut, and G. Gottschalk. 1992. Purification and characterization of $F_{420}H_2$-dehydrogenase from *Methanolobus tindarius*. Eur. J. Biochem. 203:527-531

Halboth, S. and A. Klein. 1992. *Methanococcus voltae* harbours four gene clusters potentially encoding two [NiFe] and two [NiFeSe] hydrogenases, each of the cofactor F_{420}-reducing or F_{420}-nonreducing types. Mol. Gen. Genet. 233:217-234

Hallam, S.J., N. Putnam, C.M. Preston, J.C. Detter, D. Rokhsar, P.M. Richardson, and E.F. Delong. 2004. Reverse methanogenesis: Testing the hypothesis with environmental genomics. Science. 305: 1457-1462

Harms, U., D.S. Weiss, P. Gärtner, D. Linder, and R.K. Thauer. 1995. The energy conserving N^5-methyltetrahydromethanopterin:coenzyme M methyltransferase complex from *Methanobacterium thermoautotrophicum* is composed of eight different subunits. Eur. J. Biochem. 228:640-448

Harms, U. and R.K. Thauer. 1996. Methylcobalamin:coenzyme M methyltransferase isoenzymes MtaA and MtbA from *Methanosarcina barkeri* – Cloning, sequencing and different transcription of the encoding genes, and functional overexpression of the mtaA gene in *Escherichia coli*. Eur. J. Biochem. 235:653-659

Harris, E.L.V. 1995. Concentration of the extract. In *Protein purification methods – A practical approach*. E.L.V. Harris and S.Angal, (Eds). Oxford University Press, New York, pp. 124-174

Hartmann, G.C., A.R. Klein, M. Linder, and R.K. Thauer. 1996. Purification, properties and primary structure of H_2-forming N^5-N^{10}-methylenetetrahydropmethanopterin dehydrogenase from *Methanococcus thermolithotrophicus*. Arch. Microbiol. 165:187-193

Hausinger, R.P., W.H. Orme-Johnston, and C. Walsh. 1985. Factor 390 chromophores: phosphodiester between AMP or GMP and methanogen cofactor F_{420}. Biochemistry. 24:1629-1633

Hedderich, R. A. Berkessel, and R.K. Thauer. 1989. Catalytic properties of the heterodisulfide reductase involved in the final step of methanogenesis. FEBS Lett. 255:67-71

Hedderich, R. A. Berkessel, and R.K. Thauer. 1990. Purification and properties of heterodisulfide reductase from *Methanobacterium thermoautotrophicum* (strain Marburg). Eur. J. Biochem. 193:255-261

Hedderich, R., S.P.J. Albracht, D. Linder, J. Koch, and R.K. Thauer. 1992. Isolation and characterization of polyferredoxin from *Methanobacterium thermoautotrophicum*. 298:65-68

Hedderich, R., J. Koch, D. Linder, and R.K. Thauer. 1994. The heterodisulfide reductase from *Methanobacterium thermoautotrophicum* contains sequence motifs characteristic of pyridine-nucleotide-dependent thioredoxin reductases. Eur. J. Biochem.

Hedderich, R. 2004. Energy-converting [NiFe] hydrogenases from Archaea and extremophiles: ancestors of complex I. J. Bioenerg. Biomem. 36:65-75

Heiden, S., R. Hedderich, E. Setzke, and R.K. Thauer. 1993. Purification of a cytochrome b containing H_2:heterodisulfide oxidoreductase complex from membranes of *Methanosarcina barkeri*. Eur. J. Biochem. 213:529-535

Heiden, S., R. Hedderich, E. Setzke, and R.K. Thauer. 1994. Purification of a two-subunit cytochrome-*b*-containing heterodisulfide reductase from methanol-grown *Methanosarcina barkeri*. Eur. J. Biochem. 221:855-861

Heine-Dobbernack, E., S.M. Schoberth, and H. Sahm. 1988. Relationship of intracellular conenzyme F_{420} content to growth and metabolic activity of *Methanobacterium bryantii* and *Methanosarcina barkeri*. Appl. Environ. Micro. 54:454-459

Hippe, H., D. Caspari, K. Fiebig, and G. Gottschalk. 1979. Utilization of trimethylamine and other *N*-methyl compounds for growth and methane formation by *Methanosarcina barkeri*. Proc. Natl. Acad. Sci. USA. 76:494-498

Hochheimer, A., R.A. Schmitz, R.K. Thauer, and R. Hedderich. 1995. The tungsten

formylmethanofuran dehydrogenase from *Methanobacterium thermoautotrophicum* contains sequence motifs characteristic for enzymes containing molybdopterin dinucleotide. Eur. J. Biochem. 234:910-920

Hochheimer, A., D. Linder, R.K. Thauer, and R. Hedderich. 1996. The molybdenum formylmethanofuran dehydrogenase operon and the tungsten formylmethanofuran dehydrogenase from *Methanobacterium thermoautotrophicum* – structures and transcriptional regulation. Eur. J. Biochem. 242:156-162

Hua, S. and Z. Sun. 2001. 2001. Support vector machine approach for protein subcellular localization prediction. Bioinformatics. 8:721-728

Huber, H., M.J. Hohn, R. Rachel, T. Fuchs, V.C. Wimmer, and K.O. Stetter. 2002. A new phylum of Archaea represented by a nano-sized hyperthermophilic symbiont. Nature. 417:63-67

Hungate, R.E. 1950. The anaerobic mesophilic cellulolytic bacteria. Bacteriol. Rev. 14:1-49

Ide, T., S. Bäumer, and U. Deppenmeier. 1999. Energy conservation by the H_2:heterodisulfide oxidoreductase from *Methanosarcina mazei* Gö1: Identification of two proto-translocating segments. J. Bacteriol. 181:4076-4080

Imlay, J.A. 2006. Iron-sulphur clusters and the problem with oxygen. Mol. Micro. 59:1073-1082

Ingram, J.M. and A.C. Blackwood. Year?. Microbial production of phenazines. Journal?. Vol and pages?

Jacobson, F.S., L. Daniels, J.A. Fox, C.T. Walsh, and W.H. Orme-Johnson. 1982. Purification and properties of an 8-hydroxy-5-deazaflavin-reducing hydrogenase from *Methanobacterium thermoautotrophicum*. J. Biol. Chem. 257:3385-3388

Jacobson, F. and C. Walsh. 1984. Biochemistry. 15:1054-1063

Jarrell, KF., J.R. Colvin, and G.D. Sprott. 1982. Spontaneous protoplast formation in *Methanobacterium bryantii*. J. Bacteriol. 149:346-353

Jetten, M.S.M., A.J.M. Stams, and A.J.B. Zehnder. 1992. Methanogenesis from acetate: a comparison of the acetate metabolism in *Methanothrix soehngenii* and *Methanosarcina* spp. FEMS Microbiol. Rev. 88:181-198

Jin, S.-L.C., D.K. Blanchard, and J.-S. Chen. 1983. Two hydrogenases with distinct electron-carrier specificity and subunit composition in *Methanobacterium formicicum*. Biochim. Biophys. Acta. 748:8-20

Junge, W., H. Lill, and S. Engelbrecht. 1997. ATP synthase: an electrochemical transducer with

rotatory mechanics. TIBS. 22:420-423

Kaesler, B. and P. Schönheit. 1989a. The role of sodium ions in methanogenesis. Formaldehyde oxidation to CO_2 and $2H_2$ in methanogenic bacteria is coupled with primary electrogenic Na^+ translocation at a stoichiometry of 2-3 Na^+/CO_2. Eur. J. Biochem. 184:223-232

Kaesler, B. and P. Schönheit. 1989b. The role of sodium ions in methanogenesis. CO_2 reduction to the formaldehyde level in methanogenic bacteria is coupled by a primary electrochemical potential of Na^+ generated by formaldehyde reduction to CH_4. Eur. J. Biochem. 186:309-316

Kamekura, M. 1998. Diversity of extremely halophilic bacteria. Extremophiles. 2:289-295

Kamlage, B. and M. Blaut. 1992. Characterization of cytochromes from *Methanosarcina* strain Gö1 and their involvement in electron transport during growth on methanol. J. Bacteriol. 174:3921-3927

Karrasch, M, G. Borner, and R.K. Thauer. 1990. The molybdenum cofactor of formylmethanofuran dehydrogenase from *Methanosarcina barkeri* is a molybdopterin guanine dinucleotide. FEBS Lett. 274:48-52

Kato, M.T., J.A. Field, and G. Lettinga. 1993. Methanogenesis in granular sludge exposed to oxygen. FEMS Microbiol. Lett. 114:317-324

Kell, D.B., H.J. Doddema, J.G. Morris, and G.D. Vogels. 1980. Energy coupling in methanogens. In *Proceedings of the third international symposium of microbial growth on C1 compounds*. pp.1288-1293

Keltjens, J.T., M.J. Huberts, W.H. Laarhoven, and G.D. Vogels. 1983. Structural elements of methanopterin, a novel pterin present in *Methanobacterium thermoautotrophicum*. Eur. J. Biochem. 130:537-544

Keltjens, J.T. and G.D. Vogels. 1993. Conversion of methanol and methylamines to methane and carbon dioxide. In *Methanogenesis. Ecology, physiology, biochemistry and genetics*. J.G. Ferry (ed.). Chapman and Hall, Inc. New York, pp. 209-252

Kemner, J.M. and J.G. Zeikus. 1994. Purification and characterization of membrane-bound hydrogenase from *Methanosarcina barkeri* MS. Arch. Microbiol. 161:47-54

Kemner, J.M. and J.G. Zeikus. 1994b. Regulation and function of ferredoxin-linked versus cytochrome b-linked hydrogenase in electron transfer and energy metabolism of Methanosarcina barkeri MS. Arch. Microbiol. 162:26-32

Kengen, S.W., H. W. von den Hoff, J.T. Keltjiens, C. van der Drift, and G.D. Vogels. 1991. Hydrolysis and reduction of factor 390 by cell extracts of *Methanobacterium*

thermoautotrophicum (strain ΔH). J. Bacteriol. 173:2283-2288

Kiener, A. and T. Leisinger. 1983. Oxygen sensitivity of methanogenic bacteria. Sys. Appl. Microbiol. 4:305-312

Kiener, A., R. Gall, T. Rechsteiner, and T. Leisinger. 1985. Arch. Microbiol. 143:147-150

Kiener, A., W.H. Orme-Johnson, and C.T. Walsh. 1988. Reversible conversion of coenzyme F_{420} to the 8-OH-AMP and 8-OH-GMP esters, F_{390}-A and F_{390}-G, on oxygen exposure and reestablishment of anaerobiosis in *Methanobacterium thermoautotrophicum*. Arch. Microbiol. 150:249-253

Kilgore, W.C. 1993. Greenhouse Gases and Global Climate Change. In Emissions of Greenhouse Gases in the United States 1985-1990. Energy Information Administration. Washington, DC. pp.1-10

Klein, A.R., J. Koch, K.O. Stetter, and R.K. Thauer. 1993. Two N^5, N^{10}-methylenetetrahydromethanopterin dehydrogenases in the extreme thermophile *Methanopyrus kandleri*: characterization of the coenzyme F_{420} enzyme. Arch. Microbiol. 160:186-192

Klenk, H.-P., R.A. Clayton1, J.-F. Tomb, O. White, K.E. Nelson, K. A. Ketchum, R. J. Dodson, M. Gwinn, E.K. Hickey, J.D. Peterson, D.L. Richardson, A.R. Kerlavage, D.E. Graham, N.C. Kyrpides, R.D. Fleischmann, J. Quackenbush, N.H. Lee, G.G. Sutton, S. Gill, E.F. Kirkness, B.A. Dougherty, K. McKenney, M.D. Adams, B. Loftus, S. Peterson, C.I. Reich, L.K. McNeil, J.H. Badger, A. Glodek, L. Zhou, R. Overbeek, J.D. Gocayne, J.F. Weidman, L. McDonald, T. Utterback, M.D. Cotton, T. Spriggs, P. Artiach, B.P. Kaine, S.M. Sykes, P.W. Sadow, K.P. D'Andrea, C. Bowman, C. Fujii, S.A. Garland, T. M. Mason, G. J. Olsen, C.M. Fraser, Hamilton O. Smith, C.R. Woese, and J.C. Venter. 1997. The complete genome sequence of the hyperthermophilic, sulphate-reducing archaeon *Archaeoglobus fulgidus*. Nature. 390:364-370

Kojima,k N., J.A. Fox, R.P. Hausinger, L. Daniels, W.H. Orme-Johnson, and C.T. Walsh. 1983. Paramagnetic centers in the nickel-containing, deazaflavin reducing hydrogenase of *Methanobacterium thermoautotrophicum*. Proc. Natl. Acad. Sci. USA. 80:378-382

König, H. and K.O. Stetter. 1982. Isolation and characterization of *Methanolobus tindarius*, sp. nov., a coccoid methanogen growing only on methanol and methylamines. Zbl. Bakt. Hyg., I. Abt. Orig. C. 3:478-490

Kral, T.A. and K.M. Brink. 1998. Hydrogen consumption by methanogens on the early Earth. Origins Life Evol. Biosphere. 28:311-319

Kristjansson, J.K., P. Schönheit, and R.K. Thauer. 1982. Different K_s values for hydrogen of

methanogenic bacteria and sulfate reducing bacteria: An explanation for the apparent inhibition of methanogenesis by sulfate. Arch. Microbiol. 131:278-282

Kuhn, W., K. Fiebig, H. Hippe, R.A. Mah, B.A. Huser, and G. Gottschalk. 1983. Distribution of cytochromes in methanogenic bacteria. FEMS Microbiol. Lett. 20:407-410

Künkel, A., M. Vaupel, S. Heim, R.K. Thauer, and R. Hedderich. 1997. Heterodisulfide reductase from methanol-grown cells of *Methanosarcina barkeri* is not a flavoenzyme. Eur. J. Biochem. 244:226-234

Künkel, A., J.A. Vorholt, R.K. Thauer, and R. Hedderich. 1998. An *Escherichia coli* hydrogenase-3-type in methanogenic archaea. Eur. J. Biochem. 252:467-476

Kunow, J., D. Linder, K.O. Stetter, and R.K. Thauer. 1994. $F_{420}H_2$:heterodisulfide quinone oxidoreductase from *Archaeoglobus fulgidus*. Characterization of a membrane-bound multisubunit complex containing FAD and iron-sulfur clusters. Eur. J. Biochem. 223:503-511

Laemmli, U.K. 1970. Cleavage of structural proteins during the assembly of the head of bacteriophage T4. Nature. 227:680-685

Latimer, M.T., M.H. Painter, and J.G. Ferry. 1996. Characterization of an iron-sulfur flavoprotein from *Methanosarcina thermophila*. J. Biol. Chem. 271:24023-24028

Leigh, J.A. and R.S. Wolfe. 1983. J. Biol. Chem. 258:7536-7540

Leigh, J.A., K.L. Rinehart Jr., and R.S. Wolfe. 1984. Structure of methanofuran, the carbon dioxide reduction factor of *Methanobacterium thermoautotrophicum*. J. Am. Chem. Soc. 106:3636-3640

Leigh, J.A., . Rinehart Jr., and R.S. Wolfe. 1985. Methanofuran (carbon dioxide reduction factor), a formyl carrier in methane production from carbon dioxide in *Methanobacterium*. Biochemistry. 24:995-999

Lemos, R.S., C.M.Gomes, and M.Teixeira. 2001. *Acidianus ambivalens* complex II typifies a novel family of succinate dehydrogenases. Biochem. Biophys. Res. Commun. 281:141-150

LePaglia, C. and P.L. Hartzell. 1997. Stress-induced production of biofilm in the hyperthermophile *Archaeoglobus fulgidus*. Appl. Environ. Micro. 63:3158-3163

Levitt, M.D. 1970. Oxygen tension in the gut. New Engl. J. Med. 282:1039-1040

Lienard, T. and G. Gottschalk. 1998. Cloning, sequencing, and expression of the genes encoding the sodium translocating N^5-methyltetrahydromethanopterin:coenzyme M

methyltransferase of the methylotrophic archaeon *Methanosarcina mazei* Gö1. FEBS Lett. 425:204-208

Li, Q., L.Li, T.Rejtar, D.J.Lessner, B.L.Karger, and J.G.Ferry. 2006. Electron transport in the pathway of acetate conversion to methane in the marine archaeon *Methanosarcina acetivorans*. J. Bacteriol. 188:702-710

Lin, X-L. and R. White. 1986. Occurrence of conenzyme F_{420} and its (-monoglutamyl derivative in nonmethanogenic archaebacteria. J. Bacteriol. 168:444-448

Lin, Z. and R. Sparling. 1995. Oxidation-reduction of methanol, formaldehyde, serine, and formate in *Methanosphaera stadtmanae* using ^{14}C short- and long-term labeling. Can. J. Microbiol. 41:1048-1053

Lin, Z. and R. Sparling. 1998. Investigation of serine hydroxymethyltransferase in methanogens. Can. J. Microbiol. 44:652-656.

Lissolo, T., S. Pulvin, and D. Thomas. 1984. Reactivation of the hydrogenase from *Desulfovibrio gigas* by hydrogen – Influence of redox potential. J. Biol. Chem. 259:11725-11729

Lloyd, K., L. Lapham, and A. Teske. 2006. An anerobic methane-oxidizing community of ANME-1b Archaea in hypersaline Gulf of Mexico sediments. Appl. Env. Micro. 72:7218-7230

Lorius, C., J. Jouzel, D. Raynaud, J. Hansen, and H. Le Treut. 1990. The ice-core record: climate sensitivity and future greenhouse warming. Nature. 347:139-145

Lumppio, H.L., N.V. Shenvi, A.O. Summers, G. Voordouw, and D.M. Kurtz, Jr. Rubrerythrin and rubredoxin oxidoreductase in *Desulfovibrio vulgaris*: a novel oxidative stress protection system. J. Bacteriol. 183:101-108

Lünsdorf, H., M. Niedrig, and K. Fiebig. 1991. Immunocytochemical localization of the coenzyme F_{420}-reducing hydrogenase in *Methanosarcina barkeri* Fusaro. J. Bacteriol. 173:978-984

Lyons, E.J., S. Shima, G. Buurman, S. Choudhuri, A. Batschauer, K. Steinbach, and R.K. Thauer. 2004. UV-A/blue-light inactivation of the 'metal-free' hydrogenase (HMD) from methanogenic archaea. The enzyme contains functional iron after all. Eur. J. Biochem. 271:195-204

Ma, K. and R.K. Thauer. 1990.Purification and properties of N^5,N^{10}-methylenetetrahydromethanopterin reductase from *Methanobacterium thermoautotrophicum* (strain Marburg). Eur. J. Biochem. 191:187-193

Ma, K.S. and R.K. Thauer. 1990b. N^5,N^{10}-methylenetetrahydromethanopterin reductase from

Methanosarcina barkeri. FEMS Microbiol. Lett. 70:119-124

Ma, K., C. Zirngibl, D. Linder, K.O. Stetter, and R.K. Thauer. 1991. N^5-N^{10}-methylenetetrahydropmethanopterin dehydrogenase (H_2-forming) from the extreme thermophile *Methanopyrus kandleri*. Arch. Microbiol. 156:43-48

Maeder, D.L., I. Anderson, T.S. Brettin, D.C. Bruce, P. Gilna, C.S. Han, A. Lapidus, W.W. Metcalf, E. Saunders, R. Tapia, and K.R. Sowers. The *Methanosarcina barkeri* genome: Comparative analysis with *Methanosarcina acetivorans* and *Methanosarcina mazei* reveals extensive rearrangement within Methanosarcinales genomes. J. Bacteriol. 188:7922-7931

Maeshima, M. 2000. Vacuolar H^+-pyrophosphatase. Biochim. Biophys. Acta. 1465:37-51

Mah, R.A. 1982. Methanogenesis and methanogenic partnerships. Phil. Trans. R. Soc. Lond. 297:599-616

Majander, A., M. Finel, and M. Wikström. 1994. Diphenyleneiodonium inhibits reduction of iron-sulfur clusters in the mitochondrial NADH-ubiquinone oxidoreductase (complex I). J. Biol. Chem. 269:21037-21042

Mayer, H.P. and R. Conrad. 1990. Factors influencing the population of methanogenic bacteria and the initiation of methane production upon flooding of paddy soil. FEMS Microbiol. Ecol. 73:103-112

McBride, B.C. and R.S. Wolfe. 1971. Biochemistry. 10:2317-2324

McInerney, M.J., M.P. Bryant, and N. Pfenning. 1979. Anaerobic bacterium that degrades fatty acids in syntrophic association with methanogens. Arch. Microbiol. 122:129-135

McCay, C.P. and H.D. Smith. 2005. Possibilities for methanogenic life in liquid methane on the surface of Titan. Icarus. 178:274-276

McKellar, R.C. and G.D. Sprott. 1979. Solubilization and properties of a particulate hydrogenase from *Methanobacterium* strain G2R. J. Bacteriol. 139:231-238

Meuer, J., S. Bartoschek, J. Koch, A. Künkel, and R. Hedderich. 1999. Purification and catalytic properties of Ech hydrogenase from *Methanosarcina barkeri*. Eur. J. Biochem. 265:325-335

Meuer, J., H.C. Kuettner, J.K. Zhang, R. Hedderich, and W.W. Metcalf. 2002. Genetic analysis of the archaeon *Methanosarcina barkeri* Fusaro reveals a central role for Ech hydrogenase and ferredoxin in methanogenesis and carbon fixation. Proc. Natl. Acad.

Sci. 99:5632-5637

Meyell, P-J. 1978. Introducing Methane. In Methane: Planning a Digestor. Schocken Books, New York. pp.1-5

Michel, R., C. Massanz, S. Kostka, M. Richter, and K. Fiebig. 1995. Biochemical characterization of the 8-hydroxy-5-deazaflavin-reactive hydrogenase from *Methanosarcina barkeri* Fusaro. Eur. J. Biochem. 233:727-735

Miller, T.L. and M.J. Wolin. 1983. Oxidation of hydrogen and reduction of methanol to methane is the sole energy source for a methanogen isolated from human feces. J. Bacteriol. 153:1051-1055

Miller, T.L. and M.J. Wolin. 1985. *Methanosphaera stadtmaniae* gen. nov. sp. nov.: a species that forms methane by reducing methanol with hydrogen. Arch. Microbiol. 141:116-122

Möller-Zinkhan, D., G. Börner, and R.K. Thauer. 1989. Function of methanofuran, tetrahydromethanopterin, and coenzyme F_{420} in *Archaeoglobus fulgidus*. Arch. Microbiol. 152:362-368

Moran, M., J.D. Miller, T. Kral, and D. Scott. 2005. Desert methane: Implications for life detection on Mars. Icarus. 178:277-280

Moura, I., J.J.G. Moura, B.-H. Huynh, H. Santos, J. LeGall, and A.V. Xavier. 1982. Ferredoxin from *Methanosarcina barkeri*: Evidence for the presence of a three-iron center. Eur. J. Biochem. 126:95-98

Müller, V., M. Blaut, and G. Gottschalk. 1993. Bioenergetics of methanogenesis. In *Methanogenesis. Ecology, physiology, biochemistry and genetics*. J.G. Ferry (ed.). Chapman and Hall, Inc. New York, pp. 360-406

Müller, V., C. Ruppert, and T. Lemker. 1999. Structure and function of the A_1A_0-ATPases from methanogenic archaea. J. Bioenerg. Biomem. 31:15-27

Mukhopadhyay, B. and L. Daniels. 1989. Aerobic purification of N^5,N^{10}-methylene-tetrahydromethanopterin dehydrogenase, separated from N^5,N^{10}-methenyltetrahydromethanopterin cyclohydrolase, from *Methanobacterium thermoautotrophicum* strain Marburg. Can. J. Micro. 35:499-507

Mukhopadhyay, B., E. Purwantini, and L. Daniels. 1993. Effect of methanogenic substrates on coenzyme F_{420}-dependent N^5,N^{10}-methylene-tetrahydromethanopterin dehydrogenase, N^5,N^{10}-methenyltetrahydromethanopterin cyclohydrolase and F_{420}-reducing hydrogenase activities in *Methanosarcina barkeri*. Arch. Microbiol. 159:141-146

Murakami, Eisuke, U. Deppenmeier, and S.W. Ragsdale. 2001. Characterization of the

intramolecular electron transfer pathway from 2-hydroxyphenazine to the heterodisulfide reductase from *Methanosarcina thermophila*. J. Biol. Chem. 276:2432-2439

Muth, E., E. Mörschel, and A. Klein. 1987. Purification and characterization of an 8-hydroxy-5-deazaflavin-reactive hydrogenase from *Methanococcus voltae*. Eur. J. Biochem. 169:571-577

Nair, R. and B. Rost. 2005. Mimicking cellular sorting improves prediction of subcellular localization. J. Mol. Biol. 348:85-100

Neil, A.R., D.W. Grime, and R.M.C. Dawson. 1978. Conversion of choline methyl groups through trimethylamine into methane in the rumen. Biochem. J. 170:529-535

Nelson, M.J.K., D.P. Brown, and J.G. Ferry. 1984. FAD requirement for the reduction of conenzyme F_{420} by hydrogenase from *Methanobacterium formicicum*. Biochem.Biophys.Res.Commun. 120:775-781

Nölling, J., T.D. Pihl, and J.N. Reeve. 1995. Organization and growth phase-dependent transcription of methane genes in two regions of the *Methanobacterium thermoautotrophicum* genome. J. Bacteriol. 177:2460-2468

Nölling, J., M. Ishii, J. Koch, T.D. Pihl, J.N. Reeve, R.K. Thauer, and R. Hedderich. 1995b. Characterization of a 45-kDa flavoprotein and evidence for a rubredoxin, two proteins that could participate in electron transport from H_2 to CO_2 in methanogenesis in *Methanobacterium thermoautotrophicum*. Eur. J. Biochem. 231:628-638

O'Donnell, V.B., D.G. Tew, O.T.G. Jones, and P.J. England. 1993. Studies on the inhibitory mechanism of iodonium compounds with special reference to neutrophil NADPH oxidase. Biochem. J. 290:41-49

Ollivier, B., P. Caumette, J.-L. Garcia, and R.A. Mah. 1994. Anaerobic bacteria from hypersaline environments. Microb. Rev. 58:27-38

Oremland, R.S., L.M. Marsh, and S. Polcin. 1982. Methane production and simultaneous sulphate reduction in anoxic, salt marsh sediments. Nature. 296:143-145

Orphan, V.J., K.-U. Hinrichs, W. Ussler, III, C.K. Paull, L.T. Taylor, M. Hayes, and E.F. Delong. 2001. Comparative analysis of methane-oxidizing Archaea and bacteria in anoxic marine sediments. Appl. Environ. Microbiol. 67:1922-1934

Pankhania, I.P. and J.P. Robinson. 1984. Heavy metal inhibition of methanogenesis by *Methanospirillum hungatei* GP1. FEMS Microbiol. Lett. 22:277-281

Patel, G.B., L.A. Roth, L. van den Berg, and D.S. Clark. 1976. Characterization of a strain of *Methanospirillum hungatei*. Can. J. Microbiol. 22:1404-1410

Patel, G.B. 1984. Characterization and nutritional properties of *Methanothrix concilii* sp. nov., a mesophilic, acetoclastic methanogen. Can. J. Microbiol. 30:1383-1396

Pearce, F. 1989. Methane: The hidden greenhouse gas. New Scientist. May 6:37-41

Peck, M.W. and D.B. Archer. 1989. Methods for the quantification of methanogenic bacteria. Ind. Biotech. 9:5-11

Peinemann, S., R. Hedderich, R.K. Thauer, and G. Gottschalk. ATP synthesis coupled to electron transfer from H_2 to the heterodisulfide of 2-mercaptoethanesulfonate and 7-mercaptoheptanoylthreonine phosphate in vesicle preparations of the methanogenic bacterium strain Gö1. FEBS Lett. 263:57-60

Porat, I., W. Kim, E.L. Hendrickson, Q. Xia, Y. Zhang, T. Wang, F. Taub, B.C. Moore, I.J. Anderson, M. Hackett, J.A. Leigh, and W.B. Whitman. 2006. Disruption of the operon encoding Dhb hydrogenase limits anabolic CO_2 assimilation in the archaeon *Methanococcus maripaludis*. J. Bacteriol. 188:1373-1380

Porath, J. and B. Olin. 1983. Immobilized metal ion affinity adsorption and immobilized metal ion affinity chromatography of biomaterials. Serum protein affinities for gel-immobilized iron and nickel ion. Biochemistry. 22:1621-1630

Porath, J. 1992. Immobilized metal ion affinity chromatography. Prot. Expr. Purif. 3:263-281

Preneta, A. 1995. Separation on the basis of size: gel permeation chromatography. In *Protein purification methods – A practical approach.* E.L.V. Harris and S.Angal, (Eds). Oxford University Press, New York, pp. 293-310

Price, E.C., and Cheremisinoff, P.N. 1981. Microbiology and Biochemistry. In Biogas Production and Utilization. Ann Arbor Science Publishers, Inc. pp.1-10

Raghoebarsing, A.A., A. Pol, K.T. van de Pas-Schoonen, A.J.P. Smolders, KF. Ettwig, I.C. Rijpstra, S. Schouten, J.S. Sinninghe Dansté, H.J.M. Op den Camp, M.S.M. Jetter, and M. Strous. 2006. A microbial consortium couples anaerobic methane oxidation to denitrification. Nature. 440:918-921

Ranalli, G., T.N. Whitmore, and D. Lloyd. 1986. Methanogenesis from methanol in Methanosarcina barkeri studied using inlet mass spectroscopy. FEMS Micro. Lett. 35 (2-3):119-122

Reeve, J.N., G.S. Beckler, D.S. Cram, P.T. Hamilton, J.W. Brown, J.A. Krzycki, A.F. Kolodziej, L. Alex., W.H. Orme-Johnson, and C.T. Walsh. 1989. A hydrogenase-linked gene in *Methanobacterium thermoautotrophicum* strain ΔH encodes a polyferredoxin. Proc. Natl. Acad. Sci. USA. 86:3031-3035

Romesser, J.A. and R.S. Wolfe. 1982. CDR factor, a new coenzyme required for CO_2 reduction to methane. Zentralbl. Bakteriol. Hyg. Abt. I. Orig. C. 3:271-276

Rospert, S., D. Linder, J. Ellermann, and R.K. Thauer. 1990. Two genetically distinct methyl-coenzyme M reductases in *Methanobacterium thermoautotrophicum* strain Marburg and ΔH. Eur. J. Biochem. 194:871-877

Rother, M. and W.W. Metcalf. 2004. Anaerobic growth of *Methanosarcina acetovorans* C2A on carbon monoxide: An unusual way of life for a methanogenic archaeon. Proc.Natl.Acad.Sci. 101:16929-16934

Rouvière, P.E., L. Mondelco, S. Winkler, and C.R. Woese. 1992. A detailed phylogeny for the *Methanomicrobiales*. System. Appl. Microbiol. 15:363-371

Salleh, A. 2004. Baaaaaardon me! Sheep can't stop burping. http://www.abc.net.au/science/news/enviro/EnviroRepublish_1205657.htm accessed 2006 April 12

Sauer, K., U. Harms, and R.K. Thauer. 1997. Methanol:coenzyme M methyltransferase from *Methanosarcina barkeri* – Purification, properties and encoding genes of the corrinoid protein MT1. Eur. J. Biochem. 243:670-677

Sauer, K, and R.K. Thauer. 1998. Methanol:coenzyme M methyltransferase from *Methanosarcina barkeri* – Identification of the active-site histidine in the corrinoid-harboring subunit MtaC by site-directed mutagenesis. Eur. J. Biochem. 253:698-705

Schäfer, G., M. Engelhard, and V. Müller. 1999. Bioenergetics of the Archaea. Microl. Mol. Biol. Rev. 63:570-620

Schauer, N.L. and J.G. Ferry. 1986. Composition of the coenzyme F_{420}-dependent formate dehydrogenase from *Methanobacterium formicicum*. J. Bacteriol. 165:405-411

Scheel, E. and G. Schäfer. 1990. Chemiosmotic energy conversion and the membrane ATPase of *Methanolobus tindarius*. Eur. J. Biochem. 187:727-735

Shcherbakova, V.A. and M.B. Vaĭnshtein. 2000. Methane production by the sulfate-reducing bacterium *Desulfosarcina variabilis* (abstract only). Mikrobiologia. 69:341-344

Schink, B. and I. Probst. 1980. Competitive inhibition of the membrane-bound hydrogenase of *Alcaligenes eutrophus* and molecular oxygen. Biochem. Biophys. Res. Com. 95:1563-1569

Schink, B. 1997. Energetics of syntrophic cooperation in methanogenic degradation. Microbiol Mol. Biol. Rev. 61:262-280

Schwörer, B. and R.K. Thauer. 1991. Activities of formylmethanofuran dehydrogenase, methylenetetrahydromethanopterin deyhydrogenase, methylenetetrahydromethanopterin reductase, and heterodisulfide reductase in methanogenic bacteria. Arch. Microbiol. 155:459-465

Seedorf, H., A. Dreisbach, R. Hedderich, S. Shima, and R.K. Thauer. 2004. $F_{420}H_2$ oxidase (FprA) from *Methanobrevibacter arboriphilus*, a conenzyme F_{420}-dependent enzyme involved in O_2 detoxification.

Seedorf, H., J. Kahnt, A.J. Pierik, and R.K. Thauer. 2005. *Si*-face stereospecificity at C5 of coenzyme F_{420} for $F_{420}H_2$ oxidase from methanogenic Archaea as determined by mass spectrometry. FEBS J. 272:5337-5342

Seefeldt, L.C. and D.J. Arp. 1989. Cyanide inactivation of hydrogenase from *Azotobacter vinelandii*. J. Bacteriol. 171:3298-3303

Setzke, E., R. Hedderich, S. Heiden, and R.K. Thauer. 1994. H_2:heterodisulfide oxidoreductase complex from *Methanobacterium thermoautotrophicum*. Eur. J. Biochem. 220:139-148

Shah, N.N. and D.S. Clark. 1990. Partial purification and characterization of two hydrogenases from the extreme thermophile *Methanococcus jannaschii*. Appl. Env. Micro. 56:858-863

Shima, S., M. Sordel-Klippert, M. Brioukhanov, A. Netrusov, D. Linder, and R.K. Thauer. 2001. Characterization of a heme-dependent catalase from *Methanobrevibacter arboriphilus*. Appl. Environ. Microbiol. 67:3041-3045

Shima, S., E. Warkentin, R.K. Thauer, and U. Ermler. 2002. Structure and Function of Enzymes involved in the Methanogenic Pathway Utilizing Carbon Dioxide and Molecular Hydrogen. J. Biosc and Bioeng. 93:519-530

Simianu, M., E. Murkami, J.M. Brewer, and S.W. Ragsdale. 1998. Purification and properties of the heme- and iron-sulfur-containing heterodisulfide reductase from *Methanosarcina thermophila*. Biochemistry. 37:10027-10039

Slesarev, A.I., K.V. Mezhevaya, K.S. Makarova, N.N. Polushin, O.V. Shcherbinina, V.V. Shakhova, G.I. Belova, L. Aravind, D.A. Natale, I.B. Rogozin, R.L. Tatusov, Y.I. Wolf, K.O. Stetter, A.G. Malykh, E.V. Koonin, and S.A. Kozyavkin. 2002. The complete genome of hyperthermophile *Methanopyrus kandleri* AV19 and monophyly of archael methanogens. Proc. Natl. Acad. Sci. USA. 99:4644-4649

Šmigán, P., A. Majernik, and M. Greksák. 1994. Na^+-driven ATP synthesis in *Methanobacterium thermoautotrophicum* and its differentiation from H^+-driven ATP synthesis by rhodamine 6G. FEBS Lett. 349:424-428

Smith, P.H. 1966. Microbiology of sludge methanogenesis. Develop. Ind. Microbiol. 7:156-161

Smith, D.R., L.A. Doucette-Stamm, C. Deloughery, H. Lee, J. Dubois, T. Aldredge, R. Bashirzadeh, D. Blakely, R. Cook, K. Gilbert, D. Harrison, L. Hoang, P. Keagle, W. Lumm, B. Pothier, D. Qiu, R. Spadafora, R. Vicaire, Y. Wang, J. Wierzbowski, R Gibson, N. Jiwani, A. Caruso, D. Bush, and J.N. Reeve. 1997. Complete genome sequence of *Methanobacterium thermoautotrophicum* ΔH: functional analysis and comparative genomics. J. Bacteriol. 179:7135-7155

Sorgenfrei,O., S. Müller, M. Pfeiffer, I. Sniezko, and A. Klein. 1997. The [NiFe] hydrogenases of *Methanococcus voltae*: genes, enzymes and regulation. Arch. Microbiol. 167:189-195

Sowers, K.R. and J.G. Ferry. 2002. Methanogenesis in the marine environment. In The encyclopedia of environmental microbiology. G. Bitton (ed.). John Wiley & Sons, Inc, pp. 1913-1923

Sparling, R. and L. Daniels. 1986. Source of carbon and hydrogen in methane produced from formate by *Methanococcus thermolithotrophicus*. J. Bacteriol. 168:1402-1407

Sparling, R. and L. Daniels. 1990. Regulation of formate dehydrogenase activity in *Methanococcus thermolithotrophicus*. J. Bacteriol. 172:1464-1469

Sparling, R., M.Blaut, and G.Gottschalk. 1993. Bioenergetic studies of *Methanosphaera stadtmanae*, an obligate H_2-methanol utilizing methanogen. Can. J. Microbiol. 39:742-748

Sprenger, W.W., M.C. van Belzen, J. Rosenburg, J.H.P. Hackstein, and J.T. Keltjens. 2000. *Methanomicrococcus blatticola* gen. nov., sp. nov., a methanol- and methylamine-reducing methanogen from the hindgut of the cockroach *Periplaneta americana*. Int. J. Sys. Evol. Microbiol. 50:1989-1999

Sprenger, W.W., J.H.P. Hackstein, and J.T. Keltjens. 2005. The energy metabolism of *Methanomicrococcus blatticola*: physiological and biochemical aspects. Antonie van Leewenhoek. 87:289-299

Sprott, G.D., K.M. Shaw, and T.J. Beveridge. 1987. Properties of the particulate enzyme F_{420}-reducing hydrogenase isolated from *Methanospirillum hungatei*. Can. J. Microbiol. 33:896-904

Sprott, G.D. and T.J. Beveridge. 1993. Microscoopy. In *Methanogenesis. Ecology, physiology, biochemistry and genetics*. J.G. Ferry (ed.). Chapman and Hall, Inc. New York, pp. 81-127

Stafford, D.A., D.L. Hawkes, and R. Horton. 1978. Digester Gas. In *Methane Production From Waste Organic Matter*. CRC Press, Boca Raton, Florida. pp.113-124

Steigerwald, V.J., G.S. Beckler, and J.N. Reeve. 1990. Conservation of hydrogenase and polyferredoxin structures in the hyperthermophilic archaebacterium *Methanothermus fervidus*. J. Bacteriol. 172:4715-4718

Stephenson, M. and L.H. Strickland. 1931. XXVII. Hydrogenase: a bacterial enzyme activating molecular hydrogen. I. The properties of the enzyme. Biochem. J. 25:205-214

Stojanowic, A., G.J. Mander, E.C. Duin, and R. Hedderich. 2003. Physiological role of the F_{420}-non-reducing hydrogenase (Mvh) from *Methanothermobacter marburgensis*. Arch. Microbiol. 180:194-203

Strøm, A.R., J.A. Olafsen, and H. Larsen. 1979. Trimethylamine oxide: a terminal e^- acceptor in anaerobic respiration of bacteria. J. Gen. Microbiol. 112:315-320

Storz, G. and J.A. Imlay. 1999. Oxidative stress. Curr. Opp. Microbiol. 2:188-194

Takao, M., A. Yasui, and A. Oikawa. 1991. Unique characteristics of superoxide dismutase of a strictly anaerobic archaebacterium *Methanobacterium thermoautotrophicum*. J. Biol. Chem. 266:14151-14154

Taylor, C.D. and R.S. Wolfe. 1974. J. Biol. Chem. 249:4879-4885

te Brommelstroet, B.W.T., C.M.H. Hensgens, J.T. Keltjens, C. van der Drift, and G.D. Vogels. 1990. Purification and properties of 5,10-methylenetetrahydromethanopterin reductase, a coenzyme F_{420}-dependent enzyme from *Methanobacterium thermoautotrophicum* strain delta H. J. Biol. Chem. 265:1852-1857

te Brommelstroet, B.W.T., J.W. Geerts, J.T. Keltjens, C. van der Drift, and G.D. Vogels. 1991a. Purification and properties of 5,10-methylenetetrahydromethanopterin dehydrogenase and 5,10-methylenetetrahydromethanopterin reductase, two coenzyme F_{420} dependent enzymes from *Methanosarcina barkeri*. Biochim. Biophys. Acta. 1079:293-302

te Brommelstroet, B.W.T., C.M.H. Hensgens, J.T. Keltjens, C. van der Drift, and G.D. Vogels. 1991b. Purification and characterization of coenzyme F_{420} dependent 5,10-methylenetetrahydromethanopterin dehydrogenase from *Methanobacterium thermoautotrophicum* strain delta H. Biochim. Biophys. Acta. 1073:77-84

Teh, Y.L. and S. Zinder. 1992. Acetyl-coenzyme A synthetase in the thermophilic, acetate-utilizing methanogen *Methanothrix* sp. strain CALS-1. FEMS Microbiol. Lett. 98:1-8

Teixeira, M., I. Moura, A.V. Xavier, B.H. Huynh, D.V. DerVartanian, H.D. Peck, Jr., J. LeGall, and J.J.G. Moura. 1985. Electron paramagnetic resonance studies on the mechanism of activation and the catalytic cycle of the nickel-containing hydrogenase from *Desulfovibrio gigas*. J. Biol. Chem. 260:8942-8950

Tergesteen, A. and R. Hedderich. 1999. *Methanobacterium thermoautotrophicum* encodes two multisubunit membrane-bound [NiFe] hydrogenases. Eur. J. Biochem. 264:930-943

Thauer, R.K. 1998. Biochemistry of Methanogenesis: A Tribute to Marjory Stephenson. Microbiology. 144:2377-2406

Thauer, R.K., R. Hedderich, and R. Fischer. 1993. Reactions and enzymes involved in methanogenesis from CO_2 and H_2. In *Methanogenesis. Ecology, physiology, biochemistry and genetics*. J.G. Ferry (ed.). Chapman and Hall, Inc. New York, pp. 209-252

Thauer, R.K. and S. Shima. 2006. Methane and microbes. Nature. 440:878-879

Turner, J.M. and A.J. Messenger. 1986. Occurrence, biochemistry, and physiology of phenazine pigment production. Adv. Microb. Physiol. 27:211-275

Tzeng, S.F., R.W. Wolfe, and M.P. Bryant. 1975. Factor 420-dependent pyridine nucleotide-linked hydrogenase system of *Methanobacterium ruminantium*. J. Bacteriol. 121:184-191

van Beelen, R., J.F.A. Labro, J.T. Keltjens, W.J. Geerts, G.D. Vogels, W.H. Laarhoven, W. Guut, and C.A.G. Haasnoot. 1984. Derivatives of methanopterin, a coenzyme found in methanogenesis. Eur. J. Biochem. 139:359-365

van de Wijngaard, W.M.H. and C. van der Drift. 1991. Formation of factor 390 by cell extracts of *Methanosarcina barkeri*. J. Bacteriol. 173:2710-2711

van de Wijngaard, W.M.H., J. Creemers, and C. van der Drift. 1991. Methanogenic pathways in *Methanosphaera stadtmanae*. FEMS Microbiol. Lett. 80:207-212

van der Linden, B.W. Faber, B. Bleijevens, T. Burgdorf, M. Bernhard, B. Friedrich, and S.P.J. Albracht. 2004. Selective release and functionof one of the two FMN groups in the cytoplasmic NAD^+-reducing [NiFe]-hydrogenase from *Ralstonia eutropha*. Eur. J. Biochem. 271:801-808

van der Meijden, P., H.J. Heythuysen, A. Pouwels, F.P. Houwen, C. van der Drift, and G.D. Vogels. 1983. Methyltransferases involved in methanol conversion by *Methanosarcina barkeri*. Arch. Microbiol. 134:238-242

Vanoni, M.A., E.Verzotti, G.Zanetti, and B.Curti. 1996. Properties of the recombinant β subunit of glutamate synthase. Eur. J. Biochem. 236:937-946

Vaupel, M. and R.K. Thauer. 1995. Coenzyme F_{420}-dependent N^5,N^{10}-Methylenetetrahydromethanopterin reductase (Mer) from *Methanobacterium thermoautotrophicum* strain Marburg – Cloning, sequencing, transcriptional analysis, and functional expression in *Escherichia coli* of the *mer* gene. 231:773-778

Vaupel, M. and R.K. Thauer. 1998. Two F_{420}-reducing hydrogenases in *Methanosarcina barkeri.* Arch. Microbiol. 169:201-205

Vermeij, P., F.J.M. Detmers, F.J.M. Broers, J.T. Keltjens, and C. van der Drift. 1994. Purification and characterization of coenzyme F_{430} synthetase from *Methanobacterium thermoautotrophicum* ΔH. Eur. J. Biochem. 226:185-191

Vignais, P.M., B. Billoud, and J. Meyer. 2001. Classification and phylogeny of hydrogenases. FEMS Microbiol. Rev. 25:455-501

von Bünau, R., C. Zirngibl, R.K. Thauer, and A. Klein. 1991. Hydrogen-forming and coenzyme-F_{420}-reducing methylene tetrahydromethanopterin dehydrogenase are genetically distinct enzymes in *Methanobacterium thermoautotrophicum* (Marburg). Eur. J. Biochem. 202:1205-1208

Vorholt, J.A. and R.K. Thauer. 1997. The active species of 'CO_2' utilized by formylmethanofuran dehydrogenase from methanogenic archaea. Eur. J. Biochem. 248:919-924

Wagner, D., E.-M. Pfeiffer, and E. Bock. 1999. Methane production in aerated marshland and model soils: effects of microflora and soil texture. Soil Biol. Biochem. 31:999-1006

Wang, W.C., Y.L. Yung, A.A. Lacis, T. Mo, and J.E. Hansen. 1976. Greenhouse effects due to man-made perturbations of trace gases. Science. 194:685-690

Warkentin, E., B. Mamat, M. Sordel-Klippert, M. Wicke, R.K. Thauer, M. Iwata, S. Iwata, U. Ermler, and S. Shima. 2001. Structures of $F_{420}H_2$:NADP+ oxidoreductase with and without its substrates bound. Embo J. 20:6561-6569

Wasserfallen, A., K. Huber, and T. Leisinger. 1995. Purification and structural characterization of a flavoprotein induced by iron limitation in *Methanobacterium thermoautotrophicum* Marburg. 177:2436-2441

Weiss, D.S., P. Gärtner, and R.K. Thauer. 1994. The energetics and sodium-ion dependence of N^5-methyltetrahydromethanopterin:coenzyme M methyltransferase studied with cob(I)alamin as methyl acceptor and methylcob(III)alamin as methyl donor. Eur. J. Biochem. 226:799-809

Westenberg, D.J., A. Braune, C. Ruppert, V. Müller, C. Herzberg, G. Gottschalk, and M. Blaut. 1999. The $F_{420}H_2$-dehydrogenase from *Methanolobus tindarius*: cloning of the *ffd* operon and expression of the genes in *Escherichia coli*. FEMS Microbiol. Lett. 170:389-398

White, R.H. and D. Zhou. 1993. Biosynthesis of the conenzymes in methanogens. In *Methanogenesis. Ecology, physiology, biochemistry and genetics.* J.G. Ferry (ed.).

Chapman and Hall, Inc. New York, pp.409-444

Wolfe, R.S. 1993. An historical overview of methanogeneis. In *Methanogenesis. Ecology, physiology, biochemistry and genetics.* J.G. Ferry (ed.). Chapman and Hall, Inc. New York, pp. 1-32

Woese, C. 1981. Archaebacteria. Sci. Amer. 244:98-122

Woese, C., O. Kandler, and M.L. Wheelis. 1990. Towards a natural system of organisms: Proposal for the domains Archaea, Bacteria, and Eucarya. Proc. Natl. Acad. Sci. USA. 87:4576-4579

Wong, D., Z. Lin, D.F. Juck, K.A. Terrick, and R. Sparling. 1994. Electron transfer reactions for the reduction of $NADP^+$ in *Methanosphaera stadtmanae*. FEMS Microbiol. Lett. 120:285-290

Wong, D. 1999. Elements of the electron transport pathway for *Methanosphaera stadtmanae*. Dept. of Microbiology, University of Manitoba

Woo, G.J., A. Wasserfallen, and R.S. Wolfe. 1993. Methyl viologen hydrogenase II, a new member of the hydrogenase family from *Methanobacterium thermoautotrophicum* delta H. J. Bacteriol. 175:5970-5977

Yagi, T., T. Yano, S. Di Bernardo, A. Matsuno-Yagi. 1998. Procaryotic complex Ai (NDH-1), an overview. Biochim. Biophys. Acta. 1364:125-133

Yamazaki, S., L. Tsai, and T.C. Stadtman. 1980. Stereochemical studies of 8-hydroxy-5-deazaflavin-dependent $NADP^+$ reductase from *Methanococcus vannielii*. J. Biol. Chem. 255:9025-9027

Yamazaki, S. 1982. A selenium-containing hydrogenase from *Methanococcus vannielii*. J.Biol. Chem. 257:7926-7929

Yeliseev, A., P. Gärtner, U. Harms, D. Linder, and R.K. Thauer. 1993. Function of methylcobalamin:coenzyme M methyltransferase isoenzyme II in *Methanosarcina barkeri*. Arch. Microbiol. 159:530-536

Zeikus, J.G. and D.L. Henning. 1975. *Methanobacterium arbophilicum* sp. nov. An obligate anaerobe isolated from wetwood of living trees. Antonie van Leeuwenhoek. 41:543-552

Zeikus, J.G. 1977. The biology of methanogenic bacteria. Bacteriol. Rev. 41:514-541

Zeikus, J.G., R. Kerby, and A. Krzycki. 1985. Single-carbon chemistry of acetogenic and methanogenic bacteria. Science. March 8:1167-1173

Zinder, S.H. 1993. Physiological ecology of methanogens. In *Methanogenesis. Ecology, physiology, biochemistry and genetics*. J.G. Ferry (ed.). Chapman and Hall, Inc. New York, pp. 128-206

Zirngibl, C., R. Hedderich, and R.K. Thauer. 1990. N^5-N^{10}-methylenetetrahydropmethanopterin dehydrogenase from *Methanobacterium thermoautotrophicum* has hydrogenase activity. FEBS Lett. 112-116

Zirngibl, C., W. Van Dongen, B. Schwöreer, R. Von Bünau, M. Richter, A. Klein, and R.K. Thauer. 1992. H_2-forming methylenetetrahydromethanopterin dehydrogenase, a novel type of hydrogenase without iron-sulfur clusters in methanogenic archaea. Eur. J. Biochem. 208:511-520

Appendix A - Other methanogenic media

***Methanobacterium bryantii* M.o.H.** (DSM 863) (Jarrell *et al.* 1982)	
KH_2PO_4	0.42 g/L
K_2HPO_4	0.23
$MgCl_2 \cdot 6H_2O$	0.064
$CaCl_2 \cdot 2H_2O$	0.03
NaCl	0.30
NH_4Cl	0.70
Na_2CO_3	0.16
Resazurin	1.0 mL from 0.025% stock solution
Mineral elixir	10 mL/L (or 1 mL/L from 10x stock)
$Na_2S \cdot 9H_2O$	1% (v/v) from 200 mM stock after gassing
Growth at pH 7.0 under H_2:CO_2 (pH 8.5 before gassing), growth temperature: 37°C	

Methanothermobacter marburgensis (DSM 2133) (Fuchs *et al.* 1978)	
KH_2PO_4	0.42 g/L
K_2HPO_4	0.23
$MgCl_2 \cdot 6H_2O$	0.04
$CaCl_2 \cdot 2H_2O$	0.03
NaCl	0.595
NH_4Cl	0.70
Na_2CO_3	0.16
Resazurin	1.0 mL from 0.025% stock solution
Mineral elixir	10 mL/L (or 1 mL/L from 10x stock)
$Na_2S \cdot 9H_2O$	1% (v/v) from 200 mM stock after gassing
Growth at pH 7.0 under H_2:CO_2 (pH 8.5 before gassing), growth temperature: 63°C	

Methanosaeta concilii (DSM 3671) (Patel 1984)	
KH_2PO_4	0.30 g/L
NaCl	0.60
$MgCl_2 \cdot 6H_2O$	0.10
$CaCl_2 \cdot 2H_2O$	0.08
NH_4Cl	1.00
KCO_3	4.00
Na acetate	6.80
Resazurin	1.0 mL from 0.025% stock solution
Mineral elixir	10 mL/L (or 1 mL/L from 10x stock)
Vitamin elixir	10 mL/L (or 1 mL/L from 10x stock)
$Na_2S \cdot 9H_2O$	1% (v/v) from 200 mM stock after gassing
Growth at pH 7.0 under N_2:CO_2 (pH 7.7 before gassing), growth temperature: 37°C	

Methanolobus tindarius (DSM 2278) (König and Stetter 1982)	
KCl	0.335 g/L
K_2HPO_4	0.14
$MgCl_2 \cdot 6H_2O$	4.00
$MgSO_4 \cdot 7H_2O$	3.45
$CaCl_2 \cdot 2H_2O$	0.14
NaCl	18.00
NH_4Cl	0.25
$NaHCO_3$	1.00
$Fe(NH_4)_2(SO_4)_2 \cdot 7H_2O$	0.002
Resazurin	1.0 mL from 0.025% stock solution
Mineral elixir	10 mL/L (or 1 mL/L from 10x stock)
Vitamin supplement	10 mL/L (or 1 mL/L from 10x stock)
$Na_2S \cdot 9H_2O$	1% (v/v) from 200 mM stock after gassing
Methanol	1% (v/v) from 40% stock after autoclaving
Growth at pH 6.5 under N_2:CO_2 (pH 8.3 before gassing), growth temperature: 28°C	

Methanococcus voltae (DSM 1537) (DSZM catalogue of strains, 1993)	
KCl	0.335 g/L
$MgCl_2 \cdot 6\ H_2O$	4.00
$MgSO_4 \cdot 7\ H_2O$	3.45
NH_4Cl	0.25
$CaCl_2 \cdot 2\ H_2O$	0.14
K_2HPO_4	0.14
Yeast extract	2.00
Trypticase/Tryptone	2.00
NaCl	18.00
$NaHCO_3$	5.00
$Fe(NH_4)_2(SO_4)_2 \cdot 7H_2O$	0.002
Resazurin	1.0 mL from 0.025% stock solution
$Na_2S \cdot 9\ H_2O$	1% (v/v) from 200 mM stock after gassing
Na Acetate	1.00
Mineral elixir	10 mL/L
Vitamin supplement	10 mL/L
Growth at pH 7.0 under H_2:CO_2 (pH 7.5 before gassing), growth temperature: 37°C	

Mineral elixir stock solution	
Trisodium nitrilacetate	2.02 g/L
$FeCl_3 \cdot 6H_2O$	0.21
$CoCl_2 \cdot 6H_2O$	0.20
$MnCl_2 \cdot 4H_2O$	0.10
$ZnCl_2$	0.10
$NiCl_2 \cdot 6H_2O$	0.10
$CaCl_2 \cdot 2H_2O$	0.05
$CuSO_4 \cdot 2H_2O$	0.05
$Na_2MoO_4 \cdot 2H_2O$	0.05

Vitamin supplement stock solution	
Pyridoxine-HCl	10 mg/L
Riboflavin	5
Thiamine	5
Nicotinic acid	5
p-Aminobenzoic acid	5
Lipoic acid (aka Thioctic acid)	5
Biotin	2
Folic acid	2
Cyanocobalamin	1

Appendix B - Mass Spectroscopy data for *Methanospirillum hungatei* GPI. Confirmation of the isolation of the F_{420}-reducing hydrogenase during the purification of the phenazine-dependent $F_{420}H_2$ dehydrogenase activity.

1. F_{420}-reducing hydrogenase isoenzyme II alpha subunit, *Methanosarcina barkeri* (Expect = 2.1×10^{-3})

Expectation	Sequence
3.6×10^{-3}	^{327}GTFAQHIAR^{335}
2.1×10^{-2}	^{381}GSNIHLAR^{388}
0.76	^{32}GDWLSITPVR^{41}
1.5	^{291}ANPQMEACTGVPTYDGQPVEVGPR^{314}
125.4	^{4}VVEISPTTR^{12}

2. F_{420}-reducing hydrogenase, *Methanosarcina acetovorans* C2A (Expect = 2.7×10^{-2})

Expectation	Sequence
3.6×10^{-3}	^{327}GTFAQHIAR^{335}
0.27	^{381}GTDVHIAR^{388}
0.76	^{32}GDWLSITPVR^{41}

125.4	^{4}VVEISPTTR^{12}

3. F_{420}-reducing hydrogenase isoenzyme I, *Methanosarcina barkeri* (Expect = 3.5×10^{-2})

Expectation	Sequence
3.6×10^{-3}	^{327}GTFAQHIAR^{335}
0.27	^{381}GTDVHIAR^{388}
125.4	^{4}VVEISPTTR^{12}

4. F_{420}-reducing hydrogenase isoenzyme I beta subunit, *Methanosarcina barkeri* (Expect = 0.18)

Expectation	Sequence
1.5	^{230}VGNEIWSK^{237}
0.77	^{1}MIEDPYLGK^{9}

5. F_{420}-reducing hydrogenase beta subunit, *Methanosarcina mazei* Gö1 (Expect = 0.77)

Expectation	Sequence
2.1×10^{-2}	^{195}YEQPGCHVCLDYVSSLA-DISTGSVGSPDGWSTY^{227}

0.77	^{3}EMTADPYLGK^{12}

Appendix C - Similarity of the sequences encoding for the subunits of the F_{420}-reducing hydrogenase from *Msp. hungatei* JF1 with corresponding sequences from *Ms. mazei* Gö1, *Mtb. thermoautotrophicus* ΔH, and *Mc. voltae*.

Ms. mazei Gö1 (accession number)	*Msp. hungatei* JF1		
	Identity	Positives	E value
FrhB (β) (NP_635066)	190/292 (65%)	238/292 (81%)	4e-113
FrhG (γ) (NP_635067)	183/267 (68%)	214/267 (80%)	1e-105
FrhD (δ) (NP_635068)	90/156 (57%)	120/156 (76%)	2e-49
FrhA (α) (NP_635069)	310/455 (68%)	369/455 (81%)	0.0

Mtb. thermoautotrophicus ΔH (accession number)	*Msp. hungatei* JF1		
	Identity	Positives	E value
FrhB (β) (P19499)	147/276 (53%)	201/276 (72%)	5e-81
FrhG (γ) (P19498)	122/235 (51%)	153/235 (65%)	2e-64
FrhD (δ) (P19497)	64/155 (41%)	103/155 (66%)	1e-35
FrhA (α) (P19496)	172/456 (37%)	266/456 (58%)	1e-86

Mc. voltae (accession number)	*Msp. hungatei* JF1		
	Identity	Positives	E value
FrcB (β) (Q00391)	149/275 (54%)	194/275 (70%)	2e-84
FrcG (γ) (Q00393)	121/250 (48%)	150/250 (60%)	2e-56
FrcD (δ) (CAA43497)	57/158 (36%)	94/158 (59%)	2e-20
FrcA (α) (Q00390)	180/439 (41%)	249/439 (56%)	5e-81

Appendix D - Similarity of the F_{420}-reducing hydrogenase of *Msp. hungatei* JF1 with F_{420}-reducing hydrogenases from *Methanosarcina spp.*

Blast searches performed at the National Centre for Biotechnology Information (NCBI, http://www.ncbi.nlm.nih.gov/) using sequences encoding the subunits of the F_{420}-reducing hydrogenase of Ms.mazei Gö1.

Sequences producing significant alignments (α-subunit):	(Bits)	Value
gi|20986624|gb|AE008384.1| Methanosarcina mazei strain Goe1, com	934	0.0
gi|19918815|gb|AE010299.1| Methanosarcina acetivorans str. C2A,	842	0.0
gi|72394721|gb|CP000099.1| Methanosarcina barkeri str. fusaro...	824	0.0
gi|2463278|emb|Y13763.1|MSFHMIII Methanosarcina barkeri fhm a, d	824	0.0
gi|2463273|emb|Y13764.1|MSFHMII Methanosarcina barkeri fha a, e,	816	0.0
gi|88186784|gb|CP000254.1| Methanospirillum hungatei JF-1, compl	670	0.0
gi|6626257|gb|AE000666.1| Methanothermobacter thermautotrophi...	330	5e-90

Sequences producing significant alignments (γ-subunit):	(Bits)	Value
gi|20986624|gb|AE008384.1| Methanosarcina mazei strain Goe1, com	589	2e-168
gi|72394721|gb|CP000099.1| Methanosarcina barkeri str. fusaro...	509	3e-144
gi|2463278|emb|Y13763.1|MSFHMIII Methanosarcina barkeri fhm a, d	509	3e-144
gi|2463273|emb|Y13764.1|MSFHMII Methanosarcina barkeri fha a, e,	474	7e-134
gi|19918815|gb|AE010299.1| Methanosarcina acetivorans str. C2A,	473	3e-133
gi|88186784|gb|CP000254.1| Methanospirillum hungatei JF-1, compl	381	1e-105
gi|6626257|gb|AE000666.1| Methanothermobacter thermautotrophi...	257	2e-68

Appendix D - Similarity of the F_{420}-reducing hydrogenase of *Msp. hungatei* JF1 with F_{420}-reducing hydrogenases from *Methanosarcina spp.* (cont'd)

Sequences producing significant alignments (δ-subunit):

		(Bits)	Value
gi|20986624|gb|AE008384.1|	Methanosarcina mazei strain Goe1, com	328	2e-90
gi|19918815|gb|AE010299.1|	Methanosarcina acetivorans str. C2A,	286	2e-77
gi|72394721|gb|CP000099.1|	Methanosarcina barkeri str. fusaro...	281	3e-76
gi|2463278|emb|Y13763.1|MSFHMIII	Methanosarcina barkeri fhm a, d	281	3e-76
gi|88186784|gb|CP000254.1|	Methanospirillum hungatei JF-1, compl	192	2e-49
gi|116077928|emb|AM114193.2|	Uncultured methanogenic archaeon RC	159	2e-39

Sequences producing significant alignments (β-subunit):

		(Bits)	Value
gi|20986624|gb|AE008384.1|	Methanosarcina mazei strain Goe1, com	593	2e-169
gi|72394721|gb|CP000099.1|	Methanosarcina barkeri str. fusaro...	541	6e-154
gi|2463278|emb|Y13763.1|MSFHMIII	Methanosarcina barkeri fhm a, d	541	6e-154
gi|2463273|emb|Y13764.1|MSFHMII	Methanosarcina barkeri fha a, e,	520	1e-147
gi|19918815|gb|AE010299.1|	Methanosarcina acetivorans str. C2A,	499	3e-141
gi|88186784|gb|CP000254.1|	Methanospirillum hungatei JF-1, compl	405	4e-113
gi|45047480|emb|BX957222.1|	Methanococcus maripaludis S2 complet	315	6e-86

Appendix E - Development of a protocol for the purification of the phenazine-dependent $F_{420}H_2$ dehydrogenation activity of *Methanosphaera stadtmanae*

Various column chromatography techniques were tested in order to enrich the phenazine-dependent $F_{420}H_2$ dehydrogenation activity of *Msph. stadtmanae*. The results of some of the steps are summarized here. All steps were performed under anaerobic conditions, at ambient room temperature.

1. Ammonium sulfate ($(NH_4)_2SO_4$) precipitation

$(NH_4)_2SO_4$ was added to the clarified cell-free extract (membranes removed) in successive increments to yield $(NH_4)_2SO_4$ saturation of 50, 60, and 75%. 65-75% of the phenazine-dependent $F_{420}H_2$ dehydrogenation activity was recovered in the 75% $(NH_4)_2SO_4$ pellet (Figure 6). The pellet was initially re-suspended in 200 mM KPO_4, pH 7.0, with 10 mM DTT and 5% glycerol, but in later experiments was switched to 100 mM HEPES, pH 7.0, with 5% glycerol to accommodate salt sensitive chromatographic techniques. Methyl viologen (shown here) and F_{420} H_2ase activities also precipitated out in a similar manner to the $F_{420}H_2$ dehydrogenation activity, maximally at 75% $(NH_4)_2SO_4$ saturation.

A quick word on desalting of the $F_{420}H_2$ dehydrogenation activity is discussed here. The bulk of the $F_{420}H_2$ dehydrogenation activity from *Msph. stadtmanae* preciptitates at 75% $(NH_4)_2SO_4$ saturation (~2.8 M): to make use of various column chromatography steps, such as affinity or ion-exchange chromatography, the protein must be desalted prior to application of the extract onto the respective column matrices. The desired desalting method would be to use ultrafiltration, but this technique would have to

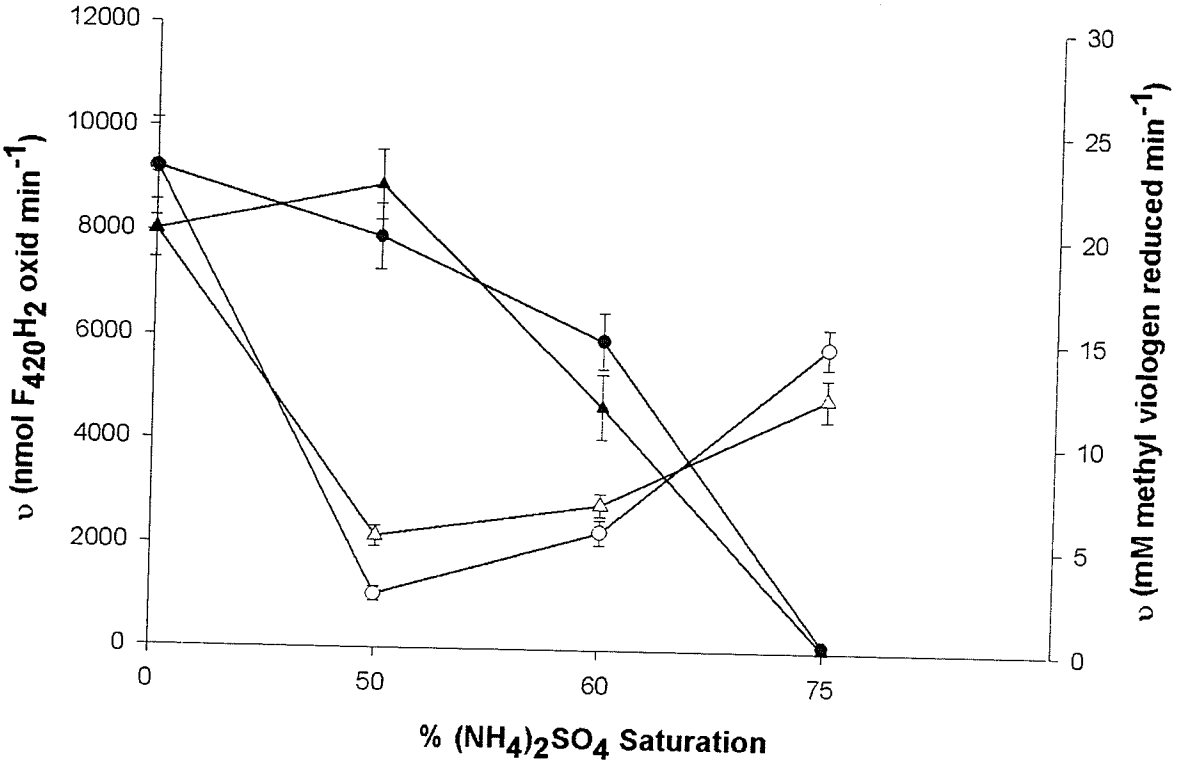

Figure 1. Ammonium sulfate ($(NH_4)_2SO_4$) precipitation profile of the $F_{420}H_2$ dehydrogenation activity from clarified cell-free extract. ●, $F_{420}H_2$ dehydrogenation activity of $(NH_4)_2SO_4$ supernatant. ○, $F_{420}H_2$ dehydrogenation activity of $(NH_4)_2SO_4$ pellet. ▲, methyl viologen-reducing hydrogenase activity of $(NH_4)_2SO_4$ supernatant. Δ, methyl viologen reducing hydrogenase activity of $(NH_4)_2SO_4$ pellet.

be conducted in the anaerobic chamber at room temperature, possibly leading to denaturation of the protein. Instead of ultra-filtration, two different desalting methods were tested, gel filtation and dialysis.

During gel filtration, the salt enters the pores of the gel beads and moves slowly through the column, while the proteins are excluded from the pores and move freely around the beads (Preneta 1995). The homogenized 75% $(NH_4)_2SO_4$ pellet (~12 mL) was loaded onto a Sephadex G-25 column (40 ml), in the anaerobic chamber at ambient room temperature; 50 mM HEPES, pH 7.0, containing 5% glycerol, 0.05% Triton-X-100, and 10 mM DTT, was used as the exchange buffer. The pooled protein was tested for activity and only 15-25% of the loaded $F_{420}H_2$ dehydrogenation activity was retained. Of note, several colored fractions separated from the main protein band during passage through the gel filtration column. These fractions were added back to the desalted protein mix prior to assay; $F_{420}H_2$ dehydrogenation activity could not be reactivated even after addition of the separated fractions.

Dialysis of the 75% $(NH_4)_2SO_4$ pellet was attempted, but this method was not anymore useful than the gel filtration step. The protein sample was loaded into semi-permeable membrane tubing and placed into the desired salt-free buffer; small molecules pass through the membrane while large molecules are retained (Harris 1995). The resuspended 75% $(NH_4)_2SO_4$ pellet was placed into pretreated Fisherbrand cellulose dialysis tubing (6000-8000 Da cut-off) and dialyzed in 50 mM HEPES, pH 7.0, containing 5% glycerol, 0.05% Triton-X-100, and 10 mM DTT. Dialysis was performed either in the anaerobic chamber (with frequent exchanges of fresh, cold buffer), or in an anaerobic 1 L Corning bottle at 4°C. The samples were dialyzed for 8 hours: for dialysis

in the anaerobic chamber the buffer was exchanged every hour; the buffer was changed after one hour, and then every two hours thereafter when dialyzed at 4°C in an anaerobic corning bottle. In either case, only 25-30% (or less) of the activity was retained after completion of dialysis. As such, dialysis was deemed to be an unsatisfactory step.

2. Metal chelate affinity chromatography

The technique of immobilized metal affinity chromatography was used in an attempt to isolate the $F_{420}H_2$ dehydrogenation activity from *Msph. stadtmanae*. This process, using Ni^{2+}-bound iminodiacetic acid, was used successfully in our studies to enrich for the phenazine-dependent $F_{420}H_2$ dehydrogenation activities from *Ms. barkeri* Fusaro and *Msp. hungatei* GP, though ultimately the observed $F_{420}H_2$ dehydrogenation activity was associated with the F_{420} H_2ase isolated from the respective methanoarchaeon.

Two separate metals were used in our studies, Ni^{2+} and Cu^{2+}. All buffers used in these processes are the same as those previously described for the purification of the dehydrogenation activities for *Msp. hungatei* GP1and *Ms. barkeri* Fusaro, except for the addition of 10 mM DTT. All buffers were made anaerobic *via* the gassing manifold and refrigerated until use. The protein, during the loading, washing, and elution steps, was kept as cool as possible using ice gel packs wrapped around the column to prevent denaturation, and all fractions were stoppered and kept cool with ice packs prior to removal from the anaerobic chamber.

Ni^{2+} was the first metal to be tested. The results are shown in Figure 2A. The $F_{420}H_2$ dehydrogenation activity did not have any significant affinity for Ni^{2+}, with only 14% of the loaded activity binding to the column matrix. To ensure that the lack of

binding by the protein was not due to over-saturation of the column, the unbound fraction was reloaded onto a freshly recharged Ni^{2+} column; the subsequently reloaded protein did not have any apparent affinity for the Ni^{2+}-bound matrix.

Cu^{2+} was also tested for its ability to bind the *Msph. stadtmanae* $F_{420}H_2$ dehydrogenation activity (Figure 2B). Cu^{2+} was tested by Denny Wong as a possible purification step to isolate the methyl viologen reducing hydrogenase from *Msph. stadtmanae*, which ultimately did not have an affinity for this particular metal ion (Wong, PhD thesis 1998). Cu^{2+} was also used by Kemner and Zeikus (1994b) to separate the F_{420} H_2ase from the F_{420}-nonreducing hydrogenase activities of *Ms. barkeri* MS; in this study, the F_{420}-nonreducing hydrogenase bound to the Cu^{2+}, whereas the F_{420} H_2ase did not bind to the column. An experiment by Choquet and Sprott (1991) found that the F_{420} H_2ase had affinity for Cu^{2+}, but the enzyme was found to be inactive upon elution from the immobilized Cu^{2+} column.

The results of our studies are shown in Figure 2B. As expected the methyl viologen reducing activity did not have any significant affinity for the immobilized Cu^{2+}, nor did the $F_{420}H_2$ dehydrogenation activity. Passage through the Cu^{2+} column resulted in over 4-fold loss in the pooled activity.

It remains to be seen whether or not other metal ions, such as Zn^{2+} or Fe^{2+}, may be useful in the enrichment of the $F_{420}H_2$ dehydrogenation activity from *Msph. stadtmanae*.

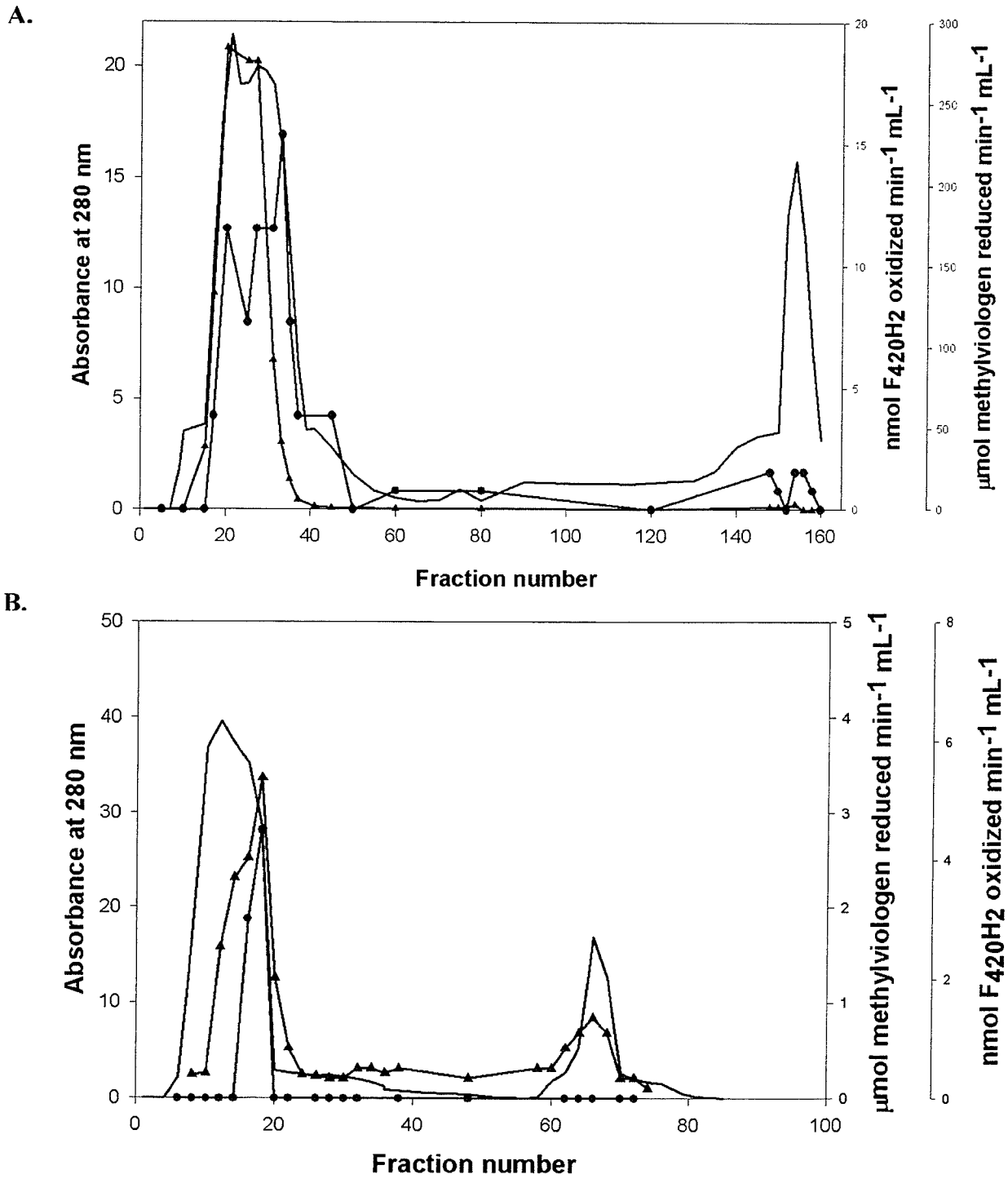

Figure 2. (A) Protein and activity profile of fractions eluted from a Ni^{+} affinity chromatography column. (B) Protein and activity profile of fractions eluted from a Cu^{2+} affinity column. A_{280}, no symbol. ●, $F_{420}H_2$ dehydrogenation activity. ▲, Methyl viologen reducing hydrogenase activity. $F_{420}H_2$ dehydrogenation activity assayed using 500 µM phenazine.

3. DEAE Sephacel (Anion exhange chromatography)

Ion-exchange chromatography is the separation of proteins on the basis of their charge (Roe 1995). Proteins carry both positive and negative charges on their surface, due in large part to the side chains of acidic and basic amino acids (Roe 1995). In low-ionic strength buffer, positively or negatively charged protein binds to ion-exchange matrices; the bound protein is eluted by increasing the ionic strength of the buffer.

DEAE Sephacel, an anion exchanging matrix, has been used in the initial enrichment process of the $F_{420}H_2$ dehydrogenase activity of *Ms. mazei* Gö1 and *Ml. tindarius*, so it was applied as step in the enrichment of the $F_{420}H_2$ dehydrogenation activity of *Msph. stadtmanae* (Figure 3A). Following $(NH_4)_2SO_4$ precipitation, the protein is desalted *via* gel filtration and then applied to the DEAE Sephacel column. Two separate peaks of activity are observed. One activity elutes without binding to the column; this activity does not appear to elute with significant hydrogenase activity. The second peak elutes within the linear 0-2 M NaCl gradient, along with a methyl-viologen reducing hydrogenase activity.

This is not an ideal method for the initial chromatography step as the protein must first be desalted; the resuspended 75% $(NH_4)_2SO_4$ protein pellet does not bind to the DEAE Sephacel matrix. The desalted protein does bind to the matrix, but the activity prior to application to the column is greatly decreased. Clarified cell-free extract (protein suspended in 200 mM KPO_4) in the absence of $(NH_4)_2SO_4$ precipitation did not have any affinity for the DEAE Sephacel.

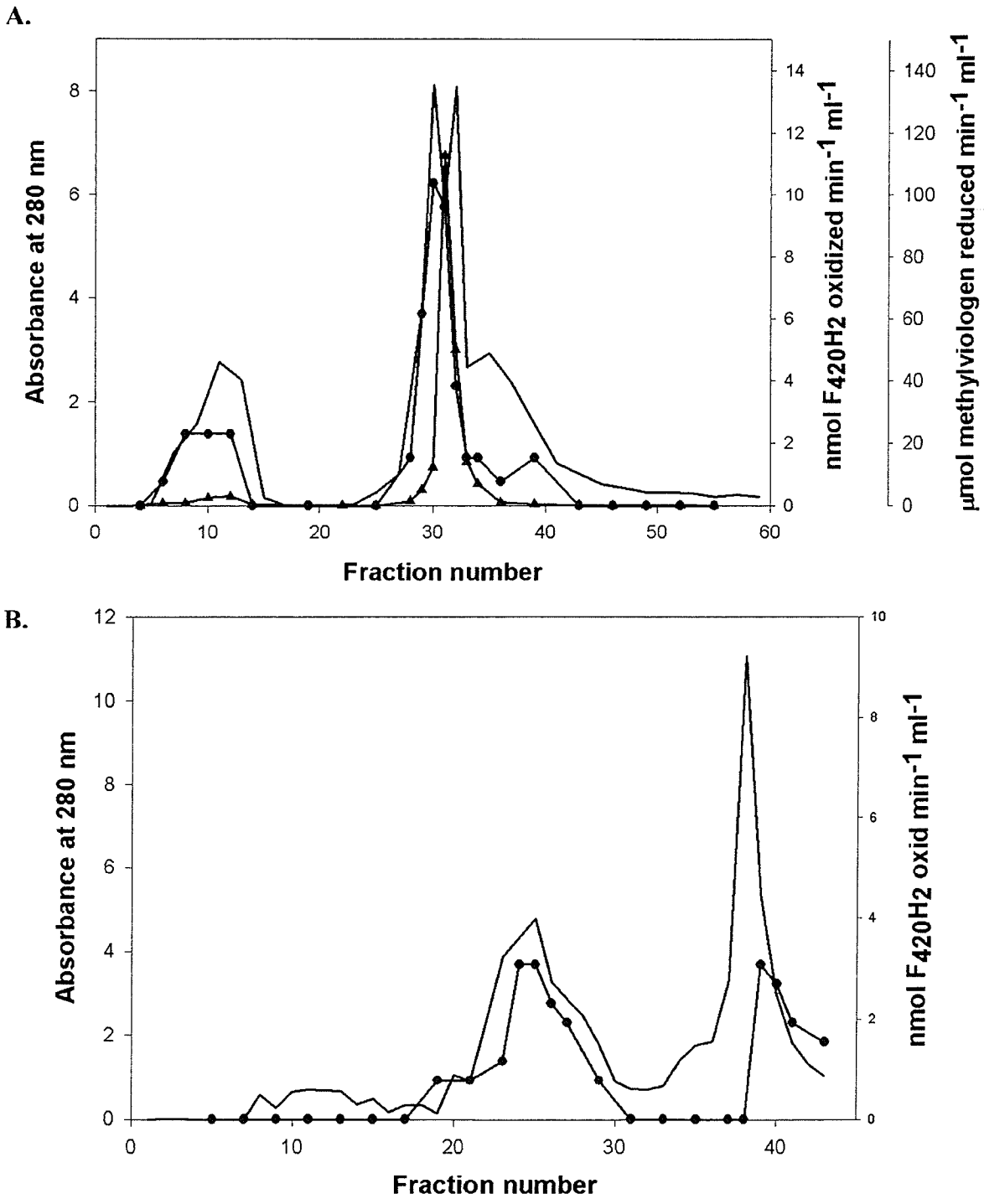

Figure 3. A. Protein and activity profile of fractions eluted from a DEAE Sephacel chromatography column. A_{280}, no symbol. $F_{420}H_2$ dehydrogenation activity, ●. Methyl viologen reduction, ▲. B. Protein and activity profile of fractions eluted from a Phenyl sepharose CL 4B column. A_{280}, no symbol. $F_{420}H_2$ dehydrogenation activity, ●. Conditions for elution as described in text. $F_{420}H_2$ dehydrogenation activity assayed using 500 µM phenazine.

4. Phenyl Sepharose CL-4B (Hydrophobic interaction chromatography)

Hydrophobic interaction chromatography involves the adsorption of protein to non-ionic groups, such as octyl or phenylalanine functionalities bound to inert matrices (Roe 1995). This requires the presence of hydrophobic patches on the protein, including amino acids such as alanine, trytophan, or phenylalanine. The addition of salts would remove the water molecules that form an ordered shell around the hydrophobic patches. The hydrophobic patches are exposed and may interact with non-ionic groups bound to the inert matrix. The protein is eluted from the matrix by decreasing the salt content (or other water miscible solvents).

Clarified cell-free extract (protein suspended in 200 mM KPO_4) was applied to Phenyl Sepharose and to Octyl Sepharose columns, with no apparent affinity. Later experiments made use of the presence of $(NH_4)_2SO_4$, at sub-precipitation saturation. The protein and activity profile of a Phenyl Sepharose column loaded with a 75% $(NH_4)_2SO_4$ saturated pellet, re-suspended in 60% $(NH_4)_2SO_4$ saturated buffer, is shown in Figure 3B. This has proven to be a convenient starting step, as it makes use of the high salt content of the protein sample. Elution of the protein also leads to desalting of the protein, enabling the use of other techniques after elution (i.e. ion exchange, affinity chromatography). The bound protein was eluted using a continuous 60-0% $(NH_4)_2SO_4$ gradient, in 50 mM HEPES, pH 7.0, with 0.05% Triton-X-100, 5% glycerol, and 10 mM DTT (Buffer A), followed by a single washing step of Buffer A to remove tightly bound protein. Two peaks of $F_{420}H_2$ dehydrogenation activity were observed during elution. One peak eluted off the column along during the continuous 60-0% $(NH_4)_2SO_4$ gradient, while the second peak eluted when the column was washed with $(NH_4)_2SO_4$ –free buffer.